



Final report

Designing farm specific nematode control programs for sheep

Project code: B.AHE.0308
Prepared by: Yan Laurenson
University of New England
Date published: 30 July 2021

PUBLISHED BY
Meat and Livestock Australia Limited
PO Box 1961
NORTH SYDNEY NSW 2059

Meat & Livestock Australia acknowledges the matching funds provided by the Australian Government to support the research and development detailed in this publication.

This publication is published by Meat & Livestock Australia Limited ABN 39 081 678 364 (MLA). Care is taken to ensure the accuracy of the information contained in this publication. However MLA cannot accept responsibility for the accuracy or completeness of the information or opinions contained in the publication. You should make your own enquiries before making decisions concerning your interests. Reproduction in whole or in part of this publication is prohibited without prior written consent of MLA.

Abstract

Designing regional and farm-specific integrated parasite management programs for sheep could be facilitated by the use of mathematical models describing the epidemiology of nematode infection. Consequently, a mathematical model capable of predicting pasture infectivity, worm burdens, drug resistance and the productive and financial consequences arising from the combination of various options for parasite control was developed. Concurrent validation studies were also carried out in New South Wales and Victoria to assess the predictive capacity of the model outputs. The development of a user interface, to assist in the operation of the mathematical model, generated a tool suitable for industry, research and educational purposes. Access to the tool, and the open-source code for the model, will be facilitated via its integration with other MLA and industry programs and web resources, such as linkage with the WormBoss website which provides an existing route to market. The provision of an open-source for the model is intended to inform researchers of underlying assumptions, allow for thorough review, remove reliance upon an individual and facilitate further development. The tool developed within this project is intended to provide a simple yet powerful resource to encourage adoption of integrated control programs by demonstrating benefit and mitigating against negative consequences in a manner specific for each farm.

Executive summary

Background

Control of internal parasites has become harder and more complex as the prevalence and severity of drench resistance has increased. Components of integrated control programs are well known but poorly adopted by sheep producers because they are uncertain of benefits. Provision of a mathematical model/tool describing the epidemiology of nematode infection may aid in the design regional control programs and support the development of farm-specific integrated parasite management programs. Such a tool may thereby encourage adoption of integrated control programs by demonstrating benefit and mitigating against negative consequences in a manner specific for each farm.

Objectives

The objective of this project was to develop a mathematical model capable of predicting pasture infectivity, worm burdens, drug resistance and the productive and financial consequences arising from the combination of various options for parasite control. Following the development of an appropriate mathematical model, a user-friendly interface will be developed to generate a tool and facilitate use of the mathematical model for the purpose of improving regional control programs and supporting the development of farm-specific programs. Further, validation studies were carried out in New South Wales and Victoria to assess the predictive capacity of the model outputs.

Methodology

A mathematical model capable of predicting pasture infectivity, worm burdens, drug resistance and the productive and financial consequences arising from the combination of various options for parasite control was developed from mathematical functions described within previously existing nematode models and parameterised in accordance with estimates provided by available literature. The completed model was validated by field studies carried out in New South Wales and Victoria to ensure regional differences in meteorological conditions and control practices were adequately captured by the model.

Results/key findings

A mathematical model and consequent tool (currently found at turnedworm-uat.une.edu.au) were successfully developed. Comparison between model predictions and field data was used to assess the predictive capacity of the model outputs. This identified some of the weaknesses of the model and a requirement to reassess the parameter estimates previously reported within available literature.

Benefits to industry

Use of the mathematical model via the tool will encourage adoption of integrated control programs by demonstrating benefit and mitigating against negative consequences in a manner specific for each farm.

Future research and recommendations

The tool should be used to generate industry and academic communications to facilitate its adoption via demonstrating the benefit of parasite control and elucidating negative interactions between parasite control options. The tool would benefit from continuing development of the underlying mathematical model to address the weaknesses identified by the validation study, and reassess parameter estimates to provide reliable prediction of the consequences of parasite control. Finally, further optimisation of the model code should be carried out to speed up processing time to improve user experience. Aside from these technical improvements, a key step will be to maximise the value for the sheep industry from the tool and open-source code. This can be achieved by integration with MLA and industry programs and web resources.

Table of contents

Abstract	2
Executive summary	3
1. Background	11
2. Objectives.....	13
3. Mathematical model	14
3.1 Weather.....	14
3.1.1 Daylight fraction	14
3.1.2 Temperature	14
3.1.3 Atmospheric pressure.....	14
3.1.4 CO ₂ and O ₂ partial pressure.....	15
3.1.5 Saturation vapour pressure	15
3.1.6 Dry air density	15
3.1.7 Psychrometric constant	15
3.1.8 Slope of saturation vapour pressure curve	15
3.1.9 Radiation.....	16
3.1.10 Wind speed	16
3.2 Pasture	17
3.2.1 Plant composition	17
3.2.2 Ground cover	18
3.2.3 Carbon assimilation via C ₃ photosynthesis.....	18
3.2.3.1 Temperature-dependence.....	18
3.2.3.2 CO ₂ compensation point.....	19
3.2.3.3 Electron transport rate	20
3.2.3.4 Net photosynthetic rate	20
3.2.4 Nitrogen uptake	21
3.2.5 Senescence	22
3.2.6 Growth	22
3.2.7 Litter decomposition	23

3.2.8	Initial parameterisation	24
3.2.9	Rates of change	26
3.2.10	Descriptors.....	27
3.2.10.1	Composition.....	27
3.2.10.2	Digestibilities	27
3.2.10.3	Gross energy and metabolizable energy	28
3.2.10.4	Pasture height and mass	28
3.3	Soil.....	29
3.3.1	Nitrogen	29
3.3.2	Hydrology.....	29
3.3.2.1	Water stress.....	29
3.3.2.2	Evapotranspiration	30
3.3.2.3	Volumetric soil water content	31
3.3.2.4	Gravimetric soil water content.....	31
3.4	Nematode ecology	32
3.4.1	Microclimatic variables.....	32
3.4.1.1	Faecal water content	33
3.4.1.2	Soil water content.....	33
3.4.1.3	Air water content.....	34
3.4.2	Free-living stages of the nematode lifecycle	34
3.4.2.1	Rates of change	34
3.4.2.2	Transition rates	35
3.4.2.3	Initial parameterisation	36
3.4.2.4	Descriptors.....	37
3.5	Supplementary feed.....	38
3.5.1	Digestibility and gross energy.....	38
3.5.2	Nitrogen descriptors	38
3.5.3	Mixed feed type.....	38
3.5.4	Availability	39
3.6	Individual animal model.....	40
3.6.1	Body composition	40

3.6.1.1 Empty body weight	40
3.6.1.2 Conceptus	40
3.6.1.3 Live weight	41
3.6.1.4 Maturity	41
3.6.1.5 Body condition score	41
3.6.2 Desired growth	42
3.6.2.1 Protein	42
3.6.2.2 Lipid.....	42
3.6.2.3 Wool.....	42
3.6.2.4 Foetus	43
3.6.2.5 Adnexa	43
3.6.3 Desired lactation.....	43
3.6.4 Nutritional requirements.....	44
3.6.4.1 Protein	44
3.6.4.2 Energy	45
3.6.5 Nutritional intake.....	46
3.6.5.1 Random environmental variation.....	46
3.6.5.2 Maximum feed intake.....	46
3.6.5.3 Feed quality descriptors	46
3.6.5.4 Pasture mass availability constraint	47
3.6.5.5 Inappetence	47
3.6.5.6 Milk intake	48
3.6.5.7 Desired feed intake.....	48
3.6.5.8 Feed intake	49
3.6.6 Gut fill	49
3.6.7 Nutrient availability via catabolism	50
3.6.8 Nutrient allocation.....	50
3.6.8.1 Parasitic protein loss.....	50
3.6.8.2 Nutrient availability	50
3.6.8.3 Maintenance	51
3.6.8.4 Pregnancy	51
3.6.8.5 Nutrient availability for lactation, body and wool growth	52

3.6.8.6 Lactation	53
3.6.8.7 Body and wool growth.....	54
3.6.8.8 Excess nutrients	56
3.6.9 Catabolism	57
3.6.10 Rates of change	57
3.6.10.1 Foetus	57
3.6.10.2 Adnexa	58
3.6.10.3 Lactation	59
3.6.10.4 Body and wool	59
3.6.11 Faeces	60
3.6.12 Parasite burden	60
3.6.13 FAMACHA® score.....	61
3.6.14 Faecal egg count	61
3.6.15 Immune response	62
3.6.16 Mortality	64
3.6.17 Initial parameterisation	65
3.6.17.1 Conceptus	65
3.6.17.2 Body composition	65
3.6.17.3 Parasite burden and immune response	66
3.7 Population model.....	68
3.8 Anthelmintic treatment and resistance	71
3.9 Scenario testing	73
3.9.1 Location	73
3.9.2 Paddock setup	73
3.9.3 Mob setup.....	74
3.9.4 Mob joining/mating.....	75
3.9.5 Mob allocation	76
3.9.6 Supplementary feed	77
3.9.7 Shearing	79
3.9.8 Anthelmintic treatment.....	79
3.9.9 Anthelmintic class efficacies.....	80

3.9.10 Economics	80
3.9.11 Optional outputs.....	81
3.10 Model outputs	82
3.10.1 Pasture traits.....	82
3.10.2 Mob traits	82
3.10.3 Phenotypic correlations, genotypic correlations and heritabilities	83
4. Validation studies	84
4.1 Site locations and initial setup.....	84
4.2 Experimental design.....	86
4.2.1 Initial pasture contamination	86
4.2.2 Monitoring period	86
4.2.3 Overview	87
4.3 Methods	88
4.3.1 Faecal egg count (bulk).....	88
4.3.2 Faecal egg count (individual)	89
4.3.3 Coproculture	90
4.3.4 Faecal egg count reduction test	92
4.3.5 Pasture sampling and analysis.....	93
4.3.6 Pasture infectivity analysis	94
4.4 Experimental diary	96
4.4.1 New South Wales.....	96
4.4.2 Victoria.....	101
4.5 Simulation procedure.....	104
4.5.1 New South Wales.....	104
4.5.2 Victoria.....	105
4.6 Results	106
4.6.1 New South Wales.....	106
4.6.1.1 Weather	106
4.6.1.2 Pasture mass and quality.....	108
4.6.1.3 Pasture infectivity	111
4.6.1.4 Live weight and body condition score	113

4.6.1.5 Faecal egg count	114
4.6.1.6 Faecal egg count reduction test	117
4.6.2 Victoria	118
4.6.2.1 Weather	118
4.6.2.2 Pasture mass and quality	120
4.6.2.3 Pasture infectivity	123
4.6.2.4 Live weight and body condition score	125
4.6.2.5 Faecal egg count	126
4.6.2.6 Faecal egg count reduction test	129
5. Tool and model accessibility	131
5.1 Tool	131
5.2 Model accessibility	131
6. Conclusion	132
6.1 Key findings	132
6.2 Benefits to industry	132
7. Future research and recommendations	133
8. References	134

1. Background

Internal parasites have been estimated to cost the Australian sheep industry in excess of \$436 million per year (Lane et al., 2015). Effective worm control relies heavily on the use of anti-parasitic drugs; however, reduced efficacy due to the evolution of drug resistance threatens the sustainability of livestock systems. As such, the cost of internal parasitism continues to increase (Kelly et al., 2010) alongside the increasing prevalence and severity of drug resistance (Playford et al., 2014). Consequently, the strategies employed to control nematode infections have increased in complexity and moved towards a more holistic approach incorporating the nutritional control of host immunity, grazing management to prepare low worm-risk pastures, selective breeding for host resistance and a more judicious use of anti-parasitic drugs. In combination these strategies must deliver effective worm control while minimising selection for drug resistance in a manner that meets the risk profile of sheep producers and the welfare concerns of consumers. WormBoss regional control programs (<http://www.wormboss.com.au/>) have been developed to satisfy these aims, but these programs would be better customised to meet regional and local needs if supported by mathematical models of the epidemiology of nematode infection. This support would be especially useful for understanding the interactions among control options (especially grazing management and anthelmintic use) and thus avoid unintended negative effects on the efficacy of worm control and drug resistance. Such models and tools would therefore improve regional control programs and support the development of farm-specific programs.

A number of mathematical models have been used to simulate nematode epidemiology around the world; however, they are of limited use and remain inaccessible to researchers and animal health advisors within Australia. In April 2009, the development of and access to a mathematical model of nematode epidemiology was identified as an industry research priority to better manage the trade-offs between production and drug resistance, and exploit known ecological barriers in nematode development (Meat & Livestock Australia, Australian Wool Innovation and Australian Cooperative Research Centre; 2009). The WormWorld model developed by Barnes and Dobson (1990) was specifically identified as a potential means of fulfilling these requirements; however, it remains inaccessible for researchers and animal health advisors.

Previously, an MLA project (B.AHE.0244; Laurenson, 2014) investigated the feasibility of developing a model to better manage nematode infections in sheep. This project reviewed seven existing and prominent nematode epidemiology models (including WormWorld) from available publications to evaluate their suitability for Australian conditions in their current form, or after customisation. Notably, each of the models reviewed were designed to address particular questions about the dynamics or control of specific nematode species in a specific host and/or agro-climatic region. Thus, whilst each model followed a generalised framework describing the population dynamics throughout the differing stages of the nematode life-cycle, certain components were only included if the authors deemed them necessary for the aim/purpose of their model. The consequence, for the purpose of simulating the impact of integrated parasite control programs on multi-species nematode infections in sheep across differing regions of Australia, was that the models reviewed incompletely described the nematode life cycle and were deemed initially unsuitable in their current form. Further issues to be noted included the dichotomy of model focus between animal production or parasitology, the disparity in the complexity of equal components between models, the minimal validation of model outputs, and the inappropriate use of models to investigate scenarios and parasite control strategies for which they were not designed to simulate.

Whilst individually the existing models were determined to be inappropriate for use in evaluating integrated parasite control programs in Australia, it was proposed that a composite model would be capable of achieving this aim. To this end, a composite model was outlined by identifying the best functions available from the existing models which were considered appropriate for the purpose of predicting the impact of nutrition, grazing management, anthelmintic treatment strategies and selective breeding for host resistance on production traits in sheep, parasitological traits and drug resistance under Australian conditions.

The availability of existing literature arising from experimental studies which support the underlying functions of each model component was also evaluated. The majority of model components were found to have sufficient supporting data. However, the full models (as a sum of components) were insufficiently validated using empirical data. Thus, field studies were proposed to provide data for validation of the model to ensure that it captures variation in regional climatic conditions and management practices.

The purpose of the present project was to develop a mathematical model capable of predicting pasture infectivity, worm burdens, drug resistance and the productive and financial consequences arising from the combination of various options for parasite control; thereby improving regional control programs and supporting the development of farm-specific programs. Further, validation studies were carried out to assess the model outputs.

Following the development of a suitable user-interface; access for industry, research and educational purposes is to be facilitated via its inclusion into the WormBoss website which provides an existing route to market. Further, it was noted in the MLA report (B.AHE.0244; Laurenson, 2014) that the absence of an open-source code for the existing models had resulted in reliance upon the individual developers, and in some cases had prevented these models from being updated once new experimental data had become available. As such, it was suggested that the source code for the mathematical model be made openly available. This would serve to inform researchers of underlying assumptions, allow for thorough review, remove reliance upon an individual and facilitate further development.

2. Objectives

- Build a composite mathematical prediction model capable of predicting the impact of nutrition, grazing management, anthelmintic treatment and selective breeding for host resistance on production, parasitism and drug resistance in sheep under Australian conditions.
- Design a user-friendly interface which allows user input (to amend pre-defined scenarios), and whose outputs include estimates of pasture infectivity, worm burdens, drench resistance, and production and financial outcomes under various Australian climate conditions. This interface to be supported by a user guide and workshop notes for advisors wishing to promote the use of the model amongst their producer clients.
- Conduct field studies to provide data for validating the model, ensuring that it reliably captures regional climatic conditions and management practices.
- Pilot the model and its user interface with producers, advisors, researchers and students and revise where necessary to improve its functionality.
- Provide the open source code for the model, to facilitate subsequent development and refinement.

3. Mathematical model

3.1 Weather

The model assumes that the user can draw on weather data including precipitation (PCP , mm d^{-1}), incoming solar radiation (R_s , $\text{MJ m}^{-2} \text{d}^{-1}$), daily maximum air temperature (T_{\max} , $^{\circ}\text{C}$), daily minimum air temperature (T_{\min} , $^{\circ}\text{C}$), wind speed (u , m s^{-1}), and vapour pressure (e_a , kPa). Further, the user is expected to input a latitude (LAT , $^{\circ}$) and elevation (z , m above sea level). Numerous meteorological variables, required by the model, were consequently calculated using these inputs.

3.1.1 Daylight fraction

The solar declination angle (δ , rad) and sunset hour angle (ω_s , rad) were estimated as (Zotarelli et al., 2010):

$$\delta = 0.409 \cdot \sin\left(\frac{2 \cdot \pi \cdot t}{365} - 1.39\right) \quad [\text{Eq. 1}]$$

$$\omega_s = \cos^{-1}\left(-\tan\left(\frac{\pi \cdot LAT}{180}\right) \cdot \tan \delta\right) \quad [\text{Eq. 2}]$$

where LAT is latitude ($^{\circ}$); and t is the julian day of year (i.e. 1st January = 1).

The daylight fraction (f_{day} , d^{-1}) was consequently estimated as:

$$f_{\text{day}} = \frac{\omega_s}{\pi} \quad [\text{Eq. 3}]$$

3.1.2 Temperature

Daylight period air temperature (T_{day} , $^{\circ}\text{C}$), daily mean air temperature (T_{mean} , $^{\circ}\text{C}$), and soil temperature (T_{soil} , $^{\circ}\text{C}$; $R^2 = 0.99$, $\text{se} = 1.69$, $F_{1,397} = 40961.58$, $p < 0.0001$) were calculated as:

$$T_{\text{day}} = T_{\min} + f_{\text{day}} \cdot (T_{\max} - T_{\min}) \quad [\text{Eq. 4}]$$

$$T_{\text{mean}} = \frac{T_{\max} + T_{\min}}{2} \quad [\text{Eq. 5}]$$

$$T_{\text{soil}} = 1.17 \cdot T_{\text{mean}} \quad [\text{Eq. 6}]$$

where f_{day} is daylight fraction (d^{-1} , section 3.1.1 Eq. 3); T_{\max} is daily maximum air temperature ($^{\circ}\text{C}$); and T_{\min} is daily minimum air temperature ($^{\circ}\text{C}$).

3.1.3 Atmospheric pressure

Daylight period atmospheric pressure (P_{day} , kPa) and daily mean atmospheric pressure (P_{mean} , kPa) were calculated as (Zotarelli et al., 2010):

$$P_x = 101.3 \cdot \left(\frac{T_x + 273 - 0.0065 \cdot z}{T_x + 273}\right)^{5.26} \quad [\text{Eq. 7}]$$

where T_x is either daylight period air temperature (T_{day} , $^{\circ}\text{C}$, section 3.1.2 Eq. 4) or daily mean air temperature (T_{mean} , $^{\circ}\text{C}$, section 3.1.2 Eq. 5) for the calculation of P_{day} and P_{mean} , respectively; and z is elevation (m above sea level).

3.1.4 CO₂ and O₂ partial pressure

The partial pressure of CO₂ (p_{CO_2} , μbar) and O₂ (p_{O_2} , μbar) were calculated as:

$$p_x = 0.01 \cdot x \cdot P_{\text{day}} \quad [\text{Eq. 8}]$$

where P_{day} is daylight period atmospheric pressure (kPa, section 3.1.3 Eq. 7); and x is either atmospheric CO₂ concentration (410.5 ppm; Mauna Loa Observatory, 2019) or atmospheric O₂ concentration (210,000 ppm) for the calculation of p_{CO_2} and p_{O_2} , respectively.

3.1.5 Saturation vapour pressure

Saturation vapour pressure (e_s , kPa) was related to daily mean air temperature (T_{mean} , °C, section 3.1.2 Eq. 5) as per the function described by Zotarelli et al. (2010):

$$e_s = 0.6108 \cdot e^{\frac{17.27 \cdot T_{\text{mean}}}{T_{\text{mean}} + 237.3}} \quad [\text{Eq. 9}]$$

3.1.6 Dry air density

Dry air density (ρ_a , kg m⁻³) was calculated as:

$$\rho_a = \frac{P_{\text{mean}}}{R_{\text{DA}} \cdot (T_{\text{mean}} + 273)} \quad [\text{Eq. 10}]$$

where P_{mean} is daily mean atmospheric pressure (kPa, section 3.1.3 Eq. 7); R_{DA} is the specific gas constant for dry air (0.287058 kJ kg⁻¹ °C⁻¹); and T_{mean} is daily mean air temperature (°C, section 3.1.2 Eq. 5).

3.1.7 Psychrometric constant

The psychrometric constant (γ , kPa °C⁻¹) was given by (Zotarelli et al., 2010):

$$\gamma = \frac{c_p \cdot P_{\text{mean}}}{\varepsilon \cdot \lambda} \quad [\text{Eq. 11}]$$

where c_p is the specific heat capacity of dry air (1.013 · 10⁻³ MJ kg⁻¹ °C⁻¹); P_{mean} is daily mean atmospheric pressure (kPa, section 3.1.3 Eq. 7); ε is the ratio molecular weight of water vapour/dry air (0.622 g⁻¹); and λ is the latent heat of vaporization (2.453 MJ kg⁻¹).

3.1.8 Slope of saturation vapour pressure curve

The slope of the relationship between saturation vapour pressure and temperature (Δ , kPa °C⁻¹) was estimated as (Zotarelli et al., 2010):

$$\Delta = \frac{4098 \cdot e_s}{(T_{\text{mean}} + 237.3)^2} \quad [\text{Eq. 12}]$$

where e_s is saturation vapour pressure (kPa, section 3.1.5 Eq. 9); and T_{mean} is daily mean air temperature (°C, section 3.1.2 Eq. 5).

3.1.9 Radiation

Net radiation (R_n , MJ m⁻² d⁻¹) was estimated in accordance with Zotarelli et al. (2010) by considering extra-terrestrial radiation (R_a , MJ m⁻² d⁻¹), clear sky solar radiation (R_{so} , MJ m⁻² d⁻¹) and net outgoing long wave solar radiation (R_{nl} , MJ m⁻² d⁻¹):

$$d_r = 1 + 0.033 \cdot \cos\left(\frac{2 \cdot \pi \cdot t}{365}\right) \quad [\text{Eq. 13}]$$

$$R_a = \frac{1440 \cdot G_{sc} \cdot d_r}{\pi} \cdot \left[\left(\omega_s \cdot \sin\left(\frac{\pi \cdot LAT}{180}\right) \cdot \sin \delta \right) + \left(\cos\left(\frac{\pi \cdot LAT}{180}\right) \cdot \cos \delta \cdot \sin \omega_s \right) \right] \quad [\text{Eq. 14}]$$

$$R_{so} = (0.75 + 0.00002 \cdot z) \cdot R_a \quad [\text{Eq. 15}]$$

$$R_{nl} = \sigma \left[\frac{(T_{\max} + 273.16)^4 + (T_{\min} + 273.16)^4}{2} \right] \cdot (0.34 - 0.14 \cdot \sqrt{e_a}) \cdot \left(1.35 \cdot \frac{R_s}{R_{so}} - 0.35 \right) \quad [\text{Eq. 16}]$$

$$R_n = (1 - f_{ref}) \cdot R_s - R_{nl} \quad [\text{Eq. 17}]$$

where d_r is the inverse relative distance Earth-Sun (Eq. 13); f_{ref} is the canopy reflectance fraction (0.23 MJ⁻¹; Farquhar et al., 1980); G_{sc} is the solar constant (0.08165 MJ m⁻² min⁻¹); LAT is latitude (°); R_s is incoming solar radiation (MJ m⁻² d⁻¹); t is the julian day of year (i.e. 1st January = 1); T_{\max} is daily maximum air temperature (°C); T_{\min} is daily minimum air temperature (°C); e_a is vapour pressure (kPa); z is elevation (m above sea level); δ is solar declination angle (rad, section 3.1.1 Eq. 1); σ is the Stefan-Boltzmann constant (4.903·10⁻⁹ MJ °C⁻⁴ m⁻² d⁻¹); and ω_s is sunset hour angle (rad, section 3.1.1 Eq. 2).

3.1.10 Wind speed

For weather data including wind speed (m s⁻¹) recorded at any given height (ht , m above ground level), the wind speed measured at 2m above ground level (u_2 , m s⁻¹) was calculated in accordance with Zotarelli et al. (2010):

$$u_2 = \frac{u_{ht}^{4.87}}{\ln(67.8 \cdot ht - 5.42)} \quad [\text{Eq. 18}]$$

3.2 Pasture

A schematic diagram of the pasture model is provided in Fig. 1. The pasture model requires user input for crude protein ($CP\%$, %), metabolizable energy (ME , MJ [kg dry matter]⁻¹) and pasture height (PHT , m) in order to define the initial values associated with plant dry matter (section 3.2.8). These inputs represent non-subjective and quantifiable traits. Pasture height can easily be measured or estimated directly from pasture. The crude protein and metabolizable energy content of plant material can be obtained by sending a sample for feed/fodder analysis using either chemical or near infrared spectroscopy techniques. This service is provided by a variety of vendors (e.g. www.feedtest.com.au) at relatively low cost.

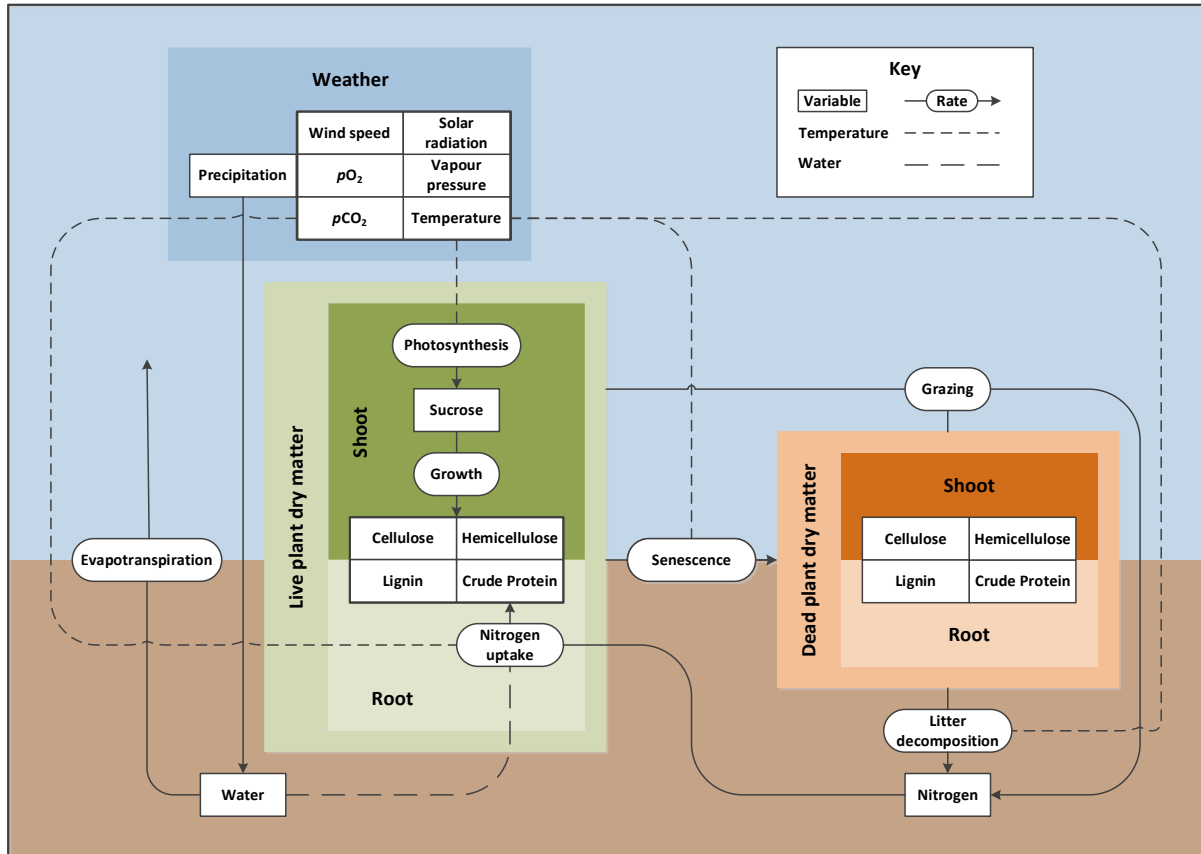


Figure 1. Schematic diagram of the pasture model.

3.2.1 Plant composition

Dead and live plant dry matter was assumed to be comprised of cellulose, crude protein, hemicellulose and lignin, with live plant dry matter also including sucrose. Further, dead and live plant dry matter were also separated into root and shoot portions. As such:

$$W_D = CL_D + CP_D + HC_D + LG_D = W_{D,RT} + W_{D,SH} \quad [\text{Eq. 19}]$$

$$W_L = CL_L + CP_L + HC_L + LG_L + SUC = W_{L,RT} + W_{L,SH} \quad [\text{Eq. 20}]$$

where CL_D , CP_D , HC_D and LG_D are the cellulose, crude protein, hemicellulose and lignin content of dead plant dry matter ($g\ m^{-2}$), respectively; CL_L , CP_L , HC_L and LG_L are the cellulose, crude protein, hemicellulose and lignin content of live plant dry matter ($g\ m^{-2}$), respectively; SUC is the sucrose content of plant dry matter ($g\ m^{-2}$); W_D is dead plant dry matter ($g\ m^{-2}$); $W_{D,RT}$ and $W_{D,SH}$ are dead

root and shoot dry matter (g m^{-2}), respectively; W_L is live plant dry matter (g m^{-2}); and $W_{L,RT}$ and $W_{L,SH}$ are live root and shoot dry matter (g m^{-2}), respectively.

The fractional carbon content of crude protein ($f_{C,CP}$, C g^{-1}) and lignin ($f_{C,LG}$, C g^{-1}) were given as 0.52 (Benedict and Osborne, 1907) and 0.64, respectively. The fractional carbon content of cellulose ($f_{C,CL}$, C g^{-1}) and sucrose ($f_{C,SUC}$, C g^{-1}) were given as:

$$f_{C,CL} = \frac{m_C \cdot n_{CL}}{M_{CL}} \quad [\text{Eq. 21}]$$

$$f_{C,SUC} = \frac{m_C \cdot n_{SUC}}{M_{SUC}} \quad [\text{Eq. 22}]$$

where m_C is the atomic mass of carbon (12 g mol^{-1}); M_{CL} is the molar mass of cellulose (162 g mol^{-1}); M_{SUC} is the molar mass of sucrose (342 g mol^{-1}); n_{CL} is the number of carbon atoms per cellulose molecule (6); and n_{SUC} is the number of carbon atoms per sucrose molecule (12).

Hence, the fractional carbon content ($f_{C,L}$, C g^{-1}) and the fractional nitrogen content of live plant dry matter ($f_{N,L}$, N g^{-1}) were calculated as:

$$f_{C,L} = \frac{f_{C,CL} \cdot (CL_L + HC_L) + f_{C,CP} \cdot CP_L + f_{C,LG} \cdot LG_L + f_{C,SUC} \cdot SUC}{W_L} \quad [\text{Eq. 23}]$$

$$f_{N,L} = \frac{f_{N,CP} \cdot CP_L}{W_L} \quad [\text{Eq. 24}]$$

where $f_{N,CP}$ is the fractional nitrogen content of crude protein (0.16 N g^{-1}).

3.2.2 Ground cover

Fractional ground cover (f_g , m^{-2}) was described as the inverse of the Beer-Lambert equation of light extinction (Monsi and Saeki, 2005):

$$f_g = 1 - e^{-k \cdot SLA \cdot f_{lam} \cdot (W_{D,SH} + W_{L,SH})} \quad [\text{Eq. 25}]$$

where f_{lam} is the lamina fraction of shoot dry matter (0.7 g^{-1} ; Thornley and Verberne, 1989); k is the canopy extinction coefficient (0.5; Zhang et al., 2014); SLA is specific leaf area ($0.02 \text{ m}^2 \text{ g}^{-1}$; Arrendondo and Schnyder, 2003); and $W_{D,SH}$ and $W_{L,SH}$ are dead and live shoot dry matter (g m^{-2}), respectively.

3.2.3 Carbon assimilation via C_3 photosynthesis

3.2.3.1 Temperature-dependence

The temperature-dependence of any variable (x) was incorporated by using the function described by Medlyn et al. (2002), which can generate both a standard and peaked Arrhenius response:

$$x = x_{25} \cdot e^{\frac{E_a \cdot (T_{day} - 25)}{298 \cdot R \cdot (T_{day} + 273)}} \cdot \frac{1 + e^{\frac{S \cdot 298 - E_d}{R \cdot 298}}}{\frac{S \cdot (T_{day} + 273) - E_d}{R \cdot (T_{day} + 273)} + 1} \quad [\text{Eq. 26}]$$

where E_a is activation energy (J mol^{-1}); E_d is deactivation energy (J mol^{-1}); R is the universal gas constant ($8.31447 \text{ J }^\circ\text{C}^{-1} \text{ mol}^{-1}$); S is the entropy factor ($\text{J }^\circ\text{C}^{-1} \text{ mol}^{-1}$); T_{day} is daylight period temperature ($^\circ\text{C}$, section 3.1.2 Eq. 4); and x_{25} is the value of variable x at 25°C .

Mesophyll conductance (g_m , $\text{mol m}^{-2} \text{s}^{-1} \text{bar}^{-1}$), maximum electron transport rate (J_{max} , $\mu\text{mol e}^- \text{m}^{-2} \text{s}^{-1}$), the Michaelis-Menten constant of Rubisco for CO_2 (K_{mC} , μbar), the Michaelis-Menten constant of Rubisco for O_2 (K_{mO} , μbar), day respiration (R_d , $\mu\text{mol CO}_2 \text{m}^{-2} \text{s}^{-1}$), the relative CO_2/O_2 specificity factor for Rubisco ($S_{\text{C/O}}$, bar^{-1}) and the maximum rate of Rubisco activity-limited carboxylation (V_{Cmax} , $\mu\text{mol CO}_2 \text{m}^{-2} \text{s}^{-1}$) were all assumed to be temperature-dependent (Table 1). Further, nitrogen-dependence was incorporated into the estimation of J_{max} at 25°C ($J_{\text{max},25}$, $\mu\text{mol e}^- \text{m}^{-2} \text{s}^{-1}$) in accordance with Harley et al. (1992):

$$J_{\text{max},25} = 95 \cdot f_{\text{N,L}} \cdot f_{\text{lam}} \cdot W_{\text{L,SH}} \quad [\text{Eq. 27}]$$

where f_{lam} is the lamina fraction of shoot dry matter (0.7 g^{-1} ; Thornley and Verberne, 1989); $f_{\text{N,L}}$ is the fractional nitrogen content of live plant dry matter (N g^{-1}), section 3.2.1 Eq. 24); and $W_{\text{L,SH}}$ is live shoot dry matter (g m^{-2}).

Consequently, the value of V_{Cmax} at 25°C ($V_{\text{Cmax},25}$, $\mu\text{mol CO}_2 \text{m}^{-2} \text{s}^{-1}$) was estimated in accordance with Leuning (2002) and Yin et al. (2004), and the value of R_d at 25°C ($R_{d,25}$, $\mu\text{mol CO}_2 \text{m}^{-2} \text{s}^{-1}$) was estimated in accordance with Farquhar et al. (1980):

$$V_{\text{Cmax},25} = \frac{J_{\text{max},25}}{1.92} \quad [\text{Eq. 28}]$$

$$R_{d,25} = 0.01 \cdot V_{\text{Cmax},25} \quad [\text{Eq. 29}]$$

Table 1. Activation energy (E_a , J mol^{-1}), deactivation energy (E_d , J mol^{-1}), entropy factor (S , $\text{J }^\circ\text{C}^{-1} \text{mol}^{-1}$), and value at 25°C (x_{25}) for the temperature-dependent variables of mesophyll conductance (g_m , $\text{mol m}^{-2} \text{s}^{-1} \text{bar}^{-1}$), maximum electron transport rate (J_{max} , $\mu\text{mol e}^- \text{m}^{-2} \text{s}^{-1}$), the Michaelis-Menten constant of Rubisco for CO_2 (K_{mC} , μbar), the Michaelis-Menten constant of Rubisco for O_2 (K_{mO} , μbar), day respiration (R_d , $\mu\text{mol CO}_2 \text{m}^{-2} \text{s}^{-1}$), the relative CO_2/O_2 specificity factor for Rubisco ($S_{\text{C/O}}$, bar^{-1}) and the maximum rate of Rubisco activity-limited carboxylation (V_{Cmax} , $\mu\text{mol CO}_2 \text{m}^{-2} \text{s}^{-1}$).

Variable	E_a	E_d	S	X_{25}
g_m	49,600 ^b	437,400 ^b	1,400 ^b	0.4 ^f
J_{max}	60,000 ^e	200,000 ^d	643 ^c	Eq. 27 ^g
K_{mC}	80,990 ^b	0	0	270 ^b
K_{mO}	23,720 ^b	0	0	165,000 ^b
R_d	46,390 ^f	0	0	Eq. 29 ^g
$S_{\text{C/O}}$	-24,460 ^b	0	0	2,800 ^b
V_{Cmax}	65,330 ^a	0	0	Eq. 28 ^g

^aBernacchi et al., 2001; ^bBernacchi et al., 2002; ^cLeuning, 2002; ^dMedlyn et al., 2002; ^eWohlfahrt et al., 1999; ^fYin and Struik, 2009; ^gprovides reference to equation within text.

3.2.3.2 CO₂ compensation point

The CO_2 compensation point in the absence of day respiration (Γ^* , μbar) was estimated as (Bernacchi et al., 2001):

$$\Gamma^* = \frac{0.5 \cdot p_{\text{O}_2}}{S_{\text{C/O}}} \quad [\text{Eq. 30}]$$

where p_{O_2} is the partial pressure of O_2 (μbar , section 3.1.4 Eq. 8); and $S_{\text{C/O}}$ is the relative CO_2/O_2 specificity factor for Rubisco (bar^{-1} , section 3.2.3.1 Eq. 26).

3.2.3.3 Electron transport rate

Photosynthetic photon flux density (*PPFD*, $\mu\text{mol photon m}^{-2} \text{s}^{-1}$) was estimated as:

$$PPFD = \frac{\alpha \cdot R_n \cdot f_g \cdot \frac{W_{L,SH}}{W_{D,SH} + W_{L,SH}}}{86,400 \cdot f_{\text{day}}} \quad [\text{Eq. 31}]$$

where f_{day} is daylight fraction (d^{-1} , section 3.1.1 Eq. 3); f_g is fractional ground cover (m^{-2} , section 3.2.2 Eq. 25); R_n is net radiation ($\text{MJ m}^{-2} \text{d}^{-1}$, section 3.1.9 Eq. 17); $W_{D,SH}$ and $W_{L,SH}$ are dead and live shoot dry matter (g m^{-2}), respectively; and α is the solar radiation conversion factor ($4,570,000 \mu\text{mol photon MJ}^{-1}$; Amthor, 2010).

The electron transport rate (J , $\mu\text{mol e}^{-} \text{m}^{-2} \text{s}^{-1}$) was consequently estimated using the non-rectangular hyperbolic function described by Marshall and Biscoe (1980):

$$J = \frac{\beta \cdot PPFD + J_{\text{max}} - \sqrt{(\beta \cdot PPFD + J_{\text{max}})^2 - 4 \cdot \zeta \cdot J_{\text{max}} \cdot \beta \cdot PPFD}}{2 \cdot \zeta} \quad [\text{Eq. 32}]$$

where J_{max} is maximum electron transport rate ($\mu\text{mol e}^{-} \text{m}^{-2} \text{s}^{-1}$, section 3.2.3.1 Eq. 26); β is the conversion efficiency of *PPDF* to J ($0.3 \text{ mol e}^{-} (\text{mol photon})^{-1}$; Medlyn et al., 2002); and ζ is the convexity factor for response of J to *PPDF* (0.7; de Pury and Farquhar, 1997).

3.2.3.4 Net photosynthetic rate

In the absence of an estimate for the partial pressure of CO_2 at the Rubisco carboxylation sites in chloroplasts, the Rubisco-limited rate of CO_2 assimilation (A_c , $\mu\text{mol CO}_2 \text{m}^{-2} \text{s}^{-1}$) and the electron transport-limited rate of CO_2 assimilation (A_l , $\mu\text{mol CO}_2 \text{m}^{-2} \text{s}^{-1}$) were estimated by solving the first root of the standard cubic equation $A^3 + pA^2 + qA + r = 0$, as per the coupled model of C_3 photosynthesis and diffusional conductance described by Yin and Struik (2009):

$$A_x = -2 \cdot \sqrt{Q} \cdot \cos\left(\frac{\varphi}{3}\right) - \frac{p}{3} \quad [\text{Eq. 33}]$$

where:

$$Q = \frac{p^2 - 3 \cdot q}{9} \quad [\text{Eq. 34}]$$

$$U = \frac{2 \cdot p^3 - 9 \cdot p \cdot q + 27 \cdot r}{54} \quad [\text{Eq. 35}]$$

$$\varphi = \cos^{-1}\left(\frac{U}{\sqrt{Q^3}}\right) \quad [\text{Eq. 36}]$$

The coefficients p , q and r were estimated as (Yin and Struik, 2009):

$$p = -\frac{d + (x_1 - R_d)/g_m + a \cdot (1/g_m + 1/g_b) + c \cdot (g_0/g_m + f_{VPD})}{m} \quad [\text{Eq. 37}]$$

$$q = \frac{d \cdot (x_1 - R_d) + a \cdot c + b \cdot (g_0/g_m + f_{VPD})}{m} \quad [\text{Eq. 38}]$$

$$r = -\frac{a \cdot b}{m} \quad [\text{Eq. 39}]$$

where f_{VPD} is the factor for describing the effect of leaf-to-air vapour difference on stomatal conductance (1.25; Yin and Struik, 2009); g_b is boundary-layer conductance ($1.5 \text{ mol m}^{-2} \text{s}^{-1} \text{bar}^{-1}$; Yin and Struik, 2009); g_m is mesophyll conductance ($\text{mol m}^{-2} \text{s}^{-1} \text{bar}^{-1}$, section 3.2.3.1 Eq. 26); g_0 is

residual stomatal conductance when irradiance approaches zero ($0.01 \text{ mol m}^{-2} \text{ s}^{-1} \text{ bar}^{-1}$; Yin and Struik, 2009); R_d is day respiration ($\mu\text{mol CO}_2 \text{ m}^{-2} \text{ s}^{-1}$, section 3.2.3.1 Eq. 26); and the coefficients a , b , c , d , m and x_1 were expressed as (Yin and Struik, 2009):

$$x_1 = \begin{cases} V_{C\max}, & \text{for } A_C \\ J/4, & \text{for } A_J \end{cases} \quad [\text{Eq. 40}]$$

$$x_2 = \begin{cases} K_{mC} \cdot (1 + p_{O_2}/K_{mO}), & \text{for } A_C \\ 2 \cdot \Gamma_*, & \text{for } A_J \end{cases} \quad [\text{Eq. 41}]$$

$$a = g_0 \cdot (x_2 + \Gamma_*) + \left(\frac{g_0}{g_m} + f_{VPD}\right) \cdot (x_1 - R_d) \quad [\text{Eq. 42}]$$

$$b = p_{CO_2} \cdot (x_1 - R_d) - \Gamma_* \cdot x_1 - R_d \cdot x_2 \quad [\text{Eq. 43}]$$

$$c = p_{CO_2} + x_2 + \left(\frac{1}{g_m} + \frac{1}{g_b}\right) \cdot (x_1 - R_d) \quad [\text{Eq. 44}]$$

$$d = x_2 + \Gamma_* + \frac{x_1 - R_d}{g_m} \quad [\text{Eq. 45}]$$

$$m = \frac{1}{g_m} + \left(\frac{g_0}{g_m} + f_{VPD}\right) \cdot \left(\frac{1}{g_m} + \frac{1}{g_b}\right) \quad [\text{Eq. 46}]$$

where J is electron transport rate ($\mu\text{mol e}^- \text{ m}^{-2} \text{ s}^{-1}$, section 3.2.3.3 Eq. 32); K_{mC} is the Michaelis-Menten constant of Rubisco for CO_2 (μbar , section 3.2.3.1 Eq. 26); K_{mO} is the Michaelis-Menten constant of Rubisco for O_2 (μbar , section 3.2.3.1 Eq. 26); p_{CO_2} is the partial pressure of CO_2 (μbar , section 3.1.4 Eq. 8); p_{O_2} is the partial pressure of O_2 (μbar , section 3.1.4 Eq. 8); $V_{C\max}$ is maximum rate of Rubisco activity-limited carboxylation ($\mu\text{mol CO}_2 \text{ m}^{-2} \text{ s}^{-1}$, section 3.2.3.1 Eq. 26); and Γ_* is the CO_2 compensation point in the absence of day respiration (μbar , section 3.2.3.2 Eq. 30).

The net photosynthetic rate (A , $\mu\text{mol CO}_2 \text{ m}^{-2} \text{ s}^{-1}$) was subsequently calculated in accordance with Farquhar et al. (1980):

$$A = \begin{cases} A_C, & \text{for } A_C \leq A_J \\ A_J, & \text{for } A_C > A_J \end{cases} \quad [\text{Eq. 47}]$$

As such, the optimum carbon assimilation rate ($C_{\text{FIX,OPT}}$, $\text{g C m}^{-2} \text{ d}^{-1}$) was estimated as:

$$C_{\text{FIX}} = A \cdot 86,400 \cdot f_{\text{day}} \cdot m_C \cdot 10^{-6} \quad [\text{Eq. 48}]$$

where m_C is the atomic mass of carbon (12 g mol^{-1}); f_{day} is daylight fraction (d^{-1} , section 3.1.1 Eq. 3).

3.2.4 Nitrogen uptake

The specific nitrogen absorption rate (SNA , $\text{g N [g live root dry matter]}^{-1} [\text{g N m}^{-2} \text{ soil}]^{-1} \text{ d}^{-1}$) was calculated using the peaked Arrhenius temperature response function described Medlyn et al. (2002), and parameterised to Clarkson et al. (1986) ($R^2 = 0.99$, $se = 1.06 \times 10^{-5}$, $F_{1,6} = 792.46$, $p < 0.001$):

$$SNA = 0.0004 \cdot e^{\frac{198,160 \cdot (T_{\text{soil}} - 25)}{298 \cdot R \cdot (T_{\text{soil}} + 273)}} \cdot \frac{1 + e^{\frac{13,520}{R \cdot 298}}}{1 + e^{\frac{740 \cdot (T_{\text{soil}} + 273) - 207,000}{R \cdot (T_{\text{soil}} + 273)}}} \quad [\text{Eq. 49}]$$

where R is the universal gas constant ($8.31447 \text{ J } ^\circ\text{C}^{-1} \text{ mol}^{-1}$); and T_{soil} is soil temperature ($^\circ\text{C}$, section 3.1.2 Eq. 6).

The optimum nitrogen uptake rate ($U_{N,OPT}$, g N m⁻² d⁻¹) was thereby estimated as:

$$U_{N,OPT} = SNA \cdot W_{L,RT} \cdot N_S \quad [\text{Eq. 50}]$$

where N_S is soil inorganic nitrogen content (g N m⁻²); and $W_{L,RT}$ is live root dry matter (g m⁻²).

The nitrogen uptake rate (U_N , g N m⁻² d⁻¹) was consequently calculated assuming that the stress constraint associated with plant available water (Ω_{PAW} , section 3.3.2.1 Eq. 113) influenced the rate of crude protein synthesis, such that

$$U_N = U_{N,OPT} \cdot \Omega_{PAW} \quad [\text{Eq. 51}]$$

3.2.5 Senescence

The deterioration of live plant dry matter with age was estimated in accordance with the function described by Woodward (1998). Hence, the relative senescence rate (ξ , g⁻¹ d⁻¹) was given as:

$$\xi = 0.00111 \cdot (T_{\text{soil}} + 3.4) \quad [\text{Eq. 52}]$$

where T_{soil} is soil temperature (°C, section 3.1.2 Eq. 6).

3.2.6 Growth

Plant carbon availability for growth (C_{AVAIL} , g C m⁻²) was assumed to be drawn from the sucrose content of plant dry matter (SUC , g m⁻²) relative to the ratio of sucrose carbon to total live plant carbon, such that:

$$C_{AVAIL} = \frac{(f_{C,SUC} \cdot SUC)^2}{f_{C,L} \cdot W_L} \quad [\text{Eq. 53}]$$

where $f_{C,L}$ is the fractional carbon content of live plant dry matter (C g⁻¹, section 3.2.1 Eq. 23); $f_{C,SUC}$ is the fractional carbon content of sucrose (C g⁻¹; section 3.2.1 Eq. 22); and W_L is live plant dry matter (g m⁻², section 3.2.1 Eq. 20).

The accretion rate of sucrose (SUC_G , g m⁻² d⁻¹) and crude protein (CP_G , g m⁻² d⁻¹) were calculated as:

$$SUC_G = \frac{C_{FIX} - C_{AVAIL}}{f_{C,SUC}} \quad [\text{Eq. 54}]$$

$$CP_G = \frac{U_N}{f_{N,CP}} \quad [\text{Eq. 55}]$$

where C_{FIX} is the carbon assimilation rate (g C m⁻² d⁻¹, section 3.2.3.4 Eq. 48); $f_{N,CP}$ is the fractional nitrogen content of crude protein (0.16 N g⁻¹); and U_N is the nitrogen uptake rate (g N m⁻² d⁻¹, section 3.2.4 Eq. 51).

The plant carbon availability for growth remaining after allocation to crude protein synthesis, was partitioned toward cellulose, hemicellulose and lignin accretion by calculating the ratio of live neutral detergent fibre carbon to total live plant carbon ($r_{C,NDF}$, g⁻¹) after considering growth and senescence:

$$r_{C,NDF} = \frac{C_{AVAIL} - f_{C,CP} \cdot CP_G + (1 - \xi) \cdot (f_{C,L} \cdot W_L - f_{C,SUC} \cdot SUC - f_{C,CP} \cdot CP_L)}{C_{FIX} + (1 - \xi) \cdot f_{C,L} \cdot W_L} \quad [\text{Eq. 56}]$$

where CP_L is the crude protein content of live plant dry matter (g m^{-2}); $f_{C,CP}$ is the fractional carbon content of crude protein (0.52 C g^{-1} ; Benedict and Osborne, 1907); and ξ is the relative senescence rate ($\text{g}^{-1} \text{ d}^{-1}$; section 3.2.5 Eq. 52).

The ratio of live acid detergent fibre carbon ($r_{C,ADF}$, g^{-1}) and live acid detergent lignin carbon ($r_{C,ADL}$, g^{-1}) to total live plant carbon were calculated such that (in agreement with section 3.2.8 Eq. 73 & 74):

$$r_{C,ADF} = 0.072 \cdot e^{2.3 \cdot r_{C,NDF}} \quad [\text{Eq. 57}]$$

$$r_{C,ADL} = 0.0043 \cdot e^{3.7 \cdot r_{C,NDF}} \quad [\text{Eq. 58}]$$

The cellulose (CL_G , $\text{g m}^{-2} \text{ d}^{-1}$), hemicellulose (HC_G , $\text{g m}^{-2} \text{ d}^{-1}$) and lignin (LG_G , $\text{g m}^{-2} \text{ d}^{-1}$) accretion rates were consequently calculated as:

$$CL_G = \frac{(r_{C,ADF} - r_{C,ADL}) \cdot (C_{\text{FIX}} + (1 - \xi) \cdot f_{C,L} \cdot W_L)}{f_{C,CL}} - (1 - \xi) \cdot CL_L \quad [\text{Eq. 59}]$$

$$HC_G = \frac{(r_{C,NDF} - r_{C,ADF}) \cdot (C_{\text{FIX}} + (1 - \xi) \cdot f_{C,L} \cdot W_L)}{f_{C,CL}} - (1 - \xi) \cdot HC_L \quad [\text{Eq. 60}]$$

$$LG_G = \frac{r_{C,ADL} \cdot (C_{\text{FIX}} + (1 - \xi) \cdot f_{C,L} \cdot W_L)}{f_{C,LG}} - (1 - \xi) \cdot LG_L \quad [\text{Eq. 61}]$$

where CL_L is the cellulose content of live plant dry matter (g m^{-2}); $f_{C,LG}$ is the fractional carbon content of lignin (0.64 C g^{-1}); HC_L is the hemicellulose content of live plant dry matter (g m^{-2}); and LG_L is the lignin content of live plant dry matter (g m^{-2}).

The fraction of new growth partitioned towards live shoot dry matter (τ_{SH} , $\text{g}^{-1} \text{ d}^{-1}$) was given as:

$$\tau_{\text{SH}} = \frac{(f_{C,CP} \cdot CP_G + C_{\text{AVAIL}}) / (C_{\text{AVAIL}} + f_{C,CP} \cdot U_{N,\text{OPT}} / f_{N,CP})}{1 + (f_{N,L} \cdot C_{\text{FIX}}) / (f_{C,L} \cdot U_{N,\text{OPT}})} \quad [\text{Eq. 62}]$$

where C_{FIX} is the carbon assimilation rate ($\text{g C m}^{-2} \text{ d}^{-1}$, section 3.2.3.4 Eq. 48); $f_{N,L}$ is the fractional nitrogen content of live plant dry matter (N g^{-1} , section 3.2.1 Eq. 24); and $U_{N,\text{OPT}}$ is the optimum nitrogen uptake rate ($\text{g N m}^{-2} \text{ d}^{-1}$, section 3.2.4 Eq. 50).

The accretion rate of root and shoot live plant dry matter ($W_{L,RT,G}$ and $W_{L,SH,G}$, respectively; $\text{g m}^{-2} \text{ d}^{-1}$) were consequently given as:

$$W_{L,RT,G} = (1 - \tau_{\text{SH}}) \cdot (CL_G + CP_G + HC_G + LG_G + SUC_G) \quad [\text{Eq. 63}]$$

$$W_{L,SH,G} = \tau_{\text{SH}} \cdot (CL_G + CP_G + HC_G + LG_G + SUC_G) \quad [\text{Eq. 64}]$$

3.2.7 Litter decomposition

Litter decomposition was predicted by the two-component model described by Kätterer et al. (1998). As such, the relative decomposition rate of dead plant dry matter (k_d , $\text{g}^{-1} \text{ d}^{-1}$) was given as:

$$k_r = 2.1 \frac{T_{\text{soil}} - 30}{10} \quad [\text{Eq. 65}]$$

$$k_d = 0.123 \cdot 0.29 \cdot k_r \cdot e^{-0.29 \cdot k_r} + (1 - 0.123) \cdot 0.0008 \cdot k_r \cdot e^{-0.0008 \cdot k_r} \quad [\text{Eq. 66}]$$

where k_r is temperature response for litter decomposition; and T_{soil} is soil temperature ($^{\circ}\text{C}$, section 3.1.2 Eq. 6).

3.2.8 Initial parameterisation

Starting values (day 1) for plant dry matter were defined using input parameters provided by the user. User inputs include crude protein ($CP\%$, %), metabolizable energy (ME , MJ [kg dry matter]⁻¹) and pasture height (PHT , m). In order to ensure initial parameterisation stays within the bounds of the model assumptions, limits were set on the user inputs, specifically:

$$0 < CP\% < 38 \quad [\text{Eq. 67}]$$

$$ME_{\min} < ME < ME_{\max} \quad [\text{Eq. 68}]$$

$$PHT > 0 \quad [\text{Eq. 69}]$$

where maximum metabolizable energy (ME_{\max} , MJ [kg dry matter]⁻¹) and minimum metabolizable energy (ME_{\min} , MJ [kg dry matter]⁻¹) were given as:

$$ME_{\max} = \begin{cases} 0.0367 \cdot CP\% + 9.356, & 0.0367 \cdot CP\% + 9.356 \geq -0.00046 \cdot CP\%^2 + 0.13 \cdot CP\% + 7.89 \\ -0.00046 \cdot CP\%^2 + 0.13 \cdot CP\% + 7.89, & 0.0367 \cdot CP\% + 9.356 < -0.00046 \cdot CP\%^2 + 0.13 \cdot CP\% + 7.89 \end{cases} \quad [\text{Eq. 70}]$$

$$ME_{\min} = -0.00046 \cdot CP\%^2 + 0.16 \cdot CP\% + 5.312 \quad [\text{Eq. 71}]$$

Neutral detergent fibre (NDF , %) was estimated as:

$$NDF = 37.8 \cdot \sqrt{0.053 \cdot CP\% + 11.5 - ME} - 0.191 \cdot CP\% + 5.97 \quad [\text{Eq. 72}]$$

Acid detergent fibre (ADF , %) was estimated using data presented by Du et al. (2016) and Jung et al. (1997) ($R^2 = 0.86$, $se = 2.67$, $F_{1,26} = 163.32$, $p < 0.0001$):

$$ADF = 7 \cdot e^{0.023 \cdot NDF} \quad [\text{Eq. 73}]$$

Acid detergent lignin (ADL , %) was estimated using data presented by Delagarde et al. (2000), Du et al. (2016) and Jung et al. (1997) ($R^2 = 0.70$, $se = 0.65$, $F_{1,69} = 158.37$, $p < 0.0001$):

$$ADL = 0.31 \cdot e^{0.037 \cdot NDF} \quad [\text{Eq. 74}]$$

The starting value for shoot dry matter (W_{SH} , g m⁻²) was estimated by resolving the relationship between pasture height and leaf area index described by Byrne et al. (2005):

$$W_{SH} = \frac{8.7 \cdot PHT}{SLA \cdot f_{lam}} \quad [\text{Eq. 75}]$$

where f_{lam} is the lamina fraction of shoot dry matter (0.7 g⁻¹; Thornley and Verberne, 1989); and SLA is specific leaf area (0.02 m² g⁻¹; Arrendondo and Schnyder, 2003).

The live fraction of shoot dry matter ($f_{L,SH}$, g⁻¹) ($R^2 = 0.72$, $se = 0.04$, $F_{1,1128} = 2953.44$, $p < 0.0001$) was estimated as:

$$f_{L,SH} = 0.2 + 0.036 \cdot (100 - NDF - CP\%) \quad [\text{Eq. 76}]$$

The live fraction of root dry matter ($f_{L,RT}$, g⁻¹) ($R^2 = 0.87$, $se = 0.04$, $F_{1,1128} = 7781.10$, $p < 0.0001$) was estimated as:

$$f_{L,RT} = 0.026 \cdot (100 - NDF) \quad [\text{Eq. 77}]$$

The shoot fraction of plant dry matter (f_{SH} , g^{-1}) was consequently estimated as:

$$f_{SH} = \frac{f_{L,SH}}{f_{L,SH} + f_{L,RT}} \quad [\text{Eq. 78}]$$

Consequently, the initial (day 1) value of dead ($W_{D,SH}$, $g\ m^{-2}$) and live ($W_{L,SH}$, $g\ m^{-2}$) shoot dry matter, as well as dead ($W_{D,RT}$, $g\ m^{-2}$) and live ($W_{L,RT}$, $g\ m^{-2}$) root dry matter, were given as:

$$W_{D,SH} = (1 - f_{L,SH}) \cdot W_{SH} \quad [\text{Eq. 79}]$$

$$W_{L,SH} = f_{L,SH} \cdot W_{SH} \quad [\text{Eq. 80}]$$

$$W_{D,RT} = (1 - f_{L,RT}) \cdot \left(\frac{W_{SH}}{f_{SH}} - W_{SH} \right) \quad [\text{Eq. 81}]$$

$$W_{L,RT} = f_{L,RT} \cdot \left(\frac{W_{SH}}{f_{SH}} - W_{SH} \right) \quad [\text{Eq. 82}]$$

The initial (day 1) crude protein content of dead (CP_D , $g\ m^{-2}$) and live (CP_L , $g\ m^{-2}$) plant dry matter were given as:

$$CP_D = (W_{D,RT} + W_{D,SH}) \cdot \frac{CP\%}{CP\% + NDF} \quad [\text{Eq. 83}]$$

$$CP_L = \frac{CP\% \cdot W_{SH}}{100 \cdot f_{SH}} - CP_D \quad [\text{Eq. 84}]$$

The initial (day 1) sucrose content of plant dry matter (SUC , $g\ m^{-2}$) was given as:

$$SUC = W_{SH} \cdot \frac{100 - NDF - CP\%}{100 \cdot f_{SH}} \quad [\text{Eq. 85}]$$

The initial (day 1) lignin content of live (LG_L , $g\ m^{-2}$) and dead (LG_D , $g\ m^{-2}$) plant dry matter were estimated as:

$$LG_L = (W_{L,RT} + W_{L,SH}) \cdot 0.0031 \cdot e^{3.7 \cdot \frac{W_{L,RT} + W_{L,SH} - CP_L - SUC}{W_{L,RT} + W_{L,SH}}} \quad [\text{Eq. 86}]$$

$$LG_D = \frac{W_{SH} \cdot ADL}{100 \cdot f_{SH}} - LG_L \quad [\text{Eq. 87}]$$

The initial (day 1) cellulose content of live (CL_L , $g\ m^{-2}$) and dead (CL_D , $g\ m^{-2}$) plant dry matter were estimated as:

$$CL_L = (W_{L,RT} + W_{L,SH}) \cdot 0.07 \cdot e^{2.3 \cdot \frac{W_{L,RT} + W_{L,SH} - CP_L - SUC}{W_{L,RT} + W_{L,SH}}} - LG_L \quad [\text{Eq. 88}]$$

$$CL_D = \frac{W_{SH} \cdot (ADF - ADL)}{100 \cdot f_{SH}} - CL_L \quad [\text{Eq. 89}]$$

Finally, the initial (day 1) hemicellulose content of dead (HC_D , $g\ m^{-2}$) and live (HC_L , $g\ m^{-2}$) plant dry matter were estimated as:

$$HC_D = W_{D,RT} + W_{D,SH} - CP_D - LG_D - CL_D \quad [\text{Eq. 90}]$$

$$HC_L = W_{L,RT} + W_{L,SH} - CP_L - SUC - LG_L - CL_L \quad [\text{Eq. 91}]$$

3.2.9 Rates of change

The rate of change for dead root ($\frac{dW_{D,RT}}{dt}$, g m⁻² d⁻¹) and shoot ($\frac{dW_{D,SH}}{dt}$, g m⁻² d⁻¹) dry matter were given by the following differential equations:

$$\frac{dW_{D,RT}}{dt} = \xi \cdot W_{L,RT} - k_d \cdot W_{D,RT} \quad [\text{Eq. 92}]$$

$$\frac{dW_{D,SH}}{dt} = \xi \cdot W_{L,SH} - k_d \cdot W_{D,SH} - DMI_{PM} \cdot \frac{W_{D,SH}}{W_{D,SH} + W_{L,SH}} \quad [\text{Eq. 93}]$$

where DMI_{PM} is pasture mass dry matter intake of a grazing population (g m⁻² d⁻¹, section 3.9.5); k_d is the relative decomposition rate of dead plant dry matter (g⁻¹ d⁻¹, section 3.2.7

Eq. 66); $W_{D,RT}$ and $W_{D,SH}$ are dead root and shoot dry matter (g m⁻²), respectively; $W_{L,RT}$ and $W_{L,SH}$ are live root and shoot dry matter (g m⁻²), respectively; and ξ is the relative senescence rate (g⁻¹ d⁻¹, section 3.2.5 Eq. 52).

The rate of change for the cellulose ($\frac{dCL_D}{dt}$, g m⁻² d⁻¹), crude protein ($\frac{dCP_D}{dt}$, g m⁻² d⁻¹), hemicellulose ($\frac{dHC_D}{dt}$, g m⁻² d⁻¹) and lignin ($\frac{dLG_D}{dt}$, g m⁻² d⁻¹) components of dead plant dry matter were given as:

$$\frac{dx_D}{dt} = \xi \cdot x_L - k_d \cdot x_D - DMI_{PM} \cdot \frac{W_{D,SH}}{W_{D,SH} + W_{L,SH}} \cdot \frac{x_D}{W_D} \quad [\text{Eq. 94}]$$

where W_D is dead plant dry matter (g m⁻², section 3.2.1 Eq. 19); x_D is either the cellulose (CL_D , g m⁻²), crude protein (CP_D , g m⁻²), hemicellulose (HC_D , g m⁻²) or lignin (LG_D , g m⁻²) component of dead plant dry matter when calculating the rate of change for each component respectively; and x_L is either the cellulose (CL_L , g m⁻²), crude protein (CP_L , g m⁻²), hemicellulose (HC_L , g m⁻²) or lignin (LG_L , g m⁻²) component of live plant dry matter when calculating the rate of change for each dead component respectively.

The rate of change for live root ($\frac{dW_{L,RT}}{dt}$, g m⁻² d⁻¹) and shoot ($\frac{dW_{L,SH}}{dt}$, g m⁻² d⁻¹) dry matter was given by the following differential equations:

$$\frac{dW_{L,RT}}{dt} = W_{L,RT,G} - \xi \cdot W_{L,RT} \quad [\text{Eq. 95}]$$

$$\frac{dW_{L,SH}}{dt} = W_{L,SH,G} - \xi \cdot W_{L,SH} - DMI_{PM} \cdot \frac{W_{L,SH}}{W_{D,SH} + W_{L,SH}} \quad [\text{Eq. 96}]$$

where $W_{L,RT,G}$ is the accretion rate of live root dry matter (g m⁻² d⁻¹, section 3.2.6 Eq. 63); and $W_{L,SH,G}$ is the accretion rate of live shoot dry matter (g m⁻² d⁻¹, section 3.2.6 Eq. 64).

The rate of change for the cellulose ($\frac{dCL_L}{dt}$, g m⁻² d⁻¹), crude protein ($\frac{dCP_L}{dt}$, g m⁻² d⁻¹), hemicellulose ($\frac{dHC_L}{dt}$, g m⁻² d⁻¹) and lignin ($\frac{dLG_L}{dt}$, g m⁻² d⁻¹) components of live plant dry matter were given as:

$$\frac{dx_L}{dt} = x_G - \xi \cdot x_L - DMI_{PM} \cdot \frac{W_{L,SH}}{W_{D,SH} + W_{L,SH}} \cdot \frac{x_L}{W_L} \quad [\text{Eq. 97}]$$

where W_L is live plant dry matter (g m⁻², section 3.2.1 Eq. 20); x_G is either the accretion of cellulose (CL_G , g m⁻² d⁻¹, section 3.2.6 Eq. 59), crude protein (CP_G , g m⁻² d⁻¹, section 3.2.6 Eq. 55), hemicellulose (HC_G , g m⁻² d⁻¹, section 3.2.6 Eq. 60) or lignin (LG_G , g m⁻² d⁻¹, section 3.2.6 Eq. 61) when calculating the rate of change for each live component respectively.

Finally, the rate of change for the sucrose component of live plant dry matter ($\frac{dSUC}{dt}$, $\text{g m}^{-2} \text{d}^{-1}$) was given as:

$$\frac{dSUC}{dt} = SUC_G - DMI_{PM} \cdot \frac{W_{L,SH}}{W_{D,SH} + W_{L,SH}} \cdot \frac{SUC}{W_L} \quad [\text{Eq. 98}]$$

where SUC is the sucrose component of live plant dry matter (g m^{-2}); and SUC_G is the accretion of sucrose ($\text{g m}^{-2} \text{d}^{-1}$, section 3.2.6 Eq. 54).

3.2.10 Descriptors

3.2.10.1 Composition

Neutral detergent fibre (NDF , %) is a measure of the fibrous (i.e. cellulose, hemicellulose and lignin) structural components of plant matter. As such, NDF was calculated as:

$$NDF = \frac{CL_L + HC_L + LG_L + CL_D + HC_D + LG_D}{W_L + W_D} \cdot 100 \quad [\text{Eq. 99}]$$

where CL_D , HC_D and LG_D are the cellulose, hemicellulose and lignin components of dead plant dry matter (g m^{-2}), respectively; CL_L , HC_L and LG_L are the cellulose, hemicellulose and lignin components of live plant dry matter (g m^{-2}), respectively; W_D is dead plant dry matter (g m^{-2} , section 3.2.1 Eq. 19); and W_L is live plant dry matter (g m^{-2} , section 3.2.1 Eq. 20).

Acid detergent fibre (ADF , %) is a measure of the cellulose and lignin structural components of plant matter. Hence, ADF was calculated as:

$$ADF = \frac{CL_L + LG_L + CL_D + LG_D}{W_L + W_D} \cdot 100 \quad [\text{Eq. 100}]$$

Acid detergent lignin (ADL , %) is a measure of the lignin structural component of plant matter. Thus, ADL was calculated as:

$$ADL = \frac{LG_L + LG_D}{W_L + W_D} \cdot 100 \quad [\text{Eq. 101}]$$

The percentage crude protein content of plant dry matter ($CP\%$, %) was given as:

$$CP\% = \frac{CP_L + CP_D}{W_L + W_D} \cdot 100 \quad [\text{Eq. 102}]$$

where CP_D and CP_L are the crude protein content of dead and live plant dry matter (g m^{-2}), respectively.

3.2.10.2 Digestibilities

Neutral detergent fibre digestibility ($NDFD$, %) and dry matter digestibility (DMD , %) were estimated in accordance with Goering and Van Soest (1975):

$$NDFD = 147.3 - 78.9 \cdot \log_{10} \left(\frac{ADL}{ADF} \cdot 100 \right) \quad [\text{Eq. 103}]$$

$$DMD = 0.98 \cdot (100 - NDF) + NDF \cdot \left(\frac{NDFD}{100} \right) - 12.9 \quad [\text{Eq. 104}]$$

where ADF is acid detergent fibre (%), section 3.2.10.1 Eq. 100); ADL is acid detergent lignin (%), section 3.2.10.1 Eq. 101); and NDF is neutral detergent fibre (%), section 3.2.10.1 Eq. 99).

Dry organic matter digestibility (*DOMD*, %) was estimated in accordance with the Australian Fodder Industry Association (2014):

$$DOMD = \frac{ME+3.001}{0.203} \quad [\text{Eq. 105}]$$

where *ME* is metabolizable energy (MJ [kg dry matter]⁻¹, section 3.2.10.3 Eq. 107).

3.2.10.3 Gross energy and metabolizable energy

Gross energy (*GE*, MJ [kg dry matter]⁻¹) was given as:

$$GE = 10 \cdot \left(-\Delta H_{c_{CL}}^{\theta} \cdot (NDF - ADL) - \Delta H_{c_{CP}}^{\theta} \cdot CP\% - \Delta H_{c_{LG}}^{\theta} \cdot ADL - \Delta H_{c_{SUC}}^{\theta} \cdot (100 - NDF - CP\%) \right) \quad [\text{Eq. 106}]$$

where *ADL* is acid detergent lignin (%; section 3.2.10.1 Eq. 101); *CP%* is the percentage crude protein content of plant dry matter (%; section 3.2.10.1 Eq. 102); *NDF* is neutral detergent fibre (%; section 3.2.10.1 Eq. 99); $\Delta H_{c_{CL}}^{\theta}$ is the heat of combustion for cellulose (-0.017457 MJ g⁻¹); $\Delta H_{c_{CP}}^{\theta}$ is the heat of combustion for crude protein (-0.0236 MJ g⁻¹; Benedict and Osborne, 1907); $\Delta H_{c_{LG}}^{\theta}$ is the heat of combustion for lignin (-0.0239 MJ g⁻¹); and $\Delta H_{c_{SUC}}^{\theta}$ is the heat of combustion for sucrose (-0.016506 MJ g⁻¹).

In the absence of an animal model determining the energy lost in faeces, urine and gastrointestinal gas, metabolizable energy (*ME*, MJ [kg dry matter]⁻¹) was calculated as:

$$ME = 0.82 \cdot \frac{DMD}{100} \cdot GE \quad [\text{Eq. 107}]$$

where *DMD* is dry matter digestibility (%; section 3.2.10.2 Eq. 104).

3.2.10.4 Pasture height and mass

Pasture height (*PHT*, m) was calculated as (Byrne *et al.*, 2005):

$$PHT = \frac{SLA \cdot f_{lam} \cdot (W_{D,SH} + W_{L,SH})}{8.7} \quad [\text{Eq. 108}]$$

where *f_{lam}* is the lamina fraction of shoot dry matter (0.7 g⁻¹; Thornley and Verberne, 1989); *SLA* is specific leaf area (0.02 m² g⁻¹; Arrendondo and Schnyder, 2003); and *W_{D,SH}* and *W_{L,SH}* are dead and live shoot dry matter (g m⁻²), respectively.

The total pasture mass of shoot dry matter (*PM_{SH}*, kg dry matter ha⁻¹) was given as:

$$PM_{SH} = 10 \cdot (W_{D,SH} + W_{L,SH}) \quad [\text{Eq. 109}]$$

The total pasture mass of shoot dry matter available for grazing (*PM_{SH,A}*, kg dry matter ha⁻¹) was calculated by taking into account the dry matter intake constraint described by Vera *et al.* (1977), such that:

$$PM_{SH,A} = PM_{SH} - 399 \cdot (1 - e^{-0.002503 \cdot PM_{SH}}) \quad [\text{Eq. 110}]$$

3.3 Soil

The soil model requires user input for soil textural type (section 3.3.2.1 Table 2) which were defined in accordance with the USDA, and the initial (day 1) inorganic soil nitrogen content ($N_{S,1}$, mg kg⁻¹) which can be obtained by sending a soil sample for laboratory testing.

3.3.1 Nitrogen

The starting (day 1) soil inorganic nitrogen content (N_S , g N m⁻²) was estimating as:

$$N_S = \frac{N_{S,1}}{10} \quad [\text{Eq. 111}]$$

where $N_{S,1}$ is the user input for inorganic soil nitrogen (mg kg⁻¹).

Soil inorganic nitrogen content (N_S , g N m⁻²) was assumed to be influenced by the nitrogen uptake rate (U_N , g N m⁻² d⁻¹, section 3.2.4 Eq. 51), the excretion of nitrogen via faeces and urine by any grazing population (N_{EXC} , g N m⁻² d⁻¹, section 3.9.5) and the relative decomposition rate of dead plant dry matter (k_d , g⁻¹ d⁻¹, section 3.2.7 Eq. 66). As such, the rate of change for soil inorganic nitrogen content ($\frac{dN_S}{dt}$, g N m⁻² d⁻¹) was given as:

$$\frac{dN_S}{dt} = k_d \cdot f_{N,CP} \cdot CP_D - U_N + N_{EXC} \quad [\text{Eq. 112}]$$

where CP_D is the crude protein content of dead plant dry matter on day 1 (g m⁻², section 3.2.8 Eq. 83); and $f_{N,CP}$ is the fractional nitrogen content of crude protein (0.16 N g⁻¹).

3.3.2 Hydrology

3.3.2.1 Water stress

The availability of water from soil was assumed to impact upon numerous processes. The hydraulic properties of soil include 'air-dry' (AD , m³ water [m³ soil]⁻¹), wilting point (WP , m³ water [m³ soil]⁻¹), field capacity (FC , m³ water [m³ soil]⁻¹) and saturation (SAT , m³ water [m³ soil]⁻¹). Values for AD , WP , FC and SAT were calculated in accordance with Saxton et al. (1986) such that they vary across soil textural types (Table 2).

Plant available water was defined as the water held in soil between FC and WP ; whereas biologically available water was defined as the water held in soil between FC and AD . As such, the stress constraints associated with plant available water (Ω_{PAW}) and biologically available water (Ω_{BAW}) were given as per Allen et al. (2005):

$$\Omega = \begin{cases} 0, & SWC_{vol} \leq x \\ \frac{SWC_{vol} - x}{0.6 \cdot (FC - WP) + WP - x}, & x < SWC_{vol} < 0.6 \cdot (FC - WP) + WP \\ 1, & SWC_{vol} \geq 0.6 \cdot (FC - WP) + WP \end{cases} \quad [\text{Eq. 113}]$$

where SWC_{vol} is volumetric soil water content (m³ water [m³ soil]⁻¹); and x is either WP or AD for the calculation of Ω_{PAW} and Ω_{BAW} , respectively.

Table 2. Hydraulic properties across soil textural type; including ‘air-dry’ (*AD*, m³ water [m³ soil]⁻¹), wilting point (*WP*, m³ water [m³ soil]⁻¹), field capacity (*FC*, m³ water [m³ soil]⁻¹) and saturation (*SAT*, m³ water [m³ soil]⁻¹).

Soil texture	Sand (%)	Silt (%)	Clay (%)	<i>AD</i>	<i>WP</i>	<i>FC</i>	<i>SAT</i>
Clay	19.5	17.5	63	0.27	0.37	0.49	0.55
Clay loam	32.5	33.5	34	0.10	0.19	0.33	0.50
Generic	40.5	34	25.5	0.07	0.14	0.28	0.48
Loam	41	40	19	0.05	0.12	0.26	0.47
Loamy sand	82	12	6	0.03	0.07	0.15	0.37
Sand	91.5	5	3.5	0.02	0.05	0.12	0.34
Sandy clay	51.5	7	41.5	0.16	0.23	0.32	0.50
Sandy clay loam	60	13	27	0.10	0.16	0.25	0.47
Sandy loam	64.5	25	10.5	0.04	0.09	0.20	0.42
Silt	7.5	87	5.5	0.03	0.10	0.31	0.42
Silty clay	6.5	47	46.5	0.16	0.27	0.43	0.54
Silty clay loam	10	56	34	0.09	0.19	0.36	0.52
Silt loam	21.5	65	13.5	0.03	0.10	0.28	0.46

3.3.2.2 Evapotranspiration

Aerodynamic resistance (r_a , s m⁻¹) was estimated in accordance with Allen et al. (1998):

$$r_a = \frac{\ln\left(\frac{z - \frac{2}{3}PHT}{0.123 \cdot PHT}\right) \cdot \ln\left(\frac{z - \frac{2}{3}PHT}{0.0123 \cdot PHT}\right)}{0.1681 \cdot u_2} \quad [\text{Eq. 114}]$$

where *PHT* is pasture height (m, section 3.2.10.4 Eq. 108); and u_2 is wind speed measured at 2m above ground level (m s⁻¹, section 3.1.10 Eq. 18).

The evaporation rate (E_v , mm d⁻¹) was consequently estimated by amending the Penman equation to account for fractional ground cover (f_g , m², section 3.2.2 Eq. 25) and the water stress constraint associated with biologically available water (Ω_{BAW} , section 3.3.2.1 Eq. 113):

$$E_v = \frac{\Delta \cdot R_n + 86,400 \cdot \rho_a \cdot c_p \cdot \frac{e_s - e_a}{r_a}}{\lambda \cdot [\Delta + \gamma]} \cdot (1 - f_g) \cdot \Omega_{BAW} \quad [\text{Eq. 115}]$$

where c_p is the specific heat capacity of dry air (1.013 · 10⁻³ MJ kg⁻¹ °C⁻¹); e_a is vapour pressure (kPa); e_s is saturation vapour pressure (kPa, section 3.1.5 Eq. 9); R_n is net radiation (MJ m⁻² d⁻¹, section 3.1.9 Eq. 17); γ is the psychrometric constant (kPa °C⁻¹, section 3.1.7 Eq. 11); Δ is slope of the saturation vapour pressure curve (kPa °C⁻¹, section 3.1.8 Eq. 12); λ is the latent heat of vaporization (2.453 MJ kg⁻¹); and ρ_a is mean daily dry air density (kg m⁻³, section 3.1.6 Eq. 10).

Canopy surface resistance (r_s , s m⁻¹) was estimated by resolving the function described by Allen et al. (2006):

$$r_s = \frac{30 \cdot (SLA \cdot f_{lam} \cdot (W_{D,SH} + W_{L,SH}) + 4)}{SLA \cdot f_{lam} \cdot (W_{D,SH} + W_{L,SH})} \quad [\text{Eq. 116}]$$

where f_{lam} is the lamina fraction of shoot dry matter (0.7 g⁻¹; Thornley and Verberne, 1989); *SLA* is specific leaf area (0.02 m² g⁻¹; Arrendondo and Schnyder, 2003); and $W_{D,SH}$ and $W_{L,SH}$ are dead and live shoot dry matter (g m⁻²), respectively.

The transpiration rate (E_T , mm d⁻¹) was consequently estimated by amending the Penman-Monteith equation to account for fractional ground cover (f_g , m², section 3.2.2 Eq. 25) and the water stress constraint associated with plant available water (Ω_{PAW} , section 3.3.2.1 Eq. 113):

$$E_T = \frac{\Delta \cdot R_n + 86,400 \cdot \rho_a \cdot c_p \frac{e_s - e_a}{r_a}}{\lambda \cdot \left[\Delta + \gamma \cdot \left(1 + \frac{r_s}{r_a} \right) \right]} \cdot f_g \cdot \frac{W_{L,SH}}{W_{D,SH} + W_{L,SH}} \cdot \Omega_{PAW} \quad [\text{Eq. 117}]$$

3.3.2.3 Volumetric soil water content

The initial volumetric soil water content on day 1 (SWC_{vol} , m³ water [m³ soil]⁻¹) was assumed to be equal to field capacity (FC , m³ water [m³ soil]⁻¹, section 3.3.2.1 Table 2). The rate of change for volumetric soil water content ($\frac{dSWC_{vol}}{dt}$, m³ water [m³ soil]⁻¹) was given as:

$$\frac{dSWC_{vol}}{dt} = \begin{cases} \frac{PCP - (E_T + E_V)}{1000}, & SAT \geq \frac{PCP - (E_T + E_V)}{1000} + SWC_{vol} \\ SAT - SWC_{vol}, & SAT < \frac{PCP - (E_T + E_V)}{1000} + SWC_{vol} \end{cases} \quad [\text{Eq. 118}]$$

where E_T is transpiration rate (mm d⁻¹, section 3.3.2.2 Eq. 117); E_V is evaporation rate (mm d⁻¹, section 3.3.2.2 Eq. 115); and PCP is precipitation (mm d⁻¹).

3.3.2.4 Gravimetric soil water content

The bulk density of soil (ρ_b , kg m⁻³) was estimated as:

$$\rho_b = (1 - SAT) \cdot \rho_p \quad [\text{Eq. 119}]$$

where SAT is the volumetric soil water content at saturation (m³ water [m³ soil]⁻¹, section 3.3.2.1 Table 2); and ρ_p is the particle density of soil (2,650 kg m⁻³).

The gravimetric soil water content (SWC_g , g water [g soil]⁻¹) was consequently calculated assuming water has a density of 1,000 kg m⁻³, such that:

$$SWC_g = \frac{SWC_{vol} \cdot 1000}{SWC_{vol} \cdot 1000 + \rho_b} \quad [\text{Eq. 120}]$$

where SWC_{vol} is volumetric soil water content (m³ water [m³ soil]⁻¹, section 3.3.2.3).

3.4 Nematode ecology

The nematode ecology model requires user input for pasture infectivity (larvae [kg dry matter]⁻¹) and paddock size (ha) in order to define the initial values associated with the number of infective larvae in soil (L_{3s}) and on herbage (L_{3h}) for each nematode species (section 3.4.2.3). A schematic diagram of the nematode ecology model is provided in Fig. 2. The model framework is based on the general lifecycle of the free-living stages of trichostrongylid gastrointestinal nematodes, where the survival within and transition between lifecycle stages was assumed to be regulated by the conditions experienced at each microclimatic station (i.e. faeces, soil and herbage).

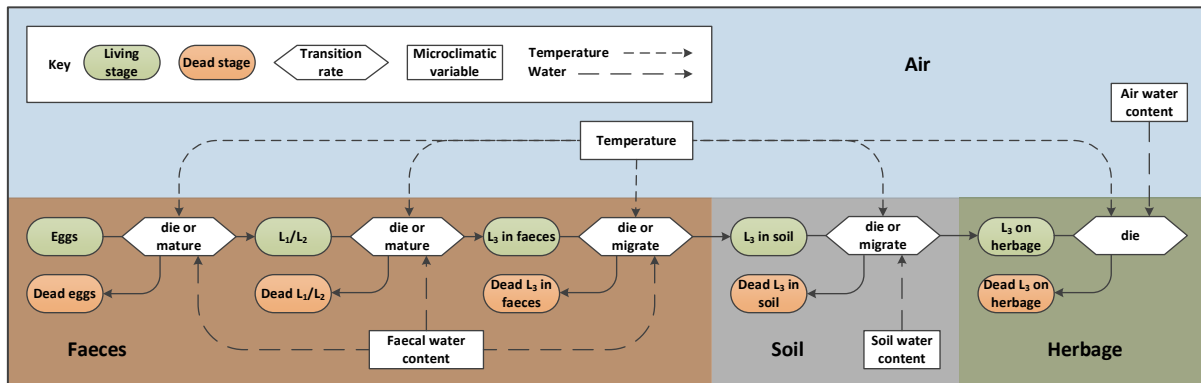


Figure 2. Schematic diagram of the free-living stages of the nematode lifecycle; including the impact of temperature and water availability on the transition rates (survival and maturation or migration) of each lifecycle stage. L_1/L_2 = first- and second-stage larvae; L_3 = third-stage larvae.

3.4.1 Microclimatic variables

Temperature and water availability are the two most important variables controlling the development, migration and survival of the free-living stages of the nematode lifecycle (Thomas, 1982). Daily mean air temperature has previously been shown to be significantly associated with the development of the free-living stages on nematodes on pasture (Reynecke et al., 2011a). Consequently, daily mean air temperature (T_{mean} , °C, section 3.1.2 Eq. 5) was used as the temperature variable influencing the dynamics of the free-living stages of the nematode lifecycle regardless of microclimatic station.

Water availability is a key determinant of the development success of the free-living stages of the nematode lifecycle (Levine and Todd, 1975). A variety of meteorological variables associated with water availability have previously been identified as impacting upon the dynamics of the free-living stages of the nematode lifecycle. These include rainfall (O'Connor et al., 2007), relative humidity (Beveridge et al., 1989; Pandey et al., 1993) and evapotranspiration (O'Connor et al., 2008). However, such factors exert their impact on free-living nematodes through the modulation of faecal and soil water content (Khadijah et al., 2013). As such, the gravimetric water content of faeces, soil and air were chosen as the most directly appropriate variables representing the water availability of each microclimatic station.

3.4.1.1 Faecal water content

Faecal water mass (FWM , g) on the day of faecal deposition was calculated in accordance with Wilson and Dudzinski (1973) ($R^2 = 0.94$), such that:

$$FWM = -64 + 1.207 \cdot FDM + 0.00216 \cdot FDM^2 \quad [\text{Eq. 121}]$$

where FDM is faecal dry matter (g, section 3.6.11 Eq. 275).

Hence, the wet faecal mass (WFM , g) and gravimetric faecal water content (FWC_g , %) on the day of faecal deposition were calculated as:

$$WFM = FWM + FDM \quad [\text{Eq. 122}]$$

$$FWC_g = 100 \cdot \frac{FWM}{WFM} \quad [\text{Eq. 123}]$$

The rate of change for gravimetric faecal water content ($\frac{dFWC_g}{dt}$, % d⁻¹) was given by the following differential equation ($R^2 = 0.95$, $se = 6.29$, $F_{1,928} = 18505.25$, $p < 0.0001$):

$$\frac{dFWC_g}{dt} = \left(0.88 \cdot (FWC_g - FWC_{g,\min}) \cdot \left(\frac{FWC_g}{80}\right)^{\nu_{FWC}} + FWC_{g,\min} + \alpha_{FWC}\right) - FWC_g \quad [\text{Eq. 124}]$$

where $FWC_{g,\min}$ is the minimum gravimetric faecal water content (7%); and ν_{FWC} (skew in growth rate) and α_{FWC} (rainfall adjustment) are given as:

$$\nu_{FWC} = \frac{8.56}{1 + e^{-2.43 \cdot (T_{\text{mean}} - 31)}} + 0.44 \quad [\text{Eq. 125}]$$

$$\alpha_{FWC} = (\beta_{FWC} \cdot (0.305625 \cdot PCP)^2 + \gamma_{FWC} \cdot 0.305625 \cdot PCP) \cdot e^{-\delta_{FWC} \cdot D} \quad [\text{Eq. 126}]$$

where D is days post-deposition; PCP is precipitation (mm d⁻¹); T_{mean} is the daily mean air temperature (°C, section 3.1.2 Eq. 5); and the coefficients β_{FWC} , γ_{FWC} and δ_{FWC} were given as:

$$\beta_{FWC} = -2 \cdot T_{\text{mean}} + 27 \quad [\text{Eq. 127}]$$

$$\gamma_{FWC} = 15 \cdot e^{0.05 \cdot T_{\text{mean}}} \quad [\text{Eq. 128}]$$

$$\delta_{FWC} = 0.09 \cdot e^{0.02 \cdot T_{\text{mean}}} \quad [\text{Eq. 129}]$$

The predicted rate of change for gravimetric faecal water content (% d⁻¹, Eq.124) could potentially result in gravimetric faecal water contents greater than 100%, consequently a maximum constraint was imposed such that:

$$FWC_g = \begin{cases} FWC_g, & \text{for } FWC_g \leq FWC_{g,\max} \\ FWC_{g,\max}, & \text{for } FWC_g > FWC_{g,\max} \end{cases} \quad [\text{Eq. 130}]$$

where $FWC_{g,\max}$ is the maximum gravimetric faecal water content (91.37%).

3.4.1.2 Soil water content

Gravimetric soil water content (SWC_g , g water [g soil]⁻¹) is provided as an output of the pasture model (section 3.3.2.4 Eq. 120). However, gravimetric soil water content does not account for the differences in biologically available water across soil textural types. Further, third-stage infective larvae are present within faeces and soil as well as on herbage. To account for discrepancies

between the biologically available water across soil textural types and microclimates, adjusted gravimetric soil water content ($SWC_{g,adj}$, %) was given as:

$$SWC_{g,adj} = (FWC_{g,max} - FWC_{g,min}) \cdot \frac{(1000 \cdot SAT + \rho_b) \cdot (1000 \cdot AD \cdot SWC_g + \rho_b \cdot SWC_g - 1000 \cdot AD)}{1000 \cdot \rho_b \cdot (SAT - AD)} + FWC_{g,min} \quad [\text{Eq. 131}]$$

where AD is the volumetric soil water content when soil is 'air-dry' (m^3 water $[\text{m}^3 \text{soil}]^{-1}$, section 3.3.2.1 Table 2); $FWC_{g,max}$ is the maximum gravimetric faecal water content (91.37%); $FWC_{g,min}$ is the minimum gravimetric faecal water content (7%); SAT is the volumetric soil water content at saturation (m^3 water $[\text{m}^3 \text{soil}]^{-1}$, section 3.3.2.1 Table 2); and ρ_b is the bulk density of soil (kg m^{-3} , section 3.3.2.4 Eq. 119).

3.4.1.3 Air water content

Gravimetric air water content (AWC_g , g water $[\text{g air}]^{-1}$) was given as:

$$AWC_g = \frac{e_a}{e_s} \quad [\text{Eq.132}]$$

where e_a is vapour pressure (kPa); and e_s is saturation vapour pressure (kPa, section 3.1.5 Eq. 9).

However, to account for discrepancies between the biologically available water across microclimates, adjusted gravimetric air water content ($AWC_{g,adj}$, %) was given as:

$$AWC_{g,adj} = (FWC_{g,max} - FWC_{g,min}) \cdot AWC_g + FWC_{g,min} \quad [\text{Eq. 133}]$$

where $FWC_{g,max}$ is the maximum gravimetric faecal water content (91.37%); and $FWC_{g,min}$ is the minimum gravimetric faecal water content (7%).

3.4.2 Free-living stages of the nematode lifecycle

The nematode ecology model framework is based on the general lifecycle of the free-living stages of trichostrongylid gastrointestinal nematodes. In brief, eggs (E) mature to third-stage infective larvae in faeces ($L3_f$) via the pre-infective larval stages (L). Infective larvae in faeces migrate into soil ($L3_s$) and then onto herbage ($L3_h$).

3.4.2.1 Rates of change

The rate of change for the egg ($\frac{dE}{dt}$, eggs d^{-1}), pre-infective larvae ($\frac{dL}{dt}$, larvae d^{-1}), infective larvae in faeces ($\frac{dL3_f}{dt}$, larvae d^{-1}), infective larvae in soil ($\frac{dL3_s}{dt}$, larvae d^{-1}) and infective larvae on herbage ($\frac{dL3_h}{dt}$, larvae d^{-1}) stages were given by the following differential equations:

$$\frac{dE}{dt} = -((1 - s_E) + \delta_E) \cdot E \quad [\text{Eq. 134}]$$

$$\frac{dL}{dt} = -((1 - s_L) + \delta_L) \cdot L + \delta_E \cdot E \quad [\text{Eq. 135}]$$

$$\frac{dL3_f}{dt} = -((1 - s_{L3,f}) + \delta_{L3,f}) \cdot L3_f + \delta_L \cdot L \quad [\text{Eq. 136}]$$

$$\frac{dL3_s}{dt} = -((1 - s_{L3,s}) + \delta_{L3,s}) \cdot L3_s + \delta_{L3,f} \cdot L3_f \quad [\text{Eq. 137}]$$

$$\frac{dL3_h}{dt} = -(1 - s_{L3,h}) \cdot L3_h + \delta_{L3,s} \cdot L3_s - L3_{h,in} \quad [\text{Eq. 138}]$$

where E is eggs; L is pre-infective larvae; $L3_f$ is infective larvae in faeces; $L3_s$ is infective larvae in soil; $L3_h$ is infective larvae on herbage; $L3_{h,in}$ is the infective larvae intake of any grazing population (larvae d^{-1} , section 3.9.5); s is the survival rate for each respective microclimatic lifecycle stage (d^{-1}); and δ is the maturation or migration rate for each respective microclimatic lifecycle stage (d^{-1}).

It should be noted that this model considers the rates of change associated with the free-living stages arising from eggs deposited on any given day. Given that the current gravimetric faecal water content will differ across deposition days (section 3.4.1.1), the egg (E), pre-infective larvae (L) and infective larvae in faeces ($L3_f$) stages of each nematode species were calculated separately for each day of deposition. In contrast the infective larvae in soil ($L3_s$) and on herbage ($L3_h$) for each nematode species were calculated irrespective of the day on which the earlier lifecycle stages were deposited onto pasture. As such, the contribution of migrating larvae to the infective larvae in soil ($L3_s$) pool of each nematode species was given as the sum of all previous depositions.

3.4.2.2 Transition rates

The microclimatic lifecycle stage specific survival rates (s , d^{-1}) and maturation or migration rates (δ , d^{-1}) were considered to be a function of both temperature and water availability. The interaction between transition rates and temperature or water availability was described using a modified β -distribution function, given as (Laurenson and Kahn, 2018):

$$\beta(x, a, b, c, d) = \frac{1}{\left(\frac{a}{a+b}\right)^a \cdot \left(1 - \frac{a}{a+b}\right)^b} \cdot \left(\frac{x-c}{d-c}\right)^a \cdot \left(1 - \frac{x-c}{d-c}\right)^b \quad [\text{Eq. 139}]$$

where the β -distribution probability density function was modified such that β is bound between 0 and 1, for a range of values of x bound between c and d . a defines the shape of the distribution relative to c , and b defines the shape of the distribution relative to d .

The impact of daily mean air temperature (T_{mean} , $^{\circ}\text{C}$, section 3.1.2 Eq. 5) and water content (WC , %) on the microclimatic lifecycle stage specific transition rates (y , d^{-1}) was consequently given as:

$$y = \beta(T_{\text{mean}}, a_T, b_T, c_T, d_T) \cdot \beta(WC, a_{WC}, b_{WC}, c_{WC}, d_{WC}) \cdot y_{\text{max}} \quad [\text{Eq. 140}]$$

where a , b , c and d are the parameters of the modified β -distribution function associated with the impact of temperature (τ) or water content (wc); and y_{max} is the maximum transition rate (d^{-1}).

Parameters c_T and d_T were set to -10 and 50 ($^{\circ}\text{C}$), respectively (Andersen et al., 1966); whereas parameters c_{WC} and d_{WC} were set to 0 and 100 (%), respectively. The input variable for water content (WC) was given as gravimetric faecal water content (FWC_g , %, section 3.4.1.1) when determining the transition rates associated with the egg (E), pre-infective larvae (L) and infective larvae in faeces ($L3_f$) microclimatic lifecycle stages; adjusted gravimetric soil water content ($SWC_{g,adj}$, %, section 3.4.1.2 Eq. 131) for infective larvae in soil ($L3_s$); and adjusted gravimetric air water content ($AWC_{g,adj}$, %, section 3.4.1.3 Eq. 133) for infective larvae on herbage ($L3_h$).

Parameters a and b of the modified β -distribution function and the maximum rates of survival (s_{max} , d^{-1}) and maturation or migration (δ_{max} , d^{-1}) were derived from available experimental data for *Trichostrongylus colubriformis* ($R^2 = 0.68$, $se = 0.10$, $F_{1,3362} = 6996$, $p < 0.0001$), *Trichostongylus vitrinus* ($R^2 = 0.70$, $se = 0.10$, $F_{1,3394} = 7756$, $p < 0.0001$) and *Teladorsagia circumcincta* ($R^2 = 0.73$, $se = 0.09$, $F_{1,3362} = 8856$, $p < 0.0001$). In the absence of experimental data for *Haemonchus contortus*, parameter estimates were calculated by adjusting the literature estimates detailed by Laurenson and Kahn (2018) in accordance with the deviation between the literature and experimental data estimates for the other species. Parameter estimates are consequently detailed in Table 3.

Table 3. Lifecycle stage specific parameter values for four nematode species, applicable to the calculation of survival (s) and maturation or migration (δ) rates.

Stage	Rate	Parameter	<i>Trichostrongylus colubriformis</i>	<i>Trichostrongylus vitrinus</i>	<i>Teladorsagia circumcincta</i>	<i>Haemonchus contortus</i>
E	s	a_T	0.424	0.100	0.100	0.831
		b_T	0.972	0.798	0.469	0.202
		a_{WC}	0.200	0.207	0.227	0.183
		b_{WC}	0.100	0.100	0.100	0.100
		s_{max}	0.853	0.926	0.863	1.000
	δ	a_T	4.506	5.438	4.178	5.147
		b_T	2.621	4.025	3.395	1.160
		a_{WC}	1.443	0.731	0.156	1.981
		b_{WC}	2.077	0.769	0.835	2.430
		δ_{max}	0.455	0.407	0.344	0.371
L	s	a_T	0.214	0.240	0.100	0.251
		b_T	0.224	0.100	0.105	0.677
		a_{WC}	0.314	0.185	0.175	0.811
		b_{WC}	0.263	0.100	0.100	0.865
		s_{max}	1.000	0.993	0.964	1.000
	δ	a_T	16.981	17.033	16.709	17.439
		b_T	10.008	12.029	10.316	12.633
		a_{WC}	3.052	2.773	1.756	2.729
		b_{WC}	0.962	0.268	0.203	0.568
		δ_{max}	0.404	0.611	0.215	0.355
L3	s	a_T	0.166	0.136	0.272	0.100
		b_T	0.100	0.113	0.100	0.100
		a_{WC}	0.143	0.632	0.117	0.130
		b_{WC}	0.100	0.205	0.100	0.100
		s_{max}	1.000	1.000	1.000	1.000
	δ	a_T	5.073	6.356	4.912	5.401
		b_T	3.191	2.427	5.177	2.339
		a_{WC}	7.716	3.802	6.598	5.157
		b_{WC}	0.565	0.100	2.940	0.945
		δ_{max}	0.351	0.379	0.236	0.150

3.4.2.3 Initial parameterisation

Egg (E), pre-infective larvae (L), and infective larvae in faeces ($L3_f$) for all nematode species were initially set to zero, i.e. it was assumed that the paddock/pasture in question had not recently been grazed.

Starting (day 1) pasture infectivity (INF , larvae [kg dry matter]⁻¹) and paddock size (PS , ha) are provided by user input. As such the total starting number of infective larvae on herbage ($L3_h$) was given as:

$$L3_h = INF \cdot PM_{SH} \cdot PS \quad [\text{Eq. 141}]$$

where PM_{SH} is the total pasture mass of shoot dry matter (kg dry matter ha⁻¹, section 3.2.10.4 Eq. 109).

However, the pasture infectivity input is not species-specific. As such, the following method was used to determine both the number of infective larvae in soil ($L3_{s,i}$) and on herbage ($L3_{h,i}$) for each nematode species:

$$\varphi_i = s_E \cdot \delta_E \cdot s_L \cdot \delta_L \cdot s_{L3,f} \cdot \delta_{L3,f} \cdot s_{L3,s} \quad [\text{Eq. 142}]$$

$$\omega_i = \varphi_i \cdot \delta_{L3,s} \cdot s_{L3,h} \quad [\text{Eq. 143}]$$

$$L3_{h,i} = L3_h \cdot \frac{\omega_i}{\omega_{\text{colu}} + \omega_{\text{vitr}} + \omega_{\text{circ}} + \omega_{\text{cont}}} \quad [\text{Eq. 144}]$$

$$L3_{s,i} = L3_{h,i} \cdot \frac{\varphi_i}{\omega_i} \quad [\text{Eq. 145}]$$

where i is nematode species ($\text{colu} = \textit{Trichostrongylus colubriformis}$, $\text{vitr} = \textit{Trichostrongylus vitrinus}$, $\text{circ} = \textit{Teladorsagia circumcincta}$, $\text{cont} = \textit{Haemonchus contortus}$); s is survival rate (d^{-1} , section 3.4.2.2); and δ is maturation or migration rate (d^{-1} , section 3.4.2.2).

It should be noted that, in the absence of gravimetric faecal water content values, the transition rates for the within faeces lifecycle stages (i.e. E , L and $L3_f$) utilised in Eq. 142 were calculated by omitting the impact of water availability.

3.4.2.4 Descriptors

Species-specific pasture infectivity (INF_i , larvae $[\text{kg dry matter}]^{-1}$) was given as:

$$INF_i = \frac{L3_{h,i}}{PM_{SH} \cdot PS} \quad [\text{Eq. 146}]$$

where $L3_{h,i}$ is the species-specific number of infective larvae on herbage; PM_{SH} is the total pasture mass of shoot dry matter (kg ha^{-1} , section 3.2.10.4 Eq. 109); and PS is paddock size (ha).

Total pasture infectivity (INF , larvae $[\text{kg dry matter}]^{-1}$) was consequently given as:

$$INF = INF_{\text{colu}} + INF_{\text{vitr}} + INF_{\text{circ}} + INF_{\text{cont}} \quad [\text{Eq. 147}]$$

where $\text{colu} = \textit{Trichostrongylus colubriformis}$; $\text{vitr} = \textit{Trichostrongylus vitrinus}$; $\text{circ} = \textit{Teladorsagia circumcincta}$; $\text{cont} = \textit{Haemonchus contortus}$.

3.5 Supplementary feed

Supplementary feed can be provided to any paddock on any given day. This requires user input defining the day of provision, feed type (cereal pellets, hay, silage or straw), quantity (SUP , kg), crude protein content ($CP\%_{sup}$, %) and metabolizable energy content (ME_{sup} , MJ kg⁻¹).

3.5.1 Digestibility and gross energy

Supplementary feed estimates for neutral detergent fibre (NDF_{sup} , %), acid detergent fibre (ADF_{sup} , %) and acid detergent lignin (ADL_{sup} , %) were calculated in accordance with section 3.2.8 (Eq. 72-74). The neutral detergent fibre digestibility ($NDFD_{sup}$, %) and dry matter digestibility (DMD_{sup} , %) of supplementary was subsequently calculated in accordance with section 3.2.10.2 (Eq. 103-104). Consequently, the gross energy content of supplementary feed (GE_{sup} , MJ kg⁻¹) was calculated by rearranging Eq. 107 (section 3.2.10.3), such that:

$$GE_{sup} = \frac{ME_{sup}}{0.82 \cdot DMD_{sup}} \cdot 100 \quad [\text{Eq. 148}]$$

3.5.2 Nitrogen descriptors

The acid detergent insoluble nitrogen concentration ($ADIN_{sup}$, kg [kg dry matter]⁻¹), fractional rate of degradation of feed nitrogen ($FRDN_{sup}$, kg [kg dry matter]⁻¹ hr⁻¹), potentially degradable nitrogen concentration (PDN_{sup} , kg [kg dry matter]⁻¹) and water soluble nitrogen concentration (WSN_{sup} , kg [kg dry matter]⁻¹) supplementary for each feed type are given in Table 4.

Table 4. Acid detergent insoluble nitrogen concentration ($ADIN$, kg [kg dry matter]⁻¹), the fractional rate of degradation of feed nitrogen ($FRDN$, kg [kg dry matter]⁻¹ hr⁻¹), potentially degradable nitrogen concentration (PDN , kg [kg dry matter]⁻¹) and water soluble nitrogen concentration (WSN , kg [kg dry matter]⁻¹) for cereal pellets, fresh forage, hay, silage and straw (AFRC, 1993).

Feed class	$ADIN$	$FRDN$	PDN	WSN
Cereal pellets	0.0004	0.27	0.48	0.47
Fresh forage	0.0012	0.12	0.67	0.24
Hay	0.0012	0.08	0.60	0.22
Silage	0.0017	0.12	0.26	0.64
Straw	0.0010	0.12	0.50	0.3

3.5.3 Mixed feed type

The provision of supplementary feed on any given day may arise from one or more supplementary feed types. As such, the crude protein content ($CP\%_{sup}$, %), metabolizable energy content (ME_{sup} , MJ kg⁻¹), dry matter digestibility (DMD_{sup} , %), gross energy content (GE_{sup} , MJ kg⁻¹), acid detergent insoluble nitrogen concentration ($ADIN_{sup}$, kg kg⁻¹), fractional rate of degradation of feed nitrogen ($FRDN_{sup}$, kg kg⁻¹ hr⁻¹), potentially degradable nitrogen concentration (PDN_{sup} , kg kg⁻¹) and water soluble nitrogen concentration (WSN_{sup} , kg kg⁻¹) of supplementary feed were given as:

$$x_{sup} = \frac{x_{sup,cer} \cdot SUP_{cer} + x_{sup,hay} \cdot SUP_{hay} + x_{sup,sil} \cdot SUP_{sil} + x_{sup,str} \cdot SUP_{str}}{SUP} \quad [\text{Eq. 149}]$$

where SUP_i and $x_{sup,i}$ are the quantity (kg) and trait value associated with each feed type, respectively (cer = cereal pellets, hay = hay, sil = silage, str = straw); and SUP (kg) is the total quantity of supplementary feed provided given as:

$$SUP = SUP_{cer} + SUP_{hay} + SUP_{sil} + SUP_{str} \quad [\text{Eq. 150}]$$

3.5.4 Availability

Available supplementary feed may arise from both supplementary feed provided on any given day and supplementary feed remaining from previous days. Hence, the rates of change for the crude protein content ($\frac{dCP\%_{sup,avail}}{dt}$, % d⁻¹), metabolizable energy content ($\frac{dME_{sup,avail}}{dt}$, MJ kg⁻¹ d⁻¹), dry matter digestibility ($\frac{dDMD_{sup,avail}}{dt}$, % d⁻¹), gross energy content ($\frac{dGE_{sup,avail}}{dt}$, MJ kg⁻¹ d⁻¹), acid detergent insoluble nitrogen concentration ($\frac{dADIN_{sup,avail}}{dt}$, kg kg⁻¹ d⁻¹), fractional rate of degradation of feed nitrogen ($\frac{dFRDN_{sup,avail}}{dt}$, kg kg⁻¹ hr⁻¹ d⁻¹), potentially degradable nitrogen concentration ($\frac{dPDN_{sup,avail}}{dt}$, kg kg⁻¹ d⁻¹) and water soluble nitrogen concentration ($\frac{dWSN_{sup,avail}}{dt}$, kg kg⁻¹ d⁻¹) of available supplementary feed were given as:

$$\frac{dx_{sup,avail}}{dt} = \frac{x_{sup,avail} \cdot (SUP_{avail} - I_{sup}) + x_{sup} \cdot SUP}{SUP_{avail} + SUP - FI_{sup}} - x_{sup,avail} \quad [\text{Eq. 151}]$$

where I_{sup} is the supplementary feed intake of any grazing population (kg, section 3.9.5); SUP is the quantity of supplementary feed provided (kg, section 3.5.3 Eq. 150); SUP_{avail} is the quantity of available supplementary feed (kg); and x_{sup} is the trait value for supplementary feed provided (section 3.5.3 Eq. 149).

The rate of change for available supplementary feed ($\frac{dSUP_{avail}}{dt}$, kg d⁻¹) was given as:

$$\frac{dSUP_{avail}}{dt} = SUP - FI_{sup} \quad [\text{Eq. 152}]$$

3.6 Individual animal model

The individual animal model requires user input for live weight (LW , kg) and the date of any prior shearing in order to define the initial values associated with body composition (section 3.6.17.2). A schematic diagram of the individual animal model is provided in Fig. 3.

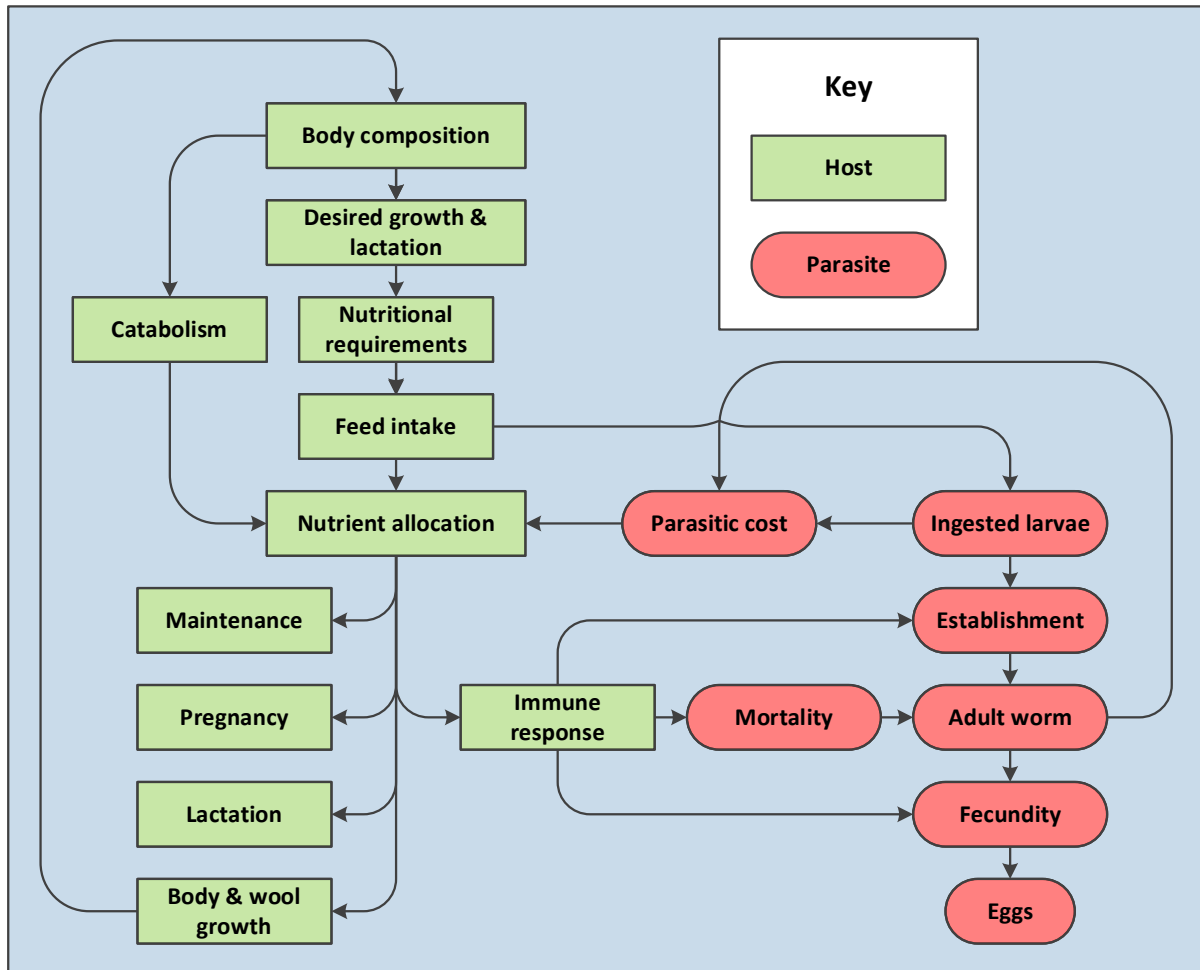


Figure 3. Schematic diagram of the individual animal model, including host-parasite interactions.

3.6.1 Body composition

3.6.1.1 Empty body weight

Fleece-free empty body weight (EBW , kg) was assumed to be comprised of ash (Ash , kg), lipid ($Lipid$, kg), protein ($Protein$, kg) and water ($Water$, kg):

$$EBW = Ash + Lipid + Protein + Water \quad [\text{Eq. 153}]$$

3.6.1.2 Conceptus

Foetal live weight (LW_f , kg) was considered as the sum of foetal ash (Ash_f , kg), lipid ($Lipid_f$, kg), protein ($Protein_f$, kg), water ($Water_f$, kg) and wool ($Wool_f$, kg), such that:

$$LW_f = Ash_f + Lipid_f + Protein_f + Water_f + Wool_f \quad [\text{Eq. 154}]$$

Conceptus adnexa (including the placenta, uterine tissues, membranes and amniotic fluid) was considered be comprised of adnexa lipid ($Lipid_a$, kg), protein ($Protein_a$, kg) and water ($Water_a$, kg). As such, the adnexa component of conceptus weight (CW_a , kg) was given as:

$$CW_a = Lipid_a + Protein_a + Water_a \quad [Eq. 155]$$

Conceptus weight (CW , kg) was consequently estimated as:

$$CW = CW_a + LW_f \quad [Eq. 156]$$

3.6.1.3 Live weight

Live weight (LW , kg) was considered to include the fleece-free empty body weight (EBW , kg, section 3.6.1.1 Eq. 153), fleece/wool weight ($Wool$, kg), gut fill (GF , kg, section 3.6.6 Eq. 216) and if applicable conceptus weight (CW , kg, section 3.6.1.2 Eq. 156):

$$LW = EBW + GF + Wool + CW \quad [Eq. 157]$$

3.6.1.4 Maturity

The body composition at maturity, for both sheep and foeti, was determined for the protein, ash, water and lipid components of fleece-free empty body weight.

Protein content at maturity ($Protein_{mat}$, kg) was given as:

$$Protein_{mat} = \alpha_{mat} \cdot EBW_{mat} \quad [Eq. 158]$$

where EBW_{mat} is the fleece-free empty body weight at maturity (kg); and α_{mat} is the proportional protein content of the fleece-free empty body weight at maturity. Both EBW_{mat} and α_{mat} were assumed to exhibit between-animal variation under partial genetic control (section 3.7).

Ash content at maturity (Ash_{mat} , kg) and water content at maturity ($Water_{mat}$, kg) were consequently calculated in accordance with Wellock et al. (2003) and Blaxter et al. (1982), respectively:

$$Ash_{mat} = 0.211 \cdot Protein_{mat} \quad [Eq. 159]$$

$$Water_{mat} = 3 \cdot Protein_{mat} \quad [Eq. 160]$$

As such, lipid content at maturity ($Lipid_{mat}$, kg) was estimated as:

$$Lipid_{mat} = EBW_{mat} - Protein_{mat} - Ash_{mat} - Water_{mat} \quad [Eq. 161]$$

3.6.1.5 Body condition score

Body condition score (BCS) was estimated assuming that the body composition at maturity represents a BCS of 2.5, and that a minimum lipid content at maturity (20% of protein at maturity) represents a BCS of 1. As such, BCS was estimated as:

$$BCS = \frac{0.3165 \cdot (Protein + Lipid) / Ash \cdot Ash_{mat} - 2 \cdot Ash_{mat} + 0.211 \cdot Lipid_{mat}}{0.211 \cdot Lipid_{mat} - 0.2 \cdot Ash_{mat}} \quad [Eq. 162]$$

where Ash is current body ash content (kg); Ash_{mat} is ash content at maturity (kg, section 3.6.1.4 Eq. 159); $Lipid$ is current body lipid content (kg); $Lipid_{mat}$ is lipid content at maturity (kg, section 3.6.1.4

Eq. 161); *Protein* is current body protein mass (kg); and *Protein_{mat}* is protein content at maturity (kg, section 3.6.1.4 Eq. 158).

3.6.2 Desired growth

3.6.2.1 Protein

Emmans (1997) previously proposed a function that approximated the relative rate of protein retention based on a Gompertz growth curve; however, in the present model the true differential of the Gompertz growth function was used. As such, desired protein accretion ($\frac{dProtein_{des}}{dt}$, kg d⁻¹) was estimated as:

$$\frac{dProtein_{des}}{dt} = Protein_{mat} \cdot \left(\frac{Protein}{Protein_{mat}} \right)^{e^{-B}} - Protein \quad [Eq. 163]$$

where *Protein* is current body protein mass (kg); *Protein_{mat}* is body protein content at maturity (kg, section 3.6.1.4 Eq. 158); and *B* is the Gompertz growth rate parameter, given as (Emmans, 1997):

$$B = \frac{0.02335}{Protein_{mat}^{0.27}} \quad [Eq. 164]$$

3.6.2.2 Lipid

Lipid accretion ($\frac{dLipid_{des}}{dt}$, kg d⁻¹) was estimated in accordance with Emmans (1997), such that:

$$\frac{dLipid_{des}}{dt} = \frac{dProtein_{des}}{dt} \cdot \frac{Lipid_{mat}}{Protein_{mat}} \cdot \beta_{lip} \cdot \left(\frac{Protein}{Protein_{mat}} \right)^{\beta_{lip}-1} \quad [Eq. 165]$$

where $\frac{dProtein_{des}}{dt}$ is desired protein accretion (kg d⁻¹, section 3.6.2.1 Eq. 163); *Lipid_{mat}* is lipid content at maturity (kg, section 3.6.1.4 Eq. 161); *Protein* is current body protein mass (kg); *Protein_{mat}* is body protein content at maturity (kg, section 3.6.1.4 Eq. 158); and β_{lip} is the constant associated with lipid deposition (Emmans, 1997):

$$\beta_{lip} = 1.46 \cdot \left(\frac{Lipid_{mat}}{Protein_{mat}} \right)^{0.23} \quad [Eq. 166]$$

3.6.2.3 Wool

Desired wool deposition ($\frac{dWool_{des}}{dt}$, kg d⁻¹) was estimated by a function derived from Cronje and Smuts (1994):

$$\frac{dWool_{des}}{dt} = 0.00085 \cdot \frac{Protein}{Protein_{mat}^{0.27}} + 0.16 \cdot \frac{dProtein_{des}}{dt} \quad [Eq. 167]$$

where $\frac{dProtein_{des}}{dt}$ is desired protein accretion (kg d⁻¹, section 3.6.2.1 Eq. 163); *Protein* is current body protein mass (kg); and *Protein_{mat}* is body protein content at maturity (kg, section 3.6.1.4 Eq. 158).

3.6.2.4 Foetus

Desired foetal protein accretion ($\frac{dProtein_{f,des}}{dt}$, kg d⁻¹), desired foetal lipid accretion ($\frac{dLipid_{f,des}}{dt}$, kg d⁻¹) and desired foetal wool deposition ($\frac{dWool_{f,des}}{dt}$, kg d⁻¹) were estimated as per the desired rates described above (sections 3.6.2.1 to 3.6.2.3 Eq. 163 to 167) by replacing the current and mature body content variables with the corresponding foetus variables.

Desired foetal ash ($\frac{dAsh_{f,des}}{dt}$, kg d⁻¹) and water ($\frac{dWater_{f,des}}{dt}$, kg d⁻¹) accretion were estimated in accordance with Wellock et al. (2003):

$$\frac{dAsh_{f,des}}{dt} = 0.211 \cdot \frac{dProtein_{f,des}}{dt} \quad [\text{Eq. 168}]$$

$$\frac{dWater_{f,des}}{dt} = \frac{dProtein_{f,des}}{dt} \cdot \frac{Water_{f,mat}}{Protein_{f,mat}} \cdot W \cdot \left(\frac{Protein_f}{Protein_{f,mat}} \right)^{w-1} \quad [\text{Eq. 169}]$$

where $Protein_f$ is current foetal protein mass (kg); $Protein_{f,mat}$ is protein content of the foetus at maturity (kg, section 3.6.1.4 Eq. 158); $Water_{f,mat}$ is water content of the foetus at maturity (kg, section 3.6.1.4 Eq. 160); and w is the constant associated with water retention (0.815; Wellock et al., 2003).

Desired foetal live weight growth ($\frac{dLW_{f,des}}{dt}$, kg d⁻¹) was consequently given as:

$$\frac{dLW_{f,des}}{dt} = \frac{dAsh_{f,des}}{dt} + \frac{dLipid_{f,des}}{dt} + \frac{dProtein_{f,des}}{dt} + \frac{dWater_{f,des}}{dt} + \frac{dWool_{f,des}}{dt} \quad [\text{Eq. 170}]$$

3.6.2.5 Adnexa

Desired adnexa protein ($\frac{dProtein_{a,des}}{dt}$, kg d⁻¹) and lipid ($\frac{dLipid_{a,des}}{dt}$, kg d⁻¹) accretion were estimated as functions derived from Ehrhardt and Bell (1995) ($R^2 = 0.97$, $se = 0.31$, $F_{1,19} = 553.11$, $p < 0.0001$):

$$\frac{dProtein_{a,des}}{dt} = 0.3127 \cdot e^{-243 \cdot e^{-0.126 \cdot EBW_{f,mat} \cdot \left(LW_f + \frac{dLW_{f,des}}{dt} \right)^{1-w}}} - Protein_a \quad [\text{Eq. 171}]$$

$$\frac{dLipid_{a,des}}{dt} = 0.2509 \cdot e^{-348 \cdot e^{-0.127 \cdot EBW_{f,mat} \cdot \left(LW_f + \frac{dLW_{f,des}}{dt} \right)^{1-w}}} - Lipid_a \quad [\text{Eq. 172}]$$

where $\frac{dLW_{f,des}}{dt}$ is desired foetal live weight growth (kg d⁻¹, section 3.6.2.4 Eq. 170); $EBW_{f,mat}$ is the fleece-free empty body weight of the foetus at maturity (kg); $Lipid_a$ is the current adnexa lipid content (kg); LW_f is the current foetal live weight (kg, section 3.6.1.2 Eq. 154); and $Protein_a$ is the current adnexa protein content (kg).

3.6.3 Desired lactation

Desired milk yield (M_{des} , kg d⁻¹) was predicted by the Wood incomplete gamma function (Wood, 1967) and parameterised in accordance with Saccareau et al. (2016):

$$M_{des} = \gamma_m \cdot t_1^{0.377} \cdot e^{-0.01 \cdot t_1} \quad [\text{Eq. 173}]$$

where t_1 is days since lambing (d); and lactation parameter γ_m was assumed to exhibit between-animal variation under partial genetic control (section 3.7).

The desired protein ($Protein_{milk,des}$, kg d⁻¹; $R^2 = 0.67$, $se = 0.003$ $F_{1,53} = 107.74$, $p < 0.0001$) and lipid ($Lipid_{milk,des}$, kg d⁻¹; $R^2 = 0.82$, $se = 0.004$, $F_{1,53} = 238.23$, $p < 0.0001$) content of milk was derived from data presented by Carta et al. (1995) and Komprej et al. (2012), such that:

$$Protein_{milk,des} = 0.032 \cdot t_1^{0.12} \cdot M_{des} \quad [Eq. 174]$$

$$Lipid_{milk,des} = 0.025 \cdot t_1^{0.21} \cdot M_{des} \quad [Eq. 175]$$

The desired lactose content of milk ($Lactose_{milk,des}$, kg d⁻¹) was derived from data presented by Hunter et al. (2015) and Morgan et al. (2006), such that ($R^2 = 0.95$, $se = 0.002$ $F_{1,36} = 710.25$ $p < 0.0001$):

$$Lactose_{milk,des} = 0.049 \cdot t_1^{0.075} \cdot e^{-0.0033 \cdot t_1} \cdot M_{des} \quad [Eq. 176]$$

3.6.4 Nutritional requirements

Only the protein and energy requirements were considered (Wellock et al., 2004), as all other nutrient requirements were assumed to be satisfied by the diet.

3.6.4.1 Protein

The protein requirement for maintenance (PR_{maint} , kg d⁻¹; Wellock et al., 2003), growth (PR_{growth} , kg d⁻¹), wool deposition (PR_{wool} , kg d⁻¹), pregnancy (PR_{preg} , kg d⁻¹) and lactation (PR_{milk} , kg d⁻¹) were given as:

$$PR_{maint} = p_{maint} \cdot \frac{Protein}{Protein_{mat}^{0.27}} \quad [Eq. 177]$$

$$PR_{growth} = \frac{dProtein_{des}}{dt} / k_{ng} \quad [Eq. 178]$$

$$PR_{wool} = \frac{dWool_{des}}{dt} / k_{nw} \quad [Eq. 179]$$

$$PR_{preg} = \left(\frac{dProtein_{a,des}}{dt} + \frac{dProtein_{f,des}}{dt} + \frac{dWool_{f,des}}{dt} \right) / k_{nc} \quad [Eq. 180]$$

$$PR_{milk} = Protein_{milk,des} / k_{nl} \quad [Eq. 181]$$

where $\frac{dProtein_{des}}{dt}$ is desired protein accretion (kg d⁻¹, section 3.6.2.1 Eq. 163); $\frac{dProtein_{a,des}}{dt}$ is the desired adnexa protein accretion (kg d⁻¹, section 3.6.2.5 Eq. 171); $\frac{dProtein_{f,des}}{dt}$ is the desired foetal protein accretion (kg d⁻¹, section 3.6.2.4); $\frac{dWool_{des}}{dt}$ is desired wool deposition (kg d⁻¹, section 3.1.6.2.3 Eq. 158); $\frac{dWool_{f,des}}{dt}$ is the desired foetal wool deposition (kg d⁻¹, section 3.6.2.4); k_{nc} is the efficiency of metabolizable protein use for concepta (0.85; AFRC, 1993); k_{ng} is the efficiency of metabolizable protein use for growth (0.59; AFRC, 1993); k_{nl} is the efficiency of metabolizable protein use for lactation (0.68; AFRC, 1993); k_{nw} is the efficiency of metabolizable protein use for wool deposition (0.26; AFRC, 1993); $Protein$ is current body protein mass (kg); $Protein_{mat}$ is protein content at maturity (kg, section 3.6.1.4 Eq. 158); p_{maint} is the constant associated with the protein requirements for maintenance (exhibits between-animal variation under partial genetic control, section 3.7); and $Protein_{milk,des}$ is the desired protein content of milk (kg d⁻¹, section 3.6.3 Eq. 174).

The total protein requirements (PR , kg d^{-1}) were consequently given as:

$$PR = PR_{\text{maint}} + PR_{\text{growth}} + PR_{\text{wool}} + PR_{\text{preg}} + PR_{\text{milk}} \quad [\text{Eq. 182}]$$

3.6.4.2 Energy

The energy requirement for maintenance (ER_{maint} , MJ d^{-1} ; Emmans and Fisher, 1986), growth (ER_{growth} , MJ d^{-1} ; Wellock et al., 2003), wool deposition (ER_{wool} , MJ d^{-1}), pregnancy (ER_{preg} , MJ d^{-1}) and lactation (ER_{milk} , MJ d^{-1}) were estimated as:

$$ER_{\text{maint}} = e_{\text{maint}} \cdot \frac{\text{Protein}}{\text{Protein}_{\text{mat}}^{0.27}} / k_{\text{m}} \quad [\text{Eq. 183}]$$

$$ER_{\text{growth}} = \left(h_{\text{P}} \cdot \frac{d\text{Protein}_{\text{des}}}{dt} + h_{\text{L}} \cdot \frac{d\text{Lipid}_{\text{des}}}{dt} \right) / k_{\text{g}} \quad [\text{Eq. 184}]$$

$$ER_{\text{wool}} = h_{\text{P}} \cdot \frac{d\text{Wool}_{\text{des}}}{dt} / k_{\text{g}} \quad [\text{Eq. 185}]$$

$$ER_{\text{preg}} = \left(h_{\text{P}} \cdot \left(\frac{d\text{Protein}_{\text{a,des}}}{dt} + \frac{d\text{Protein}_{\text{f,des}}}{dt} + \frac{d\text{Wool}_{\text{f,des}}}{dt} \right) + h_{\text{L}} \cdot \left(\frac{d\text{Lipid}_{\text{a,des}}}{dt} + \frac{d\text{Lipid}_{\text{f,des}}}{dt} \right) \right) / k_{\text{c}} \quad [\text{Eq. 186}]$$

$$ER_{\text{milk}} = \left(h_{\text{P}} \cdot \text{Protein}_{\text{milk,des}} + h_{\text{L}} \cdot \text{Lipid}_{\text{milk,des}} + h_{\text{Lac}} \cdot \text{Lactose}_{\text{milk,des}} \right) / k_{\text{l}} \quad [\text{Eq. 187}]$$

where $\frac{d\text{Lipid}_{\text{des}}}{dt}$ is desired lipid accretion (kg d^{-1} , section 3.6.2.2 Eq. 165); $\frac{d\text{Lipid}_{\text{a,des}}}{dt}$ is the desired adnexa lipid accretion (kg d^{-1} , section 3.6.2.5 Eq. 172); $\frac{d\text{Lipid}_{\text{f,des}}}{dt}$ is the desired foetal lipid accretion (kg d^{-1} , section 3.6.2.4); $\frac{d\text{Protein}_{\text{des}}}{dt}$ is desired protein accretion (kg d^{-1} , section 3.6.2.1 Eq. 163); $\frac{d\text{Protein}_{\text{a,des}}}{dt}$ the desired adnexa protein accretion (kg d^{-1} , section 3.6.2.5 Eq. 171); $\frac{d\text{Protein}_{\text{f,des}}}{dt}$ the desired foetal protein accretion (kg d^{-1} , section 3.6.2.4); $\frac{d\text{Wool}_{\text{des}}}{dt}$ is desired wool deposition (kg d^{-1} , section 3.6.2.3 Eq. 167); $\frac{d\text{Wool}_{\text{f,des}}}{dt}$ the desired foetal wool deposition (kg d^{-1} , section 3.6.2.4); e_{maint} is the constant associated with the energy requirements for maintenance (exhibits between-animal variation under partial genetic control, section 3.7); h_{L} is the heat of combustion of lipid (39.6 MJ kg^{-1}); h_{Lac} is the heat of combustion of lactose (16.5 MJ kg^{-1}); h_{P} is the heat of combustion of protein (23.8 MJ kg^{-1}); k_{c} is the efficiency of metabolizable energy utilisation for the concepta (0.133; AFRC, 1993); Protein is current body protein mass (kg); $\text{Protein}_{\text{mat}}$ is protein content at maturity (kg , section 3.6.1.4 Eq. 158); $\text{Lipid}_{\text{milk,des}}$ is the desired lipid content of milk (kg d^{-1} , section 3.6.3 Eq. 175); $\text{Lactose}_{\text{milk,des}}$ is the desired lactose content of milk (kg d^{-1} , section 3.6.3 Eq. 176); $\text{Protein}_{\text{milk,des}}$ is the desired protein content of milk (kg d^{-1} , section 3.6.3 Eq. 174); and the efficiency of metabolizable energy utilisation for maintenance (k_{m}), lactation (k_{l}) and growth (k_{g}) were given in accordance with the Agricultural and Food Research Council (AFRC, 1993):

$$k_{\text{m}} = 0.35 \cdot \frac{ME_{\text{avail}}}{GE_{\text{avail}}} + 0.503 \quad [\text{Eq. 188}]$$

$$k_{\text{l}} = 0.35 \cdot \frac{ME_{\text{avail}}}{GE_{\text{avail}}} + 0.42 \quad [\text{Eq. 189}]$$

$$k_{\text{g}} = \begin{cases} 0.78 \cdot \frac{ME_{\text{avail}}}{GE_{\text{avail}}} + 0.006, & \text{dry ewes \& rams} \\ 0.95 \cdot k_{\text{l}}, & \text{lactating ewes} \end{cases} \quad [\text{Eq. 190}]$$

where GE_{avail} is the gross energy content of available feed ($\text{MJ} [\text{kg dry matter}]^{-1}$, section 3.6.5.3 Eq. 194); and ME_{avail} is the metabolizable energy of available feed ($\text{MJ} [\text{kg dry matter}]^{-1}$, section 3.6.5.3 Eq. 194).

The total energy requirements (ER , MJ d⁻¹) were consequently given as:

$$ER = ER_{\text{maint}} + ER_{\text{growth}} + ER_{\text{wool}} + ER_{\text{preg}} + ER_{\text{milk}} \quad [\text{Eq. 191}]$$

3.6.5 Nutritional intake

3.6.5.1 Random environmental variation

Random environmental variation in feed intake (E_{FI}) was assumed to reflect the influence of external factors controlling feed intake not explicit accounted for by the model (Doeschl-Wilson et al., 2008). Random environmental variation in feed intake was achieved by pseudo-random sampling from a $N(1, \sigma_p^2)$ distribution, where σ_p^2 is phenotypic variance. The phenotypic variance for feed intake is currently set to zero; however, the ability to simulate random environmental variation in feed intake has been maintained within the model to allow for future parameterisation if necessary.

3.6.5.2 Maximum feed intake

The maximum physiological feed intake (FI_{max} , kg dry matter d⁻¹) was calculated in accordance with Lewis and Emmans (2010):

$$FI_{\text{max}} = \left(\frac{0.295 \cdot EBW}{EBW_{\text{mat}}^{0.27}} - \frac{0.195 \cdot EBW^2}{EBW_{\text{mat}}^{1.27}} \right) \cdot E_{\text{FI}} \quad [\text{Eq. 192}]$$

where E_{FI} is random environmental variation in feed intake (section 3.6.5.1); EBW is the current fleece-free empty body weight (kg, section 3.6.1.1 Eq. 153); and EBW_{mat} is the fleece-free empty body weight at maturity (kg).

3.6.5.3 Feed quality descriptors

The feed potentially ingested by an individual sheep can arise from either pasture or supplementary feed. As such, in order to calculate the quality descriptors of available feed it was first necessary to determine the fractional supplementary feed content of feed intake (f_{SUP} , kg kg⁻¹):

$$f_{\text{SUP}} = \begin{cases} \frac{SUP_{\text{avail}}}{n_{\text{sheep}} \cdot FI_{\text{max}}}, & FI_{\text{max}} > \frac{SUP_{\text{avail}}}{n_{\text{sheep}}} \\ 1, & FI_{\text{max}} \leq \frac{SUP_{\text{avail}}}{n_{\text{sheep}}} \end{cases} \quad [\text{Eq. 193}]$$

where FI_{max} is the maximum physiological feed intake (kg dry matter d⁻¹, section 3.6.5.2 Eq. 192); n_{sheep} is the number of sheep grazing a given paddock; and SUP_{avail} is the quantity of available supplementary feed (kg d⁻¹, section 3.5.4).

The crude protein content ($CP\%_{\text{avail}}$, %), metabolizable energy content (ME_{avail} , MJ [kg dry matter]⁻¹), dry matter digestibility (DMD_{avail} , %), gross energy content (GE_{avail} , MJ [kg dry matter]⁻¹), acid detergent insoluble nitrogen concentration ($ADIN_{\text{avail}}$, kg [kg dry matter]⁻¹), fractional rate of degradation of feed nitrogen ($FRDN_{\text{avail}}$, kg [kg dry matter]⁻¹ hr⁻¹), potentially degradable nitrogen concentration (PDN_{avail} , kg [kg dry matter]⁻¹) and water soluble nitrogen concentration (WSN_{avail} , kg [kg dry matter]⁻¹) of available feed were consequently calculated as:

$$x_{\text{avail}} = f_{\text{SUP}} \cdot x_{\text{sup,avail}} \cdot f_{\text{SUP}} + (1 - f_{\text{SUP}}) \cdot x \quad [\text{Eq. 194}]$$

where x is the associated trait value from pasture (section 3.2.10) or as per the nitrogen descriptors for fresh forage (section 3.5.2 Table 4); and $x_{\text{sup,avail}}$ is the associated trait value from available supplementary feed (section 3.5.4).

The metabolizable protein content of available feed (MP_{avail} , kg [kg dry matter]⁻¹) was calculated in accordance with the Agricultural and Food Research Council (AFRC, 1993). Rumen outflow rate (r_{out} , hr⁻¹) was estimated as a function of the level of feeding (LF), such that:

$$LF = \frac{ER}{ER_{\text{maint}}} \quad [\text{Eq. 195}]$$

$$r_{\text{out}} = -0.024 + 0.179 \cdot (1 - e^{-0.278 \cdot LF}) \quad [\text{Eq. 196}]$$

where ER is the total energy requirement (MJ d⁻¹, section 3.6.4.2 Eq. 191); and ER_{maint} is the energy requirement for maintenance (MJ d⁻¹, section 3.6.4.2 Eq. 183).

Quickly degradable protein (QDP , kg [kg dry matter]⁻¹) and slowly degradable protein (SDP , kg [kg dry matter]⁻¹) were calculated as:

$$QDP = WSN_{\text{avail}} \cdot \frac{CP_{\text{avail}}}{100} \quad [\text{Eq. 197}]$$

$$SDP = \frac{PDN_{\text{avail}} \cdot FRDN_{\text{avail}}}{FRDN_{\text{avail}} + r_{\text{out}}} \cdot \frac{CP_{\text{avail}}}{100} \quad [\text{Eq. 198}]$$

The effective rumen degradable protein ($ERDP$, kg [kg dry matter]⁻¹) and digestible undegradable protein (DUP , kg [kg dry matter]⁻¹) were calculated as:

$$ERDP = 0.8 \cdot QDP + SDP \quad [\text{Eq. 199}]$$

$$DUP = 0.9 \cdot \left(\frac{CP_{\text{avail}}}{100} - QDP - SDP - 6.25 \cdot ADIN_{\text{avail}} \right) \quad [\text{Eq. 200}]$$

The metabolizable protein content of available feed (MP_{avail} , kg [kg dry matter]⁻¹) was consequently calculated as:

$$MP_{\text{avail}} = 0.6375 \cdot ERDP + DUP \quad [\text{Eq. 201}]$$

3.6.5.4 Pasture mass availability constraint

The quantity of available pasture mass ($PM_{\text{SH,A}}$, kg dry matter ha⁻¹, section 3.2.10.4 Eq. 110) was assumed constrain feed intake (Vera et al., 1977). The constraint imposed by pasture mass availability was calculated by considering the fractional supplementary feed content of feed intake (f_{SUP} , kg kg⁻¹, section 3.6.5.3 Eq. 193), and the total pasture mass (PM_{SH} , kg dry matter ha⁻¹, section 3.2.10.4 Eq. 109). As such, the pasture mass availability constraint (Ω_{PM}) was given as:

$$\Omega_{\text{PM}} = f_{\text{SUP}} + (1 - f_{\text{SUP}}) \cdot \frac{PM_{\text{SH,A}}}{PM_{\text{SH}}} \quad [\text{Eq. 202}]$$

3.6.5.5 Inappetence

Components of the immune response (e.g. cytokines, gastrin etc.) are associated with inappetence, causing a reduction in feed intake (Fox et al., 1989; Greer et al., 2005). Further, Zaralis et al. (2007) reported between-breed differences in the magnitude and duration of parasite-induced reductions

in feed intake, which were proposed to be related to differences in production potential (Coop and Kyriazakis, 1999). Finally, Greer et al. (2005) reported that the magnitude of parasite-induced reductions in feed intake were greater in young lambs than older ewes, inferring a potential age or maturity effect. Consequently, inappetence (Ω_{FI}) was calculated as a function of acquired immunity Imm_{acq} , section 3.6.15 Eq. 292), the current body protein mass ($Protein$, kg) and the body protein content at maturity ($Protein_{mat}$, kg, section 3.6.1.4 Eq. 158), such that:

$$\Omega_{FI} = 1 - \left(0.3 \cdot Imm_{acq} \cdot \left(1 - \frac{Protein}{Protein_{mat}} \right) \right) \quad [\text{Eq. 203}]$$

In the present model, where the estimation of feed intake was based on the fulfillment of protein and energy requirements, parasite-induced reductions in feed intake were simulated by applying the constraints of inappetence to the protein and energy requirements. As such, the desired protein (PR_{des} , kg d⁻¹) and energy (ER_{des} , MJ d⁻¹) requirements were given as:

$$PR_{des} = \Omega_{FI} \cdot PR \quad [\text{Eq. 204}]$$

$$ER_{des} = \Omega_{FI} \cdot ER \quad [\text{Eq. 205}]$$

where ER is energy requirement (MJ d⁻¹, section 3.6.4.2 Eq. 191); and PR is protein requirement (kg d⁻¹, section 3.6.4.1 Eq. 182).

3.6.5.6 Milk intake

Suckling lambs (i.e prior to weaning) ingest milk from their mother, thereby providing both energy and protein. The energy (MI_E , MJ d⁻¹) and protein (MI_P , kg d⁻¹) provided by milk intake was calculated as:

$$MI_E = h_L \cdot Lipid_{milk} + h_{Lac} \cdot Lactose_{milk} \quad [\text{Eq. 206}]$$

$$MI_P = Protein_{milk} \quad [\text{Eq. 207}]$$

where h_L is the heat of combustion of lipid (39.6 MJ kg⁻¹); h_{Lac} is the heat of combustion of lactose (16.5 MJ kg⁻¹); $Lactose_{milk}$ is the lactose content of the mother's milk (kg, section 3.6.10.3 Eq. 268); $Lipid_{milk}$ is the lipid content of the mother's milk (kg, section 3.6.10.3 Eq. 269); and $Protein_{milk}$ is the protein content of the mother's milk (kg, section 3.6.10.3 Eq. 267).

For post-weaned lambs and sheep, the energy (MI_E , MJ) and protein (MI_P , kg) provided by milk intake was set to zero.

3.6.5.7 Desired feed intake

The desired feed intake to cover the associated requirements for energy ($FI_{des,E}$, kg d⁻¹) and protein ($FI_{des,P}$, kg d⁻¹) were calculated as:

$$FI_{des,E} = \frac{ER_{des} - MI_E}{ME_{avail}} \quad [\text{Eq. 208}]$$

$$FI_{des,P} = \frac{PR_{des} - MI_P}{MP_{avail}} \quad [\text{Eq. 209}]$$

where ER_{des} is the desired energy requirement (MJ d⁻¹, section 3.6.5.5 Eq. 205); ME_{avail} is metabolizable energy content of available feed (MJ [kg dry matter]⁻¹, section 3.6.5.3 Eq. 194); MI_E is

the energy provided by milk intake (MJ, section 3.6.5.6 Eq. 206); MI_P is the protein provided by milk intake (kg, section 3.6.5.6 Eq. 207); MP_{avail} is the metabolizable protein content of available feed (kg [kg dry matter]⁻¹, section 3.6.5.3 Eq. 201); and PR_{des} is the desired protein requirement (kg d⁻¹, section 3.6.5.5 Eq. 204).

Desired feed intake (FI_{des} , kg d⁻¹) was consequently estimated as:

$$FI_{des} = \begin{cases} FI_{des,P} \cdot E_{FI}, & FI_{des,P} \geq FI_{des,E} \\ FI_{des,E} \cdot E_{FI}, & FI_{des,P} < FI_{des,E} \end{cases} \quad [\text{Eq. 210}]$$

where E_{FI} is random environmental variation in feed intake (section 3.6.5.1).

3.6.5.8 Feed intake

Feed intake (FI , kg d⁻¹) was calculated from desired feed intake (FI_{des} , kg d⁻¹, section 3.6.5.7 Eq. 210) by considering the constraints imposed by pasture mass availability (Ω_{PM} , section 3.6.5.4 Eq. 202) and the maximum physiological feed intake (FI_{max} , kg dry matter d⁻¹, section 3.6.5.2 Eq. 192), such that:

$$FI = \begin{cases} FI_{des} \cdot \Omega_{PM}, & FI_{des} \leq FI_{max} \\ FI_{max} \cdot \Omega_{PM}, & FI_{des} > FI_{max} \end{cases} \quad [\text{Eq. 211}]$$

The energy (FI_E , MJ d⁻¹) and protein (FI_P , kg d⁻¹) provided by the ingestion of feed was consequently calculated as:

$$FI_E = FI \cdot ME_{avail} \quad [\text{Eq. 212}]$$

$$FI_P = FI \cdot MP_{avail} \quad [\text{Eq. 213}]$$

where ME_{avail} is metabolizable energy content of available feed (MJ [kg dry matter]⁻¹, section 3.6.5.3 Eq. 194); and MP_{avail} is the metabolizable protein content of available feed (kg [kg dry matter]⁻¹, section 3.6.5.3 Eq. 201).

Finally, the feed intake coming from pasture mass (FI_{PM} , kg d⁻¹) or supplementary feed (FI_{SUP} , kg d⁻¹) were given as:

$$FI_{PM} = (1 - f_{SUP}) \cdot FI \quad [\text{Eq. 214}]$$

$$FI_{SUP} = f_{SUP} \cdot FI \quad [\text{Eq. 215}]$$

where f_{SUP} is the fractional supplementary feed content of feed intake (kg kg⁻¹, section 3.6.5.3 Eq. 193).

3.6.6 Gut fill

Gut fill (GF , kg) was estimated according to Coffey et al. (2001):

$$GF = FI \cdot \left(11 - \frac{7 \cdot ME_{avail}}{15} \right) \quad [\text{Eq. 216}]$$

where FI is feed intake (kg d⁻¹, section 3.6.5.8 Eq. 211); and ME_{avail} is metabolizable energy content of available feed (MJ [kg dry matter]⁻¹, section 3.6.5.3 Eq. 194).

3.6.7 Nutrient availability via catabolism

Up to 20% of the maximum achieved body protein (P_{max} , kg) was considered as being available to meet any shortfall in protein requirements (Sykes, 2000; Houdijk et al., 2001). The total mass of body protein available via catabolism (P_{labile} , kg) was therefore calculated as:

$$P_{labile} = \begin{cases} Protein - (0.8 \cdot P_{max}), & Protein - (0.8 \cdot P_{max}) \geq 0 \\ 0, & Protein - (0.8 \cdot P_{max}) < 0 \end{cases} \quad [\text{Eq. 217}]$$

where $Protein$ is the current body protein mass (kg).

The total energy available via the catabolism of body lipid (E_{labile} , MJ) was estimated assuming that a minimum lipid:protein ratio of 0.2 is required for sheep survival (Vagenas et al., 2007a):

$$E_{labile} = \begin{cases} (Lipid - 0.2 \cdot Protein) \cdot h_L, & (Lipid - 0.2 \cdot Protein) \cdot h_L \geq 0 \\ 0, & (Lipid - 0.2 \cdot Protein) \cdot h_L < 0 \end{cases} \quad [\text{Eq. 218}]$$

where h_L is the heat of combustion of lipid (39.6 MJ kg⁻¹); $Lipid$ is the current body lipid content (kg); and $Protein$ is the current body protein content (kg).

3.6.8 Nutrient allocation

3.6.8.1 Parasitic protein loss

Gastrointestinal parasitism was assumed to result in endogenous protein loss (Yakoob et al., 1983). The nematode species-specific protein loss associated with parasitism ($P_{loss,i}$, kg d⁻¹) was given as:

$$P_{loss,i} = WB_{loss,i} \cdot WB_i + LB_{loss,i} \cdot LB_i \quad [\text{Eq. 219}]$$

where LB_i is the nematode species-specific larval burden (section 3.6.12); $LB_{loss,i}$ is the nematode species-specific protein loss per larvae (kg d⁻¹); WB_i is the nematode species-specific adult worm burden (section 3.6.12); and $WB_{loss,i}$ is the nematode species-specific protein loss per adult worm (kg d⁻¹). Both $LB_{loss,i}$ and $WB_{loss,i}$ were assumed to exhibit between-animal variation under partial genetic control (section 3.7).

The total protein loss associated with parasitism (P_{loss} , kg d⁻¹) was consequently given as:

$$P_{loss} = P_{loss,colu} + P_{loss,vitr} + P_{loss,circ} + P_{loss,cont} \quad [\text{Eq. 220}]$$

where $colu$ = *Trichostrongylus colubriformis*; $vitr$ = *Trichostrongylus vitrinus*; $circ$ = *Teladorsagia circumcincta*; $cont$ = *Haemonchus contortus*.

3.6.8.2 Nutrient availability

The energy (E_{avail} , MJ d⁻¹) and protein (P_{avail} , MJ d⁻¹) available for allocation were calculated as:

$$E_{avail} = MI_E + FI_E + E_{labile} \quad [\text{Eq. 221}]$$

$$P_{avail} = MI_P + FI_P + P_{labile} - P_{loss} \quad [\text{Eq. 222}]$$

where E_{labile} is the total energy available via the catabolism of body lipid (MJ, section 3.6.7 Eq. 218);

F_{I_E} is the energy provided by the ingestion of feed (kg d^{-1} , section 3.6.5.8 Eq. 212); F_{I_P} is the protein provided by the ingestion of feed (kg d^{-1} , section 3.6.5.8 Eq. 213); MI_E is the energy provided by the ingestion of milk (kg d^{-1} , section 3.6.5.6 Eq. 206); MI_P is the protein provided by the ingestion of milk (kg d^{-1} , section 3.6.5.6 Eq. 207); P_{labile} is the total protein available via catabolism (kg , section 3.6.7 Eq. 217); and P_{loss} is the total protein loss associated with parasitism (kg d^{-1} , section 3.6.8.1 Eq. 220).

3.6.8.3 Maintenance

The energy ($E_{\text{maint,alloc}}$, MJ d^{-1}) and protein ($P_{\text{maint,alloc}}$, kg d^{-1}) allocated to meet maintenance requirements were given as:

$$E_{\text{maint,alloc}} = \begin{cases} ER_{\text{maint}}, & E_{\text{avail}} \geq ER_{\text{maint}} \\ E_{\text{avail}}, & E_{\text{avail}} < ER_{\text{maint}} \end{cases} \quad [\text{Eq. 223}]$$

$$P_{\text{maint,alloc}} = \begin{cases} PR_{\text{maint}}, & P_{\text{avail}} \geq PR_{\text{maint}} \\ P_{\text{avail}}, & P_{\text{avail}} < PR_{\text{maint}} \end{cases} \quad [\text{Eq. 224}]$$

where E_{avail} is the energy available for allocation (MJ d^{-1} , section 3.6.8.2 Eq. 221); ER_{maint} is the energy requirement for maintenance (MJ d^{-1} , section 3.6.4.2 Eq. 183); PR_{maint} is the protein requirement for maintenance (kg d^{-1} , section 3.6.4.1 Eq. 177); and P_{avail} is the protein available for allocation (kg d^{-1} , section 3.6.8.2 Eq. 222).

3.6.8.4 Pregnancy

The energy ($E_{\text{preg,alloc}}$, MJ d^{-1}) and protein ($P_{\text{preg,alloc}}$, kg d^{-1}) allocated to meet pregnancy requirements were given in accordance with the following conditions:

1. If $(E_{\text{avail}} - E_{\text{maint,alloc}}) \geq ER_{\text{preg}}$ and $(P_{\text{avail}} - P_{\text{maint,alloc}}) \geq PR_{\text{preg}}$:

$$E_{\text{preg,alloc}} = ER_{\text{preg}} \quad [\text{Eq. 225}]$$

$$P_{\text{preg,alloc}} = PR_{\text{preg}} \quad [\text{Eq. 226}]$$

2. If $(E_{\text{avail}} - E_{\text{maint,alloc}}) \geq ER_{\text{preg}}$ and $(P_{\text{avail}} - P_{\text{maint,alloc}}) < PR_{\text{preg}}$:

$$P_{\text{preg,alloc}} = P_{\text{avail}} - P_{\text{maint,alloc}} \quad [\text{Eq. 227}]$$

$$E_{\text{preg,alloc}} = \left(h_p \cdot P_{\text{preg,alloc}} \cdot k_{\text{nc}} + h_L \cdot \left(\frac{dLipid_{\text{a,des}}}{dt} + \frac{dLipid_{\text{f,des}}}{dt} \right) \right) / k_c \quad [\text{Eq. 228}]$$

3. If $(E_{\text{avail}} - E_{\text{maint,alloc}}) < ER_{\text{preg}}$ and $(P_{\text{avail}} - P_{\text{maint,alloc}}) \geq PR_{\text{preg}}$:

$$E_{\text{preg,alloc}} = E_{\text{avail}} - E_{\text{maint,alloc}} \quad [\text{Eq. 229}]$$

$$P_{\text{preg,alloc}} = \begin{cases} PR_{\text{preg}}, & E_{\text{preg,alloc}} \geq (h_p \cdot PR_{\text{preg}} \cdot k_{\text{nc}}) / k_c \\ E_{\text{preg,alloc}} \cdot \frac{k_c}{h_p \cdot k_{\text{nc}}}, & E_{\text{preg,alloc}} < (h_p \cdot PR_{\text{preg}} \cdot k_{\text{nc}}) / k_c \end{cases} \quad [\text{Eq. 230}]$$

4. If $(E_{avail} - E_{maint,alloc}) < ER_{preg}$, $(P_{avail} - P_{maint,alloc}) < PR_{preg}$ and $(E_{avail} - E_{maint,alloc}) \geq \left(h_p \cdot (P_{avail} - P_{maint,alloc}) \cdot k_{nc} + h_L \cdot \left(\frac{dLipid_{a,des}}{dt} + \frac{dLipid_{f,des}}{dt} \right) \right) / k_c$ then $P_{preg,alloc}$ was given as per Eq. 227 and $E_{preg,alloc}$ was given as per Eq. 228.
5. If $(E_{avail} - E_{maint,alloc}) < ER_{preg}$, $(P_{avail} - P_{maint,alloc}) < PR_{preg}$, $(E_{avail} - E_{maint,alloc}) < \left(h_p \cdot (P_{avail} - P_{maint,alloc}) \cdot k_{nc} + h_L \cdot \left(\frac{dLipid_{a,des}}{dt} + \frac{dLipid_{f,des}}{dt} \right) \right) / k_c$ and $(E_{avail} - E_{maint,alloc}) \geq (h_p \cdot (P_{avail} - P_{maint,alloc}) \cdot k_{nc}) / k_c$ then $P_{preg,alloc}$ was given as per Eq. 227 and $E_{preg,alloc}$ was given as per Eq. 229.
6. If $(Energy_{avail} - E_{maint,alloc}) < ER_{preg}$, $(Protein_{avail} - P_{maint,alloc}) < PR_{preg}$ and $(Energy_{avail} - E_{maint,alloc}) < (h_p \cdot (Protein_{avail} - P_{maint,alloc}) \cdot k_{nc}) / k_c$ then $E_{preg,alloc}$ was given as per Eq. 229 and $P_{preg,alloc}$ was given as per Eq. 230.

where $\frac{dLipid_{a,des}}{dt}$ is the desired adnexa lipid accretion (kg d⁻¹, section 3.6.2.5 Eq. 172); $\frac{dLipid_{f,des}}{dt}$ is the desired foetal lipid accretion (kg d⁻¹, section 3.6.2.4); E_{avail} is the energy available for allocation (MJ d⁻¹, section 3.6.8.2 Eq. 221); $E_{maint,alloc}$ is the energy allocated to maintenance (MJ d⁻¹, section 3.6.8.3 Eq. 223); ER_{preg} is the energy requirement for pregnancy (MJ d⁻¹, section 3.6.4.2 Eq. 186); h_L is the heat of combustion of lipid (39.6 MJ kg⁻¹); k_c is the efficiency of metabolizable energy utilisation for the concepta (0.133; AFRC, 1993); k_{nc} is the efficiency of metabolizable protein use for concepta (0.85; AFRC, 1993); P_{avail} is the protein available for allocation (kg d⁻¹, section 3.6.8.2 Eq. 222); $P_{maint,alloc}$ is the protein allocated to maintenance (kg d⁻¹, section 3.6.8.3 Eq. 224); and PR_{preg} is the protein requirement for pregnancy (kg d⁻¹, section 3.6.4.1 Eq. 180).

3.6.8.5 Nutrient availability for lactation, body and wool growth

The energy ($E_{avail,prod}$, MJ d⁻¹) and protein ($P_{avail,prod}$, MJ d⁻¹) available for allocation to productive traits were calculated as:

$$E_{avail,prod} = \begin{cases} E_{avail} - E_{labile} - E_{maint,alloc} - E_{preg,alloc}, & E_{avail} - E_{labile} - E_{maint,alloc} - E_{preg,alloc} > 0 \\ 0, & E_{avail} - E_{labile} - E_{maint,alloc} - E_{preg,alloc} \leq 0 \end{cases} \quad [\text{Eq. 231}]$$

$$P_{avail,prod} = \begin{cases} P_{avail} - P_{labile} - P_{maint,alloc} - P_{preg,alloc}, & P_{avail} - P_{labile} - P_{maint,alloc} - P_{preg,alloc} > 0 \\ 0, & P_{avail} - P_{labile} - P_{maint,alloc} - P_{preg,alloc} \leq 0 \end{cases} \quad [\text{Eq. 232}]$$

where E_{avail} is the energy available for allocation (MJ d⁻¹, section 3.6.8.2 Eq. 221); E_{labile} is the total energy available via the catabolism of body lipid (MJ, section 3.6.7 Eq. 218); $E_{maint,alloc}$ is the energy allocated to maintenance (MJ d⁻¹, section 3.6.8.3 Eq. 223); $E_{preg,alloc}$ is the energy allocated to pregnancy (MJ d⁻¹, section 3.6.8.4); P_{avail} is the protein available for allocation (kg d⁻¹, section 3.6.8.2 Eq. 222); P_{labile} is the total protein available via catabolism (kg, section 3.6.7 Eq. 217); $P_{maint,alloc}$ is the

protein allocated to maintenance (kg d^{-1} , section 3.6.8.3 Eq. 224); and $P_{\text{preg,alloc}}$ is the protein allocated to pregnancy (MJ d^{-1} , section 3.6.8.4).

3.6.8.6 Lactation

The energy ($E_{\text{milk,alloc}}$, MJ d^{-1}) and protein ($P_{\text{milk,alloc}}$, kg d^{-1}) allocated to meet lactation requirements were given in accordance with the following conditions:

1. If $E_{\text{avail,prod}} \geq ER_{\text{milk}}$ and $P_{\text{avail,prod}} \geq PR_{\text{milk}}$:

$$E_{\text{milk,alloc}} = ER_{\text{milk}} \quad [\text{Eq. 233}]$$

$$P_{\text{milk,alloc}} = PR_{\text{milk}} \quad [\text{Eq. 234}]$$

2. If $E_{\text{avail,prod}} \geq ER_{\text{milk}}$ and $P_{\text{avail,prod}} < PR_{\text{milk}}$:

$$P_{\text{milk,alloc}} = P_{\text{avail,prod}} \quad [\text{Eq. 235}]$$

$$E_{\text{milk,alloc}} = \frac{(h_P \cdot P_{\text{milk,alloc}} \cdot k_{\text{nl}} + h_L \cdot \text{Lipid}_{\text{milk,des}} + h_{\text{Lac}} \cdot \text{Lactose}_{\text{milk,des}})}{k_1} \quad [\text{Eq. 236}]$$

3. If $E_{\text{avail,prod}} < ER_{\text{milk}}$ and $P_{\text{avail,prod}} \geq PR_{\text{milk}}$:

$$E_{\text{milk,alloc}} = E_{\text{avail,prod}} \quad [\text{Eq. 237}]$$

$$P_{\text{milk,alloc}} = \begin{cases} PR_{\text{milk}}, & E_{\text{milk,alloc}} \geq (h_P \cdot PR_{\text{milk}} \cdot k_{\text{nl}})/k_1 \\ E_{\text{milk,alloc}} \cdot \frac{k_1}{h_P \cdot k_{\text{nl}}}, & E_{\text{milk,alloc}} < (h_P \cdot PR_{\text{milk}} \cdot k_{\text{nl}})/k_1 \end{cases} \quad [\text{Eq. 238}]$$

4. If $E_{\text{avail,prod}} < ER_{\text{milk}}$, $P_{\text{avail,prod}} < PR_{\text{milk}}$ and $E_{\text{avail,prod}} \geq (h_P \cdot P_{\text{avail,prod}} \cdot k_{\text{nl}} + h_L \cdot \text{Lipid}_{\text{milk,des}} + h_{\text{Lac}} \cdot \text{Lactose}_{\text{milk,des}})/k_1$ then $P_{\text{milk,alloc}}$ was given as per Eq. 235 and $E_{\text{milk,alloc}}$ was given as per Eq. 236.

5. If $E_{\text{avail,prod}} < ER_{\text{milk}}$, $P_{\text{avail,prod}} < PR_{\text{milk}}$, $E_{\text{avail,prod}} < (h_P \cdot P_{\text{avail,prod}} \cdot k_{\text{nl}} + h_L \cdot \text{Lipid}_{\text{milk,des}} + h_{\text{Lac}} \cdot \text{Lactose}_{\text{milk,des}})/k_1$ and $E_{\text{avail,prod}} \geq (h_P \cdot P_{\text{avail,prod}} \cdot k_{\text{nl}})/k_1$ then $P_{\text{milk,alloc}}$ was given as per Eq. 235 and $E_{\text{milk,alloc}}$ was given as per Eq. 237.

6. If $E_{\text{avail,prod}} < ER_{\text{milk}}$, $P_{\text{avail,prod}} < PR_{\text{milk}}$ and $E_{\text{avail,prod}} < (h_P \cdot P_{\text{avail,prod}} \cdot k_{\text{nl}})/k_1$ then $E_{\text{milk,alloc}}$ was given as per Eq. 237 and $P_{\text{milk,alloc}}$ was given as per Eq. 238.

where $E_{\text{avail,prod}}$ is the energy available for allocation to productive traits (MJ d^{-1} , section 3.6.8.5 Eq. 231); ER_{milk} is the energy requirement for lactation (MJ d^{-1} , section 3.6.4.2 Eq. 187); h_L is the heat of combustion of lipid (39.6 MJ kg^{-1}); h_{Lac} is the heat of combustion of lactose (16.5 MJ kg^{-1}); h_P is the heat of combustion of protein (23.8 MJ kg^{-1}); k_1 is the efficiency of metabolizable energy use for lactation (section 3.6.4.2 Eq. 189); k_{nl} is the efficiency of metabolizable protein use for lactation

(0.68; AFRC, 1993); $Lipid_{milk,des}$ is the desired lipid content of milk ($kg\ d^{-1}$, section 3.6.3 Eq. 175); $Lactose_{milk,des}$ is the desired lactose content of milk ($kg\ d^{-1}$, section 3.6.3 Eq. 176); $P_{avail,prod}$ is the protein available for allocation to productive traits ($kg\ d^{-1}$, section 3.6.8.5 Eq. 232); and PR_{milk} is the protein requirement for lactation ($kg\ d^{-1}$, section 3.6.4.1 Eq. 181).

3.6.8.7 Body and wool growth

The energy allocated to body ($E_{body,alloc}$, $MJ\ d^{-1}$) and wool ($E_{wool,alloc}$, $MJ\ d^{-1}$) growth, as well as the protein allocated to body ($P_{body,alloc}$, $kg\ d^{-1}$) and wool ($P_{wool,alloc}$, $kg\ d^{-1}$) growth, were given in accordance with the following conditions:

1. If $(E_{avail,prod} - E_{milk,alloc}) \geq (ER_{growth} + ER_{wool})$ and $(P_{avail,prod} - P_{milk,alloc}) \geq (PR_{growth} + PR_{wool})$:

$$E_{body,alloc} = ER_{growth} \quad [Eq. 239]$$

$$E_{wool,alloc} = ER_{wool} \quad [Eq. 240]$$

$$P_{body,alloc} = PR_{growth} \quad [Eq. 241]$$

$$P_{wool,alloc} = PR_{wool} \quad [Eq. 242]$$

2. If $(E_{avail,prod} - E_{milk,alloc}) \geq (ER_{growth} + ER_{wool})$ and $(P_{avail,prod} - P_{milk,alloc}) < (PR_{growth} + PR_{wool})$:

$$P_{body,alloc} = (P_{avail,prod} - P_{milk,alloc}) \cdot \frac{PR_{growth}}{PR_{growth} + PR_{wool}} \quad [Eq. 243]$$

$$P_{wool,alloc} = (P_{avail,prod} - P_{milk,alloc}) \cdot \frac{PR_{wool}}{PR_{growth} + PR_{wool}} \quad [Eq. 244]$$

$$E_{body,alloc} = \left(h_P \cdot P_{body,alloc} \cdot k_{ng} + h_L \cdot \frac{dLipid_{des}}{dt} \right) / k_g \quad [Eq. 245]$$

$$E_{wool,alloc} = h_P \cdot P_{wool,alloc} \cdot k_{nw} / k_g \quad [Eq. 246]$$

3. If $(E_{avail,prod} - E_{milk,alloc}) < (ER_{growth} + ER_{wool})$, $(P_{avail,prod} - P_{milk,alloc}) \geq (PR_{growth} + PR_{wool})$ and $(E_{avail,prod} - E_{milk,alloc}) \geq \frac{h_P}{k_g} \cdot (PR_{growth} \cdot k_{ng} + PR_{wool} \cdot k_{nw})$

then $P_{body,alloc}$ was given as per Eq. 241, $P_{wool,alloc}$ was given as per Eq. 242, $E_{wool,alloc}$ was given as per Eq. 240, and $E_{body,alloc}$ was given as:

$$E_{body,alloc} = E_{avail,prod} - E_{milk,alloc} - E_{wool,alloc} \quad [Eq. 247]$$

4. If $(E_{avail,prod} - E_{milk,alloc}) < (ER_{growth} + ER_{wool})$, $(P_{avail,prod} - P_{milk,alloc}) \geq (PR_{growth} + PR_{wool})$ and $(E_{avail,prod} - E_{milk,alloc}) < \frac{h_P}{k_g} \cdot (PR_{growth} \cdot k_{ng} + PR_{wool} \cdot k_{nw})$:

$$P_{\text{body,alloc}} = PR_{\text{growth}} \cdot \frac{E_{\text{avail,prod}} - E_{\text{milk,alloc}}}{(h_P \cdot (PR_{\text{growth}} \cdot k_{\text{ng}} + PR_{\text{wool}} \cdot k_{\text{nw}})) / k_g} \quad [\text{Eq. 248}]$$

$$P_{\text{wool,alloc}} = PR_{\text{wool}} \cdot \frac{E_{\text{avail,prod}} - E_{\text{milk,alloc}}}{(h_P \cdot (PR_{\text{growth}} \cdot k_{\text{ng}} + PR_{\text{wool}} \cdot k_{\text{nw}})) / k_g} \quad [\text{Eq. 249}]$$

$$E_{\text{body,alloc}} = (h_P \cdot P_{\text{body,alloc}} \cdot k_{\text{ng}}) / k_g \quad [\text{Eq. 250}]$$

$$E_{\text{wool,alloc}} = h_P \cdot P_{\text{wool,alloc}} \cdot k_{\text{nw}} / k_g \quad [\text{Eq. 246}]$$

5. If $(E_{\text{avail,prod}} - E_{\text{milk,alloc}}) < (ER_{\text{growth}} + ER_{\text{wool}})$, $(P_{\text{avail,prod}} - P_{\text{milk,alloc}}) < (PR_{\text{growth}} + PR_{\text{wool}})$ and $(E_{\text{avail,prod}} - E_{\text{milk,alloc}}) \geq \left(\frac{h_P}{k_g} \cdot \left((P_{\text{avail,prod}} - P_{\text{milk,alloc}}) \cdot \frac{PR_{\text{growth}}}{PR_{\text{growth}} + PR_{\text{wool}}} \cdot k_{\text{ng}} + (P_{\text{avail,prod}} - P_{\text{milk,alloc}}) \cdot \frac{PR_{\text{wool}}}{PR_{\text{growth}} + PR_{\text{wool}}} \cdot k_{\text{nw}} \right) \right)$ then $P_{\text{body,alloc}}$ was given as per Eq. 243, $P_{\text{wool,alloc}}$ was given as per Eq. 244, $E_{\text{wool,alloc}}$ was given as per Eq. 246, and if $(E_{\text{avail,prod}} - E_{\text{milk,alloc}} - E_{\text{wool,alloc}}) \geq (h_P \cdot P_{\text{body,alloc}} \cdot k_{\text{ng}} + h_L \cdot \frac{dLipid_{\text{des}}}{dt}) / k_g$ then $E_{\text{body,alloc}}$ was given as per Eq. 245, else if $(E_{\text{avail,prod}} - E_{\text{milk,alloc}} - E_{\text{wool,alloc}}) < (h_P \cdot P_{\text{body,alloc}} \cdot k_{\text{ng}} + h_L \cdot \frac{dLipid_{\text{des}}}{dt}) / k_g$ then $E_{\text{body,alloc}}$ was given as per Eq. 247.

6. If $(E_{\text{avail,prod}} - E_{\text{milk,alloc}}) < (ER_{\text{growth}} + ER_{\text{wool}})$, $(P_{\text{avail,prod}} - P_{\text{milk,alloc}}) < (PR_{\text{growth}} + PR_{\text{wool}})$ and $(E_{\text{avail,prod}} - E_{\text{milk,alloc}}) < \left(\frac{h_P}{k_g} \cdot \left((P_{\text{avail,prod}} - P_{\text{milk,alloc}}) \cdot \frac{PR_{\text{growth}}}{PR_{\text{growth}} + PR_{\text{wool}}} \cdot k_{\text{ng}} + (P_{\text{avail,prod}} - P_{\text{milk,alloc}}) \cdot \frac{PR_{\text{wool}}}{PR_{\text{growth}} + PR_{\text{wool}}} \cdot k_{\text{nw}} \right) \right)$:

$$P_{\text{body,alloc}} = \frac{(P_{\text{avail,prod}} - P_{\text{milk,alloc}}) \cdot \frac{PR_{\text{growth}}}{PR_{\text{growth}} + PR_{\text{wool}}}}{(E_{\text{avail,prod}} - E_{\text{milk,alloc}})} \cdot \frac{h_P}{k_g} \left((P_{\text{avail,prod}} - P_{\text{milk,alloc}}) \cdot \frac{PR_{\text{growth}}}{PR_{\text{growth}} + PR_{\text{wool}}} \cdot k_{\text{ng}} + (P_{\text{avail,prod}} - P_{\text{milk,alloc}}) \cdot \frac{PR_{\text{wool}}}{PR_{\text{growth}} + PR_{\text{wool}}} \cdot k_{\text{nw}} \right) \quad [\text{Eq. 251}]$$

$$P_{\text{wool,alloc}} = \frac{(P_{\text{avail,prod}} - P_{\text{milk,alloc}}) \cdot \frac{PR_{\text{wool}}}{PR_{\text{growth}} + PR_{\text{wool}}}}{(E_{\text{avail,prod}} - E_{\text{milk,alloc}})} \cdot \frac{h_P}{k_g} \left((P_{\text{avail,prod}} - P_{\text{milk,alloc}}) \cdot \frac{PR_{\text{growth}}}{PR_{\text{growth}} + PR_{\text{wool}}} \cdot k_{\text{ng}} + (P_{\text{avail,prod}} - P_{\text{milk,alloc}}) \cdot \frac{PR_{\text{wool}}}{PR_{\text{growth}} + PR_{\text{wool}}} \cdot k_{\text{nw}} \right) \quad [\text{Eq. 252}]$$

$$E_{\text{body,alloc}} = (h_P \cdot P_{\text{body,alloc}} \cdot k_{\text{ng}}) / k_g \quad [\text{Eq. 250}]$$

$$E_{\text{wool,alloc}} = h_P \cdot P_{\text{wool,alloc}} \cdot k_{\text{nw}} / k_g \quad [\text{Eq. 246}]$$

where $\frac{dLipid_{des}}{dt}$ is desired lipid accretion ($kg\ d^{-1}$, section 3.6.2.2 Eq. 165); $E_{avail,prod}$ is the energy available for allocation to productive traits ($MJ\ d^{-1}$, section 3.6.8.5 Eq. 231); $E_{milk,alloc}$ is the energy allocated to lactation ($MJ\ d^{-1}$, section 3.6.8.6); ER_{growth} is the energy requirement for body growth ($MJ\ d^{-1}$, section 3.6.4.2 Eq. 184); ER_{wool} is the energy requirement for wool growth ($MJ\ d^{-1}$, section 3.6.4.2 Eq. 185); h_L is the heat of combustion of lipid ($39.6\ MJ\ kg^{-1}$); h_P is the heat of combustion of protein ($23.8\ MJ\ kg^{-1}$); k_g is the efficiency of metabolizable energy use for growth (section 3.6.4.2 Eq. 190); k_{ng} is the efficiency of metabolizable protein use for growth (0.59; AFRC, 1993); k_{nw} is the efficiency of metabolizable protein use for wool deposition (0.26; AFRC, 1993); $P_{avail,prod}$ is the protein available for allocation to productive traits ($kg\ d^{-1}$, section 3.6.8.5 Eq. 232); $P_{milk,alloc}$ is the protein allocated to lactation ($kg\ d^{-1}$, section 3.6.8.6); PR_{growth} is the protein requirement for body growth ($kg\ d^{-1}$, section 3.6.4.1 Eq. 178); and PR_{wool} is the protein requirement for wool growth ($kg\ d^{-1}$, section 3.6.4.1 Eq. 179).

3.6.8.8 Excess nutrients

Excess ingested energy (E_{exc} , $MJ\ d^{-1}$) and protein (P_{exc} , $kg\ d^{-1}$) were calculated as:

$$E_{exc} = E_{avail,prod} - E_{milk,alloc} - E_{body,alloc} - E_{wool,alloc} \quad [Eq. 253]$$

$$P_{exc} = P_{loss} + P_{avail,prod} - k_{nl} \cdot P_{milk,alloc} - k_{ng} \cdot P_{body,alloc} - k_{nw} \cdot P_{wool,alloc} + (1 - k_{nc}) \cdot P_{preg,alloc} \quad [Eq. 254]$$

where $E_{avail,prod}$ is the energy available for allocation to productive traits ($MJ\ d^{-1}$, section 3.6.8.5 Eq. 231); $E_{body,alloc}$ is the energy allocated to body growth ($MJ\ d^{-1}$, section 3.6.8.7); $E_{milk,alloc}$ is the energy allocated to lactation ($MJ\ d^{-1}$, section 3.6.8.6); $E_{wool,alloc}$ is the energy allocated to wool growth ($MJ\ d^{-1}$, section 3.6.8.7); k_{nc} is the efficiency of metabolizable protein use for concepta (0.85; AFRC, 1993); k_{ng} is the efficiency of metabolizable protein use for growth (0.59; AFRC, 1993); k_{nl} is the efficiency of metabolizable protein use for lactation (0.68; AFRC, 1993); k_{nw} is the efficiency of metabolizable protein use for wool deposition (0.26; AFRC, 1993); $P_{avail,prod}$ is the protein available for allocation to productive traits ($kg\ d^{-1}$, section 3.6.8.5 Eq. 232); $P_{body,alloc}$ is the protein allocated to body growth ($kg\ d^{-1}$, section 3.6.8.7); P_{loss} is the total protein loss associated with parasitism ($kg\ d^{-1}$, section 3.6.8.1 Eq. 220); $P_{milk,alloc}$ is the protein allocated to lactation ($kg\ d^{-1}$, section 3.6.8.6); $P_{preg,alloc}$ is the protein allocated to pregnancy ($MJ\ d^{-1}$, section 3.6.8.4); and $P_{wool,alloc}$ is the protein allocated to wool growth ($kg\ d^{-1}$, section 3.6.8.7).

Excess ingested energy was assumed to be retained and stored as lipid, however, excess ingested protein was assumed to be broken down and the associated nitrogen excreted as urea. The nitrogen content of urea (N_{urea} , $kg\ N\ d^{-1}$) was therefore given as:

$$N_{urea} = \frac{P_{exc}}{6.25} \quad [Eq. 255]$$

3.6.9 Catabolism

The total lipid (L_{cat} , kg d⁻¹) and protein (P_{cat} , kg d⁻¹) catabolized to meet requirements for maintenance and pregnancy were given as:

$$L_{cat} = \begin{cases} \frac{E_{\text{maint,alloc}} + E_{\text{preg,alloc}} - MI_E - FI_E}{h_L}, & E_{\text{maint,alloc}} + E_{\text{preg,alloc}} - MI_E - FI_E > 0 \\ 0, & E_{\text{maint,alloc}} + E_{\text{preg,alloc}} - MI_E - FI_E \leq 0 \end{cases} \quad [\text{Eq. 256}]$$

$$P_{cat} = \begin{cases} P_{\text{maint,alloc}} + P_{\text{preg,alloc}} + P_{\text{loss}} - MI_P - FI_P, & P_{\text{maint,alloc}} + P_{\text{preg,alloc}} + P_{\text{loss}} - MI_P - FI_P > 0 \\ 0, & P_{\text{maint,alloc}} + P_{\text{preg,alloc}} + P_{\text{loss}} - MI_P - FI_P \leq 0 \end{cases} \quad [\text{Eq. 257}]$$

where $E_{\text{maint,alloc}}$ is the energy allocated to maintenance (MJ d⁻¹, section 3.6.8.3 Eq. 223); $E_{\text{preg,alloc}}$ is the energy allocated to pregnancy (MJ d⁻¹, section 3.6.8.4); FI_E is the energy provided by the ingestion of feed (kg d⁻¹, section 3.6.5.8 Eq. 212); FI_P is the protein provided by the ingestion of feed (kg d⁻¹, section 3.6.5.8 Eq. 213); h_L is the heat of combustion of lipid (39.6 MJ kg⁻¹); MI_E is the energy provided by the ingestion of milk (kg d⁻¹, section 3.6.5.6 Eq. 206); MI_P is the protein provided by the ingestion of milk (kg d⁻¹, section 3.6.5.6 Eq. 207); P_{loss} is the total protein loss associated with parasitism (kg d⁻¹, section 3.6.8.1 Eq. 220); $P_{\text{maint,alloc}}$ is the protein allocated to maintenance (kg d⁻¹, section 3.6.8.3 Eq. 224); and $P_{\text{preg,alloc}}$ is the protein allocated to pregnancy (MJ d⁻¹, section 3.6.8.4).

3.6.10 Rates of change

3.6.10.1 Foetus

Foetal protein ($\frac{dProtein_f}{dt}$, kg d⁻¹), foetal ash ($\frac{dAsh_f}{dt}$, kg d⁻¹), foetal water ($\frac{dWater_f}{dt}$, kg d⁻¹), foetal lipid ($\frac{dLipid_f}{dt}$, kg d⁻¹) and foetal wool ($\frac{dWool_f}{dt}$, kg d⁻¹) accretion were given as:

$$\frac{dProtein_f}{dt} = \frac{dProtein_{f,des}}{dt} \cdot \frac{P_{\text{preg,alloc}}}{PR_{\text{preg}}} \quad [\text{Eq. 258}]$$

$$\frac{dAsh_f}{dt} = 0.211 \cdot \frac{dProtein_f}{dt} \quad [\text{Eq. 259}]$$

$$\frac{dWater_f}{dt} = \frac{dProtein_f}{dt} \cdot \frac{Water_{f,mat}}{Protein_{f,mat}} \cdot W \cdot \left(\frac{Protein_f}{Protein_{f,mat}} \right)^{w-1} \quad [\text{Eq. 260}]$$

$$\frac{dLipid_f}{dt} = \frac{dLipid_{f,des}}{dt} / \left(\frac{dLipid_{f,des}}{dt} + \frac{dLipid_{a,des}}{dt} \right) \cdot \frac{k_c \cdot E_{\text{preg,alloc}} - h_p \cdot P_{\text{preg,alloc}} \cdot k_{nc}}{h_L} \quad [\text{Eq. 261}]$$

$$\frac{dWool_f}{dt} = \frac{dWool_{f,des}}{dt} \cdot \frac{P_{\text{preg,alloc}}}{PR_{\text{preg}}} \quad [\text{Eq. 262}]$$

where $\frac{dLipid_{a,des}}{dt}$ is the desired adnexa lipid accretion (kg d⁻¹, section 3.6.2.5 Eq. 172); $\frac{dLipid_{f,des}}{dt}$ is the desired foetal lipid accretion (kg d⁻¹, section 3.6.2.4); $\frac{dProtein_{f,des}}{dt}$ the desired foetal protein accretion (kg d⁻¹, section 3.6.2.4); $\frac{dWool_{f,des}}{dt}$ the desired foetal wool deposition (kg d⁻¹, section 3.6.2.4); $E_{\text{preg,alloc}}$ is the energy allocated to pregnancy (MJ d⁻¹, section 3.6.8.4); h_L is the heat of combustion of lipid (39.6 MJ kg⁻¹); h_p is the heat of combustion of protein (23.8 MJ kg⁻¹); k_c is the efficiency of metabolizable energy utilisation for the concepta (0.133; AFRC, 1993); k_{nc} is the efficiency of

metabolizable protein use for concepta (0.85; AFRC, 1993); $P_{\text{preg,alloc}}$ is the protein allocated to pregnancy (MJ d^{-1} , section 3.6.8.4); PR_{preg} is the protein requirement for pregnancy (kg d^{-1} , section 3.6.4.1 Eq. 180); $Protein_f$ is current foetal protein mass (kg); $Protein_{f,mat}$ is protein content of the foetus at maturity (kg, section 3.6.1.4 Eq. 158); w is the constant associated with water retention (0.815; Wellock et al., 2003); and $Water_{f,mat}$ is water content of the foetus at maturity (kg, section 3.6.1.4 Eq. 160).

Foetal live weight growth ($\frac{dLW_f}{dt}$, kg d^{-1}) was consequently given as:

$$\frac{dLW_f}{dt} = \frac{dAsh_f}{dt} + \frac{dLipid_f}{dt} + \frac{dProtein_f}{dt} + \frac{dWater_f}{dt} + \frac{dWool_f}{dt} \quad [\text{Eq. 263}]$$

3.6.10.2 Adnexa

Adnexa protein ($\frac{dProtein_a}{dt}$, kg d^{-1}) and lipid ($\frac{dLipid_a}{dt}$, kg d^{-1}) accretion were given as:

$$\frac{dProtein_a}{dt} = \frac{dProtein_{a,des}}{dt} \cdot \frac{P_{\text{preg,alloc}}}{PR_{\text{preg}}} \quad [\text{Eq. 264}]$$

$$\frac{dLipid_a}{dt} = \frac{dLipid_{a,des}}{dt} / \left(\frac{dLipid_{f,des}}{dt} + \frac{dLipid_{a,des}}{dt} \right) \cdot \frac{k_c \cdot E_{\text{preg,alloc}} - h_p \cdot P_{\text{preg,alloc}} \cdot k_{nc}}{h_L} \quad [\text{Eq. 265}]$$

where $\frac{dLipid_{a,des}}{dt}$ is the desired adnexa lipid accretion (kg d^{-1} , section 3.6.2.5 Eq. 172); $\frac{dLipid_{f,des}}{dt}$ is the desired foetal lipid accretion (kg d^{-1} , section 3.6.2.4); $\frac{dProtein_{a,des}}{dt}$ the desired adnexa protein accretion (kg d^{-1} , section 3.6.2.5 Eq. 171); $E_{\text{preg,alloc}}$ is the energy allocated to pregnancy (MJ d^{-1} , section 3.6.8.4); h_L is the heat of combustion of lipid (39.6 MJ kg^{-1}); h_p is the heat of combustion of protein (23.8 MJ kg^{-1}); k_c is the efficiency of metabolizable energy utilisation for the concepta (0.133; AFRC, 1993); k_{nc} is the efficiency of metabolizable protein use for concepta (0.85; AFRC, 1993); $P_{\text{preg,alloc}}$ is the protein allocated to pregnancy (MJ d^{-1} , section 3.6.8.4); and PR_{preg} is the protein requirement for pregnancy (kg d^{-1} , section 3.6.4.1 Eq. 180).

Adnexa water accretion ($\frac{dWater_a}{dt}$, kg d^{-1}) was estimated as a function derived from Ehrhardt and Bell (1995) ($R^2 = 0.97$, $se = 0.31$, $F_{1,19} = 553.11$, $p < 0.0001$):

$$\frac{dWater_a}{dt} = 2.751 \cdot e^{-\frac{\left(EBW_{f,mat} \left(LW_f + \frac{dLW_f}{dt} \right)^{1-w} - 78.6 \right)^2}{800}} + 0.3662 \cdot e^{-128 \cdot e^{-0.12 \cdot EBW_{f,mat} \left(LW_f + \frac{dLW_f}{dt} \right)^{1-w}}} - Water_a \quad [\text{Eq. 266}]$$

where $\frac{dLW_f}{dt}$ is foetal live weight growth (kg d^{-1} , section 3.6.10.1 Eq. 263); $EBW_{f,mat}$ is the fleece-free empty body weight of the foetus at maturity (kg); LW_f is the current foetal live weight (kg, section 3.6.1.2 Eq. 154); w is the constant associated with water retention (0.815; Wellock et al., 2003); and $Water_a$ is water content of adnexa (kg).

3.6.10.3 Lactation

The protein ($Protein_{milk}$, kg d⁻¹), lactose ($Lactose_{milk,des}$, kg d⁻¹) and lipid ($Lipid_{milk}$, kg d⁻¹) content of milk produced by the allocation of nutrients to lactation were given as:

$$Protein_{milk} = k_{nl} \cdot P_{milk,alloc} \quad [Eq. 267]$$

$$Lactose_{milk} = Lactose_{milk,des} \cdot \frac{k_l \cdot E_{milk,alloc} - h_p \cdot Protein_{milk}}{h_L \cdot Lipid_{milk,des} + h_{Lac} \cdot Lactose_{milk,des}} \quad [Eq. 268]$$

$$Lipid_{milk} = Lipid_{milk,des} \cdot \frac{k_l \cdot E_{milk,alloc} - h_p \cdot Protein_{milk}}{h_L \cdot Lipid_{milk,des} + h_{Lac} \cdot Lactose_{milk,des}} \quad [Eq. 269]$$

where $E_{milk,alloc}$ is the energy allocated to lactation (MJ d⁻¹, section 3.6.8.6); h_L is the heat of combustion of lipid (39.6 MJ kg⁻¹); h_{Lac} is the heat of combustion of lactose (16.5 MJ kg⁻¹); h_p is the heat of combustion of protein (23.8 MJ kg⁻¹); k_l is the efficiency of metabolizable energy use for lactation (section 3.6.4.2 Eq. 189); k_{nl} is the efficiency of metabolizable protein use for lactation (0.68; AFRC, 1993); $Lactose_{milk,des}$ is the desired lactose content of milk (kg d⁻¹, section 3.6.3 Eq. 176); $Lipid_{milk,des}$ is the desired lipid content of milk (kg d⁻¹, section 3.6.3 Eq. 175); and $P_{milk,alloc}$ is the protein allocated to lactation (kg d⁻¹, section 3.6.8.6).

3.6.10.4 Body and wool

Body protein ($\frac{dProtein}{dt}$, kg d⁻¹), ash ($\frac{dAsh}{dt}$, kg d⁻¹), water ($\frac{dWater}{dt}$, kg d⁻¹), lipid ($\frac{dLipid}{dt}$, kg d⁻¹) and wool ($\frac{dWool}{dt}$, kg d⁻¹) accretion were given as:

$$\frac{dProtein}{dt} = k_{ng} \cdot P_{body,alloc} - P_{cat} \quad [Eq. 270]$$

$$\frac{dAsh}{dt} = \begin{cases} 0.211 \cdot \frac{dProtein}{dt}, & \frac{dProtein}{dt} > 0 \\ 0, & \frac{dProtein}{dt} \leq 0 \end{cases} \quad [Eq. 271]$$

$$\frac{dWater}{dt} = Water_{mat} \cdot \left(\frac{Protein + \frac{dProtein}{dt}}{Protein_{mat}} \right)^w - Water \quad [Eq. 272]$$

$$\frac{dLipid}{dt} = \frac{k_g \cdot (E_{body,alloc} + E_{exc}) - h_p \cdot P_{body,alloc} \cdot k_{ng}}{h_L} - L_{cat} \quad [Eq. 273]$$

$$\frac{dWool}{dt} = k_{nw} \cdot P_{wool,alloc} \quad [Eq. 274]$$

where $E_{body,alloc}$ is the energy allocated to body growth (MJ d⁻¹, section 3.6.8.7); E_{exc} is the excess ingested energy (MJ d⁻¹, section 3.6.8.8 Eq. 253); h_L is the heat of combustion of lipid (39.6 MJ kg⁻¹); h_p is the heat of combustion of protein (23.8 MJ kg⁻¹); k_g is the efficiency of metabolizable energy use for growth (section 3.6.4.2 Eq. 190); k_{ng} is the efficiency of metabolizable protein use for growth (0.59; AFRC, 1993); k_{nw} is the efficiency of metabolizable protein use for wool deposition (0.26; AFRC, 1993); L_{cat} is the total lipid catabolized (kg d⁻¹, section 3.6.9 Eq. 256); $P_{body,alloc}$ is the protein allocated to body growth (kg d⁻¹, section 3.6.8.7); P_{cat} is the total protein catabolized (kg d⁻¹, section 3.6.9 Eq. 257); $P_{wool,alloc}$ is the protein allocated to wool growth (kg d⁻¹, section 3.6.8.7); $Protein$ is current body protein mass (kg); $Protein_{mat}$ is protein content at maturity (kg, section 3.6.1.4 Eq. 158); w is the constant associated with water retention (0.815; Wellock et al., 2003); $Water$ is current body water mass (kg); and $Water_{mat}$ is water content at maturity (kg, section 3.6.1.4 Eq. 160).

3.6.11 Faeces

Faecal dry matter (FDM , g) was estimated as:

$$FDM = FI \cdot \left(1 - \frac{DMD_{avail}}{100}\right) \cdot 1000 \quad [\text{Eq. 275}]$$

where DMD_{avail} is the dry matter digestibility of available feed (%; section 3.6.5.3 Eq. 194); and FI is feed intake (kg d^{-1} , section 3.6.5.8 Eq. 211).

Faecal water mass (FWM , g) and wet faecal mass (WFM , g) were consequently calculated as per Eq. 121 and Eq. 122, respectively (section 3.4.1.1).

The nitrogen content of faeces (N_{faeces} , kg N d^{-1}) was given as:

$$N_{faeces} = \frac{FI \cdot CP\%_{avail} / 100 - FI_P}{6.25} \quad [\text{Eq. 276}]$$

where $CP\%_{avail}$ is the crude protein content of available feed (%; section 3.6.5.3 Eq. 194); and FI_P is the protein provided by the ingestion of feed (kg d^{-1} , section 3.6.5.8 Eq. 213).

3.6.12 Parasite burden

Infective larvae were assumed to be ingested from the pasture. As such, the species-specific larval intake (LI_i , d^{-1}) was given as:

$$LI_i = FI_{PM} \cdot INF_i \quad [\text{Eq. 277}]$$

where INF_i is the species-specific pasture infectivity (larvae $[\text{kg dry matter}]^{-1}$, section 2.4.2.4 Eq. 146); and FI_{PM} is the feed intake coming from pasture mass (kg d^{-1} , section 3.6.5.8 Eq. 214).

A proportion of ingested larvae establish ($Estab_i$, section 3.6.15 Eq. 293) within the host as adult worms following a species-specific prepatent period ($Prepat_i$, Table 5) where non-establishing infective larvae were assumed to have died prior to completing the required prepatent period. As such, the species-specific larval burden survival rate ($Surv_{LB,i}$, d^{-1}) was given as:

$$Surv_{LB,i} = Estab_i \frac{1}{Prepat_i} \quad [\text{Eq. 278}]$$

Hence, the species-specific larval burden (LB_i) was updated on a daily basis by considering incoming larvae via larval intake, the survival rate of previously ingested larvae and outgoing larvae developing to adult worms after completing the required prepatent period ($WB_{new,i}$).

The rate of change for the species-specific adult worm burden ($\frac{dWB_i}{dt}$, worms d^{-1}) was consequently calculated as:

$$\frac{dWB_i}{dt} = WB_{new,i} - Mort_{WB,i} \cdot WB_i \quad [\text{Eq. 279}]$$

where $Mort_{WB,i}$ is the species-specific mortality rate for adult worms (worms d^{-1} , section 3.6.15 Eq. 294).

The total larval burden (LB), worm burden (WB) and parasite burden (PB) across nematode species were therefore calculated as:

$$LB = LB_{\text{colu}} + LB_{\text{vitr}} + LB_{\text{circ}} + LB_{\text{cont}} \quad [\text{Eq. 280}]$$

$$WB = WB_{\text{colu}} + WB_{\text{vitr}} + WB_{\text{circ}} + WB_{\text{cont}} \quad [\text{Eq. 281}]$$

$$PB = LB + WB \quad [\text{Eq. 282}]$$

where colu = *Trichostrongylus colubriformis*; vitr = *Trichostrongylus vitrinus*; circ = *Teladorsagia circumcincta*; cont = *Haemonchus contortus*.

Table 5. The prepatent period (days) for four nematode species (Roeber et al., 2013).

<i>Trichostrongylus colubriformis</i>	<i>Trichostrongylus vitrinus</i>	<i>Teladorsagia circumcincta</i>	<i>Haemonchus contortus</i>
15	15	15	18

3.6.13 FAMACHA[®] score

Packed cell volume (PCV , %) was estimated by rearranging the multiple regression equation described by Roberts and Swan (1982) and Reynecke et al. (2011b), such that:

$$PCV = \frac{\log(WB_{\text{Haem}}) - 0.0168 \cdot LW - 3.8936}{-0.06925} \quad [\text{Eq. 283}]$$

where LW is the current live weight (kg, section 3.6.1.3 Eq. 157); and WB_{Haem} is the *Haemonchus contortus* worm burden (section 3.6.12).

FAMACHA[®] score was consequently determined in accordance with van Wyk and Bath (2002):

$$FAMACHA = \begin{cases} 1, & PCV \geq 28 \\ 2, & 23 \leq PCV < 28 \\ 3, & 18 \leq PCV < 23 \\ 4, & 13 \leq PCV < 18 \\ 5, & PCV < 13 \end{cases} \quad [\text{Eq. 284}]$$

3.6.14 Faecal egg count

Adult worms lay eggs which are deposited onto pasture within the faeces. The species-specific egg deposition ($Egg_{\text{dep},i}$, d^{-1}) was determined by the species-specific fecundity rate ($Fecund_i$, eggs worm⁻¹ d^{-1} , section 3.6.15 Eq. 298), such that:

$$Egg_{\text{dep},i} = Fecund_i \cdot WB_i \quad [\text{Eq. 285}]$$

where WB_i is the species-specific adult worm burden (section 3.6.12).

Faecal egg count is a measure of the concentration of nematode eggs within faeces and is hence subject to sampling errors. The random sampling error (S_{error}) was achieved by pseudo-random sampling from a $N(1,0.2)$ distribution (Bishop et al., 1996; Stear et al., 2009). The species-specific faecal egg count (FEC_i , eggs d^{-1}) was consequently given as:

$$FEC_i = \frac{Egg_{\text{dep},i}}{WFM} \cdot S_{\text{error}} \quad [\text{Eq. 286}]$$

where WFM is wet faecal mass (g, section 3.4.1.1 Eq. 122).

The total faecal egg count (FEC , eggs d^{-1}) across nematode species was thereby given as:

$$FEC = FEC_{colu} + FEC_{vitr} + FEC_{circ} + FEC_{cont} \quad [Eq. 287]$$

where $colu = Trichostrongylus colubriformis$; $vitr = Trichostrongylus vitrinus$; $circ = Teladorsagia circumcincta$; $cont = Haemonchus contortus$.

3.6.15 Immune response

It was assumed that the immune response was driven by recognition of the parasite burden. The species-specific parasite burden recognition ($PB_{recog,i}$) was given as:

$$PB_{recog,i} = LB_i \cdot LB_{recog,i} + WB_i \cdot WB_{recog,i} \quad [Eq. 288]$$

where LB_i is the species-specific larval burden (section 3.6.12); $LB_{recog,i}$ is the species-specific proportion of larval burden recognised (d^{-1}); WB_i is the species-specific adult worm burden (section 3.6.12); and $WB_{recog,i}$ is the species-specific proportion of adult worm burden recognised (d^{-1}). Both $LB_{recog,i}$ and $WB_{recog,i}$ are currently set as 1 for all nematode species; however, these parameters have been retained within the model to allow these values to be updated at a later date if and when experimental data becomes available.

The total parasite burden recognition (PB_{recog}) across nematode species was thereby given as:

$$PB_{recog} = PB_{recog,colu} + PB_{recog,vitr} + PB_{recog,circ} + PB_{recog,cont} \quad [Eq. 289]$$

where $colu = Trichostrongylus colubriformis$; $vitr = Trichostrongylus vitrinus$; $circ = Teladorsagia circumcincta$; $cont = Haemonchus contortus$.

As per Singleton et al. (2011), a delay between exposure and the initiation of an immune response ($PB_{recog,delay}$) was assumed. This recognition delay was assumed to exhibit between-animal variation under partial genetic control (section 3.7).

Immune recognition was assumed to be driven by protein availability. Whilst the protein requirements for the immune response were considered to be too small to be included as a nutrient requirement (section 3.6.4.1), limitations in protein availability (P_{avail} , $kg d^{-1}$, section 3.6.8.2 Eq. 222) in relation to the total protein requirements (PR , $kg d^{-1}$, section 3.6.4.1 Eq. 182) were assumed to impact upon immune recognition. Thus, immune recognition constraint associated with protein availability (Ω_{Imm}) was given as:

$$\Omega_{Imm} = \begin{cases} 1, & \frac{P_{avail} - P_{labile}}{PR} > 1 \\ \frac{P_{avail} - P_{labile}}{PR}, & 0 \leq \frac{P_{avail} - P_{labile}}{PR} \leq 1 \\ 0, & \frac{P_{avail} - P_{labile}}{PR} < 0 \end{cases} \quad [Eq. 290]$$

where P_{labile} is the total protein available via catabolism (kg , section 3.6.7 Eq. 217).

The immune recognition on any given day ($Imm_{recog,t}$) was thereby given by amending the function described by Singleton et al. (2011), such that:

$$Imm_{recog,t} = Imm_{recog,t-1} \cdot 0.5^{\frac{1}{Imm_{half}}} + \Omega_{Imm} \cdot PB_{recog,t} - PB_{recog,delay} \quad [Eq. 291]$$

where t is the current day; and Imm_{half} is the immune response half-life, which was assumed to exhibit between-animal variation under partial genetic control (section 3.7).

Acquired immunity (Imm_{acq}) was consequently calculated as a function of immune recognition (Imm_{recog} , Eq. 291), such that:

$$Imm_{acq} = 1 - e^{-\frac{Imm_{recog}}{Imm_{rate}}} \quad [\text{Eq. 292}]$$

where Imm_{rate} is the immune rate constant, which was assumed to exhibit between-animal variation under partial genetic control (section 3.7).

The acquisition of immunity was assumed to impact upon the species-specific establishment of ingested larvae ($Estab_i$), the species-specific mortality rate of adult worms ($Mort_{WB,i}$, worms d^{-1}), and the species-specific fecundity rate ($Fecund_i$, eggs worm $^{-1} d^{-1}$). $Estab_i$ and $Mort_{WB,i}$ were therefore given as:

$$Estab_i = Estab_{max,i} \cdot (1 - Imm_{acq}) \quad [\text{Eq. 293}]$$

$$Mort_{WB,i} = Mort_{WB,max,i} \cdot Imm_{acq} \quad [\text{Eq. 294}]$$

where $Estab_{max,i}$ is the species-specific maximum proportion of ingested larvae establishing; and $Mort_{WB,max,i}$ is the species-specific maximum mortality rate of adult worms (proportion d^{-1}). Both $Estab_{max,i}$ and $Mort_{WB,max,i}$ were assumed to exhibit between-animal variation under partial genetic control (section 3.7).

In addition to the impact of acquired immunity, the species-specific fecundity rate ($Fecund_i$, eggs worm $^{-1} d^{-1}$) was also assumed to be impacted by the average worm age of the resident adult worm burden (days since establishment), and density-dependent effects. The rate of change for the species-specific average worm age of the resident adult worm burden ($\frac{dWB_{age,i}}{dt}$, d^{-1}) was calculated as:

$$\frac{dWB_{age,i}}{dt} = \frac{(WB_{age,i+1}) \cdot (1 - Mort_{WB,i}) \cdot WB_i + WB_{new,i}}{(1 - Mort_{WB,i}) \cdot WB_i + WB_{new,i}} - WB_{age,i} \quad [\text{Eq. 295}]$$

where $WB_{new,i}$ is the newly established adult worms (section 3.6.12).

It was assumed that adult worms grew and became more fecund with age. As such, species-specific worm age constraint impacting upon fecundity ($\Omega_{WB,age,i}$) was given as:

$$\Omega_{WB,age,i} = 1 - e^{-\frac{WB_{age,i}}{WB_{age,const,i}}} \quad [\text{Eq. 296}]$$

where $WB_{age,const,i}$ is the species-specific worm age constant which is currently set as 7.4 for all nematode species; however, these parameters have been retained within the model to allow these values to be updated at a later date if and when experimental data becomes available.

Density-dependent effects on fecundity were considered by calculating the species-specific worm burden constraint impacting upon fecundity ($\Omega_{WB,i}$) in accordance with Bishop and Stear (2000), such that:

$$\Omega_{WB,i} = e^{-DD_{const,i} \cdot WB_i} \quad [\text{Eq. 297}]$$

where $DD_{\text{const},i}$ is the species-specific density-dependence constant. The value of $DD_{\text{const},i}$ has only been reported for *Teladorsagia circumcincta* (Bishop and Steer, 2000). However, in the absence of estimates for the other species, a value of 0.00036 was applied to all. The ability to parameterise this constant for each species has been retained within the model to allow these values to be updated at a later date if and when experimental data becomes available.

Hence, the species-specific fecundity rate ($Fecund_i$, eggs worm⁻¹ d⁻¹) was calculated by giving consideration to the impact of acquired immunity (Imm_{acq} , Eq. 292), and the constraints imposed by species-specific worm age ($\Omega_{\text{WB,age},i}$, Eq. 296) and the density-dependent effect of worm burden ($\Omega_{\text{WB},i}$, Eq. 297), such that:

$$Fecund_i = Fecund_{\text{max},i} \cdot (1 - Imm_{\text{acq}}) \cdot \Omega_{\text{WB,age},i} \cdot \Omega_{\text{WB},i} \quad [\text{Eq. 298}]$$

where $Fecund_{\text{max},i}$ is the species-specific maximum fecundity rate (eggs worm⁻¹ d⁻¹) was assumed to exhibit between-animal variation under partial genetic control (section 3.7).

3.6.16 Mortality

Sheep mortality was assumed to occur under the following circumstances:

1. $E_{\text{maint,alloc}} \neq ER_{\text{maint}} \quad [\text{Eq. 299}]$

2. $P_{\text{maint,alloc}} \neq PR_{\text{maint}} \quad [\text{Eq. 300}]$

3. $PCV < 8 \quad [\text{Eq. 301}]$

where $E_{\text{maint,alloc}}$ is the energy allocated to maintenance (MJ d⁻¹, section 3.6.8.3 Eq. 223); ER_{maint} is the energy requirement for maintenance (MJ d⁻¹, section 3.6.4.2 Eq. 183); $P_{\text{maint,alloc}}$ is the protein allocated to maintenance (kg d⁻¹, section 3.6.8.3 Eq. 224); PCV is packed cell volume (%; section 3.6.13 Eq. 283); and PR_{maint} is the protein requirement for maintenance (kg d⁻¹, section 3.6.4.1 Eq. 177).

Foetal mortality was assumed to occur if:

$$Protein_f < Protein_{f,\text{mat}} \cdot e^{-e^{G_{0,\text{mort}} + B_f(\text{gest} - \text{preg} + 1)}} \quad [\text{Eq. 302}]$$

where B_f is the foetal growth rate parameter (section 3.6.2.1 Eq. 164); gest is the gestation period (147 days); $Protein_f$ is current foetal protein mass (kg); preg is days since conception (d); $Protein_{f,\text{mat}}$ is protein content of the foetus at maturity (kg, section 3.6.1.4 Eq. 158); and the mortality threshold for the transformed degree of maturity at birth ($G_{0,\text{mort}}$) was given as:

$$G_{0,\text{mort}} = \ln(-\ln(0.04)) \quad [\text{Eq. 303}]$$

3.6.17 Initial parameterisation

3.6.17.1 Conceptus

If pregnant, foetal protein ($Protein_f$, kg), ash (Ash_f , kg), lipid ($Lipid_f$, kg), water ($Water_f$, kg), and wool ($Wool_f$, kg) were given as:

$$Protein_f = Protein_{f,mat} \cdot e^{-e^{G_0+B_f(gest-preg)}} \quad [Eq. 304]$$

$$Ash_f = 0.211 \cdot Protein_f \quad [Eq. 305]$$

$$Lipid_f = Lipid_{f,mat} \cdot \left(\frac{Protein_f}{Protein_{f,mat}} \right)^{\beta_{lip,f}} \quad [Eq. 306]$$

$$Water_f = Water_{f,mat} \cdot \left(\frac{Protein_f}{Protein_{f,mat}} \right)^w \quad [Eq. 307]$$

$$Wool_f = 0.00085 \cdot \frac{Protein_{f,mat}^{0.73}}{B_f} \cdot \ln \left(\frac{Protein_{f,mat}}{Protein_{f,mat} - Protein_f} \right) + 0.16 \cdot Protein_f \quad [Eq. 308]$$

where B_f is the foetal growth rate parameter (section 3.6.2.1 Eq. 164); $gest$ is the gestation period (147 days); $Lipid_{f,mat}$ is lipid content of the foetus at maturity (kg, section 3.6.1.4 Eq. 161); $preg$ is days since conception (d); $Protein_{f,mat}$ is protein content of the foetus at maturity (kg, section 3.6.1.4 Eq. 158); w is the constant associated with water retention (0.815; Wellock et al., 2003); $Water_{f,mat}$ is water content of the foetus at maturity (kg, section 3.6.1.4 Eq. 160); $\beta_{lip,f}$ is the constant associated with lipid deposition (section 3.6.2.2 Eq. 166); and the transformed degree of maturity at birth (G_0) was given as:

$$G_0 = \ln(-\ln(0.05)) \quad [Eq. 309]$$

Foetal live weight (LW_f , kg) was thereby calculated as per Eq. 154 (section 3.6.1.2). Adnexa lipid ($Lipid_a$, kg), protein ($Protein_a$, kg) and water ($Water_a$, kg) were consequently given as:

$$Lipid_a = 0.2509 \cdot e^{-348 \cdot e^{-0.127 \cdot EBW_{f,mat} \cdot LW_f^{1-w}}} \quad [Eq. 310]$$

$$Protein_a = 0.3127 \cdot e^{-243 \cdot e^{-0.126 \cdot EBW_{f,mat} \cdot LW_f^{1-w}}} \quad [Eq. 311]$$

$$Water_a = 2.751 \cdot e^{-\frac{(EBW_{f,mat} \cdot LW_f^{1-w} - 78.6)^2}{800}} + 0.3662 \cdot e^{-128 \cdot e^{-0.12 \cdot EBW_{f,mat} \cdot LW_f^{1-w}}} \quad [Eq. 312]$$

where $EBW_{f,mat}$ is the fleece-free empty body weight of the foetus at maturity (kg).

As such, the adnexa component of conceptus weight (CW_a , kg) and total conceptus weight (CW , kg) were calculated as per Eq. 155 and Eq. 156, respectively (section 3.6.1.2).

3.6.17.2 Body composition

The initial body composition is defined by user inputs for live weight (LW , kg) and the date of any prior shearing. An iterative process was used to solve the initial value for body protein content ($Protein$, kg) such that predicted live weight (LW , kg, section 3.6.1.3 Eq. 157) was equal to the user input. The initial ash (Ash , kg), lipid ($Lipid$, kg) and water ($Water$, kg) components were estimated as per the foetal components described above (sections 3.6.17.1 Eq. 305 to 307) by replacing the

current and mature foetal body content variables with the appropriate corresponding variables. Initial wool weight ($Wool$, kg) and gut fill (GF , kg) were given as:

$$Wool = \begin{cases} 0.00085 \cdot \frac{Protein_{mat}^{0.73}}{B} \cdot \ln\left(\frac{Protein_{mat}}{Protein_{mat}-Protein}\right) + 0.16 \cdot Protein, & \text{no prior shear} \\ Protein \cdot shear \cdot \left(\frac{0.00085}{Protein_{mat}^{0.27}} + 0.16 \cdot B \cdot \ln\left(\frac{Protein_{mat}}{Protein}\right)\right), & \text{prior shear} \end{cases} \quad [\text{Eq. 313}]$$

$$GF = \left(\frac{0.295 \cdot EBW}{EBW_{mat}^{0.27}} - \frac{0.195 \cdot EBW^2}{EBW_{mat}^{1.27}}\right) \cdot \frac{PM_{SH,A}}{PM_{SH}} \cdot \left(11 - \frac{7}{15} \cdot ME\right) \quad [\text{Eq. 314}]$$

where B is the growth rate parameter (section 3.6.2.1 Eq. 164); EBW is the fleece-free empty body weight (kg, section 3.6.1.1 Eq. 153); EBW_{mat} is the fleece-free empty body weight at maturity (kg); ME is the metabolizable energy of pasture (MJ [kg dry matter]⁻¹, section 3.2.10.3 Eq. 107); PM_{SH} is the total pasture mass (kg dry matter ha⁻¹, section 3.2.10.4 Eq. 109); $PM_{SH,A}$ is pasture mass available for grazing (kg dry matter ha⁻¹, section 3.2.10.4 Eq. 110); $Protein_{mat}$ is protein content at maturity (kg, section 3.6.1.4 Eq. 158); and $shear$ is the number of days since shearing (d).

3.6.17.3 Parasite burden and immune response

The initial species-specific larval burden (LB_i) was assumed to have arisen from the ingestion of infective larvae over a period equal to the species-specific prepatent period ($Prepat_i$, section 3.6.12 Table 5). The daily feed intake during this prior grazing period (FI_{prior} , kg d⁻¹) was estimated as:

$$FI_{prior} = \frac{GF}{11 - \frac{7}{15} \cdot ME} \quad [\text{Eq. 315}]$$

where GF is the initial gut fill (kg, section 3.6.17.2 Eq. 314); and ME is the metabolizable energy of pasture (MJ [kg dry matter]⁻¹, section 3.2.10.3 Eq. 107).

The species-specific larval burden in the absence of acquired immunity ($LB_{temp,i}$) was consequently estimated by considering the ingestion of infective larvae and the survival of infective larvae since ingestion, such that:

$$LB_{temp,i} = \sum_{n=1}^{Prepat,i} \left(FI_{prior} \cdot INF_i \cdot Estab_{max,i} \frac{Prepat,i-n}{Prepat,i} \right) \quad [\text{Eq. 316}]$$

where $Estab_{max,i}$ is the species-specific maximum proportion of ingested larvae establishing (section 3.7); and INF_i is the species-specific pasture infectivity (larvae [kg dry matter]⁻¹, section 2.4.2.4 Eq. 146).

Subsequently, the species-specific adult worm burden in the absence of acquired immunity ($WB_{temp,i}$) was estimated as:

$$WB_{temp,i} = Estab_{max,i} \cdot LB_{temp,i} \quad [\text{Eq. 317}]$$

The initial species-specific parasite burden recognition ($PB_{recog,i}$) was thereby given as:

$$PB_{recog,i} = LB_{temp,i} \cdot LB_{recog,i} + WB_{temp,i} \cdot WB_{recog,i} \quad [\text{Eq. 318}]$$

where $LB_{recog,i}$ is the species-specific proportion of larval burden recognised (d⁻¹, section 3.6.15); and $WB_{recog,i}$ is the species-specific proportion of adult worm burden recognised (d⁻¹ section 3.6.15).

The initial immune recognition (Imm_{recog}) was subsequently estimated as:

$$Imm_{recog} = \frac{Protein}{Protein_{mat}} \cdot \frac{PB_{recog}}{1 - 0.5 \frac{1}{Imm_{half}}} \quad [Eq. 319]$$

where Imm_{half} is the immune response half-life (section ???); PB_{recog} is the total parasite burden recognition (section 3.6.15 Eq. 289); $Protein$ is current body protein mass (kg); and $Protein_{mat}$ is protein content at maturity (kg, section 3.6.1.4 Eq. 158).

The initial species-specific larval burden (LB_i) and adult worm burden (WB_i) were thereby given as:

$$LB_i = LB_{temp,i} \cdot (1 - Imm_{acq}) \quad [Eq. 320]$$

$$WB_i = WB_{temp,i} \cdot (1 - Imm_{acq}) \cdot (1 - (Mort_{WB,max,i} \cdot Imm_{acq})) \quad [Eq. 321]$$

where Imm_{acq} is acquired immunity (section 3.6.15 Eq. 292); and $Mort_{WB,max,i}$ is the species-specific maximum mortality rate of adult worms (proportion d^{-1} , section 3.7).

Finally, the initial species-specific average worm age ($WB_{age,i}$, days) was given as equal to the species-specific prepatent period ($Prepat_i$, section 3.6.12 Table 5).

3.7 Population model

Between-animal variation was modelled according to Vagenas et al. (2007b) and was assumed to occur in body composition attributes, milk yield, maintenance requirements, gastrointestinal parasite tolerance, and in the immune response to gastrointestinal parasites. A simulated population of sheep were assumed to arise from mating a founder population of unrelated sires and dams. Each founder animal (sire or dam) had a breeding value (A_i), sampled from a $N(0, \sigma_A^2)$ distribution, for each trait considered to be under partial genetic control. Genetic variance (σ_A^2) was given as:

$$\sigma_A^2 = h^2 \cdot \sigma_P^2 \quad [\text{Eq. 322}]$$

where h^2 is the trait heritability; and σ_P^2 is phenotypic variation.

The trait breeding values (A_i) for each offspring were subsequently constructed as the parental average ($\frac{A_{\text{sire}} + A_{\text{dam}}}{2}$) plus a Mendelian sampling term, drawn from a $N(0, 0.5 \cdot \sigma_A^2)$ distribution (Falconer and Mackay, 1996). Maternal (M_i) and environmental (E_i) effects for the i^{th} individual were simulated by pseudo-random sampling from $N(0, \sigma_M^2)$ and $N(0, \sigma_E^2)$ distributions, respectively. The maternal effect variance (σ_M^2) and environmental effect variance (σ_E^2) were given as:

$$\sigma_M^2 = m^2 \cdot \sigma_P^2 \quad [\text{Eq. 323}]$$

$$\sigma_E^2 = (1 - h^2 - m^2) \cdot \sigma_P^2 \quad [\text{Eq. 324}]$$

where m^2 is the trait maternal effect.

The phenotypic trait value for the i^{th} individual (P_i) was subsequently given in accordance with a standard linear mixed model, such that:

$$P_i = \mu + A_i + M_i + E_i \quad [\text{Eq. 325}]$$

where μ is the trait population mean; A_i is the additive genetic deviation (breeding value) of the i^{th} individual; M_i is the additive maternal deviation (maternal effect) of the i^{th} individual; and E_i is the environmental deviation (environmental effect) of the i^{th} individual.

The maternal effects (m^2) for all traits exhibiting between-animal variation are currently set to zero; however, the ability to include maternal effects has been retained within the model to allow for future parameterisation.

A population size of 2,000 sheep (generated from mating 100 sires and 2000 dams) was chosen to ensure that trait means at each time point were estimated with precision, avoiding the need for statistical analyses of the outputs. With this population size, the expected standard error of each mean value within the simulation is $\sigma/100$, where σ is the trait standard deviation at that time point. Therefore, even with extremely variable traits such as faecal egg count, which have a coefficient of variation close to 100%, the standard error of the mean will only be 5% of the mean value.

Further, it should be noted that all trait phenotypes were assumed to be normally distributed, thus distributions such as the over-dispersion of faecal egg count described by Bishop and Stear (1997) occur as a consequence of the functions that underlie the model rather than as a result of direct input.

The body composition traits assumed to exhibit between-animal variation include the fleece-free empty body weight at maturity (EBW_{mat} , kg, section 3.6.1.4 Eq. 158), and the proportional protein content of the fleece-free empty body weight at maturity (α_{mat} , section 3.6.1.4 Eq. 158). These body composition traits were assumed to be breed and gender specific (where crossbreeds can be calculated as a weighted average of the appropriate breeds). Heritability (h^2) estimates for

both EBW_{mat} and α_{mat} were given as 0.5 for all breeds and genders, whilst the population mean and coefficient of variance are given in Table 6.

Table 6. Breed and gender specific population means (μ) and coefficients of variation (CV) for body composition traits exhibiting between-animal variation. EBW_{mat} is fleece-free empty body weight at maturity (kg), and α_{mat} is the proportional protein content of the fleece-free empty body weight at maturity.

Parameter	Gender	Male		Female	
	Breed	μ	CV^a	μ	CV^a
EBW_{mat}	Border Leicester	113	0.225	90	0.225
	Dorset	104	0.110	70	0.100
	Merino	81	0.125	56	0.125
	Suffolk	126	0.225	87	0.150
α_{mat}	Border Leicester	0.13	0.070	0.12	0.110
	Dorset	0.17	0.030	0.15	0.050
	Merino	0.18	0.030	0.16	0.050
	Suffolk	0.15	0.070	0.13	0.080

^aPhenotypic variance (σ_p^2) = ($\mu \cdot CV$)²

Whilst only the body composition traits exhibiting between-animal variation are currently provided as breed and gender specific, the ability to provide breed and gender specific parameters for all other traits exhibiting between-animal variation has been retained within the model.

The other traits assumed to exhibit between-animal variation include the lactation parameter influencing milk yield (γ_m , section 3.6.3 Eq. 173); the constants associated with the energy (e_{maint} , section 3.6.4.2 Eq.183) and protein (p_{maint} , section 3.6.4.1 Eq. 177) requirements for maintenance; the parasite tolerance constants associated the protein loss per larvae (LB_{loss} , kg d⁻¹, section 3.6.8.1 Eq. 219) and per adult worm (WB_{loss} , kg d⁻¹, section 3.6.8.1 Eq. 219); the immune response constants determining the delay between exposure and the initiation of an immune response ($PB_{recog, delay}$, days, section 3.6.15 Eq. 291), the immune response half-life (Imm_{half} , days, section 3.6.15 Eq. 291) and the immune acquisition rate (Imm_{rate} , section 3.6.15 Eq. 292); and the parasite resistance constants associated with the maximum proportion of ingested larvae establishing ($Estab_{max}$, section 3.6.15 Eq. 293), the maximum mortality rate of adult worms ($Mort_{WB, max}$, proportion d⁻¹, section 3.6.15 Eq. 294) and the maximum fecundity rate ($Fecund_{max}$, eggs worm⁻¹ d⁻¹, section 3.6.15 Eq. 298). The population mean (μ), coefficient of variance (CV) and heritability (h^2) of these traits are provided in Table 7.

All traits, other than those associated with parasite tolerance and resistance, were assumed to be uncorrelated (Doeschl-Wilson et al., 2008). The traits associated with parasite resistance ($Estab_{max}$, $Mort_{WB, max}$ and $Fecund_{max}$) were assumed to be a function of overlapping effector mechanisms (components of the Th2 immune response) (Jenkins and Allen, 2010), and as such strongly genetically and phenotypically correlated ($r = +0.5$). Similarly, the traits describing parasite tolerance (LB_{loss} and WB_{loss}) were also assumed to be strongly genetically and phenotypically correlated ($r = +0.5$). Subsequently, a Cholesky decomposition of the variance covariance matrix for correlated traits was used to generate the appropriate covariances.

Table 7. The population mean (μ), coefficients of variation (CV) and heritability (h^2) of traits exhibiting between-animal variation.

Parameter	Description	Category	Nematode species	μ	CV ^a	h^2
γ_m	Milk yield parameter	Lactation		0.739 ^b	0.25 ^b	0.33 ^b
e_{maint}	Maintenance energy requirement constant	Maintenance		1.870	0.15 ^c	0.25 ^c
p_{maint}	Maintenance protein requirement constant			0.004 ^c	0.15 ^c	0.25 ^c
LB_{loss}	Protein loss per larvae ($\mu\text{g d}^{-1}$)	Parasite tolerance	<i>T. colubriformis</i>	121 ^g	0.2	0.00
			<i>T. vitrinus</i>	121 ^g		
			<i>T. circumcincta</i>	126 ^f		
			<i>H. contortus</i>	123 ^g		
WB_{loss}	Protein loss per adult worm ($\mu\text{g d}^{-1}$)	Parasite tolerance	<i>T. colubriformis</i>	865 ^g	0.2	0.00
			<i>T. vitrinus</i>	865 ^g		
			<i>T. circumcincta</i>	898 ^f		
			<i>H. contortus</i>	876 ^g		
$PB_{\text{recog, delay}}$	Parasite burden recognition delay			7.000 ^d	0.10	0.00
Imm_{half}	Immune response half-life	Immune response		8.100 ^d	0.10	0.00
Imm_{rate}	Immune acquisition rate constant			350,000	0.25	0.25 ^c
$Estab_{\text{max}}$	Maximum proportion of larvae establishing		<i>T. colubriformis</i>	0.65 ^e	0.05 ^c	0.00 ^c
			<i>T. vitrinus</i>	0.65		
			<i>T. circumcincta</i>	0.74 ^e		
			<i>H. contortus</i>	0.59 ^e		
$Mort_{\text{WB, max}}$	Maximum mortality rate of adult worms	Parasite resistance	<i>T. colubriformis</i>	0.05 ^e	0.05 ^c	0.00 ^c
			<i>T. vitrinus</i>	0.05		
			<i>T. circumcincta</i>	0.11 ^e		
			<i>H. contortus</i>	0.12 ^e		
$Fecund_{\text{max}}$	Maximum fecundity rate		<i>T. colubriformis</i>	400 ^e	0.05 ^c	0.00 ^c
			<i>T. vitrinus</i>	400		
			<i>T. circumcincta</i>	240 ^e		
			<i>H. contortus</i>	3500 ^e		

^aPhenotypic variance (σ_p^2) = $(\mu \cdot CV)^2$; ^bSaccareau et al. (2016); ^cDoeschl-Wilson et al. (2008);

^dSingleton et al. (2011); ^eKao et al. (2000); ^fparameterised to Coop et al. (1982); ^gbased on comparison between the impact of *T. circumcincta* and the productive impact of the other species reported by Mavrot et al. (2015).

Simulation of a population allows for the calculation of the heritabilities, genetic correlations and phenotypic correlations of the model output traits. The heritability of and correlations between the following traits were calculated: live weight, empty body weight, body condition score, wool weight, FAMACHA[®] score, LN(faecal egg count +1), LN(larval burden +1), LN(worm burden +1) and LN(parasite burden +1).

3.8 Anthelmintic treatment and resistance

A total of 7 anthelmintic classes were considered, including the benzimidazole group (*BZ*, ‘white’, e.g. albendazole, fenbendazole, oxfendazole), the levamisole group (*LV*, ‘clear’, e.g. levamisole), the macrocyclic lactone group (*ML*, ‘mectins’, e.g. ivermectin, abamectin, moxidectin), the amino-acetonitrile derivative group (*AD*, e.g. monepantel), the spiroindole group (*SI*, e.g. derquantel), the organophosphate group (*OP*, e.g. naphthalophos) and the salicylanilides/phenols group (*SA*, e.g. closantel).

As per Barnes et al. (1995), resistance was determined by any number of independent genes (n_{gen}), each consisting of two alleles, *R* (resistant) and *S* (susceptible). Assuming a neutral mode of inheritance, anthelmintic efficacy was determined by the number of *R* alleles present. Since each nematode has $2n_{gen}$ alleles, there are $2n_{gen} + 1$ possible genotypes containing 0 to $2n_{gen}$ *R* alleles. The initial proportion of each genotype ($p_{gen,i}$) within the wider nematode population (on pasture and within host lifecycle stages) was subsequently calculated as:

$$p_{gen,i} = \frac{(2n_{gen})!}{(2n_{gen}-i-1)!(i-1)!} \cdot \left(1 - \frac{effic}{100}\right)^{i-1} \cdot \left(\frac{effic}{100}\right)^{2n_{gen}-i-1} \quad [\text{Eq. 326}]$$

where *effic* is the initial anthelmintic class efficacy (%; provided by user input); and *i* is genotype (1 to $2n_{gen} + 1$).

Anthelmintic treatment was assumed to impact both the infective larval burden (*LB*) and the adult worm burden (*WB*) resident within the host. The impact of anthelmintic treatment on the proportion of each genotype (for either the infective larval burden or the adult worm burden) was given as:

$$p_{gen,i} = p_{gen,i} \cdot \frac{i-1}{2n_{gen}} \quad [\text{Eq. 327}]$$

The infective larval burden (*LB*) and adult worm burden (*WB*) surviving anthelmintic treatment were consequently given as:

$$LB = LB \cdot \sum_{i=1}^{2n_{gen}+1} p_{gen,LB,i} \quad [\text{Eq. 328}]$$

$$WB = WB \cdot \sum_{i=1}^{2n_{gen}+1} p_{gen,WB,i} \quad [\text{Eq. 329}]$$

where $p_{gen,LB,i}$ is the proportion of genotype *i* for the larval burden (calculated as per Eq. 327); and $p_{gen,WB,i}$ is the proportion of genotype *i* for the worm burden (calculated as per Eq. 327).

The resistance genotype proportions within the larval and worm burdens were subsequently updated to ensure the new proportions added to 1, such that:

$$p_{gen,i} = p_{gen,i} \cdot \frac{p_{gen,i}}{\sum_{i=1}^{2n_{gen}+1} p_{gen,i}} \quad [\text{Eq. 330}]$$

Further, these resistance genotype proportions were updated daily to account for the influence ingested larvae, the establishment of new adult worms from the larval burden and the mortality rate of the adult worm burden.

The anthelmintic class efficacy against the resident adult worm burden (% $effic_{WB}$) was calculated by considering the total proportion of resistance alleles within the resident adult worm burden ($p_{R,WB}$), such that:

$$p_{R,WB} = \sum_{i=1}^{2n_{gen}+1} p_{gen,WB,i} \quad [\text{Eq. 331}]$$

$$effic_{WB} = (1 - p_{R,WB}) \cdot 100 \quad [\text{Eq. 332}]$$

The proportion of each resistance genotype within the eggs deposited ($p_{gen,egg,i}$) by the adult worm burden on any given day was consequently calculated assuming Hardy-Weinberg equilibrium, such that:

$$p_{gen,egg,i} = \frac{(2n_{gen})!}{(2n_{gen}-i-1)!(i-1)!} \cdot p_{R,WB}^{i-1} \cdot (1 - p_{R,WB})^{2n_{gen}-i-1} \quad [\text{Eq. 333}]$$

The resistance genotype proportions within the free-living lifecycle stages on pasture were also updated on a daily basis to account for the transition dynamics that determine the total population of each stage. The anthelmintic class efficacy of the infective larvae on herbage (% $effic_{L3h}$) was calculated to provide an indication of the difference between the resistance status of the pasture compared to the nematode burden resident within the host population. This may be considered as the anthelmintic class efficacy for a burden that would arise within a tracer sheep from ingestion of the current infective larvae on herbage. $effic_{L3h}$ was calculated as per Eq. 331 and 332 by replacing the worm burden variables with the associated variables for the infective larvae on herbage.

Whilst the ability to define the number of genes involved in the calculation of anthelmintic resistance has been retained within the model, currently all anthelmintic classes were assumed to be controlled by three independent genes (i.e. a trigenic mechanism). Further, the resistance status of each anthelmintic class was calculated independently inferring no cross-resistance; whereas complete side-resistance was assumed between actives within each class (i.e. each active within an anthelmintic class was not simulated separately).

The resistance/efficacy of each anthelmintic class was simulated separately for each nematode species. All anthelmintic classes were assumed to be effective against all nematode species except the salicylanilides/phenols group (SA) which was considered to only be effective against *Haemonchus contortus*. For all nematode species, the resistance genotypes were assumed to be equally fit (i.e. no fitness disadvantage). As such, any apparent reversion towards susceptibility occurs as a consequence of the dynamics of the nematode lifecycle. For anthelmintic class efficacies provided across nematode species, fluctuations occur due to changes in the proportional contribution of each nematode species, which may be expected to have different resistance profiles. Differences in the resistance profile of each nematode species arise from differences in the species-specific parasite burdens and *refugia* (free-living stages) at the time of any previous anthelmintic treatment.

A total of 62 anthelmintic formulation options (registered for use in Australia) were included within the model. Each was defined by specifying the constituent anthelmintic classes as well as the duration of efficacy against each nematode species in accordance with the WormBoss Drench Database (www.wormboss.com.au/sheep-goats/drenches.php). For formulations containing more than one anthelmintic class, additive efficacy was assumed by simulating the impact of each sequentially.

3.9 Scenario testing

3.9.1 Location

The location for any given scenario can be defined by the user inputs required for section 3.1. These include the latitude (LAT , °) and elevation (z , m above sea level), as well as the provision of meteorological variables covering the period which the user wishes to simulate. The input meteorological variables include: rainfall/precipitation (PCP , mm d⁻¹), solar radiation (R_s , MJ m⁻² d⁻¹), the daily maximum air temperature (T_{max} , °C), the daily minimum air temperature (T_{min} , °C), the vapour pressure at 9am ($e_{a,9}$, kPa), the vapour pressure at 3pm ($e_{a,3}$, kPa) and the wind speed measured at 10m above ground level (u_{10} , m s⁻¹).

The wind speed measured at 10m above ground level (u_{10} , m s⁻¹) is specified as a user input due to the provision of this variable within Australian meteorological databases. This variable is converted to the wind speed measured at 2m above ground level (u_2 , m s⁻¹) within the model in accordance with Eq. 18 (section 3.1.10).

The inputs for vapour pressure at 9am ($e_{a,9}$, kPa) and vapour pressure at 3pm ($e_{a,3}$, kPa) are used to calculate daily average vapour pressure (e_a , kPa). As such, if the 9am and 3pm variables are unavailable these inputs can both be populated by the daily average vapour pressure (e_a , kPa).

3.9.2 Paddock setup

The user can define an unlimited number of paddocks which are numbered sequentially (Fig. 4). For each paddock user inputs are required to define: the initial crude protein content of plant dry matter ($CP\%$, %, section 3.2.8), the initial metabolizable energy content of plant dry matter (ME , MJ [kg dry matter]⁻¹, section 3.2.8), the initial pasture height (PHT , m), the soil textural type (as per section 3.3.2.1 Table 2), the initial inorganic soil nitrogen content ($N_{s,1}$, mg kg⁻¹, section 3.3.1 Eq. 111), the paddock size (PS , ha) and the initial pasture infectivity (INF , larvae [kg dry matter]⁻¹, section 3.4.2.3).

Initial paddock values

Paddock	Crude Protein (%)	Metabolizable energy (MJ kg ⁻¹)	Pasture height (m)	Soil type	Soil nitrogen content (mg kg ⁻¹)	Paddock size (ha)	Paddock infectivity (infective larvae kg ⁻¹)
1	8.7	8	0.2	Clay loam ▼	120	10	0
2	9.5	7.8	0.3	Sandy clay loam ▼	40	7	3200
+							

Figure 4. Initial concept design for the paddock setup user-interface.

Due to the underlying pasture model assumptions relating to plant composition, the user input for the initial crude protein content of plant dry matter ($CP\%$, %) must be between 0 and 38% (section 3.2.8 Eq. 67), and the initial metabolizable energy content of plant dry matter (ME , MJ [kg dry matter]⁻¹) must be between the maximum and minimum values specified by Eq. 70 and Eq. 71, respectively (section 3.2.8).

The initial pasture height (PHT , m) was specified as a user input that can be easily measurable/estimated value. Where the initial pasture mass is known (PM_{SH} , kg dry matter ha⁻¹), the initial pasture height can be estimated as:

$$PHT = \frac{SLA \cdot f_{lam} \cdot PM_{SH}}{87} \quad [\text{Eq. 334}]$$

where f_{lam} is the lamina fraction of shoot dry matter (0.7 g⁻¹; Thornley and Verberne, 1989); and SLA is specific leaf area (0.02 m² g⁻¹; Arrendondo and Schnyder, 2003).

3.9.3 Mob setup

The user can define an unlimited number of mobs which are numbered sequentially (Fig. 5). For each mob user inputs are required to define: the mob size (*MS*, sheep), the mob gender (*MG*; female, male or mixed), the breed composition (% Border Leicester, Dorset, Merino and Suffolk), the prior shear date (yyyy-mm-dd, if applicable) and the initial mean live weight at first allocation (*LW*, kg).

Initial mob values									
Mob	Number of sheep	Sex	Breed composition (%)				Prior shear date*	Mean live weight (kg)	
			Border Leicester	Dorset	Merino	Suffolk			
1	15	female ▼	0	0	100	0	2014-11-24 ▼	35.5	-
2	21	male ▼	33.4	20.3	0	46.3	▼	60	-
+									

* Prior shear date is optional, leave blank for no prior shear date.

Figure 5. Initial concept design for the mob setup user-interface.

The breed composition inputs were used to generate a population of 2,000 sheep (section 3.7), where the population mean (μ), coefficients of variation (*CV*) and heritability (h^2) of traits exhibiting between-animal variation were thereby given as a weighted average of the specified breed composition. The mob gender input was used to determine the population means (μ) and coefficients of variation (*CV*) for body composition traits exhibiting between-animal variation. For mixed gender mobs, the population of 2,000 sheep was considered to be comprised of 1,000 females and 1,000 males.

Due to each mob being simulated as a population of 2,000 sheep, certain variables required adjustment to account for mob size (*MS*, sheep). The considerations included to account for mob size are provided in section 3.9.5.

The initial mean live weight at first allocation (*LW*, kg) for each mob was used to calculate the initial body composition of each individual animal within the simulated population. To account for between-animal variation in these initial body composition traits, the initial mean live weight was first used to determine the mob average current body protein content ($Protein_{mob}$, kg) as per section 3.6.17.2 using the population mean values for the proportional protein content of the fleece-free empty body weight at maturity (α_{mat} , section 3.7) and the fleece-free empty body weight at maturity (EBW_{mat} , kg, section 3.7). $Protein_{mob}$ was subsequently used to estimate the mob's initial level of maturity (Mat_{mob}) such that:

$$Mat_{mob} = \frac{Protein_{mob}}{\alpha_{mat} \cdot EBW_{mat}} \quad [Eq. 335]$$

The initial body protein content (*Protein*, kg) of each individual animal within a simulated population was consequently given as:

$$Protein = Mat_{mob} \cdot Protein_{mat} \quad [Eq. 336]$$

where $Protein_{mat}$ is the protein content at maturity (kg, section 3.6.1.4 Eq. 158) for each individual animal.

The remaining body composition traits were thereby calculated for each individual animal in accordance with section 3.6.17.2.

3.9.4 Mob joining/mating

The user can define an unlimited number of joining/mating events which are numbered sequentially (Fig. 6). For each mating event user inputs are required to define: the date of mating (yyyy-mm-dd), and the mobs to be mated.

Mating/joining

Join	Date	Mob 1	Mob 2
1	2015-04-01 ▼	1 ▼	2 ▼ -
+			

Available mobs

Mob	Sex	Breed composition (%)			
		Border Leicester	Dorset	Merino	Suffolk
1	female	0	0	100	0
2	male	33.4	20.3	0	46.3

Figure 6. Initial concept design for the mating event input user-interface.

The mobs available for mating are provided as per the user inputs for mob setup (section 3.9.3). When defining the mobs to be mated, these mobs must be of opposite gender. It should be noted that the ability to mate mobs of mixed gender is not currently supported by the model. Further, female mobs can not be mated if they are already pregnant from a previously specified mating (where the gestation period is given as 147 days) or if they are currently nursing pre-weaning lambs (see section 3.9.5).

Offspring were assumed to be born following a 147 day gestation period from the date of mating. Each ewe was assumed to give birth to a single lamb such that the model retains a population size of 2,000 for the offspring mob. Hence, the mob size (*MS*, sheep) of the offspring mob was given as equal to that of the maternal mob.

Offspring mobs were numbered sequentially by adding the total number of mobs specified at mob setup (section 3.9.3) to the mating event from which they arose. For example, if 2 mobs were specified at mob setup and 1 mating event was specified, then the offspring arising from mating event 1 would be given as mob 3 (2+1).

All offspring mobs were assumed to be of mixed gender. Further, traits exhibiting between-animal variation (section 3.7) were defined assuming that the breed composition of the offspring mob was given by the average of the parental mobs. The routine used to generate each population used the same pseudo-random number seed on each occasion. As such, the i^{th} individual within the offspring population represents the progeny of the i^{th} individual within the maternal and paternal populations. This consideration is particularly important when considering the milk intake (section 3.6.5.6) of any suckling lamb (i.e. which ewe is nursing which lamb).

3.9.5 Mob allocation

To enable grazing strategies such as paddock rotation, each mob can be allocated to any paddock on any given date. The user can define an unlimited number of mob allocations (Fig. 7). For each mob allocation user inputs are required to define: the mob, the paddock, and the date of allocation (yyyy-mm-dd).

Mob allocation to paddocks

Allocation	Mob	Paddock	Date
1	1	1	2015-01-01
2	2	2	2015-02-20
3	2	remove	2015-04-02
4	3	2	2015-11-30
+			

Available mobs

Mob	Sex	Breed composition (%)			
		Border Leicester	Dorset	Merino	Suffolk
1	female	0	0	100	0
2	male	33.4	20.3	0	46.3
3	mixed	offspring from join 1, available for allocation from: 2015-08-26*			

*Offspring will be automatically allocated to the paddock of the mother mob (i.e. does not require explicit allocation). Weaning can be simulated by allocating either the mother mob or offspring mob to a different paddock following birth (date available for allocation).

Figure 7. Initial concept design for the mob allocation user-interface.

Allocations can be made on any date, where the first allocation of any given mob does not need to be the first date of the simulated period. Each mob was assumed to remain on its allocated paddock until a subsequent allocation is specified. Further, each mob can be removed from the simulation on any date by allocating the mob to paddock 0. Offspring mobs are automatically allocated to the same paddock as the maternal mob at birth. Weaning can be simulated by allocating either the maternal mob or the offspring mob to a different paddock on any date following birth.

Once the paddock allocation of each mob is defined, adjustments can be made to account for the influence of paddock size (PS , ha) and mob size (MS , sheep) on the variables that link the different model components. These include the total pasture mass dry matter intake of mobs grazing any given paddock (DMI_{PM} , $g\ m^{-2}\ d^{-1}$, section 3.2.9), the total supplementary feed intake of mobs grazing any given paddock (I_{sup} , kg, section 3.5.4), the total quantity of nitrogen excreted by mobs grazing any given paddock (N_{exc} , $g\ N\ m^{-2}\ d^{-1}$, section 3.3.1), the total infective larvae intake of mobs grazing any given paddock ($L3_{h,in}$, larvae d^{-1} , section 3.4.2.1), the total number of nematode eggs deposited by mobs grazing any given paddock (Egg_{dep} , eggs d^{-1}) and the number of sheep grazing a given paddock (n_{sheep} , section 3.6.5.3 Eq, 193)

The total pasture mass dry matter intake of any mobs grazing the same paddock (DMI_{PM} , $g\ m^{-2}\ d^{-1}$) was calculated as the sum of the intake of each mob, where the pasture mass intake of each mob ($DMI_{PM,mob}$, $g\ m^{-2}\ d^{-1}$) was given as:

$$DMI_{PM,mob} = \frac{MS}{20000 \cdot PS} \cdot \sum_{i=1}^{2000} FI_{PM,i} \quad [\text{Eq. 337}]$$

where $Fl_{PM,i}$ is the pasture mass feed intake of the i^{th} individual within a population of 2,000 sheep (kg d^{-1} , section 3.6.5.8 Eq. 214).

The total supplementary feed intake of mobs grazing the same paddock (I_{sup} , kg) was calculated as the sum of the intake of each mob, where the supplementary feed intake of each mob ($I_{\text{sup,mob}}$) was given as:

$$I_{\text{sup,mob}} = \frac{MS}{2000} \cdot \sum_{i=1}^{2000} Fl_{\text{SUP},i} \quad [\text{Eq. 338}]$$

where $Fl_{\text{SUP},i}$ is the supplementary feed intake of the i^{th} individual within a population of 2,000 sheep (kg d^{-1} , section 3.6.5.8 Eq. 215).

The total quantity of nitrogen excreted by mobs grazing the same paddock (N_{exc} , $\text{g N m}^{-2} \text{d}^{-1}$) was calculated as the sum of nitrogen excreted by each mob, where the nitrogen excretion of each mob ($N_{\text{exc,mob}}$, $\text{g N m}^{-2} \text{d}^{-1}$) was given as:

$$N_{\text{exc,mob}} = \frac{MS}{20000 \cdot PS} \cdot \sum_{i=1}^{2000} (N_{\text{urea},i} + N_{\text{faeces},i}) \quad [\text{Eq. 339}]$$

where $N_{\text{urea},i}$ is the nitrogen content of urea of the i^{th} individual within a population of 2,000 sheep (kg N d^{-1} , section 3.6.8.8 Eq. 255); and $N_{\text{faeces},i}$ is the nitrogen content of faeces of the i^{th} individual within a population of 2,000 sheep (kg N d^{-1} , section 3.6.11 Eq. 276).

The total infective larvae intake of mobs grazing the same paddock ($L3_{\text{h,in}}$, larvae d^{-1}) was calculated as the sum of larval intake of each mob, where the infective larvae intake of each mob (LI_{mob} , larvae d^{-1}) was given as:

$$LI_{\text{mob}} = \frac{MS}{2000} \cdot \sum_{i=1}^{2000} LI_i \quad [\text{Eq. 340}]$$

where LI_i is the larval intake of the i^{th} individual within a population of 2,000 sheep (larvae d^{-1} , section 3.6.12 Eq. 277).

The total number of nematode eggs deposited by mobs grazing the same paddock (Egg_{dep} , eggs d^{-1}) was calculated as the sum of egg deposition of each mob, where the egg deposition of each mob ($Egg_{\text{dep,mob}}$, eggs d^{-1}) was given as:

$$Egg_{\text{dep,mob}} = \frac{MS}{2000} \cdot \sum_{i=1}^{2000} Egg_{\text{dep},i} \quad [\text{Eq. 341}]$$

where $Egg_{\text{dep},i}$ is the egg deposition of the i^{th} individual within a population of 2,000 sheep (larvae d^{-1} , section 3.6.14 Eq. 285).

Finally, the number of sheep grazing the same paddock (n_{sheep}) was calculated as the sum of the mob size (MS , sheep) of each mob.

3.9.6 Supplementary feed

Supplementary feed is provided on a paddock basis, i.e. will be available to all mobs allocated to a particular paddock at any given date. The user can define an unlimited number of supplementary feed provisions (Fig. 8). Each supplementary feed is defined by user inputs specifying: the paddock to which the supplementary feed is to be provided, the date of provision (yyyy-mm-dd), the supplementary feed type (cereal pellets, hay, silage or straw), the quantity of supplementary feed provided (SUP , kg), the crude protein content ($CP\%_{\text{sup}}$, %), and the metabolizable energy content (ME_{sup} , MJ kg^{-1}).

Supplementary feed inputs

Supplementary feed	Provided to paddock	Date	Feed type	Quantity (kg)	Crude Protein (%)	Metabolizable energy (MJ kg ⁻¹)	
1	1	2015-04-10	Cereal pellets	6	15	12	-
2	1	2015-04-10	Straw	4.5	5	7.1	-
3	2	2015-03-10	Silage	10	6.9	10.5	-
+							

Mob allocation to paddocks

Allocation	Mob	Paddock	Date
1	1	1	2015-01-01
2	2	2	2015-02-20
3	2	remove	2015-04-02
4	3	2	2015-11-30

Figure 8. Initial concept design for the supplementary feed input user-interface.

When providing cereal pellets as supplementary feed, straw is often also provided as a source of roughage. As such, supplementary feed of mixed feed types can be specified by the provision of two separate supplementary feeds to the same paddock on the same day.

Due to the underlying assumptions relating to composition of supplementary feed, the user input for the crude protein content of supplementary feed ($CP\%_{sup}$, %) must be between 0 and 89.8%, and the metabolizable energy content of supplementary feed (ME_{sup} , MJ kg⁻¹) must be between the maximum and minimum values given as:

$$ME_{sup,max} = -0.000026 \cdot CP\%_{sup}^2 + 0.052 \cdot CP\%_{sup} + 11.48 \quad [\text{Eq. 342}]$$

$$ME_{sup,min} = -0.00046 \cdot CP\%_{sup}^2 + 0.16 \cdot CP\%_{sup} + 5.312 \quad [\text{Eq. 343}]$$

3.9.7 Shearing

The user can define an unlimited number of shearing events (Fig. 9). Each shearing event is defined by user inputs specifying: the mob to be sheared, and the date of the shearing event (yyyy-mm-dd).

The sheared wool weight ($Wool_{shear}$, kg) of all individuals within any simulated was initially set to zero. On the day of shearing, the current wool weight ($Wool$, kg) was added to the sheared wool weight ($Wool_{shear}$, kg) and then the current wool weight ($Wool$, kg) was set to zero.

Shearing

Shear	Mob		Date		
1	1	▼	2015-10-01	▼	-
2	2	▼	2015-03-15	▼	-
+					

Available mobs

Mob	Sex	Breed composition (%)			
		Border Leicester	Dorset	Merino	Suffolk
1	female	0	0	100	0
2	male	33.4	20.3	0	46.3
3	mixed	offspring from join 1, available for shearing from: 2015-08-26			

Figure 8. Initial concept design for the shearing event input user-interface.

3.9.8 Anthelmintic treatment

An unlimited number anthelmintic treatments can be defined by the user (Fig. 9). Each anthelmintic treatment is defined by user inputs specifying: the mob to be treated, the date of the treatment (yyyy-mm-dd), the anthelmintic formulation (62 options available), the treatment protocol (entire mob, fixed mob percentage or by trait threshold), the trait used to determine which individuals to treat (body condition score, faecal egg count, FAMACHA[®] score, growth rate or live weight), the trait threshold determining treatment, and the percentage of the population to be treated (%).

Treatments											
Treatment	Mob		Date		Formulation		Protocol ¹		Trait ²	Threshold ³	Percentage ⁴ (%)
1	1	▼	2015-02-01	▼	Alben (Virbac)	▼	Entire mob	▼	None		
2	1	▼	2015-11-08	▼	Hat-trick (Ancare)	▼	Fixed mob %	▼	Live weight (kg)		50
3	1	▼	2015-11-08	▼	Zolvix (Elanco)	▼	By trait threshold	▼	Faecal egg count (eggs g-1)	500	
4	2	▼	2015-01-05	▼	Cydectin Long-Acting Injection (Virbac)	▼	Entire mob	▼	None		
+											

¹Only entire mob treatments can be selected for dates before or at first allocation

²Only required for 'fixed mob %' or 'by trait threshold' treatment protocols

³Only required for 'by trait threshold' protocol

⁴Only required for 'fixed mob %' protocol

Available mobs

Mob	Sex	Breed composition (%)			
		Border Leicester	Dorset	Merino	Suffolk
1	female	0	0	100	0
2	male	33.4	20.3	0	46.3
3	mixed	offspring from join 1, available for treatment from: 2015-08-26			

Figure 9. Initial concept design for the anthelmintic treatment input user-interface.

When targeted selective treatment is simulated (fixed mob percentage or threshold treatment protocols) the traits available to determine which individuals get treated were: body condition score (*BCS*, section 3.6.1.5 Eq. 162), faecal egg count (*FEC*, eggs d⁻¹, section 3.6.14 Eq. 287), FAMACHA[®] score (section 3.6.13 Eq. 284), growth rate ([g live weight] d⁻¹), and live weight (*LW*, kg, section 3.6.1.3 Eq. 157). For all traits except *FEC*, values from the day prior to treatment were used. For *FEC* the values from five days prior to treatment were used to allow laboratory processing time. When the treatment protocol was specified to be 'by trait threshold'; trait values greater than the specified threshold were treated for *FEC* and FAMACHA[®] score; and trait values less than the specified threshold were treated for *BCS*, growth rate and *LW*. When the treatment protocol was specified to be a 'fixed mob percentage', the individuals within a simulated population were treated according to the highest values for *FEC* and FAMACHA[®] score, and the lowest values for *BCS*, growth rate and *LW*.

3.9.9 Anthelmintic class efficacies

The initial anthelmintic efficacy for each of the seven anthelmintic classes considered by the model can be defined by user input (Fig. 10). These anthelmintic classes include the benzimidazole group (*BZ*, 'white', e.g. albendazole, fenbendazole, oxfendazole), the levamisole group (*LV*, 'clear', e.g. levamisole), the macrocyclic lactone group (*ML*, 'mectins', e.g. ivermectin, abamectin, moxidectin), the amino-acetonitrile derivative group (*AD*, e.g. monepantel), the spiroindole group (*SI*, e.g. derquantel), the organophosphate group (*OP*, e.g. naphthalophos) and the salicylanilides/phenols group (*SA*, e.g. closantel).

The user input for the initial anthelmintic class efficacy must be between 0 and 99.99%. Not all initial anthelmintic class efficacies need to be specified. If the initial anthelmintic class efficacy is unknown/unspecified then the initial anthelmintic class efficacy is automatically set to 99.99%.

Initial anthelmintic class efficacies

Input	Class ¹		Efficacy ² (%)	
1	LV	▼	90	-
2	SI	▼	72.5	-
3	SA	▼	83.2	-
+				

¹BZ = benzimidazole group ('white'), e.g. albendazole, fenbendazole, oxfendazole

LV = levamisole group ('clear'), e.g. levamisole

ML = macrocyclic lactone group ('mectins'), e.g. ivermectin, abamectin, moxidectin

AD = amino-acetonitrile derivative group, e.g. monepantel

SI = spiroindole group, e.g. dequantel

OP = organophosphate group, e.g. naphthalophos

SA = salicylanilides/phenols group, e.g. closantel

²0-99.99%, SA efficacy should be considered as the efficacy against *Haemonchus contortus* (Barber's pole)

Figure 10. Initial concept design for the anthelmintic class efficacy input user-interface.

3.9.10 Economics

The user can input economic values for any of the available mobs (Fig. 11). The economic values include the trade price of meat ($Meat_{price}$, cents [kg carcass weight]⁻¹), and the trade price of wool ($Wool_{price}$, cents [kg clean wool]⁻¹). If no economic inputs are provided for any mob, then the model assumes zero values.

Economic inputs					
Input	Mob		Meat price (¢ kg ⁻¹ carcass weight)	Wool price (¢ kg ⁻¹ clean wool)	
1	1	▼	700	1400	-
2	2	▼	740	1520	-
3	3	▼	720	1460	-
+					

Available mobs					
Mob	Sex	Breed composition (%)			
		Border Leicester	Dorset	Merino	Suffolk
1	female	0	0	100	0
2	male	33.4	20.3	0	46.3
3	mixed	offspring from join 1			

Figure 10. Initial concept design for the economic input user-interface.

Carcass weight ($W_{carcass}$, kg) was calculated in accordance with Shija et al. (2013), such that:

$$W_{carcass} = 0.6142 \cdot EBW \quad [Eq. 344]$$

where EBW is the fleece-free empty body weight (kg, section 3.6.1.1 Eq. 153)

The economic meat value (AUD_{meat} , \$AUD) for each mob was consequently calculated as:

$$AUD_{meat} = Meat_{price} \cdot \frac{MS}{200000} \cdot \sum_{i=1}^{2000} W_{carcass,i} \quad [Eq. 345]$$

where MS is mob size (sheep); and $W_{carcass,i}$ is the carcass weight of the i^{th} individual within a population of 2,000 sheep (kg).

The economic wool value (AUD_{wool} , \$AUD) for each mob was calculated as:

$$AUD_{wool} = Wool_{price} \cdot \frac{MS}{200000} \cdot \sum_{i=1}^{2000} (Wool_i + Wool_{shear,i}) \quad [Eq. 346]$$

where MS is mob size (sheep); $Wool_i$ is the current wool weight of the i^{th} individual within a population of 2,000 sheep (kg); and $Wool_{shear,i}$ is the sheared wool weight of the i^{th} individual within a population of 2,000 sheep (kg, section 3.9.7).

3.9.11 Optional outputs

The calculation of phenotypic correlations, genotypic correlation and heritabilities are computationally time consuming and only of interest to a narrow selection of users. Consequently, these are given as optional outputs (Fig. 11).

Optional outputs*	
Output	
Phenotypic correlations	×
Heritabilities	
Genotypic correlations	×

*Optional outputs require additional complex calculations that may be time-consuming

Figure 11. Initial concept design for the optional output user-interface.

3.10 Model outputs

3.10.1 Pasture traits

Available pasture traits include:

1. Neutral detergent fibre (%)
2. Acid detergent fibre (%)
3. Acid detergent lignin (%)
4. Crude protein (%)
5. Dry matter digestibility (%)
6. Dry organic matter digestibility (%)
7. Metabolizable energy (MJ kg⁻¹)
8. Pasture mass (kg ha⁻¹)
9. Pasture mass available for grazing (kg ha⁻¹)
10. Volumetric soil water content (m³ water [m³ soil]⁻¹)
11. *H.contortus* pasture infectivity (infective larvae kg⁻¹)
12. *T.circumcincta* pasture infectivity (infective larvae kg⁻¹)
13. *T.colubriformis* pasture infectivity (infective larvae kg⁻¹)
14. *T.vitrinus* pasture infectivity (infective larvae kg⁻¹)
15. Total pasture infectivity (infective larvae kg⁻¹)
16. Benzimidazole efficacy (%)
17. Levamisole efficacy (%)
18. Macrocylic lactone efficacy (%)
19. Amino-acetonitrile efficacy (%)
20. Spiroindole efficacy (%)
21. Organophosphate efficacy (%)
22. Salicylanide efficacy (%)

3.10.2 Mob traits

Available mob traits include:

1. Live weight (kg)
2. Empty body weight (kg)
3. Body condition score
4. Wool weight (kg)
5. FAMACHA score
6. Mortality (%)
7. Total mob carcass weight (kg)
8. Total mob wool production (kg)
9. Total mob meat value (\$)
10. Total mob wool value (\$)
11. *H.contortus* faecal egg count (eggs g⁻¹)
12. *T.circumcincta* faecal egg count (eggs g⁻¹)
13. *T.colubriformis* faecal egg count (eggs g⁻¹)
14. *T.vitrinus* faecal egg count (eggs g⁻¹)
15. Total faecal egg count (eggs g⁻¹)
16. *H.contortus* larval burden

17. *T.circumcincta* larval burden
18. *T.colubriformis* larval burden
19. *T.vitrinus* larval burden
20. Total larval burden
21. *H.contortus* worm burden
22. *T.circumcincta* worm burden
23. *T.colubriformis* worm burden
24. *T.vitrinus* worm burden
25. Total worm burden
26. *H.contortus* total burden
27. *T.circumcincta* total burden
28. *T.colubriformis* total burden
29. *T.vitrinus* total burden
30. Total burden
31. Benzimidazole efficacy (%)
32. Levamisole efficacy (%)
33. Macrocyclic lactone efficacy (%)
34. Amino-acetonitrile efficacy (%)
35. Spiroindole efficacy (%)
36. Organophosphate efficacy (%)
37. Salicylanide efficacy (%)

3.10.3 Phenotypic correlations, genotypic correlations and heritabilities

Heritabilities are provided for; and phenotypic and genotypic correlations are provided between; the following traits:

1. Live weight (kg)
2. Empty body weight (kg)
3. Body condition score
4. Wool weight (kg)
5. Famacha score
6. Log-transformed faecal egg count (eggs g⁻¹)
7. Log-transformed larval burden
8. Log-transformed worm burden
9. Log-transformed total burden

4. Validation studies

The objective of the field studies was to provide data for model validation ensuring the capture of regional climatic conditions and management practices. As such field studies were proposed to run at two distinct locations in New South Wales and Victoria representing summer and winter rainfall regions, respectively.

4.1 Site locations and initial setup

The New South Wales study was carried out at UNE Rural Properties (Maxwellton) in Armidale NSW (latitude: -30.5°, elevation: 980m); whereas, the Victoria study was carried out at 'Lal Lal' (300 Yendon-Mount Egerton Road, Yendon) (latitude: -37.7°, elevation: 509m).

Each site consisted of 4 replicate paddocks (2 ha each) and a laneway (Fig. 12). Each paddock had access to water, and a Davis Instruments wireless Vantage Pro 2 weather station was installed in the laneway.

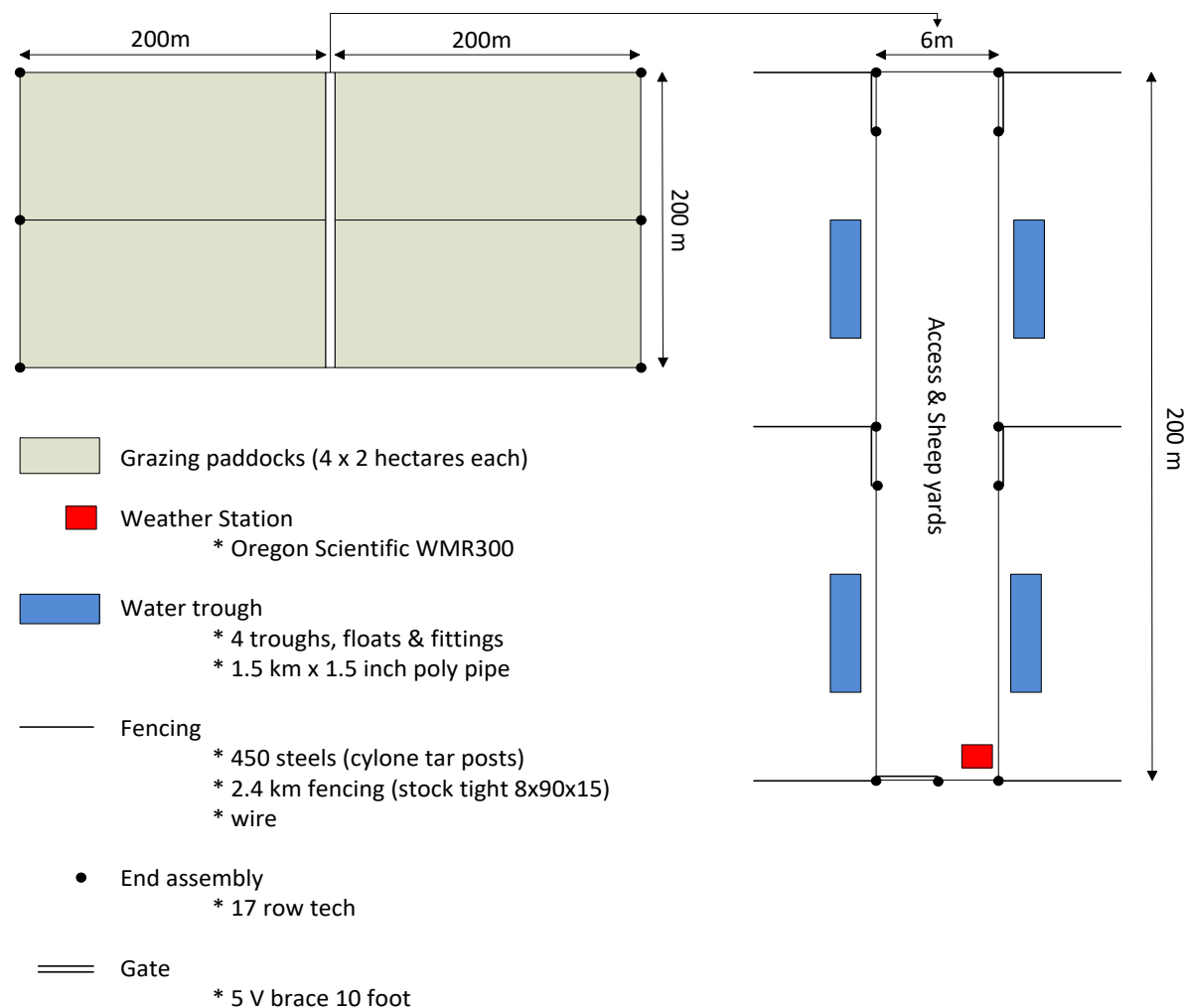


Figure 12. Initial proposed experimental site design.

The site setup at Maxwellton (Armidale, NSW) differed slightly from this design due to the availability of existing infrastructure as part of the UNE Rural Properties. These facilities included 4 paddocks (2 ha each) each with access to water and a laneway. The only difference between the site setup and the initially proposed site design (Fig. 12) was the orientation of the paddocks in relation to the laneway (4 paddocks on one side of a laneway). The weather station was consequently installed within one of the paddock to allow for more central placement. Figure 13 provided an annotated satellite image of the Maxwellton (NSW) experimental site.



Figure 13. Maxwellton (NSW) experimental site indicating the 4 paddocks (2 ha each), and the location of the weather station (x).

The site setup at Lal Lal (Yendon, VIC) matched the initially proposed site design (Fig. 12). Photographs of the Lal Lal (VIC) experimental site are provided in Fig. 14.



Figure 13. Lal Lal (VIC) experimental site. a) Central laneway, b) Paddocks 1 & 2, c) Paddocks 3 & 4, d) Weather station.

4.2 Experimental design

The original experimental design for the validation studies is provided below.

4.2.1 Initial pasture contamination

- A 'donor' flock of 80 Merino yearlings will be grazed on the experimental site (20 yearlings per paddock). On the day of placement, faecal samples (bulk of 'donor' flock) will be taken for:
 - Faecal egg count (FEC).
 - Coproculture/larval differentiation to determine nematode genus percentages.
- One week following placement of the 'donor' flock (when coproculture/larval differentiation results are available), a decision needs to be made as to whether the 'donor' flock requires artificial infection. If bulk FEC indicated >400epg, and the coproculture/larval differentiation identified *Haemonchus*, *Trichostrongylus* and *Teladorsagia* each contributing >20%; then no artificial infection is required. Otherwise, the 80 Merino yearlings will be drenched (Initial effective combination: Zolvix + albendazole/levamisole/abamectin) to remove existing infection.
- Two weeks following placement, if artificial infection is required then the 80 Merino yearlings should be given a mixed nematode genus bolus (sourced from VHR/Invetus), and subsequently be left to graze the experimental site to generate the initial pasture larvae contamination.
- Bulk (paddock) faecal samples will be taken from the 80 Merino yearlings at weekly intervals to confirm egg deposition and nematode genus prevalence.
- Twelve weeks following placement of the 'donor' flock, the 80 Merino yearlings will be moved to a holding paddock for a faecal egg count reduction test (FECRT) to determine initial anthelmintic class & genus efficacy.

4.2.2 Monitoring period

- Immediately following removal of 'donor flock', 60 Merino weaners should be tagged and treated with short acting anthelmintic to remove existing infection (Initial effective combination: Zolvix + albendazole/levamisole/abamectin). The following measurements should be taken:
 - Live weight (each sheep).
 - Body condition score (each sheep).
 Weaners should then be allocated to the paddocks (15 weaners x 4 paddocks) ensuring equal distribution of live weight & body condition score.
- After one week (following placement of weaners), the following measurements/samples should be taken (& analysed):
 - Faecal samples for bulk FEC (each paddock) to confirm removal of existing infection.
 - Pasture samples (per paddock) for pasture quality, mass & infectivity.
- At monthly intervals (following placement of weaners) the following measurements/samples should be taken (& analysed):
 - Live weight (each sheep).
 - Body condition score (each sheep).
 - Faecal samples (each sheep) for individual FEC and paddock coproculture.
 - Pasture samples (each paddock) for pasture quality, mass & infectivity.

- In regards to anthelmintic treatment:
 - No strategic treatments.
 - Drench at high mean WEC threshold (e.g. for Armidale mean FEC >1500 eggs g⁻¹).
 - All paddocks are to be treated the same.
 - All treatments should be with a single active, rotating the use of albendazole or abamectin at each occasion. Levamisole is not to be used, we test for levamisole resistance in the FECRT to check that there are no changes in resistance in the absence of its use.
- FECRT to be carried out at the end of each year following flock removal from the experimental site. Merino weaners to be replaced at the start of the second year following the design described above.

4.2.3 Overview

Table 8. Overview of validation study experimental design.

Study Day	Activity
0	80 Merino yearlings placed onto paddocks to generate initial pasture larval contamination. Faecal samples collected for bulk (flock) FEC and coproculture.
7	Results of coproculture determine requirement for artificial infection. If no artificial infection required, bulk paddock FEC and coproculture. If artificial infection required, drench to remove existing infection.
14	If no artificial infection required then bulk paddock FEC and coproculture (to monitor egg & genus deposition). If artificial infection required, bulk FEC to confirm removal of existing infection, then artificial challenge administered.
21, 28, 35, 42, 49, 56, 63, 70 & 77	Bulk paddock FEC and coproculture (to monitor egg & genus deposition).
84	80 Merino yearlings removed from paddocks for FEC reduction test.
85	60 Merino weaners placed onto paddocks: Live weight measurement, body condition scoring & anthelmintic drench (to remove pre-existing infections).
92	Bulk paddock FEC to confirm removal of existing infection. Pasture samples collected from each paddock for pasture quality, mass & infectivity analysis.
122, 152, 182, 212, 242, 272, 302, 332, 362, 392 & 422	Live weight & body condition scoring. Faecal samples collected for individual FEC (each animal) & coproculture (each paddock). Drenching if required according to WEC threshold. Pasture samples collected from each paddock for pasture quality, mass & infectivity analysis.
449	60 Merino sheep removed from paddocks for FEC reduction test.
450	60 replacement Merino weaners placed onto paddocks: Live weight measurement, condition scoring & anthelmintic drench (to remove pre-existing infections).
457	Bulk paddock FEC to confirm removal of existing infection. Pasture samples collected from each paddock for pasture quality, mass & infectivity analysis.
487, 517, 547, 577, 607, 637, 667, 697, 727, 757 & 787	Live weight & body condition scoring. Faecal samples collected for individual FEC (each animal) & coproculture (each paddock). Drenching if required according to WEC threshold. Pasture samples collected from each paddock for pasture quality, mass & infectivity analysis.
814	60 Merino sheep removed from paddocks for FEC reduction test.
840	All analysis completed. End of experiment.

4.3 Methods

4.3.1 Faecal egg count (bulk)

- a. Faecal sampling:
 1. Collect 50g of freshly deposited faeces from each paddock (ensuring that the sample is representative of entire grazing flock on paddock).
 2. Place each sample into a container.
 3. Label each container (paddock and sampling date).
Samples can be stored in a 4°C fridge for up to one week.

- b. Laboratory procedure:
 1. Place bulk faecal sample into 1000ml plastic beaker (separate beaker per paddock).
 2. Crush samples with spatula until all pellets blended together.
 3. For each sample, tare scales with a 250ml collection jar and weigh out 30g of faecal sample (**A**). Retain the remaining faecal sample for coproculture.
 4. Add 150ml water (**B**) to each 30g faecal sample.
 5. Mix samples using a homogeniser with a large mixing blade.
 6. Prepare 5 Whitlock Universal counting slide chambers (per 30g faecal sample) by filling each chamber with 600µl (**C**) saturated salt solution (specific gravity = 1.2).
 7. Place a large sieve into each sample and draw 5 aliquots of 150µl (**D**) from within the sieve.
 8. Carefully add each aliquot to the Whitlock counting slide chambers containing the saturated salt solution (150µl per chamber).
 9. Allow slides to sit for 2 minutes to float parasite eggs to surface.
 10. Identify and count strongylid eggs (oval shaped, 80-90 microns longs) within the grided area of each slide chamber (**E**, 0.5ml) using a compound microscope at x40 magnification (x4 objective, x10 eyepieces).
 11. Calculate the mean average egg count of the five chambers (**F**, eggs).
 12. Faecal egg count (FEC, epg) is calculated as:

$$FEC = \frac{1}{\frac{A}{A+B} \cdot \frac{D}{C+D}} \cdot F = 60 \cdot F \quad [\text{Eq. 347}]$$

where **A** is the faecal sample (30g), **B** is the quantity of distilled water added to the faecal sample (150ml), **C** is the quantity of saturated salt solution added to each Whitlock slide chamber (600µl), **D** is the quantity of diluted faecal sample added to each Whitlock slide chamber (150µl), **E** is the quantity of the sample within the grided area of the Whitlock slide chamber (0.5ml), and **F** is the mean average egg count of five chambers.

13. Record paddock, sampling date & FEC.

4.3.2 Faecal egg count (individual)

- a. Faecal sampling:
1. Collect 5g of faeces from the rectum of each animal (new glove for each animal).
 2. Place each sample into a container.
 3. Label each container (animal ID, paddock or drench group and sampling date).
Samples can be stored in a 4°C fridge for up to one week.
- b. Laboratory procedure:
1. Tare scales and weigh out 3g of each sample (**A**). Remaining faecal samples should be retained for coproculture.
 2. Add 15ml (**B**) distilled water to each sample.
 3. Homogenise each sample.
 4. Fill each chamber of a Whitlock Universal counting slide with 600µl (**C**) saturated salt solution (specific gravity = 1.2). Two chambers required per sample.
 5. Place a small sieve into each sample and draw 2 aliquots of 150µl (**D**) from within the sieve.
 6. Carefully add each aliquot to the Whitlock Universal counting slide chambers containing the saturated salt solution (150µl per chamber).
 7. Allow slide to sit for 2 minutes to float parasite eggs to surface.
 8. Identify and count strongylid eggs (oval shaped, ~80-90 microns long) within the gridded area of the slide chamber (**E**, 0.5ml) using a compound microscope at x40 magnification (x4 objective, x10 eyepieces). Repeat for the second chamber.
 9. Calculate the mean average egg count of the two chambers (**F**, eggs).
 10. Faecal egg count (FEC, eggs/g) is calculated as:

$$FEC = \frac{1}{\frac{A}{A+B} \cdot \frac{D}{C+D}} \cdot F = 60 \cdot F \quad [\text{Eq. 347}]$$

where **A** is the faecal sample (3g), **B** is the quantity of distilled water added to the faecal sample (15ml), **C** is the quantity of saturated salt solution added to each Whitlock slide chamber (600µl), **D** is the quantity of diluted faecal sample added to each Whitlock slide chamber (150µl), **E** is the quantity of the sample within the gridded area of the Whitlock slide chamber (0.5ml), and **F** is the mean average egg count of two chambers.

11. Record Animal ID, paddock or drench group, sampling date & FEC.

4.3.3 Coproculture

- a. Day 1:
 1. Label 500ml jar (paddock or drench group & sampling date).
 2. Tare scale with 500ml jar.
 3. Transfer all faeces (remainder of faecal samples following individual or bulk FEC) into 500ml jar. (1 jar per paddock or drench group).
 4. Weigh faecal sample (**A**, g).
 5. Crush sample with spatula until all pellets are blended together.
 6. Add an equal quantity of vermiculite (**A**, g) to jar.
 7. Carefully add water and mix thoroughly through sample until vermiculite and faeces fully blended. Sample should be moist enough to hold together and cut into chunks with spatula, but not wet.
 8. Use spatula to fill in air pockets. Compress gently but do not compact heavily.
 9. Place lid on jar but leave loose to allow air into jar.
 10. Place in 23°C incubator for 7 days.

- b. Day 7:
 11. Remove jar from incubator and remove lid.
 12. Fill jar with water.
 13. Use water bottle to fill jar until meniscus forms.
 14. Place petri dish (glass or plastic) over the top and carefully invert. Add water to petri dish until about half full.
 15. Leave for a minimum of 1 hour.
 16. Use pipette to draw liquid out of petri dish and place into 15ml conical centrifuge tube (minimum of 5ml).
 17. Label tube (paddock or drench group & sampling date).
 18. Place sample in the fridge until ready to count.

- c. Counting:
 19. Draw up a small amount of liquid with larvae from the bottom of the conical centrifuge tube using a pipette.
 20. Drop one drop onto a clean slide.
 21. Add one drop of Lugol's iodine (1g iodine and 2g potassium iodide in 100ml distilled water) to kill and stain larvae.

22. Cover with a coverslip.
23. Place slide under compound microscope at 200x magnification (x20 objective, x10 eyepieces).
24. Run up and down the slide (being careful not to go over the same area) and record the number of larvae of each genus (*Haemonchus*, *Teladorsagia* & *Trichostrongylus*) on a counter until a total of 100 larvae have been counted. If less than 100, repeat procedure with a second slide until 100 is reached. Genus counts consequently represent percentage prevalence.
25. Record paddock or drench group, sampling date & genus counts.

4.3.4 Faecal egg count reduction test

The Faecal Egg Count Reduction Test (FECRT) detailed below follows the procedure described by Coles et al. (2006), and the interpretation of data is modified (to account for changes in control group FECs at pre- and post-treatment) from that described by Coles et al. (1992).

a. Procedure:

1. Randomly allocate sheep to a drench group (control, albendazole, levamisole, abamectin). For the 'donor flock', 5 sheep per paddock should be allocated to each drench group. For weaners, 3 sheep per paddock should be allocated the albendazole, levamisole & abamectin drench groups, and 6 sheep should be allocated to the control group.
2. For 'donor flock', tag sheep to identify individual and drench group. For weaners, record animal ID (tag) and drench group.
3. Collect faecal samples for individual FEC and drench group coproculture.
4. Individually weight sheep and give the manufacturer recommended dose orally for the BZ, LEV & ABA drench groups. The control group receives no drench.
5. Place all sheep in holding paddock.
6. After 14 days, collect faecal samples to carry out individual FEC and drench group coproculture.

b. Interpretation:

1. Calculate the average FEC (from individual FECs) for each drench group (& control) and for both the pre-treatment and 14 day post-treatment FECs.
2. Calculate the average genus FEC for each drench group (& control) and for both the pre-treatment and 14 day post-treatment FECs, by multiplying the average FECs by the proportion of each genus (determined from pre- and post-treatment coprocultures).
3. Percentage reduction (R, %) for each genus and for each drench group is consequently calculated in accordance with McKenna (2006):

$$R = 100 \cdot \left(1 - \frac{\bar{X}_{14}}{\bar{X}_0} \cdot \frac{\bar{C}_0}{\bar{C}_{14}} \right) \quad [\text{Eq. 348}]$$

where \bar{X}_0 is the mean average pre-treatment genus FEC for the drench group, \bar{X}_{14} is the mean average post-treatment genus FEC for the drench group, \bar{C}_0 is the mean average pre-treatment genus FEC for the control group, and \bar{C}_{14} is the mean average post-treatment genus FEC for the control group.

4.3.5 Pasture sampling and analysis

The following procedures should be carried out for each of the 4 paddocks on each sampling occasion.

a. Pasture sampling:

The following pasture sampling technique was described by Waller et al. (1981).

1. Identify 6 representative sites from the paddock using a stratified random approach.
2. At each site, place a metal quadrat (**A**, 0.1m²).
3. Use lawn clippers to cut pasture samples from a single quadrat at approximately 0.5cm from ground (do not collect litter layer).
4. Place clippings from each site into a labelled (site, paddock & sampling date) paper bag.

b. Laboratory procedure:

1. Tare scales with an appropriately sized container (sufficient to hold the 6 pasture samples).
2. Transfer the 6 pasture samples into the container to create a bulk paddock pasture sample.
3. Weigh & record the bulk pasture sample (**B**, kg).
4. Calculate pasture mass of paddock (kg) as:

$$\text{Pasture mass (kg)} = \frac{1}{n \cdot A} \cdot p \cdot B \quad [\text{Eq. 349}]$$

where *n* is the number of sampling sites (*n* = 6), **A** is the area of the metal quadrat (0.1m²), *p* is the area of the paddock (*p* = 20,000m²), **B** is the weight of the bulk pasture sample (kg).

5. Record paddock, sampling date, and pasture mass.
6. Mix bulk pasture sample to ensure an even distribution of site samples throughout the bulk sample.
7. Transfer an appropriate quantity of the bulk pasture sample into a FeedTest sample bag and send (without delay) to FeedTest (<http://www.feedtest.com.au/>) for pasture quality analysis (Fodder Quality Package (NIR)). N.B. Pasture mass (kg) can be converted to Pasture mass (kg dry matter) when results of pasture quality analysis are obtained.
8. Place the remaining bulk pasture sample into a coarse (1mm aperture) mesh.
9. Label mesh bag (paddock & sampling date).
10. Carry out pasture infectivity analysis.

4.3.6 Pasture infectivity analysis

The following pasture larval recovery technique was described by O'Connor (2007c) as a modification of the technique given by Martin et al. (1990).

- a. Day 1:
 1. Label a 20L bucket (paddock & sampling date).
 2. Suspend mesh bag (containing pasture sample) inside 20L bucket.
 3. Cover with 10L of water.
 4. Add 25g non-ionic detergent.
 5. Soak for 6 hours.
 6. Remove mesh bag (containing pasture sample).
 7. Rinse pasture sample (in mesh bag) twice with 4L of water, and drain into 20L bucket (total volume of water should now be ~18L).
 8. Leave overnight to sediment.
 9. Place mesh bag (containing pasture sample) into an 80°C oven for 3 days.
- b. Day 2:
 10. Syphon off supernatant from 20L bucket, leaving sediment in ~4L of water.
 11. Pour the sediment (and 4L of water) through a coarse (1mm aperture) sieve into a polyethylene bag with a V-shaped base.
 12. Label polyethylene bag (paddock & sampling date).
 13. Suspend bag overnight to sediment.
- c. Day 3:
 14. Pierce polyethylene bag above sediment and allow supernatant to drain.
 15. Pierce bottom of V-shaped polyethylene bag and rinse sediment into a 250ml jar with 50-80ml of 70% ethanol.
 16. Label jar (paddock & sampling date).
 17. Leave to stand overnight.
- d. Day 4:
 18. Remove excess alcohol.
 19. Record volume of remaining sediment (**A**, ml).
 20. Mix sediment (swirl).

21. Transfer a 3ml subsample (**B**) to a 15ml conical centrifuge tube.
22. Add 7ml of potassium iodide (KI) solution (r.d. 1.4).
23. Label conical centrifuge tube (paddock & sampling date).
24. Mix by inversion.
25. Centrifuge (at 1400g) for 6 minutes (to separate larvae from soil sediment).
26. Collect supernatant.
27. Dilute supernatant up to 50ml with de-ionised water.
28. Centrifuge (at 1400g) for 6 minutes (to sediment larvae).
29. Remove supernatant, retaining 0.8-1.5ml (**C**) larval sediment and water.
30. Transfer replicate 0.2ml subsamples of larval solution (**D**) to two chambers of a Whitlock Universal counting slide, each containing 0.4ml potassium iodide (KI, r.d. 1.6) to float larvae.
31. Stain solution with 1 drop of Lugol's iodine (1g iodine and 2g potassium iodide in 100ml distilled water).
32. Identify and count larvae by genus (*Haemonchus*, *Teladorsagia*, *Trichostrongylus*) using a compound microscope at x40 magnification (x4 objective, x10 eyepieces) for each chamber of the slide.
33. Remove mesh bag (containing herbage sample) from 80°C oven and weigh (**E**, kg dry matter).
34. The larvae (L3) per kg dry matter (DM) for each genus is consequently calculated as:

$$L3/kg\ DM = \frac{L3(chamber\ 1)+L3(chamber\ 2)}{2} \cdot \frac{A \cdot C}{B \cdot D \cdot E} \quad [Eq.\ 350]$$

where **A** is the volume of sediment (ml), **B** is the quantity of the subsample (3ml), **C** is the volume of larval sediment (ml), **D** is the quantity of subsample added to each chamber of a Whitlock Universal counting slide (0.2ml), and **E** is the pasture sample dry weight (kg).

35. Record paddock, sampling date & L3/kg DM for each genus.

4.4 Experimental diary

All events occurring at the New South Wales and Victoria sites are detailed below.

4.4.1 New South Wales

All animal research carried out at the NSW experimental site received animal ethics committee approval from the University of New England (authority no: AEC17-017 & AEC18-029).

01-November-2017: 80 Merino yearlings were drenched with 7.5ml Triguard (Merial) and 3.5ml Zolvix (Elanco), and then randomly allocated to one of four paddocks (20 sheep per paddock).

08-November-2017: Bulk paddock FECs confirmed clearance of any pre-existing infections.

15-November-2017: Bulk paddock FECs continued to confirmed clearance of any pre-existing infections. Consequently, all 80 Merino yearlings were given a 5ml oral formulation containing 500 *Haemonchus contortus*, 3000 *Teladorsagia circumcincta*, 1000 *Trichostrongylus colubriformis*, 1000 *Trichostrongylus vitrinus* infective larvae (provided by Invetus, NSW). Following the administration of artificial infections, the yearlings were re-allocated to the 4 paddocks (20 sheep per paddock).

22-November-2017 to 20-December-2017: Bulk faecal samples were taken from each paddock (for bulk FEC) at weekly intervals.

21-December-2017: Bulk paddock FECs from 20th December indicated that paddocks 1 and 4 had FECs > 1500 eggs g⁻¹. Faecal samples from each sheep in paddocks 1 and 4 were analysed to determine individual FECs. All sheep with a FEC > 2000 eggs g⁻¹ were drenched with 7ml Triguard (Merial). This included 5 sheep from paddock 1 and 6 sheep from paddock 4.

27-December-2017: Bulk faecal samples taken from each paddock (for bulk FEC).

28-December-2017: Bulk paddock FECs from 27th December indicated that paddocks 2 and 3 had FECs > 1500 eggs g⁻¹. Faecal samples from each sheep in paddocks 2 and 3 were analysed to determine individual FECs. All sheep with a FEC > 2000 eggs g⁻¹ were drenched with 7ml Triguard (Merial). This included 6 sheep from paddock 2 and 4 sheep from paddock 3.

3-January-2018 to 17-January-2018: Bulk faecal samples were taken from each paddock (for bulk FEC) at weekly intervals.

24-January-2018: All 80 Merino yearlings were removed from the experimental paddocks. Each sheep had a faecal sample taken (for pre-treatment FEC), and was weighed and assigned to one of four anthelmintic treatment groups for a FECRT. 5 sheep from each paddock were randomly allocated to each of four treatment groups (Abamectin, Albendazole, Levamisole, control (no treatment)), such that each treatment group contained a total of 20 sheep. Each sheep was treated according to the manufacturers recommended dosage (ml kg⁻¹). All 80 Merino yearlings were then moved to a holding paddock.

25-January-2018: 60 freshly weaned Merino lambs were drenched with 4ml HAT-TRICK (Merial) and 2ml Zolvix (Elanco), and given injections of 1ml Ultravac 5 in 1 (Zoetis) and 0.5ml Selovin LA (Bayer). Each lamb was weighed and assessed for body condition score. Lambs were then randomly allocated to the four experimental paddocks (15 per paddock).

31-January-2018: Bulk faecal samples taken from each paddock (for bulk FEC).

5-February-2018: Pasture samples taken from each paddock for pasture quality, mass and infectivity analysis.

7-February-2018: Faecal samples were sampled from all 80 Merino yearlings (for post-treatment FEC), and then released from the experiment.

14-February-2018 & 21-February-2018: Bulk faecal samples taken from each paddock (for bulk FEC).

28-February-2018: Faecal samples collected from all 60 lambs (for individual FEC). Further, each was weighed and assessed for body condition score.

2-March-2018: The mean FEC of faecal samples collected on 28th February 2018 was > 1500 eggs g⁻¹. Consequently, all 60 lambs were treated with 5ml Alben (albendazole).

5-March-2018: Pasture samples taken from each paddock for pasture quality, mass and infectivity analysis.

13-March-2018: Bulk faecal samples taken from each paddock (for bulk FEC).

28-March-2018: Faecal samples collected from all 60 lambs (for individual FEC). Further, each was weighed and assessed for body condition score. Following FEC analysis the mean FEC was > 1500 eggs g⁻¹. Consequently, all 60 lambs were treated with 8ml Virbamec (abamectin).

9-April-2018: Pasture samples taken from each paddock for pasture quality, mass and infectivity analysis.

11-April-2018: Bulk faecal samples taken from each paddock (for bulk FEC). Following FEC analysis, paddocks 1 to 3 were found to have a mean FEC of 380 eggs g⁻¹; however, paddock 4 had a FEC of 6780 eggs g⁻¹. Due to animal health and welfare concerns, faecal samples were collected from the 15 lambs in paddock 4 (for individual FEC) to confirm the bulk FEC results. These samples were analysed and resulted in a mean FEC of 18392 eggs g⁻¹. Consequently, the 15 lambs in paddock 4 were treated with 6ml Alben (albendazole).

13-April-2018: Following the spike in mean FEC for paddock 4 on 11th April 2018, it was decided that the 45 lambs in paddocks 1 to 3 should be treated with 7ml Alben (albendazole) as a precautionary measure.

15-April-2018: Lamb mortality in paddock 4. A post-mortem examination was carried out to determine the cause of death. Whilst the treatment on 11th April 2018 was effective (post-mortem faecal sampling and FEC analysis), the lamb was found to have succumb to anaemia. This was most likely due to an inability to recover from the spike in FEC reported for paddock 4 on 11th April 2018. An adverse event report to this effect was consequently submitted to the UNE animal ethics committee.

26-April-2018: Faecal samples collected from all 59 remaining lambs (for individual FEC). Further, each was weighed and assessed for body condition score.

2-May-2018: Bulk faecal samples taken from each paddock (for bulk FEC).

7-May-2018: Pasture samples taken from each paddock for pasture quality, mass and infectivity analysis.

9-May-2018 to 23-May-2018: Bulk faecal samples taken weekly from each paddock (for bulk FEC).

30-May-2018: Faecal samples collected from all 59 lambs (for individual FEC). Further, each was weighed and assessed for body condition score.

4-June-2018: Pasture samples taken from each paddock for pasture quality, mass and infectivity analysis.

13-June-2018 & 20-June-2018: Bulk faecal samples taken from each paddock (for bulk FEC).

27-June-2018: Faecal samples collected from all 59 lambs (for individual FEC). Further, each was weighed and assessed for body condition score.

5-July-2018: Pasture samples taken from each paddock for pasture quality, mass and infectivity analysis.

11-July-2018: Bulk faecal samples taken from each paddock (for bulk FEC).

12-July-2018: Due to increased bulk FEC from 11th July 2018, faecal samples collected from all 15 lambs in paddock 3 (for individual FEC).

25-July-2018: Faecal samples collected from all 59 lambs (for individual FEC). Further, each was weighed and assessed for body condition score.

23-August-2018: Pasture samples taken from each paddock for pasture quality, mass and infectivity analysis.

28-August-2018: Faecal samples collected from all 59 lambs (for individual FEC). Further, each was weighed and assessed for body condition score.

24-September-2018: Pasture samples taken from each paddock for pasture quality, mass and infectivity analysis.

3-October-2018: Faecal samples collected from all 59 lambs (for individual FEC). Further, each was weighed and assessed for body condition score.

4-October-2018: Based on the FEC results from faecal samples collected on 3rd October 2018, all 59 weaners were treated with 10ml Virbamec (abamectin).

12-October-2018: Faecal samples were collected from 6 randomly selected lambs to confirm suspected abamectin resistance. Consequently, all 59 weaners were treated with 10ml Alben (albendazole).

22-October-2018: Faecal samples collected from all 59 lambs (for individual FEC). Further, each was weighed and assessed for body condition score.

23-October-2018: All 59 lambs sheared.

24- October-2018: All 59 lambs were weighed to record post-shearing weights.

31-October-2018: Pasture samples taken from each paddock for pasture quality, mass and infectivity analysis.

6-November-2018: Bulk faecal samples taken from each paddock (for bulk FEC).

19-November-2018: Faecal samples collected from all 59 lambs (for individual FEC). Further, each was weighed and assessed for body condition score.

26-November-2018: Bulk faecal samples taken from each paddock (for bulk FEC).

30-November-2018: Pasture samples taken from each paddock for pasture quality, mass and infectivity analysis.

6-December-2018: Bulk faecal samples taken from each paddock (for bulk FEC).

11-December-2018: Faecal samples collected from all 59 lambs (for individual FEC). Further, each was weighed and assessed for body condition score.

13-December-2018: All 59 sheep treated with 12.5ml Virbamec (abamectin).

19-December-2018: Bulk faecal samples taken from each paddock (for bulk FEC).

21-December-2018: All 59 sheep treated with 10ml Alben (albendazole).

27-December-2018: Bulk faecal samples taken from each paddock (for bulk FEC).

2-December-2018: Pasture samples taken from each paddock for pasture quality, mass and infectivity analysis.

10-January-2019: Bulk faecal samples taken from each paddock (for bulk FEC).

23-January-2019: All 59 Merino yearlings were removed from the experimental paddocks. Each sheep had a faecal sample taken (for pre-treatment FEC) and was weighed and assessed for body condition score, and assigned to one of four anthelmintic treatment groups for a FECRT. 15 sheep were randomly allocated to the Abamectin, Albendazole and Levamisole treatment groups, and the remaining sheep (14) were allocated to a no treatment control group. Each sheep was treated according to the manufacturers recommended dosage (ml kg^{-1}). All 59 Merino yearlings were then moved to a holding paddock.

7-February-2019: Faecal samples were taken from all 59 Merino yearlings (for post-treatment FEC), and then released from the experiment.

8-February-2019: 60 freshly weaned Merino lambs were drenched with 4ml HAT-TRICK (Merial) and 2ml Zolvix (Elanco). Each lamb was weighed and assessed for body condition score. Lambs were then randomly allocated to the four experimental paddocks (15 per paddock).

12-February-2019: Pasture samples taken from each paddock for pasture quality, mass and infectivity analysis.

14-February-2019: Bulk faecal samples taken from each paddock (for bulk FEC).

26-February-2019: Faecal samples collected from all 60 lambs (for individual FEC). Further, each was weighed and assessed for body condition score.

15-March-2019: Bulk faecal samples taken from each paddock (for bulk FEC).

27-March-2019: Faecal samples collected from all 60 lambs (for individual FEC). Further, each was weighed and assessed for body condition score.

3-April-2019: Bulk faecal samples taken from each paddock (for bulk FEC).

10-April-2019: Bulk faecal samples taken from each paddock (for bulk FEC). All 60 lambs weighed and assessed for body condition score and treated with 6ml Alben (albendazole).

24-April-2019: Faecal samples collected from all 60 lambs (for individual FEC). Further, each was weighed and assessed for body condition score.

8-May-2019: Bulk faecal samples taken from each paddock (for bulk FEC). All 60 lambs weighed and assessed for body condition score.

22-May-2019: Faecal samples collected from all 60 lambs (for individual FEC). Further, each was weighed and assessed for body condition score.

7-June-2019: Bulk faecal samples taken from each paddock (for bulk FEC).

19-June-2019: Faecal samples collected from all 60 lambs (for individual FEC). Further, each was weighed and assessed for body condition score.

24-June-2019: Field study terminated. Drought conditions had led to a reliance on supplementary feeding, and the monitoring of sheep indicated that they were no longer gaining weight (animal welfare concern). All sheep removed from the experiment and the University of New England animal ethics committee notified.

Table 9. Supplementary feeding regime at the NSW experimental site. CP = crude protein content (%), ME = metabolizable energy content (MJ kg⁻¹), Quantity = kg sheep⁻¹, Supply = week⁻¹.

Date	Cereal pellets			Straw			Supply
	Quantity	CP	ME	Quantity	CP	ME	
19-June-2018 to 26-June-2018	0.10	14	9	0	0	0	3
27-June-2018 to 17-July-2018	0.20	14	9	0	0	0	3
18-July-2018 to 26-July-2018	0.20	14	9	0	0	0	7
27-July-2018 to 31-August-2018	0.30	14	9	0	0	0	7
1-September-2018 to 15-September-2018	0.30	21	10.5	0	0	0	7
16-September-2018 to 1-October-2018	0.30	14	9	0	0	0	7
2-October-2018 to 8-October-2018	0.25	14	9	0	0	0	7
9-October-2018 to 15-October-2018	0.20	14	9	0	0	0	7
16-October-2018 to 31-October-2018	0.15	14	9	0	0	0	7
25-February-2019 to 16-March-2019	0.05	14	9	0	0	0	3
19-March-2019 to 25-March-2019	0.10	14	9	0	0	0	3
27-March-2019 to 28-March-2019	0.10	14	9	0	0	0	7
29-March-2019 to 2-April-2019	0.10	14	9	0.02	9.4	9.1	7
3-April-2019 to 8-May-2019	0.20	14	9	0.03	9.4	9.1	7
9-May-2019 to 23-June-2019	0.30	14	9	0.04	9.4	9.1	7

4.4.2 Victoria

10-November-2017: 80 Merino yearlings were randomly allocated to one of four paddocks (20 per paddock).

15-November-2017: All 80 Merino yearlings were drenched with a combination of Monepantel, Abamectin, Fenbendazole and Levamisole. Bulk faecal samples taken from each paddock (for bulk FEC & coproculture).

22-November-2017: Bulk faecal samples taken from each paddock (for bulk FEC & coproculture). All 80 Merino yearlings were given a 5ml oral formulation containing 500 *Haemonchus contortus*, 3000 *Teladorsagia circumcincta*, 1000 *Trichostrongylus colubriformis* and 1000 *Trichostrongylus vitrinus* infective larvae (provided by Invetec, NSW).

29-November-2017 to 7-March-2018: Bulk faecal samples taken from each paddock (for bulk FEC & coproculture) at weekly intervals.

14-March-2018: Bulk faecal samples taken from each paddock (for bulk FEC & coproculture). All 80 Merino yearlings had an individual faecal sample taken (for pre-treatment FEC) and were assigned to one of four anthelmintic treatment groups for a FECRT. 5 sheep from each paddock were randomly allocated to each of four treatment groups (Abamectin, Fenbendazole, Levamisole, control (no treatment)), such that each treatment group contained a total of 20 sheep. All sheep were treated accordingly and were returned to the experimental paddocks (to minimise *Haemonchus* contamination of other areas of the farm, as this parasite is not endemic to Lal Lal).

26-March-2018: Faecal samples were sampled from all 80 Merino yearlings (for post-treatment FEC), and then released from the experiment. 60 Merino weaners were drenched with a combination of Abamectin, Monepantel, Fenbendazole and Levamisole. Each lamb was weighed and assessed for body condition score. Lambs were then randomly allocated to the four experimental paddocks (15 per paddock). Pasture samples taken from each paddock for pasture quality, mass and infectivity analysis.

5-April-2018: Bulk faecal samples taken from each paddock (for bulk FEC).

23-April-2018: Pasture samples taken from each paddock for pasture quality, mass and infectivity analysis.

27-April-2018: Faecal samples collected from all lambs (for individual FEC). Further, each was weighed and assessed for body condition score.

21-May-2018: Pasture samples taken from each paddock for pasture quality, mass and infectivity analysis.

25-May-2018: Faecal samples collected from all lambs (for individual FEC & paddock coproculture). Further, each was weighed and assessed for body condition score.

30-May-2018: All lambs drenched with Abamectin.

22-June-2018: Faecal samples collected from all lambs (for individual FEC & paddock coproculture). Further, each was weighed and assessed for body condition score.

25-June-2018: Pasture samples taken from each paddock for pasture quality, mass and infectivity analysis.

27-June-2018: All lambs drenched with Fenbendazole.

27-July-2018: Faecal samples collected from all lambs (for individual FEC & paddock coproculture). Further, each was weighed and assessed for body condition score. Pasture samples taken from each paddock for pasture quality, mass and infectivity analysis.

1-August-2018: All lambs drenched with Abamectin.

31-August-2018: Faecal samples collected from all lambs (for individual FEC & paddock coproculture). Further, each was weighed and assessed for body condition score. Pasture samples taken from each paddock for pasture quality, mass and infectivity analysis.

6-September-2018: All lambs drenched with Fenbendazole.

1-October-2018 & 26-October-2018: Faecal samples collected from all lambs (for individual FEC & paddock coproculture). Further, each was weighed and assessed for body condition score. Pasture samples taken from each paddock for pasture quality, mass and infectivity analysis.

5-November-2018: All lambs drenched with Abamectin.

26-November-2018 & 19-December-2018: Faecal samples collected from all lambs (for individual FEC & paddock coproculture). Further, each was weighed and assessed for body condition score. Pasture samples taken from each paddock for pasture quality, mass and infectivity analysis.

27-December-2018: All lambs drenched with Fenbendazole.

29-January-2019: Faecal samples collected from all lambs (for individual FEC & paddock coproculture). Further, each was weighed and assessed for body condition score. Pasture samples taken from each paddock for pasture quality, mass and infectivity analysis.

31-January-2019: All lambs drenched with Abamectin.

4-March-2019: Faecal samples collected from all lambs (for individual FEC & paddock coproculture). Further, each was weighed and assessed for body condition score. Pasture samples taken from each paddock for pasture quality, mass and infectivity analysis.

19-March-2019: Faecal samples collected from all individuals (for pre-treatment FEC). Each sheep was then assigned to one of four anthelmintic treatment groups (Abamectin, Fenbendazole, Levamisole or control) for a FECRT, and treated accordingly.

1-April-2019: Faecal samples collected from all individuals (for post-treatment FEC) as part of FECRT, and then released from the experiment. 60 Merino weaners were drenched with Zolvix (Elanco). The lambs were then randomly allocated to the four experimental paddocks (15 per paddock).

5-April-2019, 7-May-2019 & 4-June-2019: Faecal samples collected from all lambs (for individual FEC). Further, each was weighed and assessed for body condition score. Pasture samples taken from each paddock for pasture quality, mass and infectivity analysis.

13-June-2019: All lambs drenched with Fenbendazole.

28-June-2019, 5-August-2019, 10-September-2019, 8-October-2019 & 6-November-2019: Faecal samples collected from all lambs (for individual FEC & paddock coproculture). Further, each was weighed and assessed for body condition score. Pasture samples taken from each paddock for pasture quality, mass and infectivity analysis.

3-December-2019: Faecal samples collected from all lambs (for individual FEC & paddock coproculture). Further, each was weighed and assessed for body condition score. Pasture samples taken from each paddock for pasture quality, mass and infectivity analysis. All lambs drenched with Abamectin.

10-January-2020, 10-February-2020 & 10-March-2020: Faecal samples collected from all 60 lambs (for individual WEC & paddock coproculture). Further, each was weighed and assessed for body condition score. Pasture samples taken from each paddock for pasture quality, mass and infectivity analysis.

8-April-2020: Faecal samples collected from all individuals (for pre-treatment FEC). Further, each was weighed and assessed for body condition score. Each sheep was then assigned to one of three anthelmintic treatment groups (Abamectin, Fenbendazole or control) for a FECRT, and treated accordingly.

20-April-2020: Faecal samples collected from all individuals lambs (for post-treatment FEC), and then released from the experiment.

Table 10. Supplementary feeding regime at the VIC experimental site. CP = crude protein content (%), ME = metabolizable energy content (MJ kg⁻¹), Quantity = kg paddock⁻¹.

Date	Hay		
	Quantity	CP	ME
19-February-2019	300	4.2	6.9
11-March-2019	300	4.2	6.9
25-March-2019	300	4.2	6.9
8-April-2019	300	4.2	6.9
10-May-2019	300	4.2	6.9
24-May-2019	300	4.2	6.9
7-June-2019	300	4.2	6.9
21-June-2019	300	4.2	6.9

4.5 Simulation procedure

4.5.1 New South Wales

The New South Wales validation study was simulated by setting the latitude and elevation inputs to -30.5° and 980m, respectively. The required weather inputs were provided by the weather station records from 1st November 2017 to 24th June 2019. The entire experimental site was represented by a single 8-hectare paddock with a clay loam soil textural type. The paddock had an initial pasture crude protein content of 5%, an initial pasture metabolizable energy protein content of 7 MJ kg⁻¹, an initial pasture height of 0.43m, and an initial soil inorganic nitrogen content of 20mg kg⁻¹. Further, the pasture was assumed to have an initial infectivity of 0 larvae [kg dry matter]⁻¹.

Three mobs were simulated to represent the Merino yearlings used for initial pasture contamination, and the Merino weaners used in the first and second year of the validation study. The Merino yearlings mob consisting of 80 individuals had an initial mean live weight of 60kg; whereas the year 1 and 2 Merino weaner mob each consisting of 60 individuals had an initial mean live weight of 18.8kg and 18.5kg, respectively. The Merino yearlings were first allocated to the simulated paddock on 1st November 2017 and removed on 24th January 2018. The year 1 Merino weaners were first allocated to the simulated paddock on 25th January 2018 and removed on 23rd January 2019. The year 2 Merino weaners were first allocated to the simulated paddock on 8th February 2019 and remained until the end of the simulation period.

Supplementary feed was supplied to the paddock as per Table 9 (section 4.4.1).

All individuals within the Merino yearling mob received an artificial challenge containing 500 *Haemonchus contortus*, 3000 *Teladorsagia circumcincta*, 1000 *Trichostrongylus colubriformis* and 1000 *Trichostrongylus vitrinus* infective larvae on 15th November 2017. The initial anthelmintic class efficacy of the artificial challenge was set to 96.4% for the benzimidazole group, 97.2% for the levamisole group, and 94.6% for the macrocyclic lactone group. Anthelmintic treatments (Albendazole, Abamectin and Levamisole) were later administered to any Merino yearling with a FEC > 2000 eggs g⁻¹ on 21st December 2017 and 28th December 2017.

All individuals within the year 1 Merino weaner mob received anthelmintic treatments on 25th January 2018 (Abamectin, Monepantel, Albendazole and Levamisole), 2nd March 2018 (Albendazole), 28th March 2018 (Abamectin), 12th April 2018 (Albendazole), 4th October 2018 (Abamectin), 12th October 2018 (Albendazole), 13th December 2018 (Abamectin) and 21st December 2018 (Albendazole). Further, all individuals within the year 1 Merino weaner mob were sheared on 23rd October 2018.

All individuals within the year 2 Merino weaner mob received anthelmintic treatments on 8th February 2019 (Abamectin, Monepantel, Albendazole and Levamisole), and 10th April 2019 (Albendazole).

4.5.2 Victoria

The Victoria validation study was simulated by setting the latitude and elevation inputs to -37.7° and 509m, respectively. The required weather inputs were provided by the weather station records from 22nd November 2017 to 20th April 2020. The entire experimental site was represented by a single 8-hectare paddock with a clay loam soil textural type. The paddock had an initial pasture crude protein content of 8.5%, an initial pasture metabolizable energy protein content of 7 MJ kg^{-1} , an initial pasture height of 0.2m, and an initial soil inorganic nitrogen content of 121 mg kg^{-1} . Further, the pasture was assumed to have an initial infectivity of 0 larvae $[\text{kg dry matter}]^{-1}$.

Three mobs were simulated to represent the Merino yearlings used for initial pasture contamination, and the Merino weaners used in the first and second year of the validation study. The Merino yearlings mob consisted of 80 individuals had an initial mean live weight of 60kg; whereas the year 1 and 2 Merino weaner mob each consisting of 60 individuals had an initial mean live weight of 23.4kg and 26.9kg, respectively. The Merino yearlings were first allocated to the simulated paddock on 22nd November 2017 and removed on 26th March 2018. The year 1 Merino weaners were first allocated to the simulated paddock on 26th March 2018 and removed on 1st April 2019. The year 2 Merino weaners were first allocated to the simulated paddock on 1st April 2019 and remained until the end of the simulation period.

1200kg hay (CP = 4.2%, ME = 6.9 MJ kg^{-1}) was supplied to the paddock on 19th February 2019, 11th March 2019, 25th March 2019, 8th April 2019, 10th May 2019, 24th May 2019, 7th June 2019 and 21st June 2019.

All individuals within the Merino yearling mob received an artificial challenge containing 500 *Haemonchus contortus*, 3000 *Teladorsagia circumcincta*, 1000 *Trichostrongylus colubriformis* and 1000 *Trichostrongylus vitrinus* infective larvae on 22nd November 2017. The initial anthelmintic class efficacy of the artificial challenge was set to 70.7% for the benzimidazole group, 96.8% for the levamisole group, and 96.1% for the macrocyclic lactone group. Anthelmintic treatments were later administered to the Merino yearling mob in accordance with a FEC reduction test on 14th March 2018; where 20 individuals received Abamectin, 20 individuals received Fenbendazole, 20 individuals received Levamisole and 20 individuals remained untreated (control).

All individuals within the year 1 Merino weaner mob received anthelmintic treatments on 26th March 2018 (Abamectin, Monepantel, Fenbendazole and Levamisole), 30th May 2018 (Abamectin), 27th June 2018 (Fenbendazole), 1st August 2018 (Abamectin), 6th September 2018 (Fenbendazole), 5th November 2018 (Abamectin), 27th December 2018 (Fenbendazole) and 31st January 2019 (Abamectin). Further, anthelmintic treatments were administered to the year 1 Merino weaner mob in accordance with a FEC reduction test on 19th March 2019; where 12 individuals received Abamectin, 12 individuals received Fenbendazole, 12 individuals received Levamisole and the remaining individuals remained untreated (control).

All individuals within the year 2 Merino weaner mob received anthelmintic treatments on 1st April 2019 (Monepantel), 13th June 2019 (Fenbendazole), and 3rd December 2019 (Abamectin). Further, anthelmintic treatments were administered to the year 2 Merino weaner mob in accordance with a FEC reduction test on 8th April 2020; where 19 individuals received Abamectin, 19 individuals received Fenbendazole and the remaining individuals remained untreated (control).

4.6 Results

4.6.1 New South Wales

4.6.1.1 Weather

The meteorological data recorded at the New South Wales experimental site is provided for: rainfall (mm d^{-1} , Fig. 14), solar radiation ($\text{MJ m}^{-2} \text{d}^{-1}$, Fig. 15), maximum and minimum daily temperature ($^{\circ}\text{C}$, Fig. 16), vapour pressure (kPa, Fig. 17), and windspeed measure at 2m (m s^{-1} , Fig. 18).

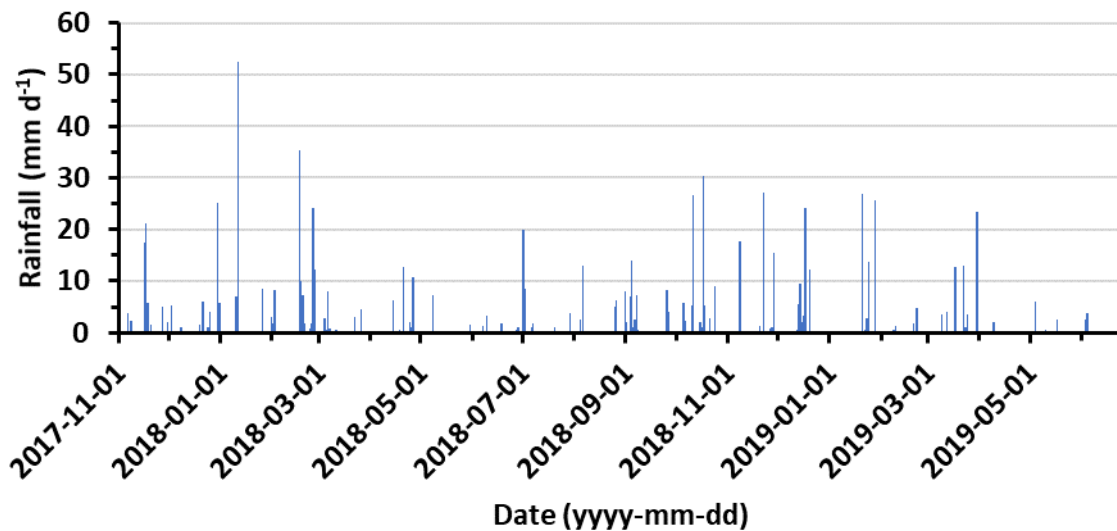


Figure 14. Rainfall (mm d^{-1}) at the New South Wales experimental site.

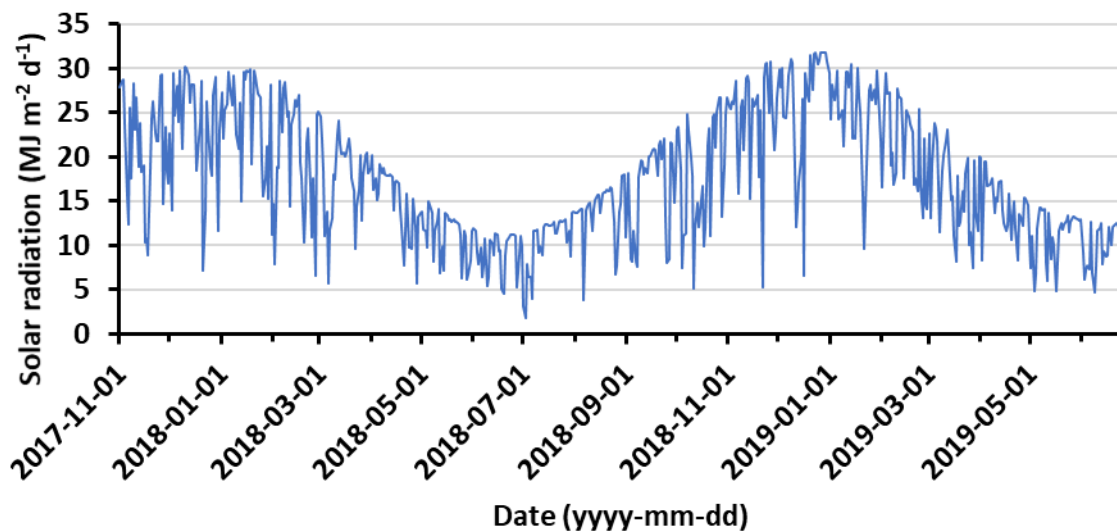


Figure 15. Rainfall (mm d^{-1}) at the New South Wales experimental site.

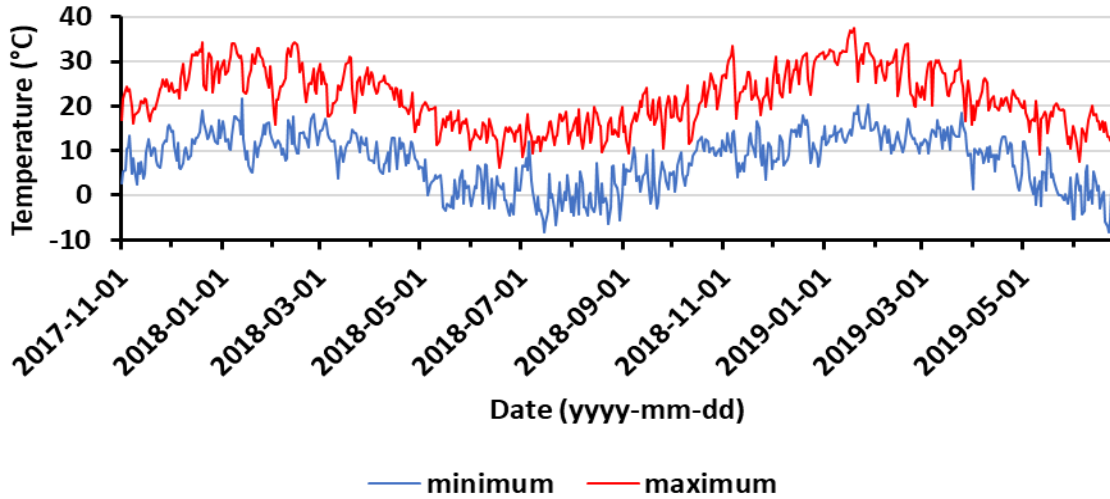


Figure 16. Daily temperature (°C) at the New South Wales experimental site.

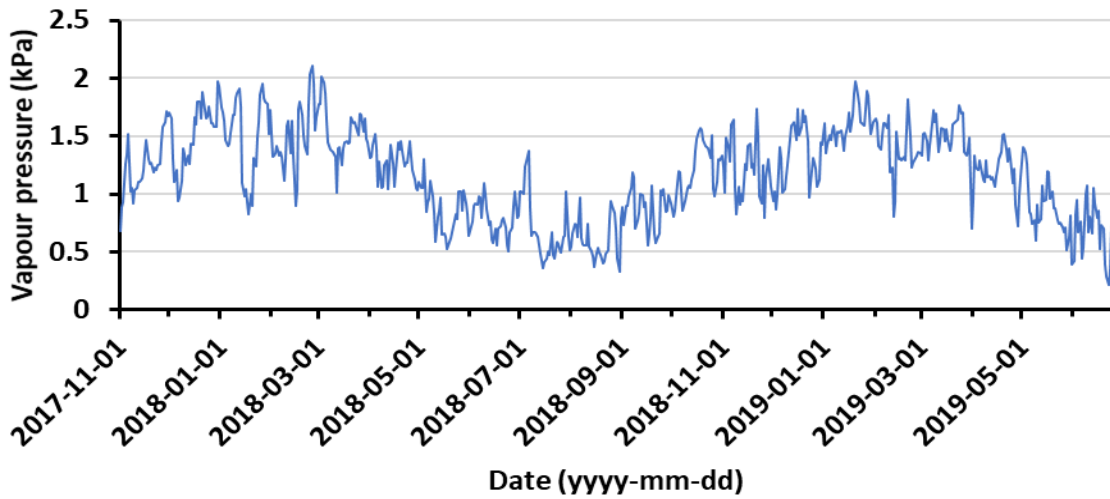


Figure 17. Vapour pressure (kPa) at the New South Wales experimental site.

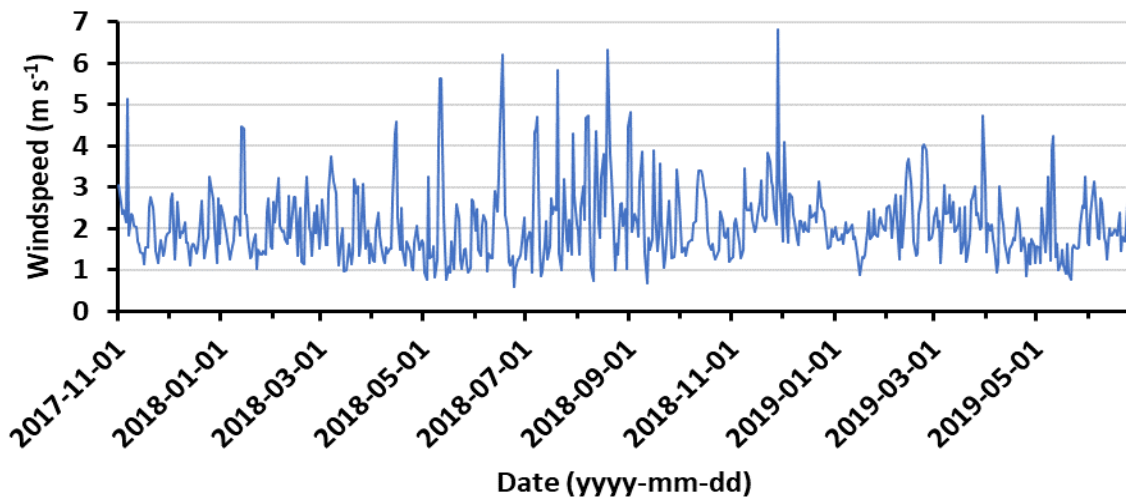


Figure 18. Windspeed at 2m (m s⁻¹) at the New South Wales experimental site.

4.6.1.2 Pasture mass and quality

The observed and predicted values for pasture mass (kg) and various indicators of pasture quality are provided in Figures 19 to 24, and linear regression statistics are provided in Table 11. Whilst the predicted values for each trait follow the same trends as the observed trait values, it should be noted that predicted metabolizable energy, dry matter digestibility, neutral detergent fibre and acid detergent fibre were consistently higher than the respective observations. Further, the linear regression statistics indicate a poor non-significant relationship between observed and predicted crude protein content. This suggests that further development of the pasture model should focus on the components covering nitrogen dynamics.

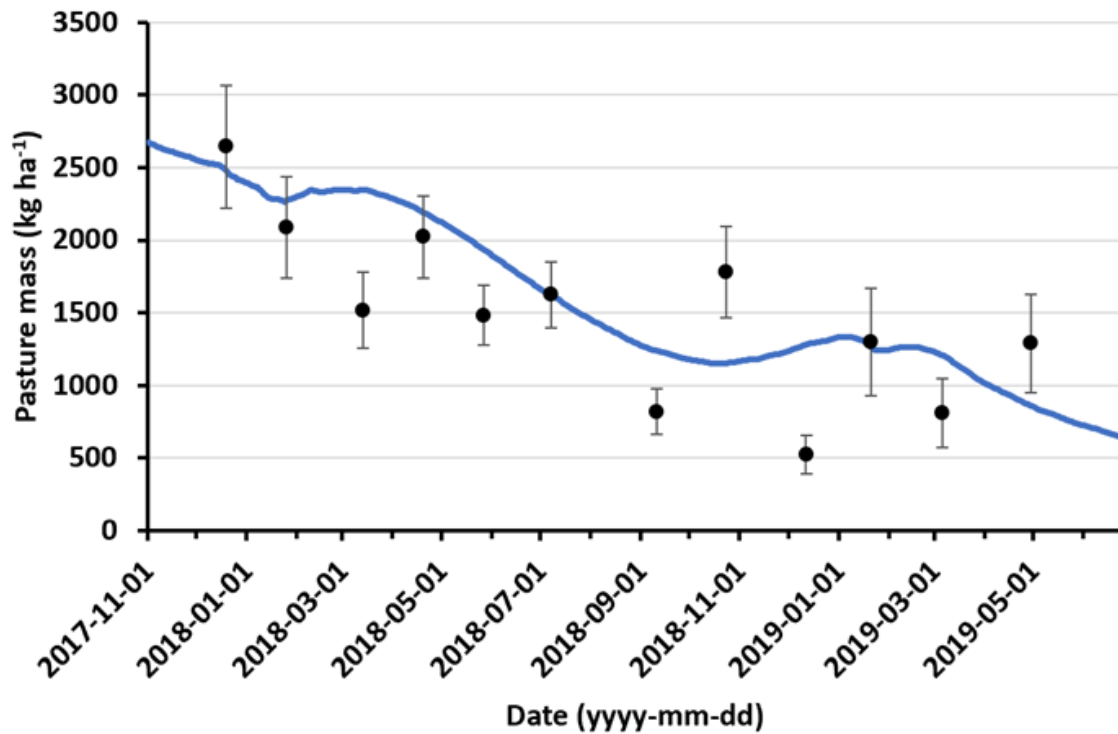


Figure 19. Predicted and observed pasture mass (kg ha⁻¹) for the New South Wales experimental site. Predictions are provided by a solid blue line, and observations are provided by the circular plot points (error bars indicate the standard error).

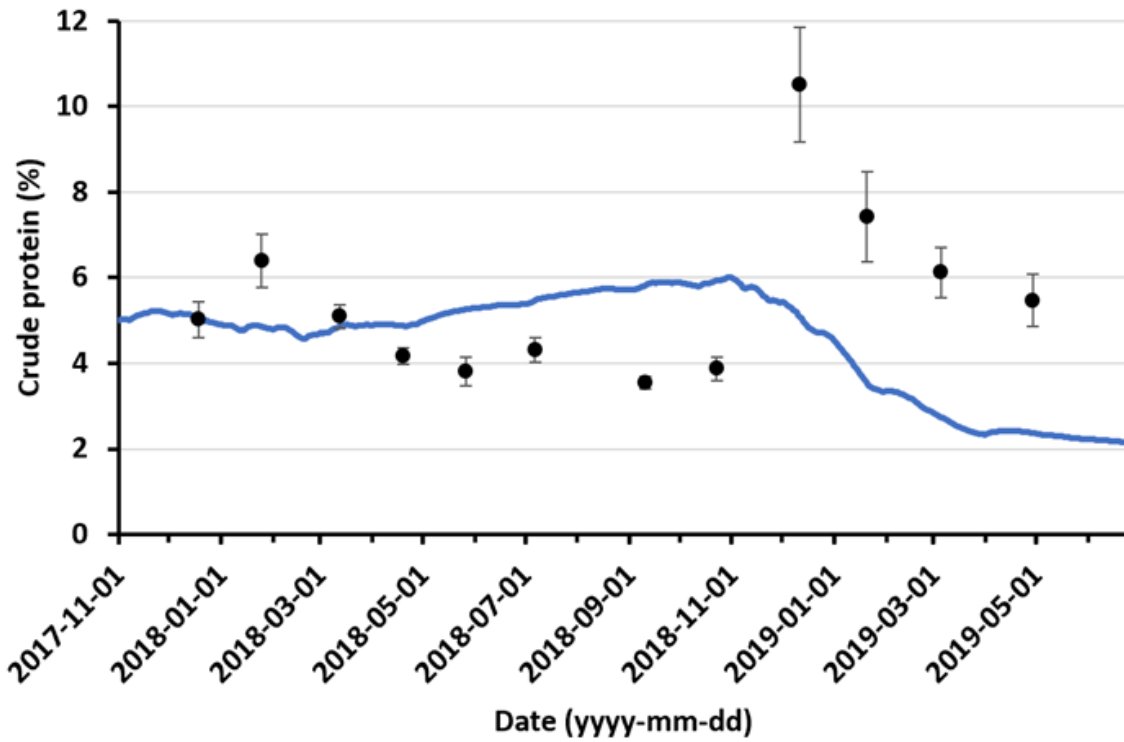


Figure 20. Predicted and observed crude protein content (%) for the New South Wales experimental site. Predictions are provided by a solid blue line, and observations are provided by the circular plot points (error bars indicate the standard error).

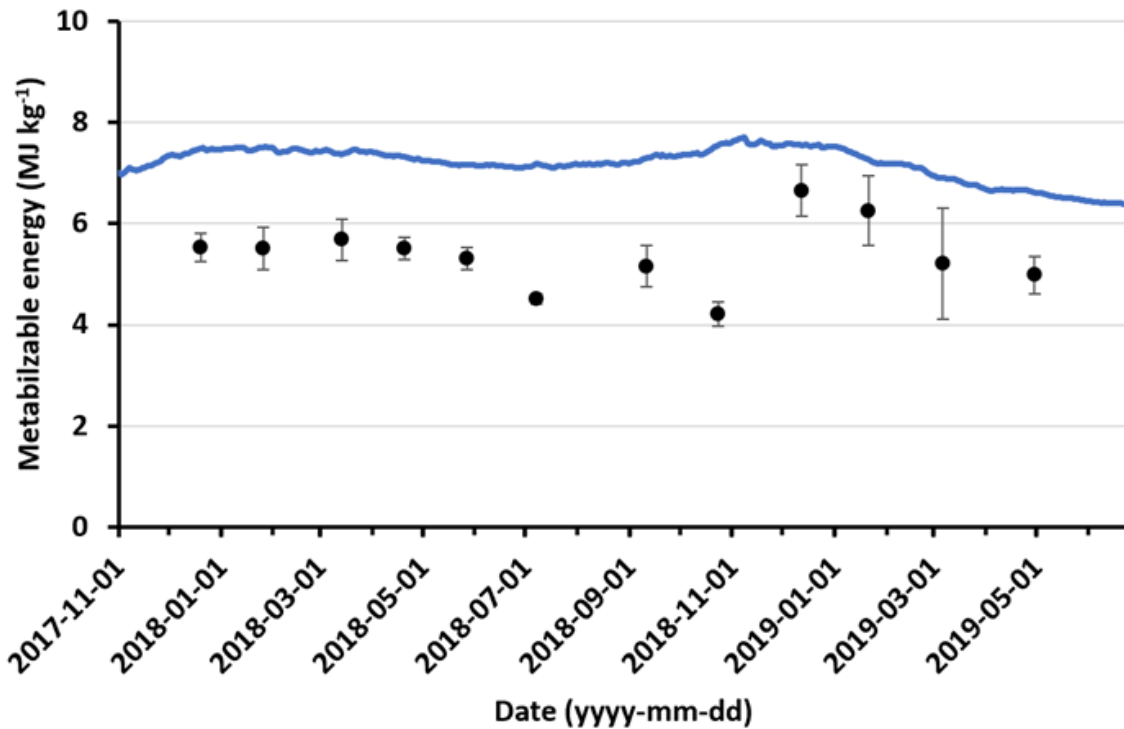


Figure 21. Predicted and observed metabolizable energy (MJ kg^{-1}) for the New South Wales experimental site. Predictions are provided by a solid blue line, and observations are provided by the circular plot points (error bars indicate the standard error).

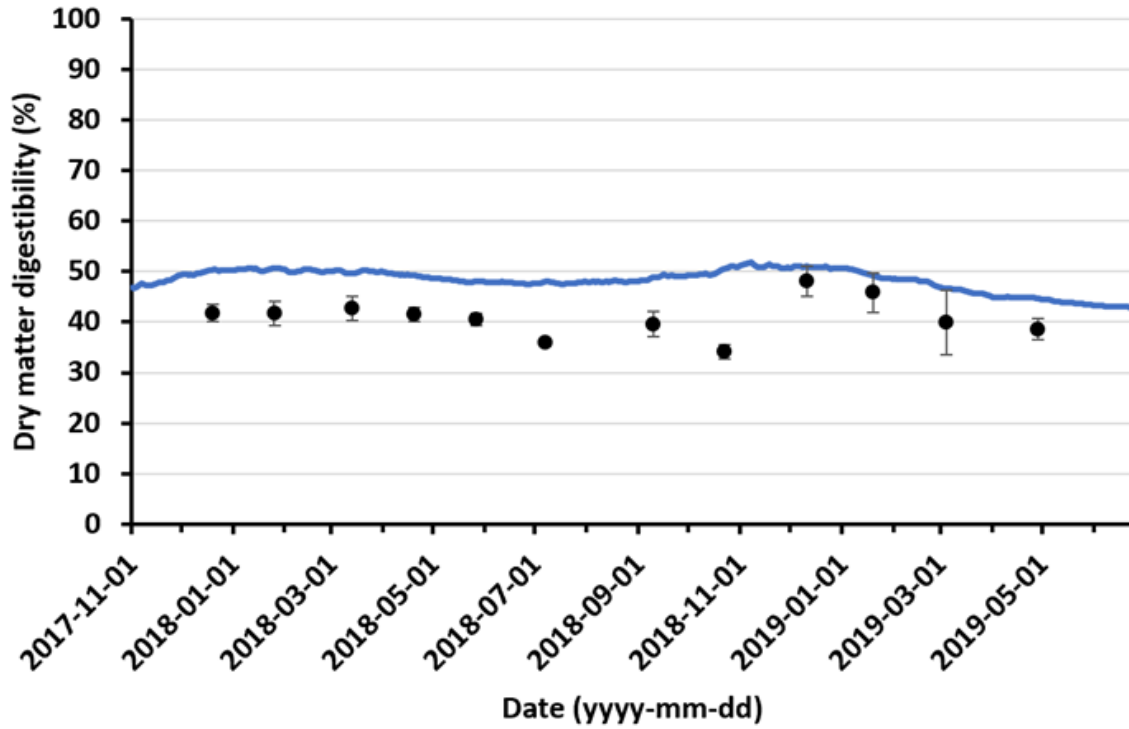


Figure 22. Predicted and observed dry matter digestibility (%) for the New South Wales experimental site. Predictions are provided by a solid blue line, and observations are provided by the circular plot points (error bars indicate the standard error).

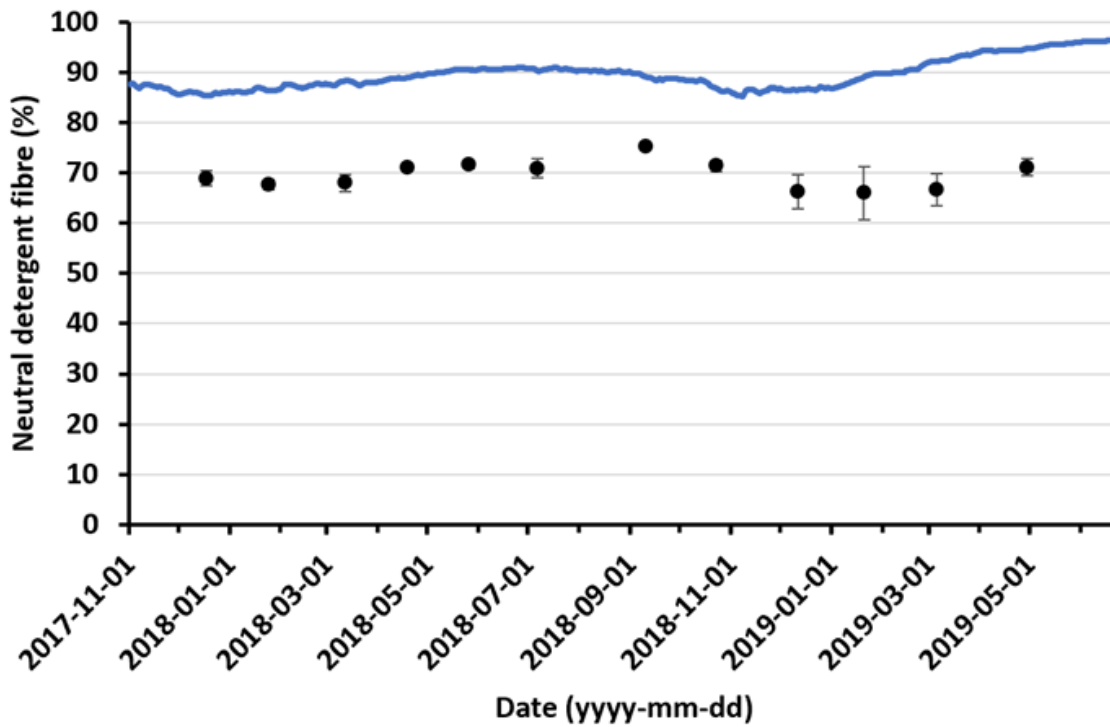


Figure 23. Predicted and observed neutral detergent fibre (%) for the New South Wales experimental site. Predictions are provided by a solid blue line, and observations are provided by the circular plot points (error bars indicate the standard error).

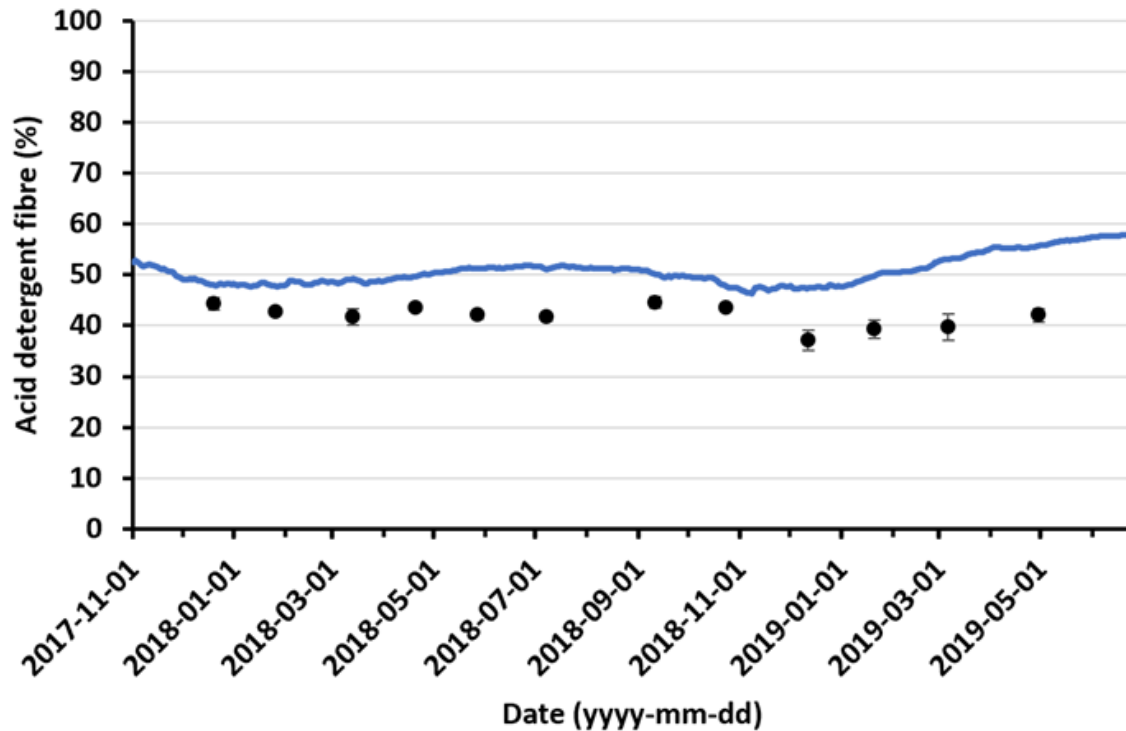


Figure 24. Predicted and observed acid detergent fibre (%) for the New South Wales experimental site. Predictions are provided by a solid blue line, and observations are provided by the circular plot points (error bars indicate the standard error).

Table 11. Linear regression statistics for pasture mass and the pasture quality descriptors.

Trait	R^2	Standard error	$F_{1,10}$	gradient	y-intercept	p
Pasture mass	0.58	332	12.62	0.590	787.42	<0.01
Crude protein	0.01	0.785	0.083	0.035	4.898	0.78
Metabolizable energy	0.41	0.134	6.868	0.158	6.488	<0.05
Dry matter digestibility	0.40	0.977	6.539	0.196	41.338	<0.05
Neutral detergent fibre	0.74	0.870	28.32	0.499	53.838	<0.0005
Acid detergent fibre	0.39	1.265	6.352	0.435	31.465	<0.05

4.6.1.3 Pasture infectivity

The observed and predicted values for pasture infectivity (larvae kg^{-1}) are provided in Fig. 25 and Fig. 26, respectively. Observed pasture infectivity values were high, potentially representing an issue with the laboratory method used to measure this trait (section 4.3.6). In contrast, the predicted pasture infectivity range (0 to 4500 larvae kg^{-1}) fell within the trickle challenge levels investigated by Coop et al. (1982), thereby representing a much more realistic scale than the observed values. However, no significant linear regression was found between the observed and predicted pasture infectivity values indicating that the differences were not confined to the absolute values.

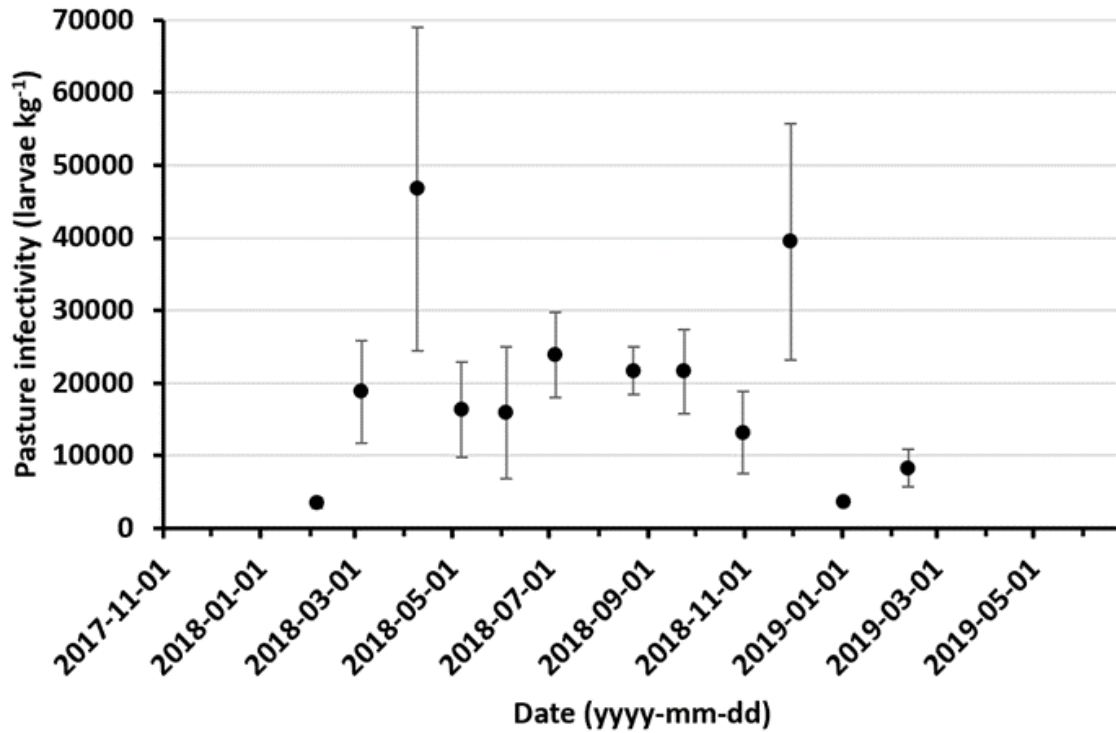


Figure 25. Observed pasture infectivity (larvae kg⁻¹) for the New South Wales experimental site. Error bars indicate the standard error.

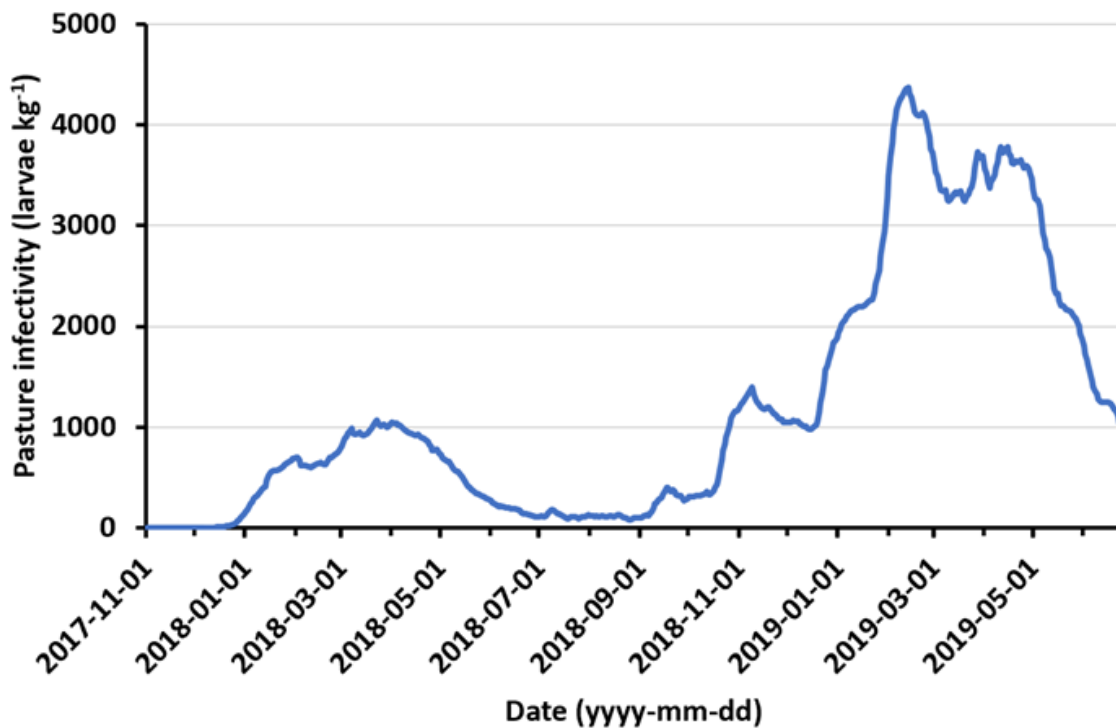


Figure 26. Predicted pasture infectivity (larvae kg⁻¹) for the New South Wales experimental site.

4.6.1.4 Live weight and body condition score

The observed and predicted values for live weight (kg) and body condition score are provided in Fig. 27 and Fig. 28, respectively; and linear regression statistics are provided in Table 12. Predicted live weight for the year 1 Merino weaners were similar to the observed values; however, the live weight predictions for the year 2 Merino weaners increased at a rapid rate diverging from the observed values. Drought conditions led to low pasture mass at the time of placement of the weaners on 8th February 2019, and consequently these animals were maintained via supplementary feed. Whilst observed live weights remained reasonably stable, supplementary feeding was not sufficient to maintain the simulated population of 2000 sheep resulting in a mortality rate of 99.95%. The remaining individual (being on the extremity of a normal distribution) had very low protein and energy requirements for maintenance (and thus managed to survive) whilst also having a fast intrinsic growth rate. As such the predicted live weight (calculated as the average of living animals) appeared to diverge from the observed values, when in fact the simulated population fared worse than the sheep within the experimental study. This suggests that the model assumption underlining the fractional supplementary feed content of feed intake may need to be readdressed (Eq. 193, section 3.6.5.3). Similarly, the predicted body condition scores were in reasonable agreement with the observed values for the year 1 Merino weaners, and over-predicted for the year 2 Merino weaners (again calculated as an average of living individuals). Nevertheless, the linear regression statistics between predicted and observed body condition scores was very good.

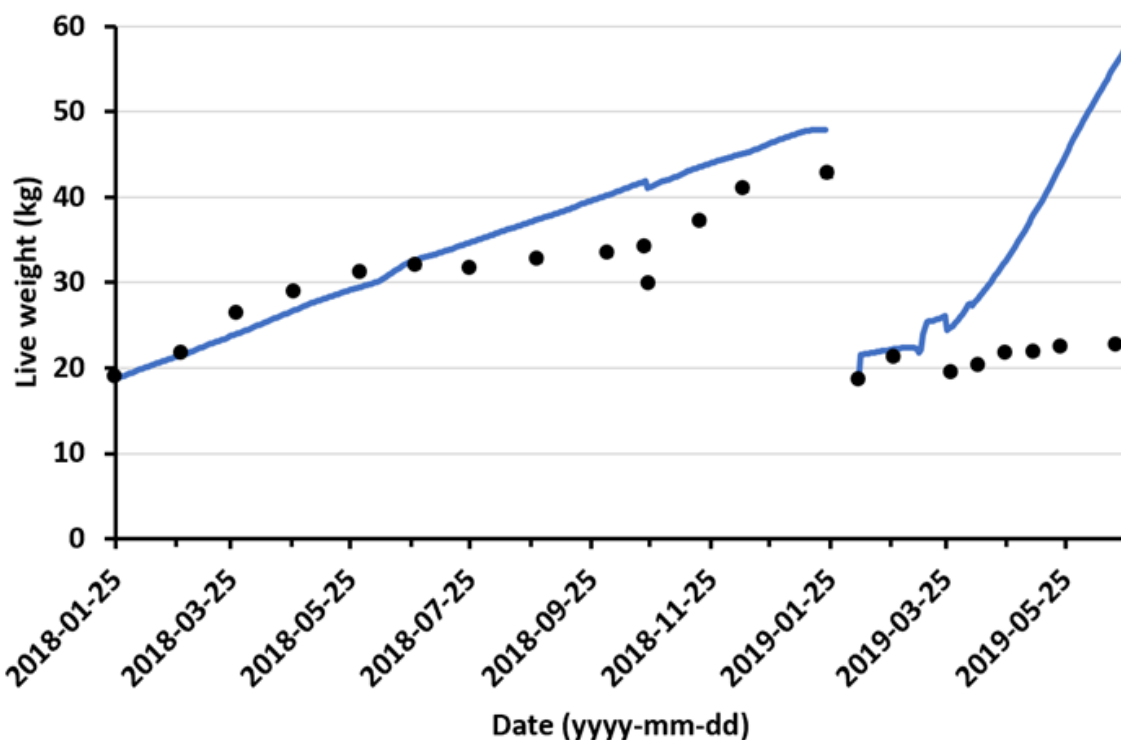


Figure 27. Predicted and observed live weight (kg) for the New South Wales experimental site. Predictions are provided by a solid blue line, and observations are provided by the circular plot points (error bars indicate the standard error).

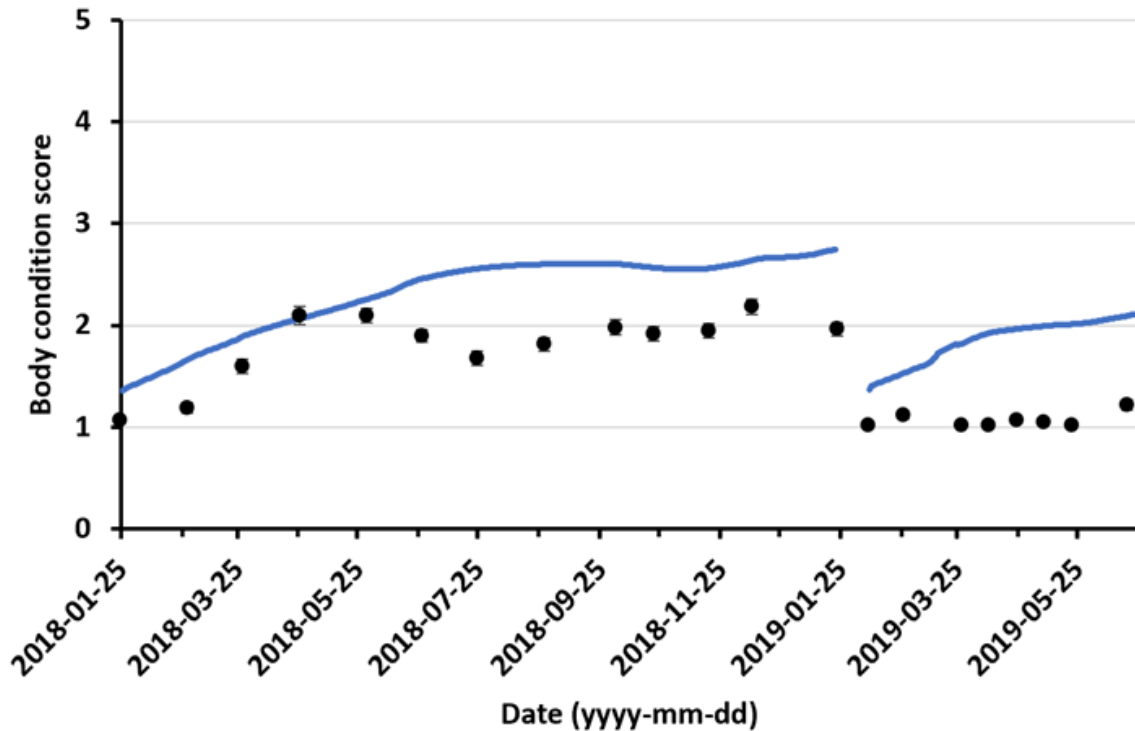


Figure 28. Predicted and observed body condition score for the New South Wales experimental site. Predictions are provided by a solid blue line, and observations are provided by the circular plot points (error bars indicate the standard error).

Table 12. Linear regression statistics for live weight and body condition score.

Trait	R^2	Standard error	$F_{1,20}$	gradient	y-intercept	p
Live weight	0.34	8.499	10.46	0.814	11.49	<0.005
Body condition score	0.63	0.271	32.44	0.757	0.988	<0.0001

4.6.1.5 Faecal egg count

The observed and predicted values for faecal egg count (FEC, eggs g^{-1}) are provided across nematode species (Fig. 29); and for *Haemonchus contortus* (Fig. 30), *Trichostrongylus* (Fig. 31) and *Teladorsagia circumcincta* (Fig. 32). Corresponding linear regression statistics are provided in Table 12. In general, across nematode species predicted FECs were greater than the observed FECs. In agreement with the observed FECs, predicted FECs were predominantly *Haemonchus contortus*. However, FECs were predicted for *Teladorsagia circumcincta* but absent in the observed FECs. Linear regression statistics were poor and non-significant for all species except the *Trichostrongylus* spp. FECs. This would thereby indicate a requirement to review the parameters determining the establishment, mortality and fecundity of each nematode species; and the functions describing faecal output (section 3.6.11).

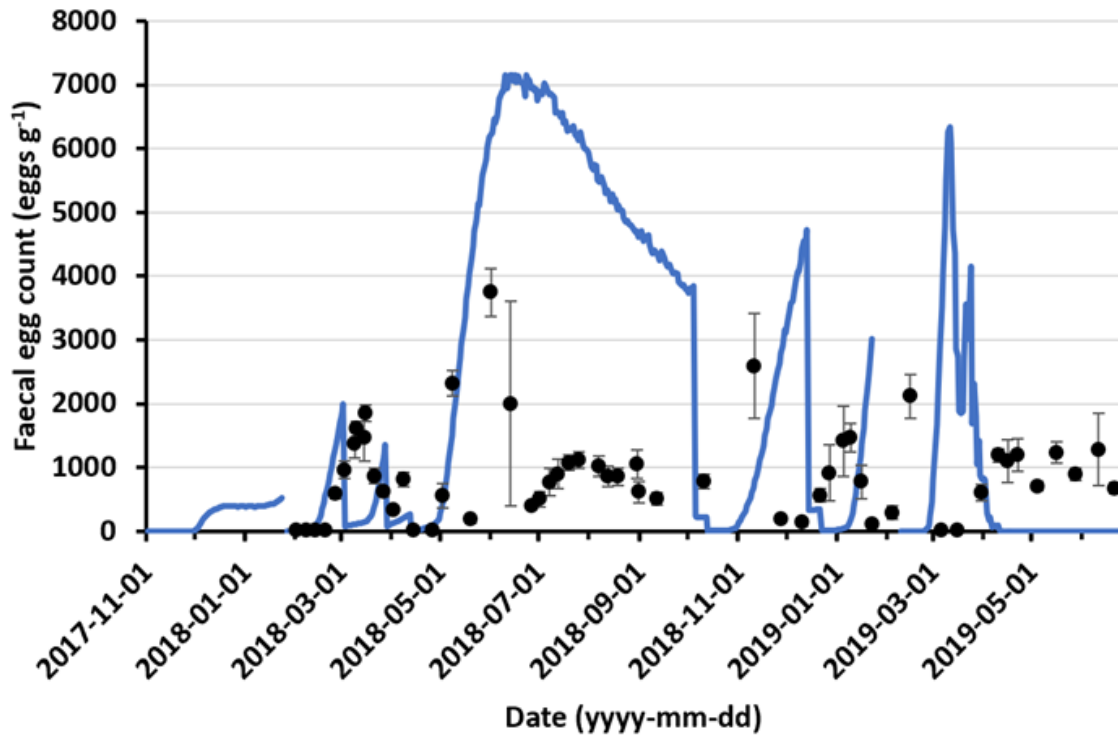


Figure 29. Predicted and observed faecal egg count (eggs g⁻¹) across nematode species for the New South Wales experimental site. Predictions are provided by a solid blue line, and observations are provided by the circular plot points (error bars indicate the standard error).

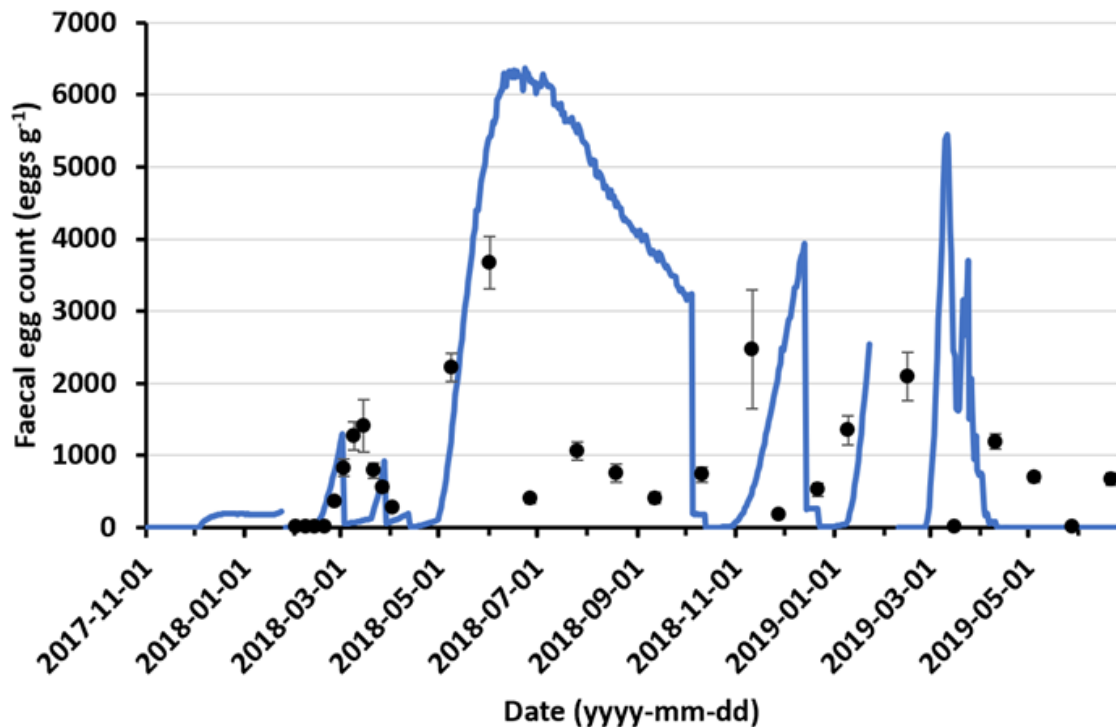


Figure 30. Predicted and observed faecal egg count (eggs g⁻¹) of *Haemonchus contortus* for the New South Wales experimental site. Predictions are provided by a solid blue line, and observations are provided by the circular plot points (error bars indicate the standard error).

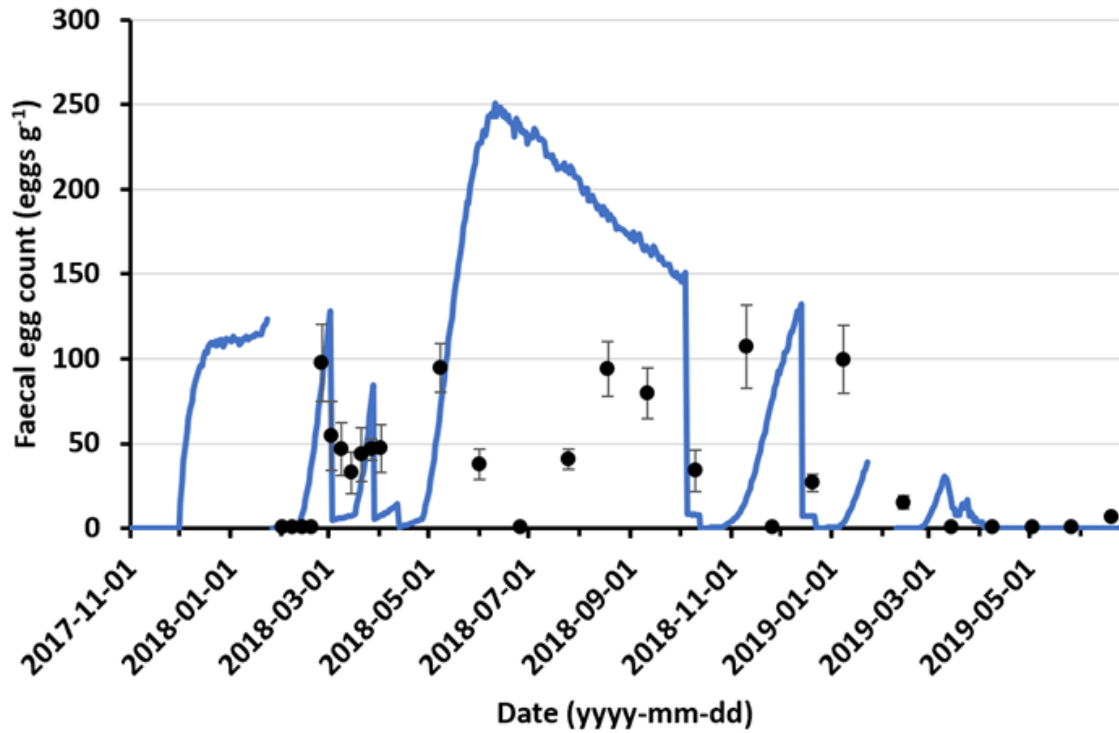


Figure 31. Predicted and observed faecal egg count (eggs g⁻¹) of *Trichostrongylus* spp. for the New South Wales experimental site. Predictions are provided by a solid blue line, and observations are provided by the circular plot points (error bars indicate the standard error).

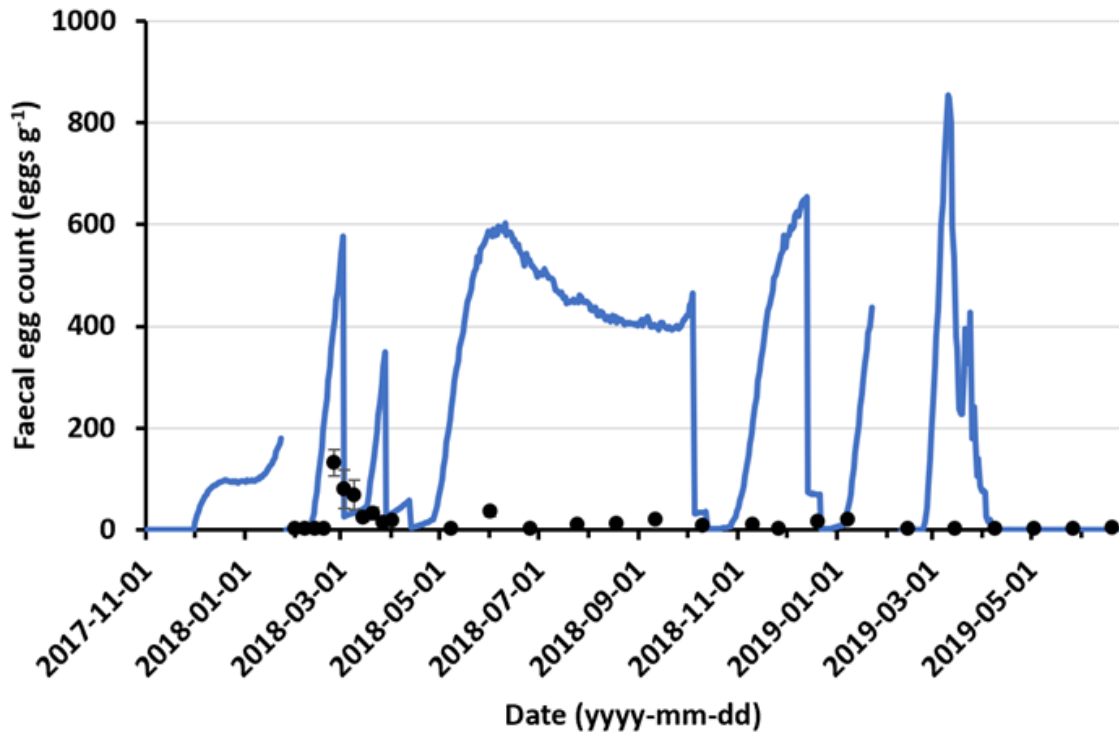


Figure 32. Predicted and observed faecal egg count (eggs g⁻¹) of *Teladorsagia circumcincta* for the New South Wales experimental site. Predictions are provided by a solid blue line, and observations are provided by the circular plot points (error bars indicate the standard error).

Table 13. Linear regression statistics for the faecal egg count predictions.

Species	R^2	Standard error	$F_{1,26}$	gradient	y-intercept	p
All	0.05	2279	2.61	0.682	1119	0.11
<i>Haemonchus</i>	0.06	1919	1.78	0.563	840	0.19
<i>Trichostrongylus</i>	0.58	50	35.30	1.563	20.96	<0.0005
<i>Teladorsagia</i>	0.01	222	0.20	-0.647	216	0.66

4.6.1.6 Faecal egg count reduction test

The faecal egg count reduction test (FECRT) carried out on the exiting 'donor' flock on 24th January 2018 indicated a 94.6% efficacy for the benzimidazole group, 97.2% for the levamisole group, and 94.6% for the macrocyclic lactone group. By 23rd January 2019, a follow up FECRT, indicated a minor increase in the efficacy of all anthelmintic classes with a benzimidazole group efficacy of 97.6%, a macrocyclic lactone group efficacy of 96.2%, and a levamisole group efficacy of 99.4%. No FECRT test was conducted in 2020 due to the cessation of the experiment as a consequence of drought conditions.

The initial efficacy of the benzimidazole group, the levamisole group, and the macrocyclic lactone group within the simulations were set to the results of the FECRT carried out on 24th January 2018. Due to lack of use, the predicted levamisole efficacy remained at 97.2% throughout the simulation. The predicted benzimidazole group efficacy reduced from 96.4% on 24th January 2018 to 96.23% on 23rd January 2019. Similarly, the predicted the macrocyclic lactone group efficacy reduced from 94.6% on 24th January 2018 to 94.18% on 19th March 2019.

4.6.2 Victoria

4.6.2.1 Weather

The meteorological data recorded at the Victoria experimental site is provided for: rainfall (mm d^{-1} , Fig. 33), solar radiation ($\text{MJ m}^{-2} \text{d}^{-1}$, Fig. 34), maximum and minimum daily temperature ($^{\circ}\text{C}$, Fig. 35), vapour pressure (kPa, Fig. 36), and windspeed measure at 2m (m s^{-1} , Fig. 37).

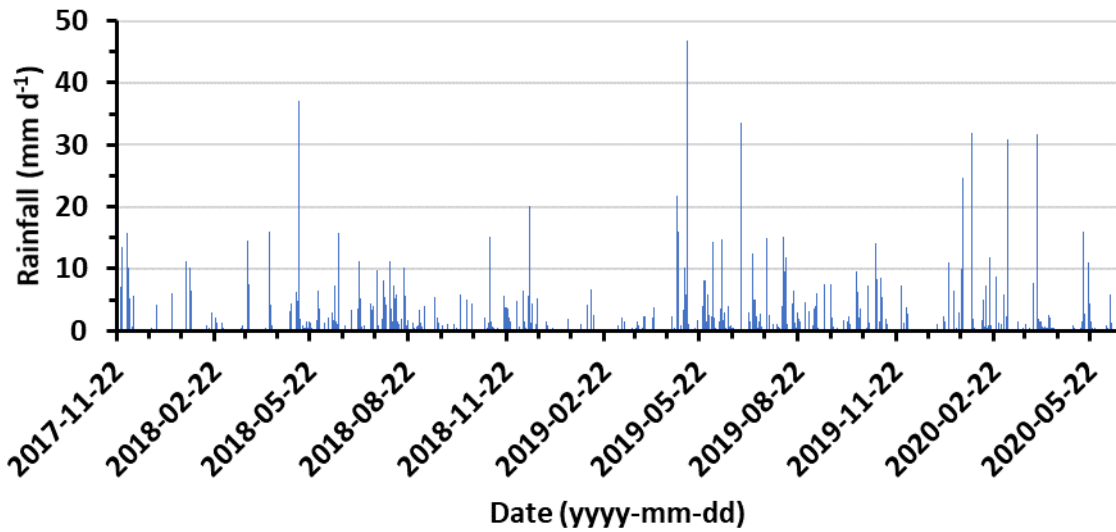


Figure 33. Rainfall (mm d^{-1}) at the Victoria experimental site.

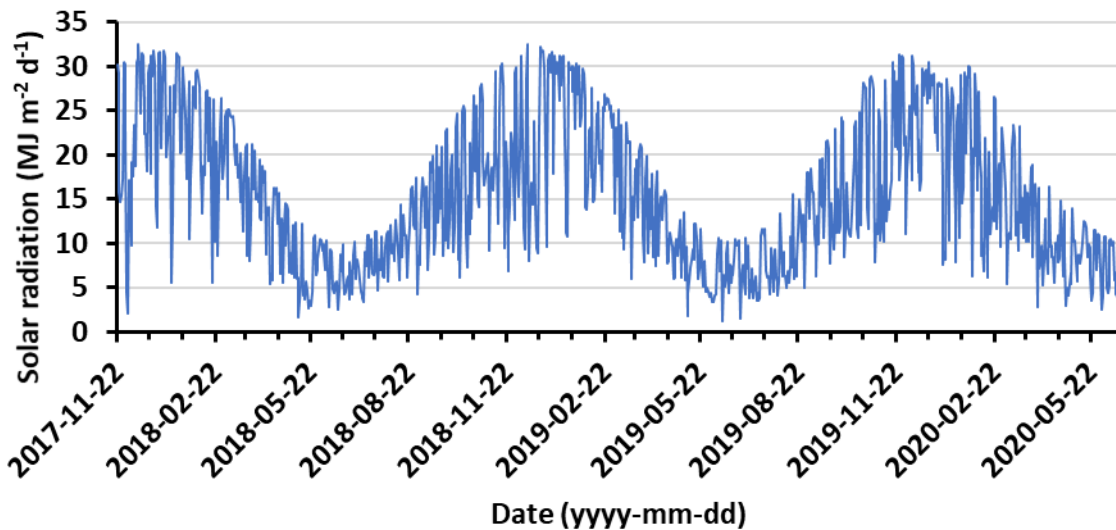


Figure 34. Rainfall (mm d^{-1}) at the Victoria experimental site.

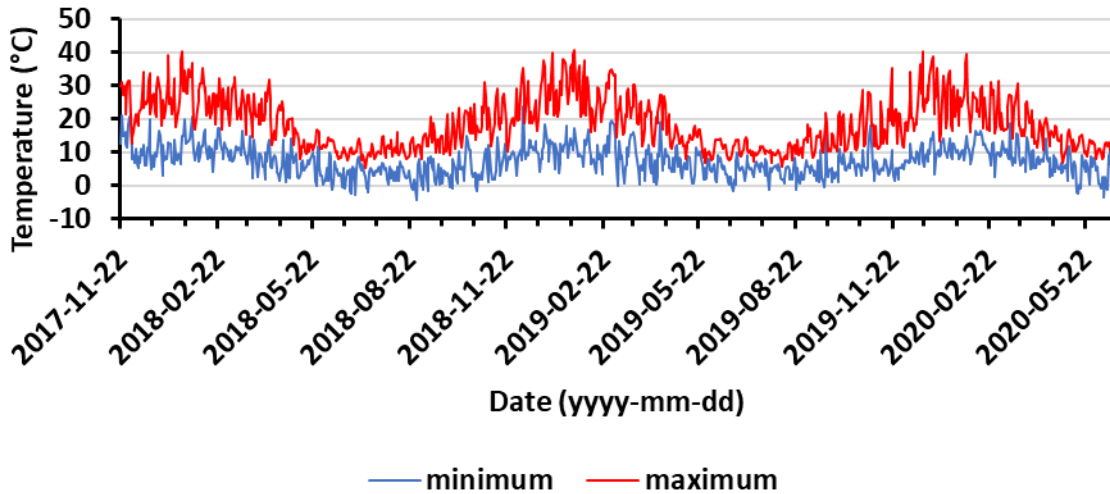


Figure 35. Daily temperature (°C) at the Victoria experimental site.

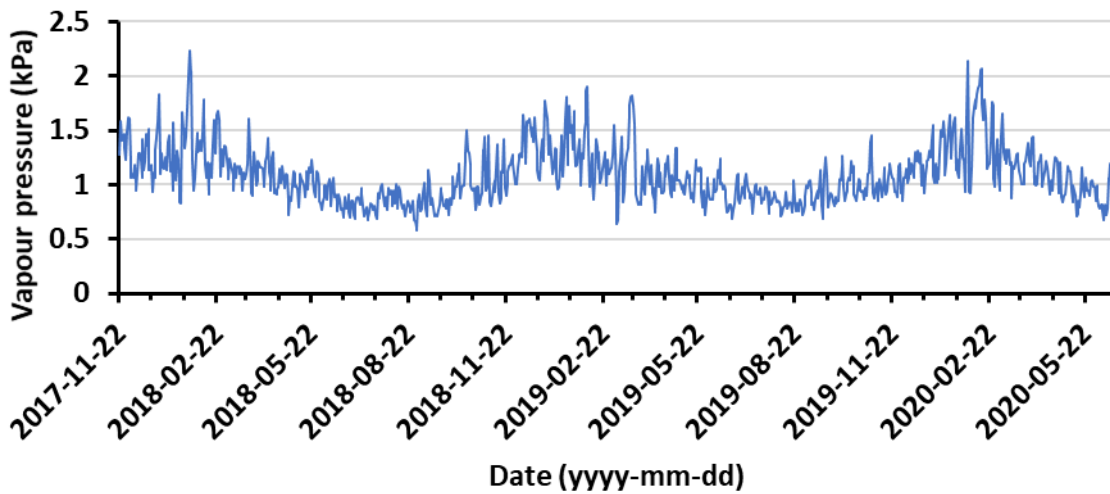


Figure 36. Vapour pressure (kPa) at the Victoria experimental site.

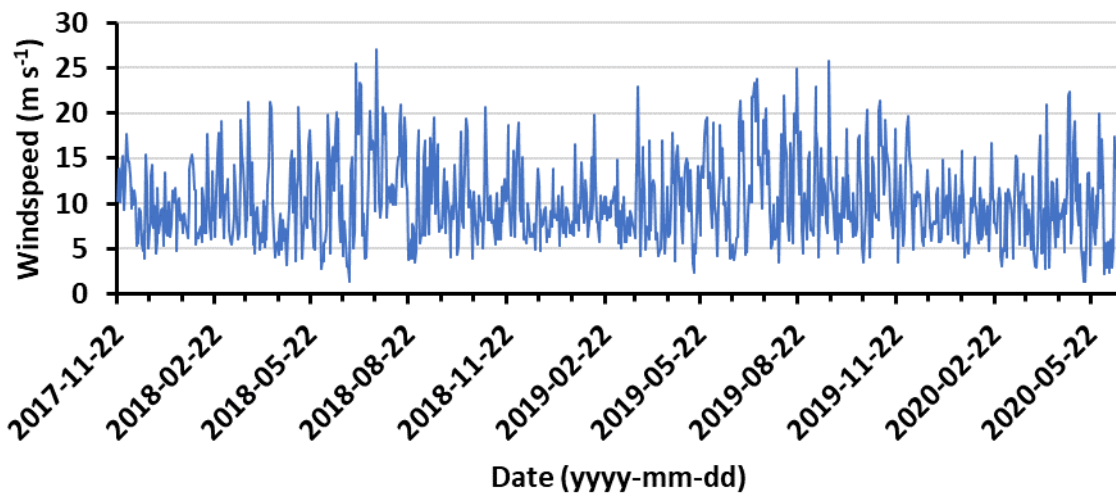


Figure 37. Windspeed at 2m (m s⁻¹) at the Victoria experimental site.

4.6.2.2 Pasture mass and quality

The observed and predicted values for pasture mass (kg) and various indicators of pasture quality are provided in Figures 38 to 43, and linear regression statistics are provided in Table 14. Whilst the predicted values for each trait follow the same trends as the observed trait values, it should be noted that predicted neutral detergent fibre and acid detergent fibre were consistently higher than the respective observations. Further, the simulations were found to be very sensitive to the input specifying the initial soil inorganic nitrogen content (mg kg^{-1}), indicating that the current nitrogen dynamics of the pasture model may be over-simplistic.

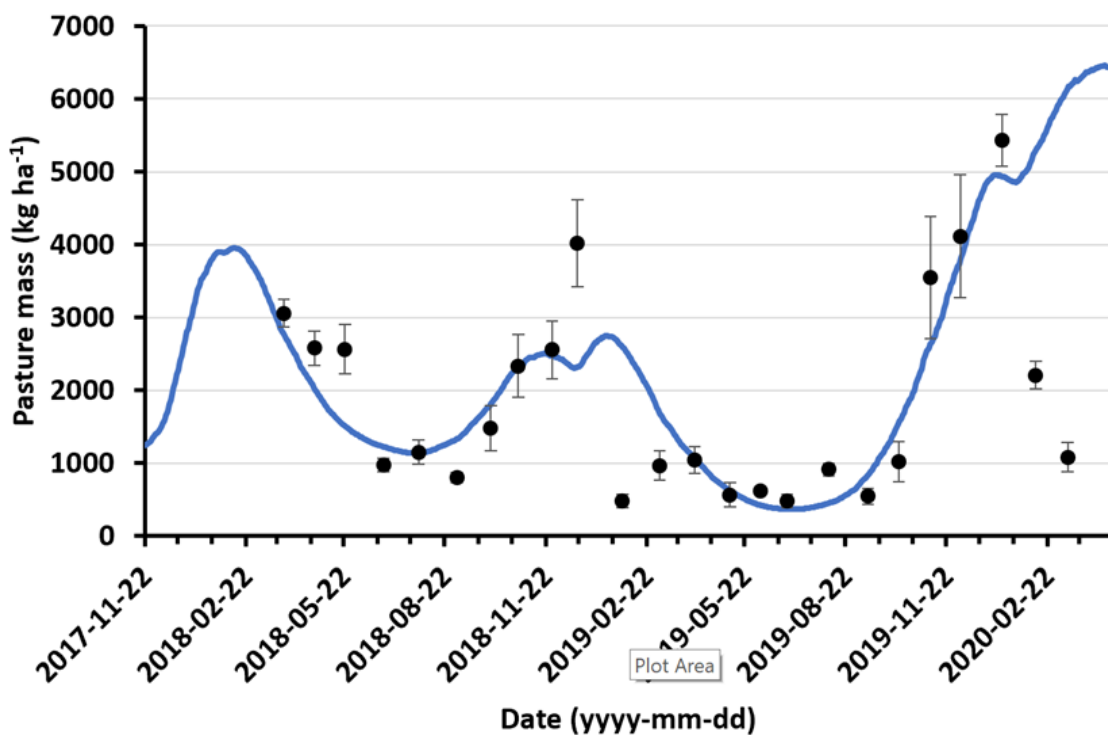


Figure 38. Predicted and observed pasture mass (kg ha^{-1}) for the Victoria experimental site. Predictions are provided by a solid blue line, and observations are provided by the circular plot points (error bars indicate the standard error).

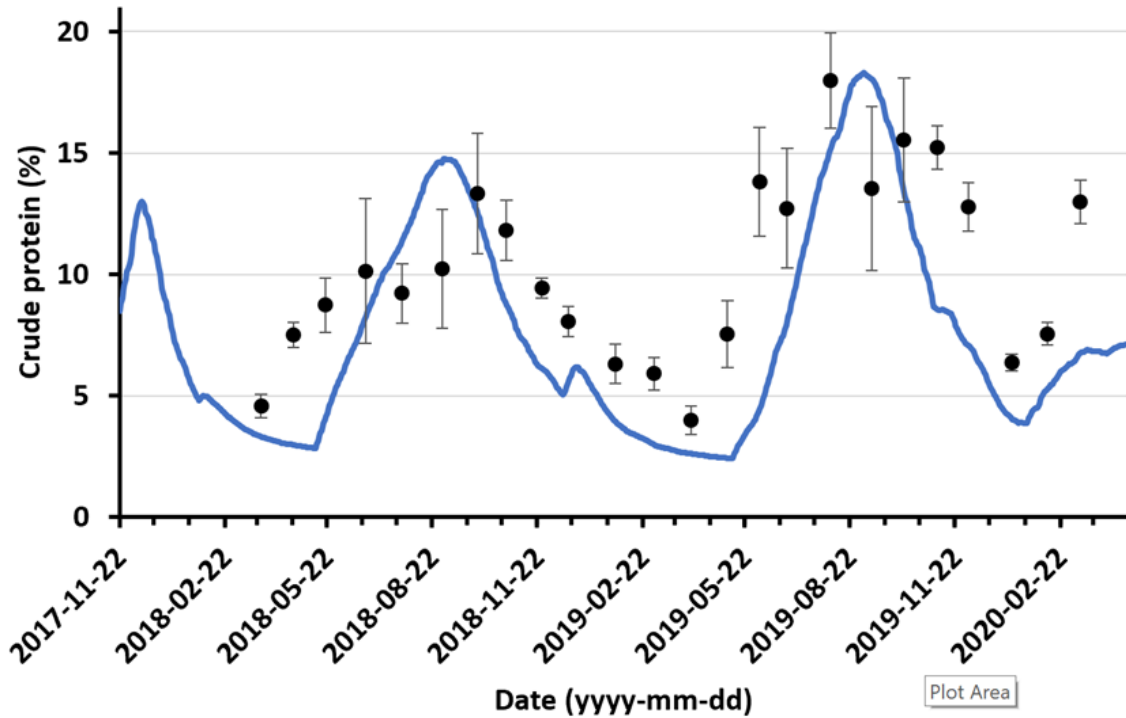


Figure 39. Predicted and observed crude protein content (%) for the Victoria experimental site. Predictions are provided by a solid blue line, and observations are provided by the circular plot points (error bars indicate the standard error).

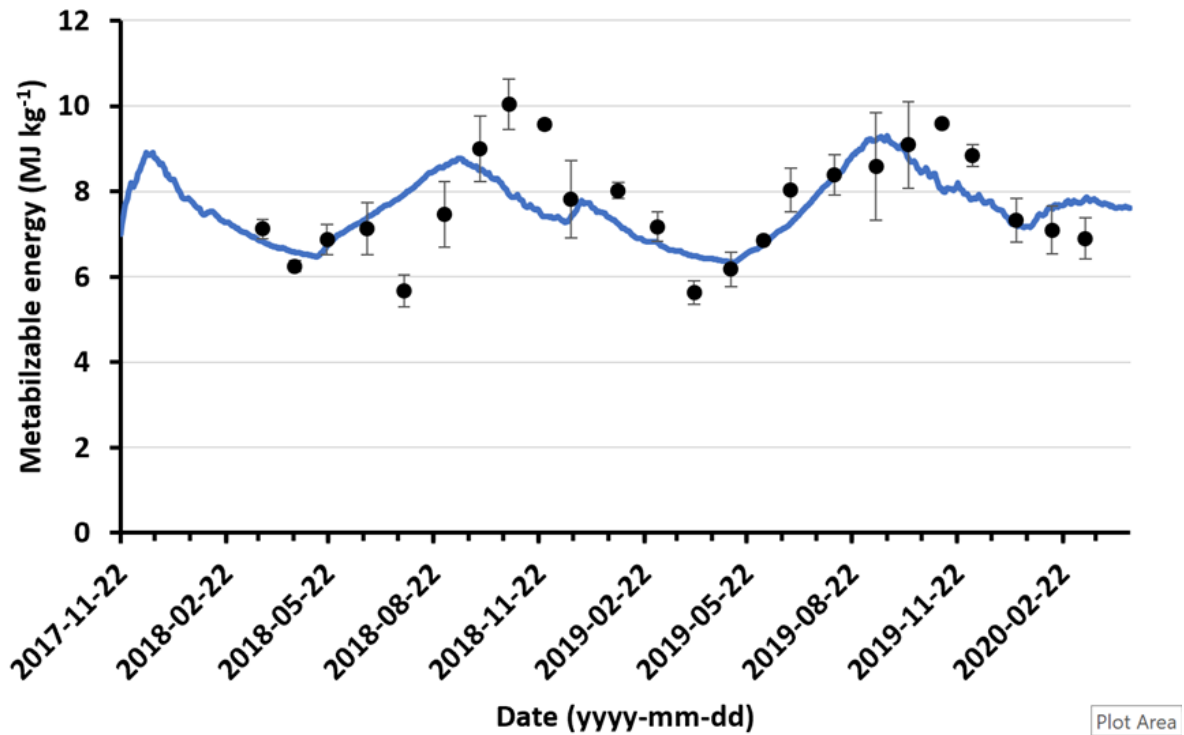


Figure 40. Predicted and observed metabolizable energy (MJ kg^{-1}) for the Victoria experimental site. Predictions are provided by a solid blue line, and observations are provided by the circular plot points (error bars indicate the standard error).

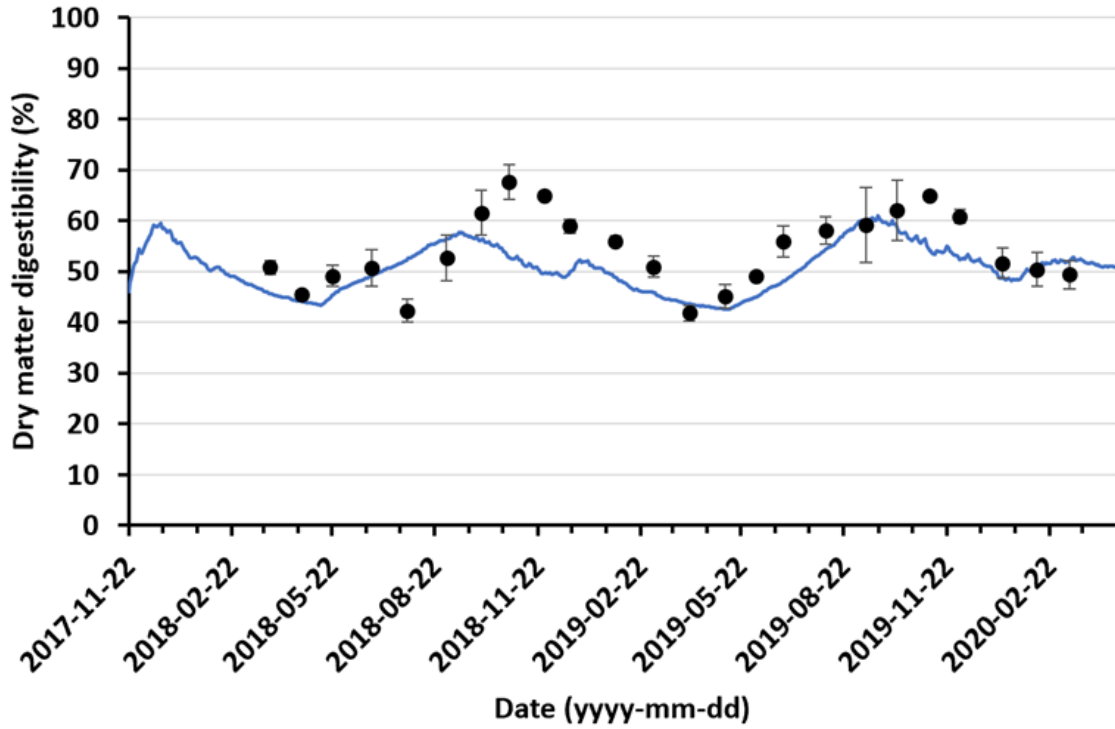


Figure 41. Predicted and observed dry matter digestibility (%) for the Victoria experimental site. Predictions are provided by a solid blue line, and observations are provided by the circular plot points (error bars indicate the standard error).

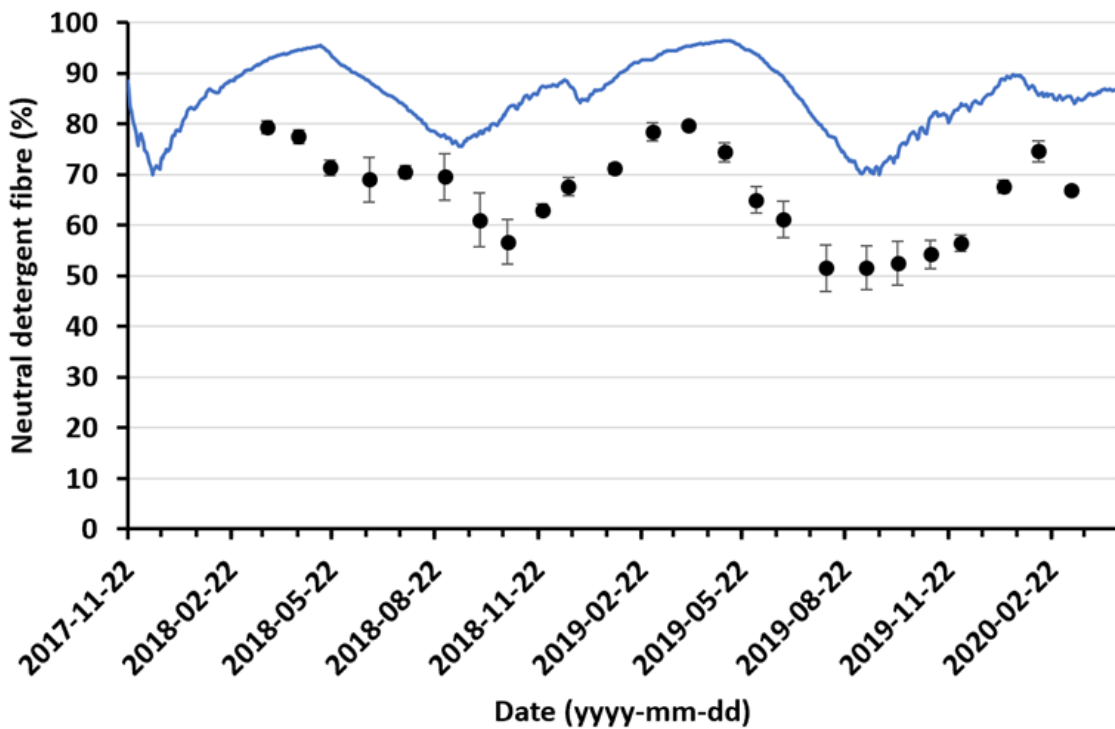


Figure 42. Predicted and observed neutral detergent fibre (%) for the Victoria experimental site. Predictions are provided by a solid blue line, and observations are provided by the circular plot points (error bars indicate the standard error).

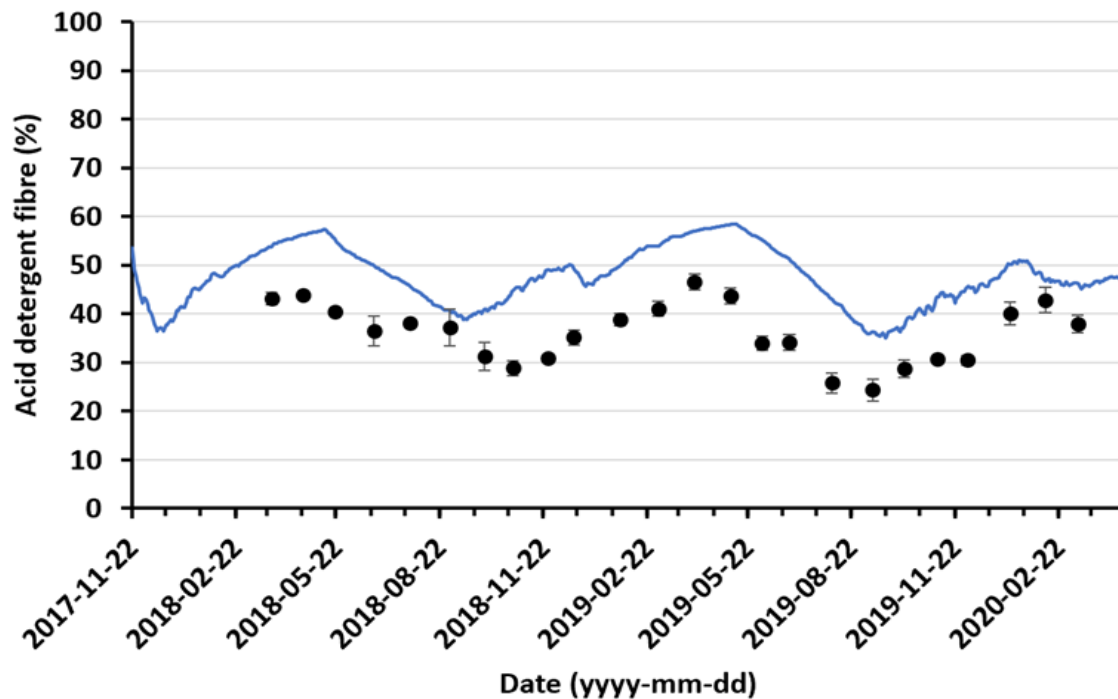


Figure 43. Predicted and observed acid detergent fibre (%) for the Victoria experimental site. Predictions are provided by a solid blue line, and observations are provided by the circular plot points (error bars indicate the standard error).

Table 14. Linear regression statistics for pasture mass and the pasture quality descriptors.

Trait	R^2	Standard error	$F_{1,22}$	gradient	y-intercept	p
Pasture mass	0.30	1317	9.52	0.614	988.36	<0.01
Crude protein	0.51	3.215	22.85	0.854	-1.196	<0.0001
Metabolizable energy	0.37	0.635	12.67	0.379	4.610	<0.005
Dry matter digestibility	0.38	3.850	13.57	0.404	28.216	<0.005
Neutral detergent fibre	0.59	4.500	31.93	0.591	47.170	<0.0001
Acid detergent fibre	0.58	4.076	30.41	0.763	21.021	<0.0001

4.6.2.3 Pasture infectivity

The observed and predicted values for pasture infectivity (larvae kg^{-1}) are provided in Fig. 44 and Fig. 45, respectively. Observed pasture infectivity values were extremely high, potentially representing an issue with the laboratory method used to measure this trait (section 4.3.6). In contrast, predicted pasture infectivity values were extremely low, suggesting a requirement to further refine the parameters describing the dynamics of nematode lifecycle and/or the influence of the host immune response. Nevertheless, despite differences in the absolute values of observed and predicted pasture infectivity the directionality of change over the year was broadly similar. Hence, a significant regression equation was found ($F_{1,22} = 8.566$, $p < 0.01$), with an adjusted R^2 of 0.28. Predicted pasture infectivity was equal to 0.0000228 of the observed pasture infectivity + 5.591, with a standard error of 4.765.

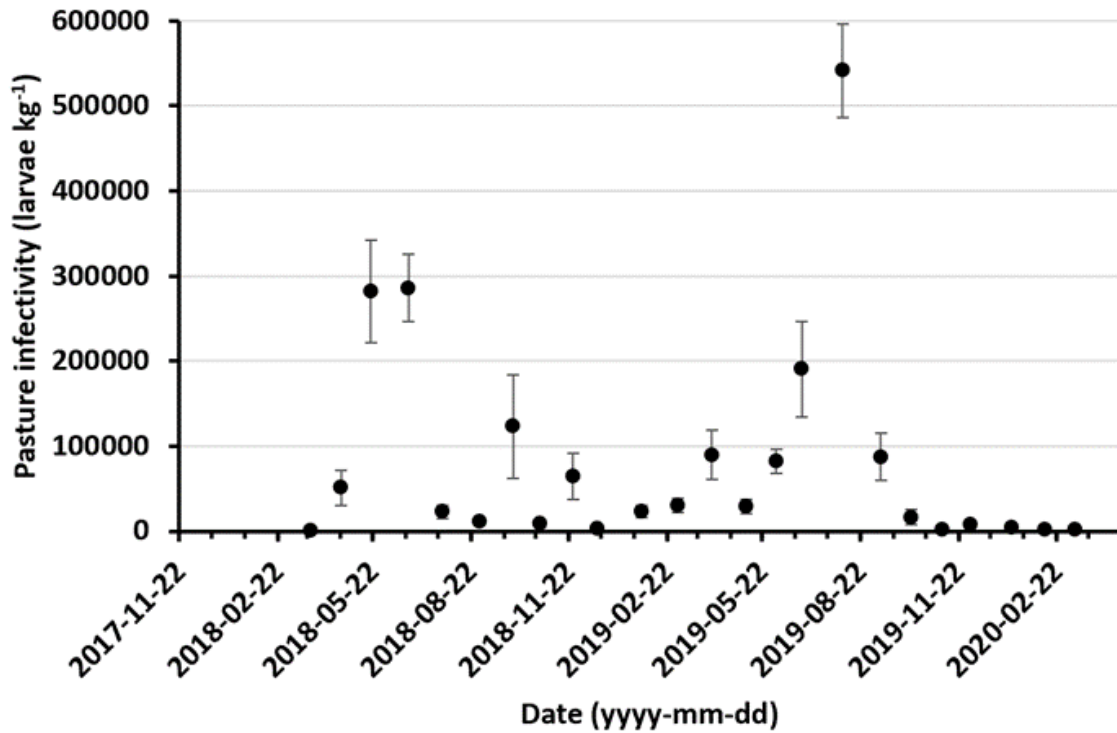


Figure 44. Observed pasture infectivity (larvae kg⁻¹) for the Victoria experimental site. Error bars indicate the standard error.

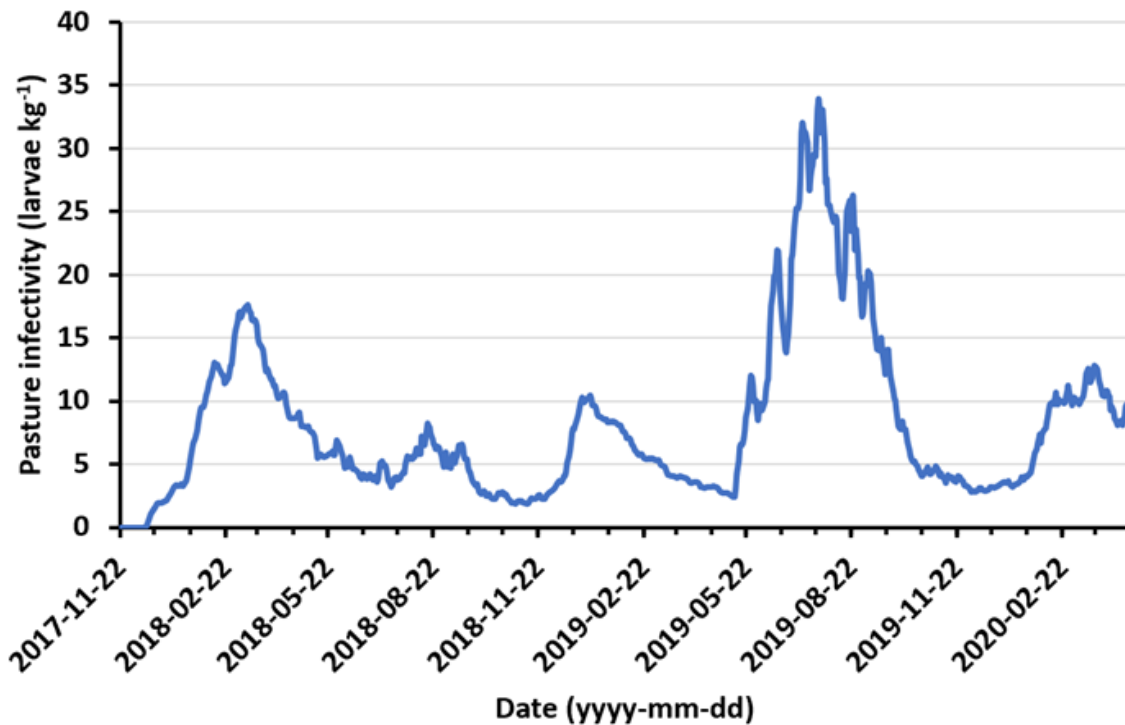


Figure 45. Predicted pasture infectivity (larvae kg⁻¹) for the Victoria experimental site.

4.6.2.4 Live weight and body condition score

The observed and predicted values for live weight (kg) and body condition score are provided in Fig. 46 and Fig. 47, respectively; and linear regression statistics are provided in Table 15. Predicted live weight increased at a faster rate than the observed values. Due to the low level of predicted pasture infectivity (section 4.6.2.3), the resultant predictions for larval and adult worm burdens and associated protein loss may also be too low. This would consequently lead to increased rate of live weight gain for the predictions in comparison to the observed values. Notably, the initial predicted reductions in live weight for the year 2 Merino weaners coincides with a period of pasture mass scarcity (Fig. 39, section 4.6.2.2). As supplementary feeding was simulated, this suggests that the model assumption underlining the fractional supplementary feed content of feed intake may need to be readdressed (Eq. 193, section 3.6.5.3). Nevertheless, the linear regression statistics for live weight gain were very good (Table 15). In contrast, it is important to note that the linear regression statistics for body condition score were very poor and not significant. Predicted body condition score was consistently lower than the observed values. This is also likely to occur as a consequence of low levels of protein loss due to parasitism, such that the ratio of body lipid to body protein remains low (i.e. a low body condition score).

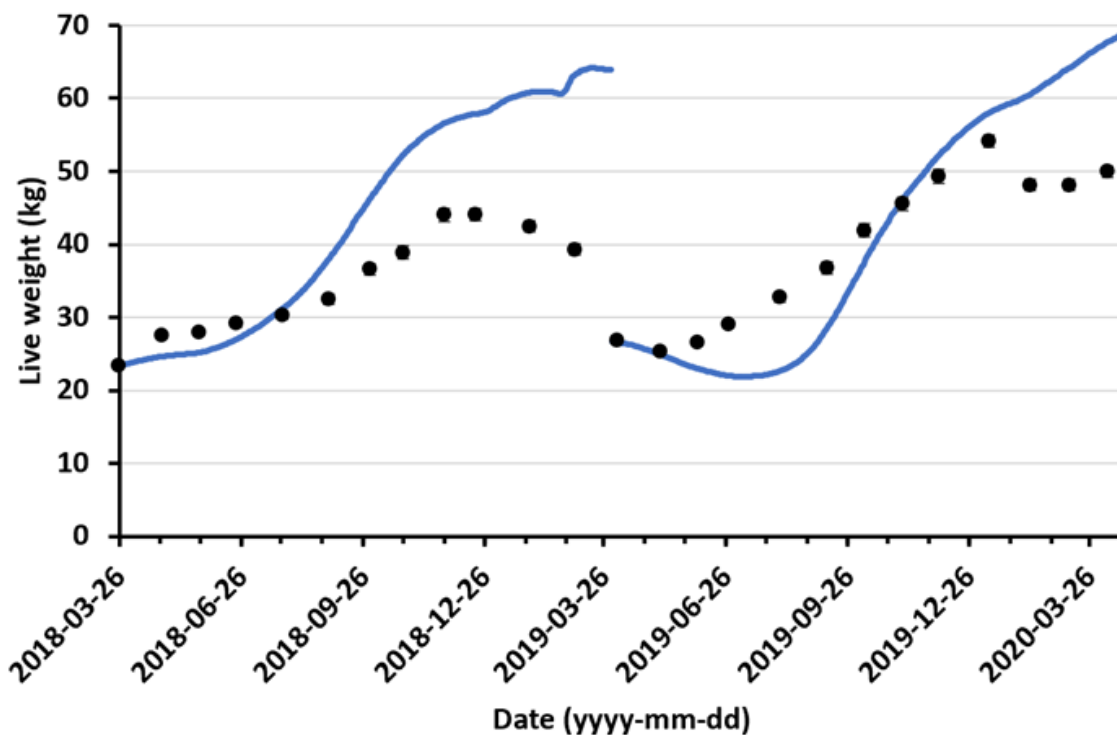


Figure 46. Predicted and observed live weight (kg) for the Victoria experimental site. Predictions are provided by a solid blue line, and observations are provided by the circular plot points (error bars indicate the standard error).

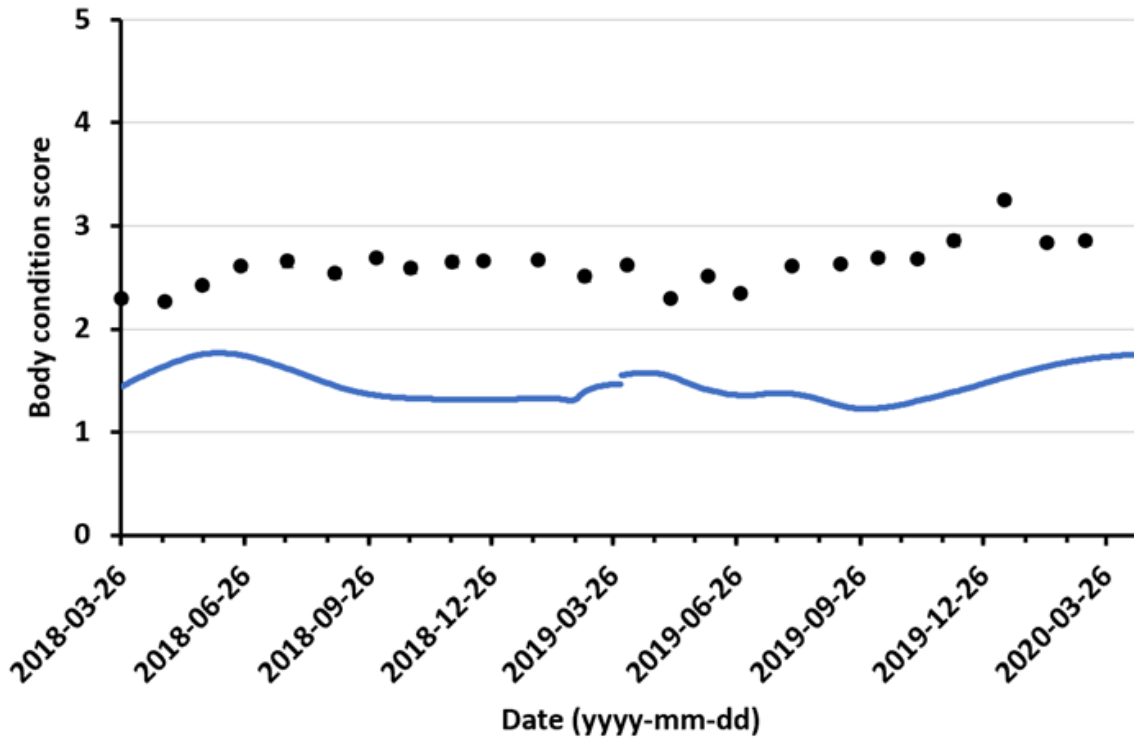


Figure 47. Predicted and observed body condition score for the Victoria experimental site. Predictions are provided by a solid blue line, and observations are provided by the circular plot points (error bars indicate the standard error).

Table 15. Linear regression statistics for live weight and body condition score.

Trait	R ²	Standard error	F _{1,23}	gradient	y-intercept	p
Live weight	0.78	7.887	79.70	1.567	-16.724	<0.0001
Body condition score	0.04	0.162	0.037	-0.030	1.533	0.85

4.6.2.5 Faecal egg count

The observed and predicted values for faecal egg count (eggs g⁻¹) are provided across nematode species (Fig. 48); and for *Haemonchus contortus* (Fig. 49), *Trichostrongylus* (Fig. 50) and *Teladorsagia circumcincta* (Fig. 51). Corresponding linear regression statistics are provided in Table 16. Following artificial infection on 22nd November 2017, the faecal egg count (FEC) of the ‘donor’ flock rose for all nematode species. Whilst the FEC predictions also rose during this period, the predicted FEC of all nematode species was lower than the observed values. This would thereby indicate a requirement to review the parameters determining the establishment, mortality and fecundity of each nematode species; and the functions describing faecal output (section 3.6.11). Following placement of the year 1 Merino weaners on 26th March 2018, FECs continued to be observed (predominantly *Trichostrongylus* spp.) despite the frequent use of anthelmintics. In contrast, the frequent use of anthelmintics, alongside the low pasture infectivity predictions (section 4.6.2.3), led to very low FEC predictions for all nematode species. Following placement of the year 2 Merino weaners on 1st April 2019, FECs continued to be observed for *Teladorsagia circumcincta*. Predicted FECs for the *Trichostrongylus* spp. were extremely low, similar to the observed *Trichostrongylus* FECs; and

Teladorsagia circumcincta FEC predictions rose (albeit to lower levels than the observed values). However, in contrast to the observed *Haemonchus contortus* FECs, which remained close to zero from 22nd June 2018, *Haemonchus contortus* FEC predictions rose following placement of the year 2 Merino weaners. This was likely due to low pasture infectivity predictions resulting in low larval and adult worm burdens and thereby hampering the acquisition of immunity; as well as the high fecundity of *Haemonchus contortus*; such that even a small *Haemonchus* challenge was sufficient to result in the FEC predictions for this nematode species. These differences between the observed and predicted FECs resulted in an R^2 of 0.21 (across nematode species). Whilst this may appear poor, this represents a markable improvement upon previous modelling efforts.

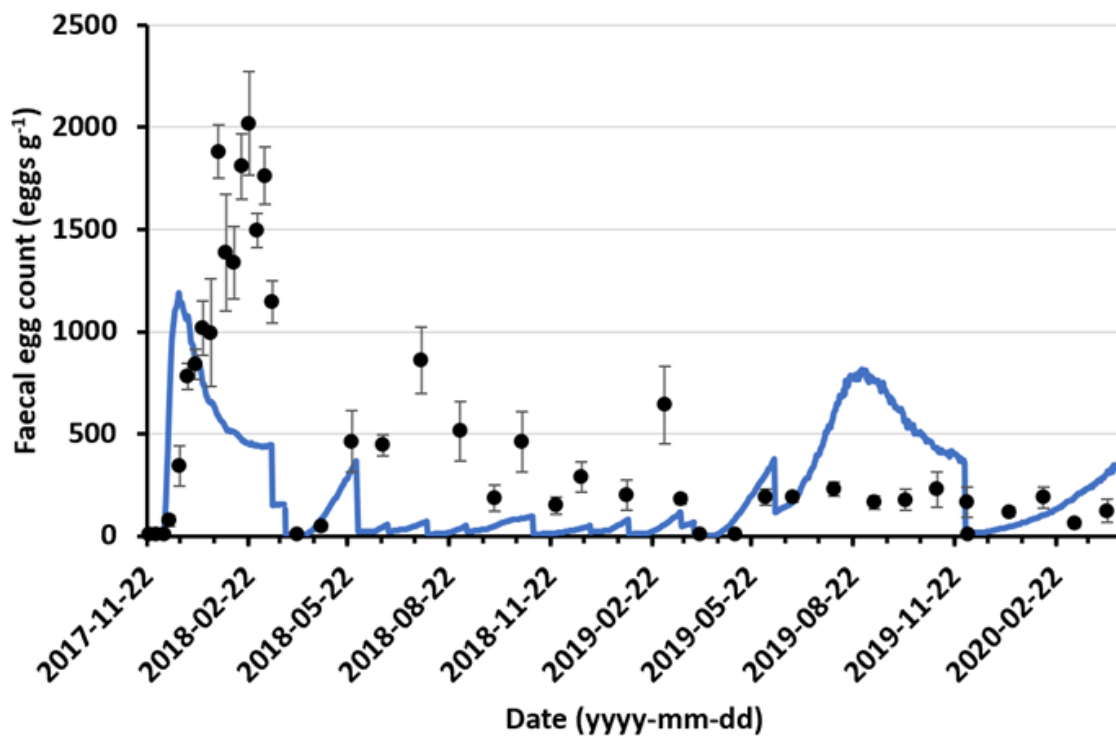


Figure 48. Predicted and observed faecal egg count (eggs g⁻¹) across nematode species for the Victoria experimental site. Predictions are provided by a solid blue line, and observations are provided by the circular plot points (error bars indicate the standard error).

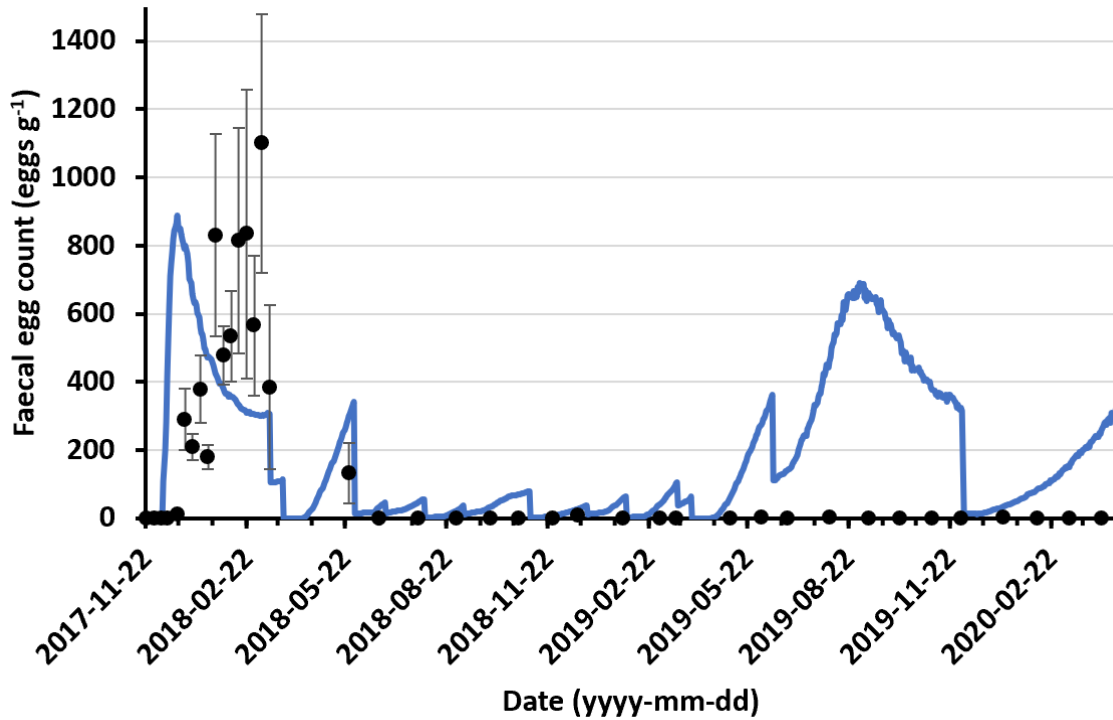


Figure 49. Predicted and observed faecal egg count (eggs g⁻¹) of *Haemonchus contortus* for the Victoria experimental site. Predictions are provided by a solid blue line, and observations are provided by the circular plot points (error bars indicate the standard error).

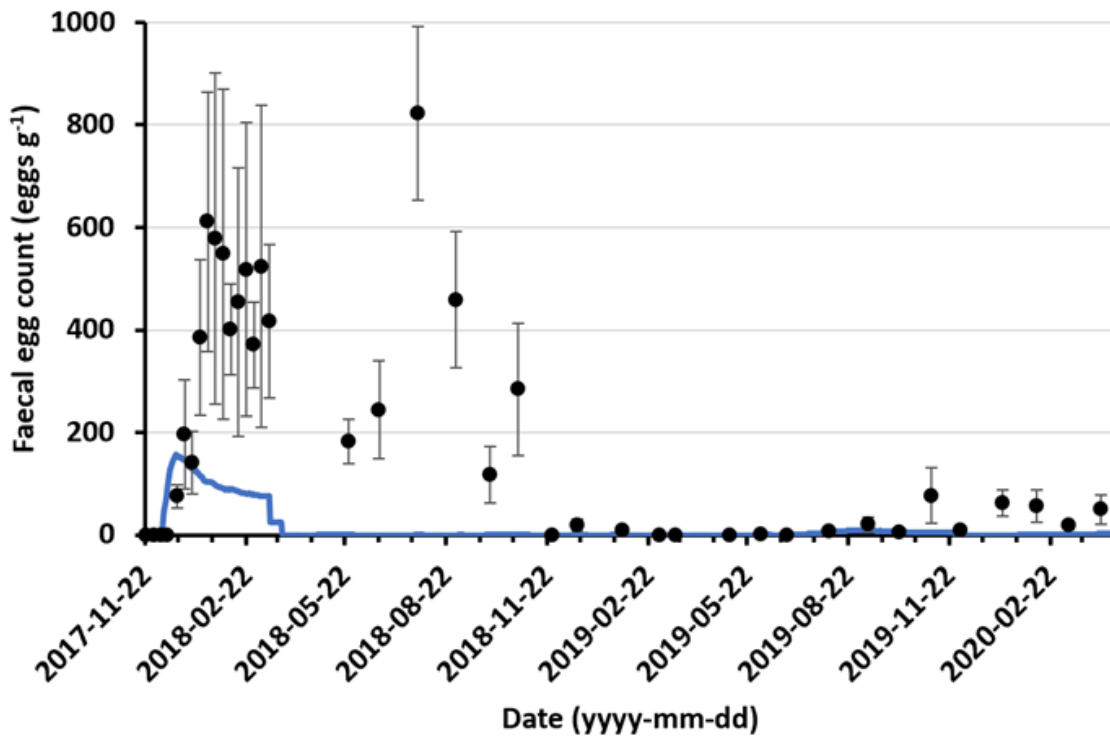


Figure 50. Predicted and observed faecal egg count (eggs g⁻¹) of *Trichostrongylus* spp. for the Victoria experimental site. Predictions are provided by a solid blue line, and observations are provided by the circular plot points (error bars indicate the standard error).

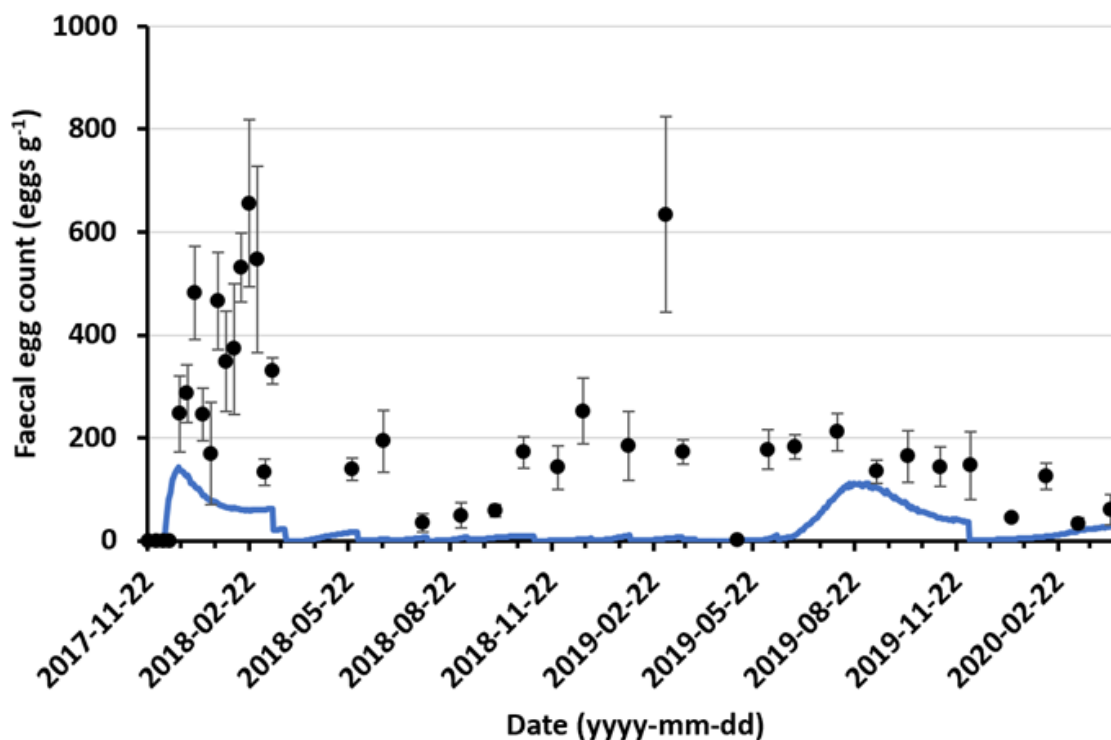


Figure 51. Predicted and observed faecal egg count (eggs g⁻¹) of *Teladorsagia circumcincta* for the Victoria experimental site. Predictions are provided by a solid blue line, and observations are provided by the circular plot points (error bars indicate the standard error).

Table 16. Linear regression statistics for the faecal egg count predictions.

Species	R ²	Standard error	F _{1,42}	gradient	y-intercept	p
All	0.21	287	11.25	0.248	189	<0.005
<i>Haemonchus</i>	0.11	230	4.60	0.266	221	<0.05
<i>Trichostrongylus</i>	0.24	23	11.96	0.055	7.45	<0.005
<i>Teladorsagia</i>	0.17	38	7.67	0.095	21	<0.01

4.6.2.6 Faecal egg count reduction test

The faecal egg count reduction test (FECRT) carried out on the exiting 'donor' flock on 14th March 2018 indicated a 70.7% efficacy for the benzimidazole group, 96.8% for the levamisole group, and 96.1% for the macrocyclic lactone group. By 19th March 2019, a follow up FECRT, indicated a macrocyclic lactone group efficacy of 59.2%, and a levamisole group efficacy of 72.1%. By the FECRT carried out on 4th April 2020, the macrocyclic lactone group efficacy had reduced to 53.5%.

Whilst the observed reduction in the macrocyclic lactone group efficacy could be attributed to the frequent use of anthelmintics (as a consequence of a low regional treatment threshold), a reduction in levamisole efficacy was also observed despite a lack of use (included in the FECRT as a positive control). As such, the observed reduction in the macrocyclic lactone group efficacy was likely a consequence of attempting to determine efficacy from low faecal egg counts rather than as a

consequence of anthelmintic use. This was also the likely reason for the failure to determine the benzimidazole group in the FECRTs carried out on 19th March 2019 and 4th April 2020.

The initial efficacy of the benzimidazole group, the levamisole group, and the macrocyclic lactone group within the simulations were set to the results of the FECRT carried out on 14th March 2018. Due to lack of use, the predicted levamisole efficacy remained at 96.8% throughout the simulation. The predicted benzimidazole group efficacy reduced from 70.7% on 14th March 2018 to 70.28% on 19th March 2019, and then rose again to 70.65% by 4th April 2020. Similarly, the predicted the macrocyclic lactone group efficacy reduced from 96.1% on 14th March 2018 to 94.55% on 19th March 2019, and then rose again to 95.32% by 4th April 2020. As no fitness disadvantages were included within the model, the apparent reversion towards susceptibility predicted from 19th March 2019 to 4th April 2020 were likely a consequence of fluctuations in the species proportions of the resident parasitic burden. Nevertheless, minor reductions in the efficacies of the benzimidazole and macrocyclic lactone groups were predicted when considering the starting and ending efficacies of the simulation. These reductions in predicted efficacies were small despite low levels of predicted pasture infectivity (i.e. *refugia*) as predicted parasitic burdens were also small.

5. Tool and model accessibility

5.1 Tool

The tool (Turned Worm) is currently available at turnedworm-uat.une.edu.au but this url may change as integration with the ParaBoss suite of websites is completed. The site contains a User Guide and a number of Information Buttons to assist users in the use of the Turned Worm model.

5.2 Model accessibility

The current site, turnedworm-uat.une.edu.au, also provides full access to the mathematical model as open-source code (folder – zipped) and to model documentation through the download of a zipped folder.

6. Conclusion

6.1 Key findings

This project successfully developed a mathematical model describing the epidemiology of nematode infection that could predict pasture infectivity, worm burdens, drug resistance and the productive and financial consequences arising from the combination of various options for parasite control. The validation field studies identified various model weaknesses. Most notably, the sensitivity of the pasture model to user inputs describing the initial soil inorganic nitrogen content, the model components accounting for the impact of supplementary feeding, and a reliance upon parameter estimates from published literature derived from experimental studies where confounding effects within the experimental design may have influenced the determination of appropriate values. Further, the processing time for simulations is currently excessive. Whilst attempts were made to reduce processing time by optimising the model code, and providing optional outputs for time consuming processes (i.e. the calculation of heritabilities, phenotypic correlations and genotypic correlations), further code optimisation could significantly reduce processing time.

6.2 Benefits to industry

Control of internal parasites has become harder and more complex as the prevalence and severity of drench resistance has increased. Components of integrated control programs are well known but poorly adopted by sheep producers because they are uncertain of benefits. Advisors remain concerned about negative consequences when integrated control programs are poorly implemented: for example, drenching sheep moving into low worm-risk paddocks can increase drench resistance. The tool developed within this project will provide a simple yet powerful resource to encourage adoption of integrated control programs by demonstrating benefit and mitigating against negative consequences in a manner specific for each farm.

7. Future research and recommendations

The tool should be used to generate industry and academic communications to facilitate its adoption via demonstrating the benefit of parasite control and elucidating negative interactions between parasite control options.

Further, the tool would benefit from continuing development of the underlying mathematical model to address the weaknesses identified by the validation study. These efforts should initially be focussed on:

1. Addressing the sensitivity of the pasture model to user inputs describing the initial soil inorganic nitrogen content by providing a more comprehensive description of nitrogen dynamics.
2. Readdressing the model components accounting for the impact of supplementary feeding.
3. Reassessing parameter estimates from published literature that describe the dynamics of the nematode lifecycle and host-parasite interactions to provide more reliable prediction of the model's parasitological outputs.

Finally, processing time and memory requirement are currently excessive and this limits the number of paddocks, mobs and period for the simulations in the tool. Whilst attempts were made to reduce processing time by optimising the model code, and providing optional outputs for time consuming processes (i.e. the calculation of heritabilities, phenotypic correlations and genotypic correlations), further code optimisation could significantly reduce processing time. For example, the model currently simulates 2000 individuals for every mob. This requirement was included to facilitate the simulation of targeted treatments and the estimation of outputs that would aid in the development of selective breeding programs. However, in the instance where no targeted treatments are specified by user input and the optional outputs for heritabilities, phenotypic correlations and genotypic correlations are not requested; then there is no requirement to simulate 2000 individuals for every mob. Under such scenarios only a single individual representing the population mean need to be simulated, and thus a 2000-fold decrease in processing time could be achieved.

Notwithstanding these comments, the tool provides industry advisors, producers and students for the first time, with the ability to independently explore the impacts of nematode infection and the consequences of various treatment regimens for production and anthelmintic resistance. Such investigations can be used to develop farm specific nematode control programs. The next step for MLA and UNE is to plan how this tool can be integrated with MLA and industry programs and web resources and supported by a communication plan.

8. References

- Agricultural and Food Research Council, AFRC. (1993). *Energy and Protein Requirements of Ruminants. An Advisory Manual Prepared by the AFRC Technical Committee on Response to Nutrients*. CAB International, Wallingford, UK.
- Allen, R.G., Pereira, L.S., Raes, D., Smith, M. (1998). Crop evapotranspiration – Guidelines for computing crop water requirements – FAO Irrigation and drainage paper 56. Food and Agriculture Organization of the United Nations, Rome.
https://appgeodb.nancy.inra.fr/biljou/pdf/Allen_FAO1998.pdf [verified: 16/05/2019]
- Allen, R.G., Pereira, L.S., Smith, M., Raes, D., Wright, J.L. (2005). FAO-56 Dual crop coefficient method for estimating evaporation from soil and application extensions. *Journal of Irrigation and Drainage Engineering* **131**: 2-13
- Allen, R.G., Pruitt, W.O., Wright, J.L., Howell, T.A., Ventura, F., Snyder, R., Itenfisu, D., Steduto, P., Berengena, J., Baselga Yrisarry, J., Smith, M., Pereira, L.S., Raes, D., Perrier, A., Alves, I., Walter, I., Elliott, R. (2006). A recommendation on standardized surface resistance for hourly calculation of reference ET₀ by the FAO56 Penman-Monteith method. *Agricultural Water Management* **81**: 1-22
- Amthor, J.S. (2010). From sunlight to phytomass: on the potential efficiency of converting solar radiation to phyto-energy. *New Phytologist* **188**: 939-959
- Andersen, F.L., Wang, G.-T., Levine, N.D. (1966). Effect of temperature on survival of the free-living stages of *Trichostrongylus colubriformis*. *The Journal of Parasitology* **52**: 713-721
- Arrendondo, J.T., Schnyder, H. (2003). Components of leaf elongation rate and their relationship to specific leaf area in contrasting grasses. *New Phytologist* **158**: 305-314
- Australian Fodder Industry Association (AFIA). (2014). Method 2.2R – calculation of metabolisable energy. In 'AFIA – Laboratory Methods Manual: a reference manual of standard methods for the analysis of fodder.' pp. 91–92. (AFIA: Melbourne) Available at
https://www.afia.org.au/files/AFIALabManua_v8_rm.pdf [verified: 16/05/2019]
- Barnes E.H., Dobson R.J. (1990) Population dynamics of *Trichostrongylus colubriformis* in sheep: computer model to simulate grazing systems and the evolution of anthelmintic resistance. *International Journal for Parasitology* **20**: 823-831
- Barnes, E.H., Dobson, R.J., Barger, I.A. (1995). Worm Control and Anthelmintic Resistance: Adventures with a Model. *Parasitology Today* **11**: 56-63
- Benedict, F.G., Osborne, T.B. (1907). The heat of combustion of vegetable proteins. *Journal of Biological Chemistry* **3**: 119-133
- Bernacchi, C.J., Singaas, E.L., Pimentel, C., Portis, A.R., Long, S.P. (2001). Improved temperature response functions for models of Rubisco-limited photosynthesis. *Plant, Cell and Environment* **24**: 253-259
- Bernacchi, C.J., Portis, A.R., Nakano, H., von Caemmerer, S., Long, S.P. (2002). Temperature response of mesophyll conductance. Implication for the determination of Rubisco enzyme kinetics and for limitations to photosynthesis in vivo. *Plant Physiology* **130**: 1992-1998
- Beveridge, I., Pullman, A.L., Martin, R.R., Barelds, A. (1989). Effects of temperature and relative humidity on development and survival of the free-living stages of *Trichostrongylus colubriformis*, *T. rugatus* and *T. vitrinus*. *Veterinary Parasitology* **33**: 143-153

- Bishop, S.C., Bairden, K., McKellar, Q.A., Park, M., Steer, M.J. (1996). Genetic parameters for faecal egg count following mixed, natural, predominantly *Ostertagia circumcincta* infection and relationships with live weight in young lambs. *Animal Science* **63**: 423-428
- Bishop, S.C., Stear, M.J. (1997). Modelling responses to selection for resistance to gastro-intestinal parasites in sheep. *Animal Science* **64**: 469-478
- Bishop, S.C., Stear, M.J. (2000). The use of a gamma-type function to assess the relationship between the number of adult *Teladorsagia circumcincta* and total egg output. *Parasitology* **121**: 435-440
- Blaxter, K.L., Fowler, V.A., Gill, J.C. (1982). A study of the growth of sheep to maturity. *The Journal of Agricultural Science* **98**: 405-420
- Byrne, K.A., Kiely, G., Leahy, P. (2005). CO₂ fluxes in adjacent new and permanent temperate grasslands. *Agricultural and Forest Meteorology* **135**: 82-92
- Carta, A., Sanna, S.R., Casu, S. (1995). Estimating lactation curves and seasonal effects for milk, fat and protein in Sarda dairy sheep with a test day model. *Livestock Production Science* **44**: 37-44
- Clarkson, D.T., Hopper, M.J., Jones, L.H.P. (1986). The effect of root temperature on the uptake of nitrogen and the relative size of the root system in *Lolium perenne*. I. Solutions containing both NH₄⁺ and NO₃⁻. *Plant, Cell and Environment* **9**: 535-545
- Coffey, M.P., Emmans, G.C., Brotherstone, S. (2001). Genetic evaluation of dairy bulls for energy balance traits using random regression. *Animal Science* **73**: 29-40
- Coles, G.C., Bauer, C., Borgsteede, F.H.M., Geerts, S., Klei, T.R., Taylor, M.A., Waller, P.J. (1992). World Association for the Advancement of Veterinary Parasitology (W.A.A.V.P.) methods for the detection of anthelmintic resistance in nematodes of veterinary importance. *Veterinary Parasitology*, **44**: 35-44
- Coles, G.C., Jackson, F., Pomroy, W.E., Prichard, R.K., von Samson-Himmelstjerna, G., Silvestre, A., Taylor, M.A., Vercruyse, J. (2006). The detection of anthelmintic resistance in nematodes of veterinary importance. *Veterinary Parasitology*, **136**: 167-185
- Coop, R.L., Kyriazakis, I. (1999). Nutrition-parasite interaction. *Veterinary Parasitology* **84**: 187-204
- Coop, R.L., Sykes, A.R., Angus, K.W. (1982). The effect of three levels of intake of *Ostertagia circumcincta* larvae on growth rate, food intake and body composition of growing lambs. *The Journal of Agricultural Science* **98**: 247-255
- Cronje, P.B., Smuts, M. (1994). Nutrient partitioning in merino rams with different wool growth-rates. *Animal Production* **59**: 55-60
- de Pury, D.G.G., Farquhar, G.D. (1997). Simple scaling of photosynthesis from leaves to canopies without the errors of big-leaf models. *Plant, Cell and Environment* **20**: 537-557
- Delagarde, R., Peyraud, J.L., Delaby, L., Faverdin, P. (2000). Vertical distribution of biomass, chemical composition and pepsin-cellulose digestibility in a perennial ryegrass sward: interaction with month of year, regrowth age and time of day. *Animal Feed Science and Technology*. **84**: 49-68
- Doeschl-Wilson, A.B., Vagenas, D., Kyriazakis, I., Bishop, S.C. (2008). Exploring the assumptions underlying genetic variation in host nematode resistance. *Genetics Selection Evolution* **40**: 241

- Du, S., Xu, M., Yao, J. (2016). Relationship between fibre degradation kinetics and chemical composition of forages and by-products in ruminants. *Journal of Applied Animal Research* **44**: 189-193
- Ehrhardt, R.A., Bell, A.W. (1995). Growth and metabolism of ovine placenta during mid-gestation. *Placenta* **16**: 727-741
- Emmans, G.C. (1997). A method to predict the food intake of domestic animals from birth to maturity as a function of time. *Journal of Theoretical Biology* **186**: 189-200
- Emmans, G.C., Fisher, C. (1986). Problems of Nutritional theory. In *Nutritional Requirements and Nutritional Theory* (ed. Fisher, C. and Boorman, K.N.), pp 9-57. Butterworths, London.
- Falconer, D.S., Mackay, T.F.C. (1996). Introduction to quantitative genetics, 4th ed. Longman, UK.
- Farquhar, G.D., von Caemmerer, S., Berry, J.A. (1980). A biochemical model of photosynthetic CO₂ assimilation in leaves of C₃ species. *Planta* **149**: 78-90
- Fox, M.T., Gerrelli, D., Pitt, S.R., Jacobs, D.E., Gill, M., Gale, D.L. (1989). *Ostertagia ostertagi* infection in the calf: effects of a trickle challenge on appetite, digestibility, rate of passage of digesta and liveweight gain. *Research in Veterinary Science* **47**: 294-298
- Goering, H.K., Van Soest, P.J. (1975). Forage fiber analyses. (Apparatus, reagents, procedures and some applications). Agricultural Handbook No. 379. ARSUSDA, Washington, DC.
- Greer, A.W., Stankiewicz, M., Jay, N.P., McAnulty, R.W., Sykes, A.R. (2005). The effect of concurrent corticosteroid induced immune-suppression and infection with the intestinal parasite *Trichostrongylus colubriformis* on food intake and utilization in both immunologically naïve and competent sheep. *Animal Science* **80**: 89-99
- Harley, P.C., Thomas, R.B., Reynolds, J.F., Strain, B.R. (1992). Modelling photosynthesis of cotton grown in elevated CO₂. *Plant, Cell and Environment* **15**: 271-282
- Houdijk, J.M., Jessop, N.S., Kyriazakis, I. (2001). Nutrient partitioning between reproductive and immune functions in animals. *Proceedings of the Nutritional Society* **60**: 515-525
- Hunter, T.E., Suster, D., DiGiocomo, K., Dunshea, F.R., Cummins, L.J., Egan, A.R., Leury, B.J. (2015). Milk production and body composition of single-bearing East Friesian x Romney and Border Leicester x Merino ewes. *Small Ruminant Research* **131**: 123-129
- Jung, H.G., Mertens, D.R., Payne, A.J. (1997). Correlation of acid detergent lignin and klason lignin with digestibility of forage dry matter and neutral detergent fiber. *J. Dairy Sci.* **80**: 1622-1628
- Kao, R.R., Leathwick, D.M., Roberts, M.G., Sutherland, I.A. (2000). Nematode parasites of sheep: a survey of epidemiological parameters and their application in a simple model. *Parasitology* **121**: 85-103
- Kätterer, T., Reichstein, M., Andrén, O., Lomander, A. (1998). Temperature dependence of organic matter decomposition: a critical review using literature data analysed with different models. *Biology and Fertility of Soils* **27**: 258-262
- Kelly, G.A., Kahn, L.P., Walkden-Brown, S.W. (2010). Integrated parasite management for sheep reduces the effects of gastrointestinal nematodes on the Northern Tablelands of New South Wales. *Animal Production Science* **50**: 1043-1052

- Khadijah, S., Kahn, L.P., Walkden-Brown, S.W., Bailey, J.N., Bowers, S.F. (2013). Effect of simulated rainfall timing on faecal moisture and development of *Haemonchus contortus* and *Trichostrongylus colubriformis* eggs to infective larvae. *Veterinary Parasitology* **192**: 199-210
- Komprej, A., Gorjanc, G., Kompan, D., Kovač, M. (2012). Lactation curves for milk yield, fat, and protein content in Slovenian dairy sheep. *Czech Journal of Animal Science* **57**: 231-239
- Lane, J., Jubb, T., Shephard, R., Webb-Ware, J., Fordyce, G. (2015). Priority list of endemic diseases for the red meat industries. Meat & Livestock Australia, Final Report of Project B.AHE.0010, Sydney, Australia. ISBN 9781741918946
- Laurenson, Y.C.S.M. (2014). Evaluating the feasibility of developing a model to better manage nematode infections of sheep. Meat & Livestock Australia, Final Report of Project B.AHE.0244, Sydney, Australia. ISBN 9781740362795
- Laurenson, Y.C.S.M., Kahn, L.P. (2018). A mathematical model to predict the risk arising from the pasture infectivity of four nematode species in Australia. *Animal Production Science* **58**: 1504-1514
- Leuning, R. (2002). Temperature dependence of two parameters in a photosynthesis model. *Plant, Cell and Environment* **25**: 1205-1210
- Levine, N.D., Todd, K.S. (1975). Micrometeorological factors involved in development and survival of free-living stages of the sheep nematodes *Haemonchus contortus* and *Trichostrongylus colubriformis*. A review. *International Journal of Biometeorology* **19**: 174-183
- Lewis, R.M., Emmans, G.C. (2010). Feed intake of sheep as affected by body weight, breed, sex, and feed composition. *Journal of Animal Science* **88**: 467-480
- Marshall, B., Biscoe, P.V. (1980). A model for C₃ leaves describing the dependence of net photosynthesis on irradiance. *Journal of Experimental Biology* **31**: 29-39
- Martin, R.R., Beveridge, I., Pullman, A.L., Brown, T.H. (1990). A modified technique for the estimation of the number of infective larvae present on pasture, and its application in the field under South Australian conditions. *Veterinary Parasitology*, **37**: 133-143
- Mauna Loa Observatory (2019). <https://esrl.noaa.gov/gmd/ccgg/trends/graph.html> [verified: 16/05/2019]
- Mavrot, F., Hertzberg, H., Torgerson, P. (2015). Effect of gastro-intestinal nematode infection on sheep performance: a systematic review and meta-analysis. *Parasites & Vectors* **8**: 557
- McKenna, P.B. (2006). A comparison of faecal egg count reduction test procedures. *New Zealand Veterinary Journal* **54**: 202-203
- Meat & Livestock Australia, Australian Wool Innovation, Australian Sheep Industry Cooperative Research Centre. (2009). RD&E INVESTMENT PRIORITIES 2009/2012, SHEEP INTERNAL PARASITE MANAGEMENT; 15th April 2009, Sydney NSW, Australia.
- Medlyn, B.E., Dreyer, E., Ellsworth, D., Forstreuter, M., Harley P.C., Kirschbaum, M.U.F., Le Roux, X., Montpied, P., Strassmeyer, J., Walcroft, A., Wang, K., Loustau, D. (2002). Temperature response of parameters of a biochemically based model of photosynthesis. II. A review of experimental data. *Plant, Cell and Environment* **25**: 1167-1179
- Monsi, M., Saeki, T. (2005). On the factor light in plant communities and its importance for matter production. *Annals of Botany* **95**: 549-567

- Morgan, J.E., Fogarty, N.M., Nielsen, S., Gilmour, A.R. (2006). Milk yield and milk composition from grazing primiparous non-dairy crossbred ewes. *Australian Journal of Agricultural Research* **57**: 377-387
- O'Connor, L.J. (2007). Ecology of the free-living stages of *Haemonchus contortus* in a cool temperate environment. PhD thesis, University of New England, Australia.
- O'Connor, L.J., Kahn, L.P., Walkden-Brown, S.W. (2007). The effects of amount, timing and distribution of simulated rainfall on the development of *Haemonchus contortus* to the infective larval stage. *Veterinary Parasitology* **146**: 90-101
- O'Connor, L.J., Kahn, L.P., Walkden-Brown, S.W. (2008). Interaction between the effects of evaporation rate and amount of simulated rainfall on development of the free-living stages of *Haemonchus contortus*. *Veterinary Parasitology* **155**: 223-234
- Pandey, V.S., Chaer, A., Dakkak, A. (1993). Effect of temperature and relative humidity on survival of eggs and infective larvae of *Ostertagia circumcincta*. *Veterinary Parasitology* **49**: 219-227
- Playford, M.C., Smith, A.N., Love, S., Besier, R.B., Kluver, P., Bailey J.N. (2014). Prevalence and severity of anthelmintic resistance in sheep nematodes in Australia (2009-2012). *Australian Veterinary Journal* **92**: 464-471
- Reynecke, D.P., Waghorn, T.S., Oliver, A-M.B., Miller, C.M., Vlassoff, A., Leathwick, D.M. (2011a). Dynamics of the free-living stages of sheep intestinal parasites on pasture in the North Island of New Zealand. 2. Weather variables associated with development. *New Zealand Veterinary Journal* **59**: 287-292
- Reynecke, D.P., van Wyk, J.A., Gummow, B., Dorny, P., Boomker, J. (2011b). A stochastic model accommodating the FAMACHA[®] system for estimating worm burdens and associated risk factors in sheep naturally infected with *Haemonchus contortus*. *Veterinary Parasitology* **177**: 231-241
- Roberts, J.L., Swan, R.A. (1982). Quantitative studies of ovine haemonchosis. 2. Relationship between total worm counts of *Haemonchus contortus*, haemoglobin values and body weight. *Veterinary Parasitology* **9**: 201-209
- Roeber, F., Jex, A.R., Gasser, R.B. (2013). Impact of gastrointestinal parasitic nematodes of sheep, and the role of advanced molecular tools for exploring epidemiology and drug resistance – an Australian perspective. *Parasites & Vectors* **6**: 153
- Saccareau, M., Moreno, C.R., Kyriazakis, I., Faivre, R., Bishop, S.C. (2016). Modelling gastrointestinal parasitism infection in a sheep flock over two reproductive seasons: *in silico* exploration and sensitivity analysis. *Parasitology* **143**: 1509-1531
- Saxton, K.E., Rawls, W.J., Romberger, J.S., Papendick, R.I. (1986). Estimating generalized soil-water characteristics from texture. *Soil Science Society of America Journal* **50**: 1031-1036
- Shija, D.S., Mtenga, L.A., Kimambo, A.E., Laswai, G.H., Mushi, D.E., Mgheni, D.M., Mwilawa, A.J., Shirima, E.J.M., Safari, J.G. (2013). Preliminary evaluation of slaughter value and carcass composition of indigenous sheep and goats from traditional production system in Tanzania. *Asian-Australian Journal of Animal Sciences* **26**: 143-150
- Singleton, D.R., Stear, M.J., Matthews, L. (2011). A mechanistic model of developing immunity to *Teladorsagia circumcincta* infection in lambs. *Parasitology* **138**: 322-332

- Stear, M.J., Boag, B., Cattadori, I., Murphy, L. (2009). Genetic variation in resistance to mixed, predominantly *Teladorsagia circumcincta* nematode infection of sheep: from heritabilities to gene identification. *Parasite Immunology* **31**: 274-282
- Sykes, A.R. (2000). Environmental effects on animal production: the nutritional demands of nematode parasite exposure in sheep. *Asian Australasian Journal of Animal Sciences* **13**: 343-350
- Thomas, R.J. (1982). The ecological basis of parasite control: nematodes. *Veterinary Parasitology* **11**: 9-24
- Thornley, J.H.M., Verberne, E.L.J. (1989). A model of nitrogen flows in grassland. *Plant, Cell and Environment* **12**: 863-886
- Vagenas, D., Bishop, S.C., Kyriazakis, I. (2007a). A model to account for the consequences of host nutrition on the outcome of gastrointestinal parasitism in sheep: logic and concepts. *Parasitology* **134**: 1263-1277
- Vagenas, D., Doeschl-Wilson, A., Bishop, S.C., Kyriazakis, I. (2007b). In silico explorations of the effects of host genotype and nutrition on the genetic parameters of lambs challenged with gastrointestinal parasites. *International Journal for Parasitology* **37**: 1617-1630
- van Wyk, J.A., Bath, G.F. (2002). The FAMACHA[®] system for managing haemonchosis in sheep and goats by clinically identifying individual animals for treatment. *Veterinary Research* **33**: 509-529
- Vera, R.R., Morris, J.G., Koong, L.,-J. (1977). A quantitative model of energy intake and partition in grazing sheep in various physiological states. *Animal Production* **25**: 133-153
- Waller, P.J., Dobson, R.J., Donald, A.D., Thomas, R.J. (1981). Populations of strongylid nematode infective stages in sheep pastures: comparison between direct pasture sampling and tracer lambs as estimators of larval abundance. *International Journal for Parasitology*, **11**: 359-367
- Wellock, I.J., Emmans, G.C., Kyriazakis, I. (2003). Modelling the effects of thermal environment and dietary composition on pig performance. *Animal Science* **77**: 255-266
- Wellock, I.J., Emmans, G.C., Kyriazakis, I. (2004). Describing and predicting growth in the pig. *Animal Science* **78**: 379-388
- Wilson, A.D., Dudzinski, M.L. (1973). Influence of the concentration and volume of saline water on the food intake of sheep, and on their excretion of sodium and water in urine and faeces. *Australian Journal of Agricultural Research* **24**: 245-256
- Wohlfahrt, G., Bahn, M., Haubner, E., Horak, I., Michaeler, W., Rottmar, K., Tappeiner, U., Cernusca, A. (1999). Inter-specific variation of the biochemical limitation to photosynthesis and related leaf traits of 30 species from mountain grassland ecosystems under different land use. *Plant, Cell and Environment* **22**: 1281-1296
- Wood, P.D.P. (1967). Algebraic model of the lactation curve in cattle. *Nature* **216**: 164-165
- Woodward, S.J.R. (1998). Quantifying different causes of leaf and tiller death in grazed perennial ryegrass swards. *New Zealand Journal of Agricultural Research* **41**: 149-159
- Yakoob, A.Y., Holmes, P.H., Parkins, J.J., Armour, J. (1983). Plasma protein loss associated with gastrointestinal parasitism in grazing sheep. *Research in Veterinary Science* **34**: 58-63
- Yin, X., van Oijen, M., Schapendonk, A.H.C.M. (2004). Extension of a biochemical model for the generalized stoichiometry of electron transport limited C₃ photosynthesis. *Plant, Cell and Environment* **27**: 1211-1222

Yin, X., Struick, P.C. (2009). C₃ and C₄ photosynthesis models: An overview from the perspective of crop modelling. *NJAS – Wageningen Journal of Life Sciences* **57**: 27-38

Zaralis, K., Tolkamp, B.J., Houdijk, J.G.M., Wylie, A.R.G., Kyriazakis, I. (2007). Effect of nematode infection on anorexia and leptin levels in lambs of two breeds. *Journal of Animal and Feed Sciences* **16**: 405--410

Zhang, L., Hu, Z., Fan, J., Zhou, D., Tang, F. (2014). A meta-analysis of the canopy light extinction coefficient in terrestrial ecosystems. *Frontiers of Earth Science* **8**: 599-609

Zotarelli, L., Dukes, M.D., Romero, C.C., Migliaccio, K.W., Morgan, K.T. (2010). Step by step calculation of the Penman-Monteith Evapotranspiration (FAO-56 Method). AE459. The Institute of Food and Agricultural Sciences, Agricultural and Biological Engineering Department, University of Florida. Revised August 2015. Retrieved from: <http://edis.ifas.ufl.edu/ae459> [verified: 16/05/2019]